Plastic Buckling

of

Columns and Plates

Shirin Jowhari Moghadam

BEng (Hons), MSc, DIC

May 2015

A thesis submitted in fulfilment
of the requirements for the degree of
Doctor of Philosophy of
Imperial College London

Department of Civil and Environmental Engineering
Imperial College London
London SW7 2AZ

Declaration

I confirm that this thesis is my own work and that any material from published or unpublished work from others is appropriately referenced.

Acknowledgements

I would like to gratefully acknowledge the support of various people and their distinct contributions to my PhD, one of the most incredible incidents of my life which has been a truly life-changing experience.

Undertaking a PhD is a wonderful, but mostly an overwhelming journey and it would not have been possible to carry on without the help of my supervisor, my family and my friends. First and foremost I want to express my sincere gratitude to my supervisor, Professor Bassam Izzuddin, for his continuous and invaluable support, guidance and encouragement throughout my PhD life. It has been an honour and a privilege to work with you, Professor.

I want to extend my deepest and heartfelt gratitude to my wonderful family for your unconditional love, for your endless patience and for your persistent encouragement and most importantly for giving me the opportunity to follow my dreams. Thanks a million Dad, Mum, Shafa and Shima. How can I ever thank you enough.. My special thanks goes to Matthew, who has been there for me along the way, through all of the ups and downs.

I also would like to take this opportunity to thank all my friends particularly Alex#1, Caterina, Francisco, Amir Abbas, Aliyyah, Marianna, Corrado, Alex#2, Eleni, my colleagues in room 317A and the lovely people of Imperial College for being by my side and always giving me reasons to cheer up.

زندگی خالی نیست:

مهربانی هست، سیب هست، ایمان هست..

آری

تا شقایق هست، زندگی باید کرد.

Sohrab Sepehri

Abstract

The theory of buckling strength of compression members in the plastic range has been extensively studied, and numerical methods already exist which deal with such behaviour. However, there is a significant research interest in developing analytical models for the plastic buckling, largely driven by the need for simplified mechanics-based design tools, but also by the desire for enhanced understanding of this complex phenomenon.

A thorough investigation into the inelastic buckling of columns and plates reveals the existence of two well-known inconsistencies recognised as the "Column Paradox" and the "Plate Plastic Buckling Paradox". In the current research, addressing the conceptual issues related to the plastic buckling of columns and plates, including the two associated paradoxes, has been achieved by means of development and application of analytical models that are verified against nonlinear finite element analysis. These models are based on sound principles of structural mechanics and are intended to illustrate the mechanics of the plastic buckling response of stocky columns/plates by means of a simplified analytical approach, from the point of buckling initiation and considering the post-buckling response. In these models, the Rotational Spring Analogy is used for formulating the geometric stiffness matrix, whereas the material stiffness matrix is obtained with due consideration for the spread of material plasticity.

It is shown that the buckling of stocky perfect columns starts at the Engesser load while the von Karman upper limit is typically not realised due to tensile yielding at the outer fibre of the column cross-section. Furthermore, it is established that beyond a threshold level of imperfection, as evaluated directly from the developed model, the plastic post-buckling response of columns is barely affected by a further increase in the out-of-straightness.

Besides identifying previous misconceptions in the research literature, the proposed analytical models for the plastic buckling of plates have proven to offer valuable insight into factors that influence the plastic buckling of stocky plates, and hence succeeded in resolving the long-standing paradox. It is the major contention of this

thesis, verified through extensive studies, that the “Plate Plastic Buckling Paradox” is resolved with the correct application of plasticity theory, considering not only the influence of initial imperfections but also the interaction between flexural and planar actions.

Table of Contents

List of Tables

List of Figures

Notation

Abbreviations

1D	One dimensional
2D	Two dimensional
FE	Finite Element
MDOF	Multiple Degree of Freedom
N.A.	Neutral Axis
RSA	Rotational Spring Analogy
SDOF	Single Degree of Freedom
DMV	Donnell-Mushtari-Vlasov

Symbols

$\{B\}$	Curvatures
$[D]$	Elastic constitutive matrix
$[E_t]$	Tangent modulus matrix
$[E_{tb}]$	Tangent modulus matrix for Conventional Incremental Theory
$[K_E]$	Material stiffness matrix
$[K_G]$	Geometric stiffness matrix
$[K_T]$	Tangent stiffness matrix
$\{N\}$	Normal to yield surface
$\{s\}$	Deviatoric stress
$\{U\}$	Associated buckling mode
a	Length of plate
A	Area
a_i and b_i	Coefficients in Hutchinson's asymptotic expansions
b	Width of plate/column
c	Hardening function in yield rule
d	Length of unloading region in Hutchinson's model
E	Young's modulus
$\bar{E}$	Equivalent flexural modulus

E_R	Reduced modulus
E_s	Secant modulus
E_t	Tangent modulus
f	Yield surface
F	Axial force
F_1 and F_2	Normal force increments in von Karman theory
G	Shear modulus
G_s	Secant shear modulus
G_t	Tangent shear modulus
h	Thickness of plate/Depth of column cross-section
h_e	Depth of unloading zone
I	Second-moment of area
J_2	Second invariant of deviatoric stress
k	Plate instability coefficient
k_e	Nominal material stiffness
k_g	Nominal geometric stiffness
k_θ	Stiffness of distributed equivalent rotational spring
k_ρ	Rotational stiffness of spring
L	Length of column/Depth of Hutchinson's column model
$\tilde{L}$	Length of Hutchinson's column model
M_x and M_y	Bending moments in x- and y-direction
n	Number of transverse half-waves
N_x, N_y and N_{xy}	Nominal loading in x- and y- directions and nominal shear loading
P	Applied load
P_0	Load at which strain reversal initiates
P_c	Instantaneous buckling load
P_{ce}	Critical elastic buckling load
P_{cr}	Critical buckling load
P_E	Euler's formula
P_{max}	Maximum buckling resistance (load at which tensile yielding initiates)
P_R	Reduced-modulus load

P_t	Tangent-modulus load
P_Y	Yield load
r	Radius of gyration
S	Elastic section modulus
w	Buckling mode
w_0	Maximum amplitude of transverse displacement at centre
$\bar{w}$	Normalised mode
$w_{0i,max}$	Threshold level of imperfection
w_i	Weighting factor
W^p	Plastic work per unit volume
x_c	Length of elastic region for Class 2 column
x_e	Length of unloading zone
x_s	Length of elastic region in large imperfections
y	Depth from neutral axis
y_e	Instantaneous neutral axis
y_R	von Karman neutral axis
$\{\alpha\}$	Total translation of centre of yield surface
β	Ratio of biaxial loading
$d\lambda$	Positive scalar increment in plastic component of strain increment
γ_{xy}	Shear strain
Δ	Increment sign
δ	Infinitesimal increment sign
ε_{ep}	Effective strain
$\{\varepsilon_p\}$	Plastic strains
η	Plasticity reduction factor/effective tangent material modulus
η_l	Effective tangent material modulus without shear/twisting component
θ	Rotation of column in Hutchinson's model
$\{\theta\}$	Slope of buckling mode
K	Parameter defining the size of yield surface
λ	Slenderness ratio/Accumulated plastic strain
μ	Hardening parameter

ν	Poisson's ratio
ρ	Load factor
σ_{cr}	Critical buckling stress
σ_e	Effective stress
$\sigma_x(\sigma_1)$ and $\sigma_y(\sigma_2)$	Planar normal stresses in x- and y-direction
σ_Y	Yield strength
τ_{xy}	Planar shear stress
φ	A scalar function related to the material property
$_0$ (subscript)	Initial values
^{o} (superscript)	
$_b$ (subscript)	Bottom
$_c$ (subscript)	Centroidal
$_f$ (subscript)	Flexural
$_m$ (subscript)	Mid-plane
$_t$ (subscript)	Top

CHAPTER 1

Introduction

1.1 Background

The primary concern in compression elements in many engineering structures such as aircrafts, ships and offshore structures is about the instability characteristics of the element. This structural instability is known as buckling, the phenomenon in which the structure subject to compression undergoes visibly large transverse displacements, as illustrated in Figure 1.1. On the other hand, considerations of minimum use of material within a structural member can lead to one relatively small dimension (e.g. plate thickness or a column cross-sectional dimension) compared to the other dimensions, which in turn reduces the buckling capacity, thus potentially influencing the overall load carrying capacity. However, in designing the structures mentioned above there is often a need to utilise a greater resistance than the material yield strength and hence the buckling of stocky members becomes of interest. Accordingly, it is essential to understand the buckling phenomenon and to predict its influence on the overall structural resistance.

Figure 1.1 Phenomenon of buckling

Plates and plated members are widely used in various engineering structures, such as buildings, box girder bridges, wind turbines and offshore structures (Figure 1.2), to

name but a few, while columns represent the dominant structural component in most structures. The focus of this thesis is on the stocky columns and plates, where buckling occurs at stresses greater than the proportional yield limit of the material used in fabrication of the structure. Such structures are normally designed using the buckling equations available for the elastic structures, with some approximation applied when the elastic buckling loads exceed the yield limit. While advanced numerical modelling using nonlinear finite element (FE) analysis can model the influence of the material yielding on the buckling, its computational demands has meant that its use is restricted to the design of important structures or to the assessment of existing structures, such as the push-over analysis of offshore jackets. For the majority of typical structures, a stocky plate or column is assumed in the current design practice to provide a maximum resistance equal to the yield load, which can be conservative and ignores the increase in strength due to strain hardening. However, in order to realise any related benefits, it is important to develop simplified models that capture the influence of material plasticity on the buckling response.

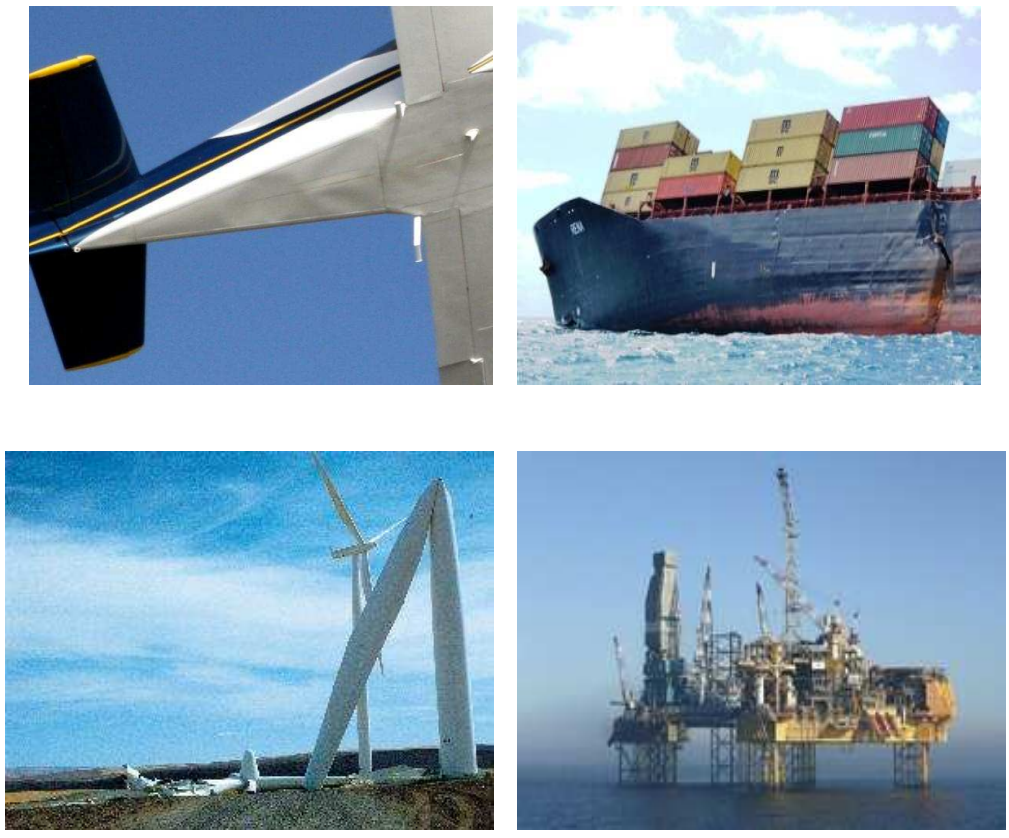

Figure 1.2 Plate buckling

Under an increasing applied load beyond the elastic limit of the material, elasto-plastic materials such as structural steel, aluminium and stainless steel exhibit both reversible elastic and irreversible plastic deformations. In the case of the structural steel, the stress-strain relationship is linear (i.e. obeying Hooke's law) up to the yield strength beyond which the material deforms plastically, typically with increasing stress due to the strain hardening but at a much lower rate. In the plastic range or the strain hardening zone, the stress-strain relations become nonlinear as the deformations increase with a decreasing stiffness. Hence, the main difficulty of establishing a simplified method for the inelastic buckling analysis is the fact that the material stiffness for structures with material nonlinearity is not uniquely defined in the plastic range (Izzuddin, 2007c). Hence, it would be necessary to select an appropriate material stiffness founded on sound constitutive relations and allowing for the true incremental response of the structure. On the other hand, buckling of a structure typically arises when the geometric stiffness becomes sufficiently 'negative' to overcome the 'positive' material stiffness. Consequently, the buckling response of stocky structures becomes quite complicated as a result of the interaction between geometric and material nonlinearities.

The theory of buckling strength of compression members has the most extensive history in the study of strength of materials. However, there is significant research interest in developing analytical models for the plastic buckling, largely driven by the need for simplified mechanics-based design tools, but also by the desire for enhanced understanding of this complex phenomenon.

The very first formulation of the law relating stresses and strains was due to Robert Hooke in 1660 who discovered that the deformation of an elastic body is proportional to the forces acting on it. This formulation is known as Hooke's law of elasticity and is valid in the case of sufficiently small deformations. Over a century later in 1807, Thomas Young represented the factor of proportionality in Hooke's law and introduced a numerical constant E that describes the elastic properties of a solid undergoing compression/tension only in one direction, the so called Young's modulus of elasticity. Subsequent to the introduction of Poisson's ratio in 1811, Hooke's law was generalised to describe the linear stress-strain constitutive relations within the elastic range for multi-axial stress states. However, when the material is

stressed beyond its yield strength, it undergoes irreversible plastic deformations where Hooke's law is no longer valid and therefore a different approach is required to describe the constitutive law.

The earliest attempt to establish a buckling formula was made by Euler (1744). He studied Bernoulli's finding in 1705 regarding the moment-curvature relation on the basis of Hooke's law in a bent rod and presented the column formula that is still used to predict the critical elastic buckling load of columns. Local instability of plates was first investigated by Bryan in 1891 where he obtained a theoretical solution to the problem of a simply-supported plate subject to a uniform compression. Up to this stage, numerous investigations had been carried out on the elastic buckling of plates under various loadings and boundary conditions. The calculation of the critical buckling stress of columns and of compressive members made up of plates is well established in the elastic region. However, this is only applicable to slender columns and plates and therefore not to short columns and stocky plates where the buckling stress exceeds the elastic limit. The complication starts with columns and plates having slenderness ratios below a specific limit, where the elastic buckling load exceeds the yield load, in which case the actual plastic buckling load becomes affected by the entire stress-strain relationship of the material including the tangent modulus E_t.

Column was the first type of structure for which buckling was studied in the plastic range. Engesser (1889) proposed the use of the tangent modulus E_t in the Euler buckling formula. However, at the same time Considère (1891) believed that the column buckling response is positively affected by unloading on the column convex side and that the value of effective modulus must be between E and E_t. Almost two decades later, von Karman suggested his well-known double-modulus E_R theory founded on Engesser's theory and Considère's idea. However, the extensive tests carried out showed that von Karman's reduced-modulus theory resulted in considerably higher buckling stresses. This paradox was addressed by Shanley (1947) who stated that the tangent modulus E_t is the correct effective modulus to be employed for the buckling beyond the proportional limit, and that the unloading of one side of the column does not occur at buckling. Soon after, Duberg and Wilder (1952) carried out a theoretical study on column behaviour in the plastic range

allowing for initial imperfections and employing a realistic material model, where they also concluded that tangent-modulus load is the critical load at which the column starts to buckle.

In the case of plate buckling, the earliest attempts were made by Bleich (1924), Gerard (1945), Timoshenko & Gere (1961), who suggested the replacement of Young's modulus in the elastic critical buckling stress of plates by a reduced modulus such as the tangent modulus or the secant modulus. However, a proper investigation of the buckling of plates beyond the elastic range requires a knowledge of the constitutive relations between the stresses and strains. On this topic, two main theories of plasticity have been introduced: Deformation Theory and Incremental Theory. The former was initially proposed by Hencky (1924) and was further developed by Ilyushin (1947), whereas the latter was further developed by Handelman and Prager (1948). The main difference between the two theories is that the Deformation Theory relates the total strain to the stress state and hence assumes a unique relation between stress and strain which is independent of the history of loading, while the Incremental Theory relates the increments of strains to the increments of stress thus accounting for load path dependency. Although Incremental Theory is widely accepted as the more correct theory, it furnishes bifurcation loads that are much larger than the predictions of Deformation Theory, and more importantly the experimental results are in favour of the solutions given by the Deformation Theory. This perplexing outcome has since been referred to as the "Plate Plastic Buckling Paradox". Numerous numerical, experimental and analytical investigations into this well-known paradox have been carried out, as presented in Chapter 2, though no substantial explanation supported by sound principles of mechanics of materials has been offered so far.

1.2 Scope, Objectives and Originality of Thesis

Today the elasto-plastic buckling analysis of structures is studied by means of rigorous numerical methods such as the finite element method; however, this numerical method is still considered to be too involved for a direct application in the design and assessment practice, and it does not provide significant insight into the main factors influencing the nonlinear response. On the other hand, analytical models are beneficial as i) they are efficient, ii) they potentially enhance understanding of the problem, and iii) they are more amenable for application in design/assessment

practice. However, this comes at the cost of lack of generality. While extensive research has been undertaken to improve the current theories for the plastic buckling analysis of columns and plates, there is still no generally applicable analytical method for such problems. In particular, the Plate Plastic Buckling Paradox relating to the plates has evaded researchers until this date, thus reflecting major shortcomings in the existing analytical models for the plastic buckling of plates.

Within this brief context, the main objectives of the current work are:

1. development of a rational analytical model for the plastic buckling of stocky columns;
2. investigation of the key parameters influencing the plastic column buckling;
3. comparison of the general characteristics of the plastic buckling in columns and plates using nonlinear FE analysis;
4. development of a rational analytical model for the plastic buckling of stocky plates based on sound principles of mechanics of materials; and
5. investigation of the key parameters influencing the plastic plate buckling, and shedding light on the Plate Plastic Buckling Paradox.

Besides the novel developments in the two proposed analytical models for the plastic buckling of columns and plates, this work makes the following original contributions:

1. identification of the role of the initial imperfections in the plastic buckling of columns, including the presence of a threshold imperfection level;
2. establishing that the plastic buckling resistance of the stocky columns is limited by tensile yielding;
3. demonstrating the crucial influence of the initial imperfections on the plastic buckling resistance of the stocky plates; and
4. showing that the incorporation of the interaction between planar and flexural actions achieves a final and conclusive resolution of the Plastic Buckling Paradox for stocky plates.

1.3 Organisation of Thesis

In this chapter, a brief background relating to the plastic buckling of columns and plates is presented, which is followed by highlighting the scope, objectives and originality of the current research.

Chapter 2 presents an extensive literature review of the developments in the plastic buckling of columns and plates to date, highlights the shortcomings of the existing methods of analysis, and identifies the main gaps of knowledge which will be addressed in the subsequent chapters.

In Chapter 3, an analytical model for the plastic buckling of columns is presented, which considers for the first time the spread of plasticity over the cross-section and along the member length. In addition to establishing some key features of the plastic buckling, the imperfection sensitivity in the plastic range is studied, and as a result a threshold level of imperfection for very stocky columns is identified.

In Chapter 4, a comparative parametric study is undertaken on the plastic buckling of columns and plates using the nonlinear analysis program ADAPTIC (Izzuddin, 1991). The study compares the plastic buckling response for the two types of element from the initiation of buckling to the maximum buckling resistance, with the primary aim of establishing whether an analytical plastic bucking model for stocky plates could be based on the previously developed model for stocky columns.

Building on the outcomes of Chapter 4, which indicate the plastic buckling of plates is inherently different from that of columns, Chapter 5 focuses on the analytical modelling requirements of plates. In particular, consideration is given to the Plate Plastic Buckling Paradox and a recent attempt by Becque (2010) to resolve this paradox in an analytical model. It is shown that Becque's approach to reducing the shear modulus is not rational, and an explanation based on the accepted principles of material plasticity is offered.

Chapter 6 questions the widely accepted notion that the reduction in the shear modulus in the plastic range alone accounts for the inaccuracy of the Incremental Theory. To this end, an analytical model for the elasto-plastic buckling analysis of

plates is proposed founded on the findings of Chapter 5, generalised to consider other pertinent issues, and applied to gain further insight into the plastic buckling of plates and to resolve the Plate Plastic Buckling Paradox. In addition to establishing some key features of the plastic buckling in stocky plates, the crucial role of initial imperfections for such structural elements is highlighted.

Chapter 7 generalises the analytical model developed in Chapter 6 to address plates with different aspect ratios, buckling modes and subject to various loading conditions, where relevant parametric studies are undertaken.

Finally, Chapter 8 summarises the achievements and main conclusions of this work, and provides suggestions for further future work on the plastic buckling of structures.

CHAPTER 2

Literature Review

2.1 Introduction

The most common type of analysis in structural mechanics and engineering design is the linear static analysis, where a linear relationship between stress and strain forms the basis of "Theory of Elasticity" and Hooke's law in its general form is used to describe this relationship. However, only some structures will fail at a load causing stresses smaller than the material yield limit, typically by elastic buckling. Many structures made of metals such as steel would in fact develop material plasticity at certain levels of loading, following which load redistribution occurs, and final failure may be due to the development of a plastic mechanism or inelastic buckling. Particularly in the latter case, both material and geometric nonlinearities are encountered. Geometric nonlinearities can arise due to significant internal stresses and/or significant changes in the geometry during loading relative to the initial undeformed configuration. On the other hand, material nonlinearity arises due to nonlinearity in the stress-strain relation, where the "Theory of Plasticity" is typically employed for modelling the material nonlinearity in metals.

For more than a century, there has been a significant amount of research conducted on the elasto-plastic buckling analysis of structures, involving experimental, analytical and numerical methods. However, regardless of the major research topics and numerous investigations in this field, buckling of metal structures continues to attract research interest. In this chapter, a comprehensive review of literature is undertaken on the plastic buckling analysis of metallic columns and plates, where specific reference is made to paradoxes that have been encountered by previous researchers, with at least one of these paradoxes remaining largely unresolved. This is followed by reviewing existing simplified plastic buckling analysis methods and the typical treatment of plastic buckling in design codes.

2.2 Plastic Buckling of Columns

The history of column buckling theory dates back to over 270 years with the pioneering work of Leonhard Euler (Euler, 1744). He studied the moment-curvature relation of a bent pin-ended rod and established a critical load, which has since been known as the Euler load, at which a slender elastic column can be held in a bent configuration under an axial load $P_E=\pi^2EI/L^2$. Euler's formula is considered as the earliest design formula in engineering history.

Elasto-plastic buckling of columns was first investigated by Engesser in 1889 (Engesser, 1889) who proposed the use of a "tangent-modulus" $E_t=d\sigma/d\varepsilon$, defined as the slope of the stress-strain curve at the critical stress, as an effective modulus for the buckling analysis in the plastic range leading to $P_t= \pi^2E_tI/L^2$ for a pin-ended column. However, at the same time Considère (1891) believed that the column resistance is enhanced by unloading on its convex side, and that the value of effective modulus must be between E and E_t. As a result, the maximum buckling load of a column would be underestimated by Engesser's load, which was considered to over-simplify the determination of the plastic buckling resistance with the effective modulus varying over the cross-section due to elastic unloading. A few years later Jasinski (1895) pointed out that Engesser's tangent-modulus theory was not correct and presented the reduced-modulus theory based on Considère's work but could not calculate the reduced modulus theoretically. Subsequently, Engesser (1895) acknowledged the mistake in his original theory and showed how to calculate the reduced modulus (also known as Considère–Engesser theory) for different cross-sections (Gere and Goodno, 2012).

Almost two decades later, von Karman (1910) suggested his well-known "double modulus" or "reduced-modulus" theory founded on Engesser's theory and Considère's idea; throughout the rest of this thesis, the term "reduced-modulus" will be used to refer to von Karman's theory. He assumed that the column buckles at a constant axial load P, and adopted the Euler-Bernoulli hypothesis of plane sections remaining plane and normal to the centroidal reference line of the column. When the column buckles, the concave side of the column undergoes further compression, associated with plastic loading, while the convex side undergoes incremental

extension, leading to elastic unloading, and as a result there will be a neutral axis at which the axial strain does not change (Figure 2.1). The distances from the concave and convex sides of the column are denoted by h_1 and h_2, so that $h=h_1+h_2$. Since the tangent modulus E_t is used for the plastic loading zone, while Young's modulus E is used for the elastic unloading zone, a bilinear stress distribution within the cross-section is formed. As a consequence of these assumptions, the resultants of the normal stress increments $F_1=bh_1E_th_1\kappa/2$ and $F_2= bh_2Eh_2\kappa/2$ will be of opposite sign and equal magnitude to ensure incremental axial equilibrium, leading to $h_1 = h\sqrt{E_t}\Big/\left(\sqrt{E}+\sqrt{E_t}\right)$ for a rectangular solid section and an effective reduced modulus $E_R = 4EE_t\Big/\left(\sqrt{E}+\sqrt{E_t}\right)^2$ for the tangential flexural response of a rectangular cross-section (Bazant and Cedolin, 1991). Similar to the tangent modulus load, von Karman's reduced modulus buckling load is obtained from Euler's formula with Young's modulus E replaced by E_R, leading to $P_R= \pi^2E_RI/L^2$ for a pin-ended column. To validate his theory, von Karman performed a series of careful tests on specimens of rectangular and idealised H-cross-sections. However, subsequent work (Templin *et al.*, 1938;van den Broek, 1945;Sandorff, 1946) showed that the reduced-modulus theory predicts significantly larger buckling loads compared with experiments conducted on columns.

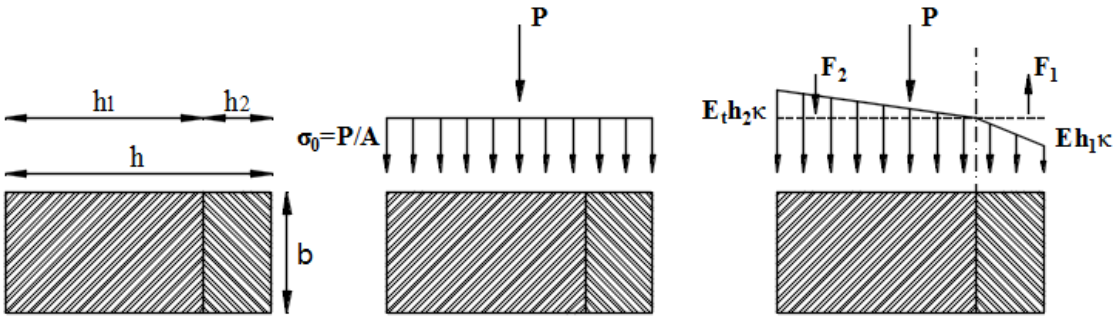

Figure 2.1 Assumed incremental stress distribution over rectangular cross-section for reduced-modulus load (Bazant and Cedolin, 1991)

Von Karman's reduced-modulus buckling load is obtained based on the assumption that the column buckles under a constant load, i.e. he considered a simple bifurcation problem, and thus a unique critical load is predicted for a stocky column on the basis

of its geometry and material properties. The difference between the two buckling loads (i.e. tangent- and reduced-modulus loads) presented a paradox, until 1946 when Shanley showed in his well-known article "The Column Paradox" (Shanley, 1946) that, unlike the elastic buckling case, there is no unique critical buckling load for a column in the inelastic range. He questioned the assumption of a constant load at bifurcation made in the reduced-modulus approach because it assumes that the column remains straight up to the maximum load (i.e. bifurcation load). However, there is some strain reversal taking place within the cross-section, which in turn provides the additional stiffness leading to a critical load greater than the tangent-modulus load. According to Shanley, this represented a paradox since in his view it is impossible to have strain reversal in a straight column (although it will be shown later that a Class 2 column would exhibit strain reversal even though the column is straight). Therefore he concluded (Shanley, 1946) that the plastic buckling theory of the column should be reviewed on the basis that buckling occurs simultaneously with an increasing axial load, and that the maximum buckling load is attained somewhere between P_t and P_R (Figure 2.2). The main shortcoming of the reduced-modulus approach is that it overestimates the initial buckling load, since the prefect column becomes unstable on the trivial path above the Engesser load.

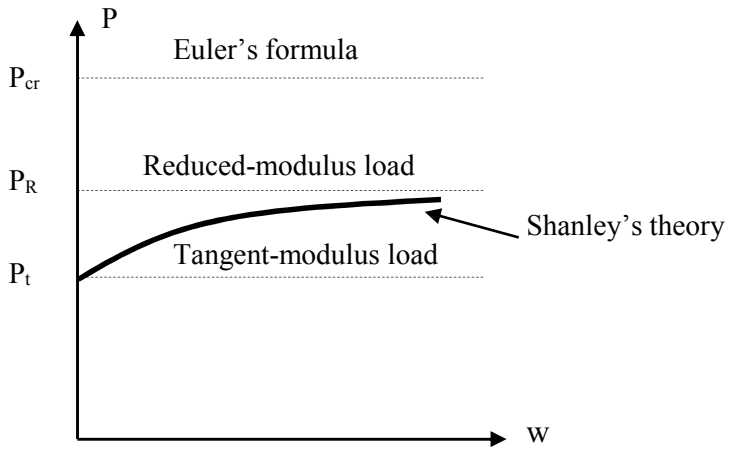

Figure 2.2 Shanley's theory compared to tangent-modulus and reduced-modulus theories

Subsequently in 1947, Shanley stated that the tangent-modulus E_t is the correct effective modulus to be employed for buckling beyond the proportional limit and that the unloading of one side of the column does not occur until the tangent-modulus load is reached (Shanley, 1947). He validated his theory by performing various tests on columns with rectangular sections followed by an analytical model consisting of a simplified two-flange column Figure 2.3. His model column consisted of two rigid bars which are connected by two small axial elements (links) at the centre of the column. With analogy to reduced-modulus theory, he assumed that under an increasing load the element on the concave side undergoes increasing compressive stress while the element on the convex side undergoes decreasing compressive stress, each with the corresponding moduli (i.e. E_t for loading and E for unloading elements). Satisfying the conditions of axial and moment equilibrium, an expression for the applied load P and the lateral deflection d of the column is obtained. Assuming a constant tangent modulus E_t, he concluded that for a perfect column buckling starts at the Engesser tangent-modulus load P_t, at which the lateral deflection takes place, and the load will increase until it approaches the reduced-modulus load P_R.

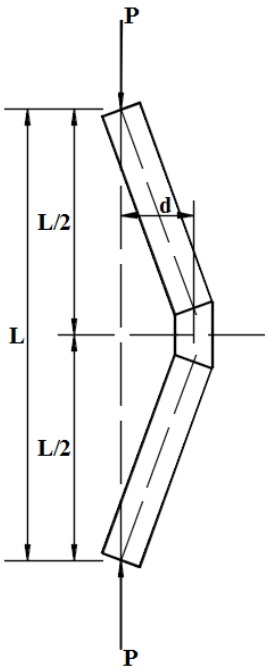

Figure 2.3 Shanley's simplified two-flanged column (Shanley, 1947)

Duberg and Wilder (1952) carried out a theoretical study on column behaviour in the plastic range allowing for initial imperfections and a realistic Ramberg-Osgood (1943) material model. In their study they also concluded that if the behaviour of a perfectly straight column is regarded as the limiting behaviour of a bent column as its initial imperfection vanishes, the tangent-modulus load is the critical buckling load of the column; i.e. the load at which the column starts to buckle. Two decades later, Hutchinson evaluated the plastic buckling in the context of the generalised stability theory (Hutchinson, 1973a;b, 1974), and his method has been considered since as the most successful analytical method in predicting the maximum buckling load of geometrically perfect and imperfect columns. For elastic structures, the critical load corresponds to a bifurcation load, and hence Koiter's general theory which is based on an asymptotic perturbation technique can be used to evaluate the initial post-buckling and imperfection sensitivity (Koiter, 1960). In plastic buckling, however, the bifurcation load does not occur at a constant load, and therefore the development of a similar approach to Koiter's introduces more difficulties (Christensen and Byskov, 2008). Nevertheless, in 1974, Hutchinson published an overview of the developments in plastic buckling analysis, including his own contribution which evaluates Shanley's model in the spirit of Koiter's asymptotic method (Hutchinson, 1974).

Hutchinson uses a rigid-rod model similar to Shanley's simple model except for the fact that this cantilever column model was originally (Hutchinson, 1972) being supported by two springs as a representation of the outer and the inner fibres of the cross-section (the so called discrete Shanley-type model) and a third spring at the top so as to incorporate the geometric nonlinearities into the model, as shown in Figure 2.4a. However, in later work, Hutchinson (1973b) presents his method of plastic buckling analysis by means of a continuum version of his previous simple model, in the sense that the column is supported by a continuous row of springs, as illustrated in Figure 2.4b, to capture the spread of plasticity over the cross-section depth, although no real cross-section was indicated in his earlier works. As can be seen, this simple model has two degrees of freedom: the downward vertical displacement u and the rotation θ.

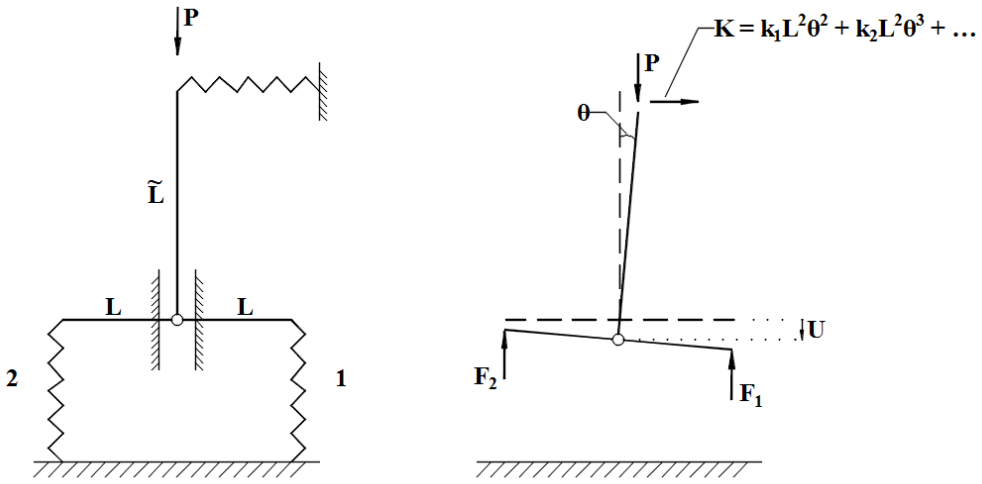

a. Discrete Shanley-type model (Hutchinson, 1972)

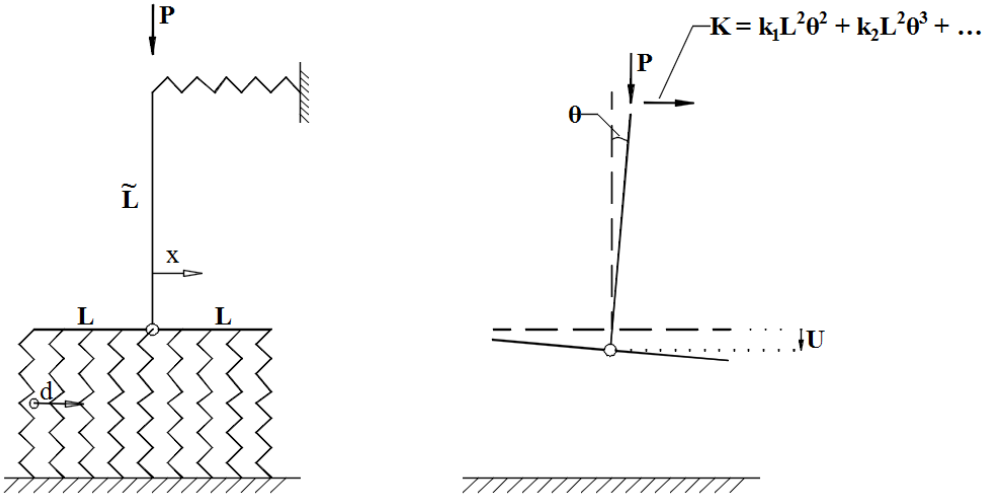

b. Continuous model (Hutchinson, 1973b)

Figure 2.4 Hutchinson's rigid-rod model

The lowest bifurcation load of a perfect column in the plastic range is the tangent-modulus load, which is given by Hutchinson for his model as $P_t = 2E_tL^3/(3\tilde{L})$, from which the elastic unloading starts at least at one point, and the region of elastic unloading expands as deflections increase (indicated by d in Figure 2.4b). By satisfying the conditions of axial and flexural equilibrium, through employing a

tangent modulus E_t for the plastic loading zone ($d<x<L$) and Young's modulus E for the unloading zone ($-L<x<d$), Hutchinson obtains two coupled nonlinear differential equations, which are then solved approximately by means of asymptotic expansions relating the applied load P to the rotation of the column θ using fractional powers (Hutchinson, 1973b):

$$\begin{aligned} P/P_t &= 1+a_1\theta+a_2\theta^{3/2}+a_3\theta^2+a_4\theta^{5/2}+... \\ d/L &= -1-\frac{3}{2}b_2\theta^{1/2}-2b_3\theta-\frac{5}{2}b_4\theta^{3/2}+... \end{aligned} \tag{2.1}$$

where the coefficients a_i and b_i are related to material and geometric properties of the column. On the basis of this expansion, an approximate estimate of the maximum buckling load of the column can be calculated by truncating the above series: $P_{max}/P_t = 1+4a_1^3/(27a_2^2)$.

Hutchinson (1974) uses a Ramberg-Osgood stress-strain relationship to introduce a nonlinear material behaviour and obtains maximum buckling loads which are typically only slightly greater than the tangent-modulus load P_t. He further applies his asymptotic model to initially imperfect columns for which his analysis breaks up into two parts. The first expansions are derived for the inelastic behaviour of columns before any elastic unloading takes place which yield asymptotic expressions for load-deflection at the onset of elastic unloading. Other expansions are then derived for the plastic behaviour after the elastic unloading has taken place. The new expansions, asymptotic in character and derived in terms of the amplitude of initial imperfection, are considerably involved and provide adequate accuracy for very small imperfections.

Although Hutchinson's plastic buckling model may yield important features of post-buckling behaviour of both perfect and imperfect columns, there are notable shortcomings in his approach, including the important question as to whether his simplified link-spring models are directly applicable to the plastic buckling assessment of real columns. Indeed, Hutchinson (1974) states that his column model is the simplest meaningful model that is capable of illustrating some aspects of the analytical character of an initial post-bifurcation behaviour. In this respect, his model

is quite elementary in the sense that no real cross-section is considered and that the spread of plasticity is only captured through the cross-section and not along the column length. Later on in a review of plastic buckling Hutchinson (1974) used the approximate strain-displacement relations of Donnell-Mushtari-Vlasov (DMV) theory (Donnell, 1933;Mushtari, 1938;Vlasov, 1964) of plates and shells for an accurate analysis of post-bifurcation behaviour of columns in the plastic range to estimate the maximum support load for both solid circular and rectangular cross-sections. It will be shown in Chapter 3 that even this prediction of maximum load overestimates the numerical solution by a large margin.

Hutchinson's work has since been used in other related research work (Christensen and Byskov, 2008;Needleman and Tvergaard, 1982;van der Heijden, 1979) aiming to enhance his model for more accurate predictions of buckling resistance of the columns in the plastic range. However, until now, analytical models for the plastic column buckling are based on a grossly simplified rigid bar/column assumption, and neglect the spread of plasticity along the column length. Above all, a reasonably accurate estimate of the maximum plastic bucking load of a stocky column has not yet been determined; as will be shown in Chapter 3, tensile yielding on the convex side of a buckled column determines the maximum plastic buckling resistance, yet it has been completely ignored in all previous analytical models of plastic column buckling.

Besides initial imperfections, the effect of residual stresses on the plastic buckling of columns was been investigated by performing both analytical and experimental studies (Camotim and Roorda, 1985, 1993), where it was concluded that the presence of residual stresses significantly affects the bucking behaviour of columns in the plastic range. In their proposed method, based on Hill's general bifurcation theory and Hutchinson's asymptotic expansion, the influence of residual stresses on the terms of the asymptotic expansion is first determined, and then a combined effect on the load carrying capacity (i.e. squash load) and an estimate of the maximum load is investigated (Camotim and Roorda, 1993). It was found out that independently of the constitutive relation considered in the analysis, the residual stresses can increase or reduce the strength depending on their sign, where the differences in load carrying capacity are larger than the corresponding differences in maximum load (Camotim

and Roorda, 1985). Despite their potential significance, the effect of residual stresses on the plastic buckling of columns and plates will not be addressed in the current research.

Since the tangent-modulus buckling load P_t is the lowest load at which buckling is initiated, it is still regarded as the practical buckling load in design formulas for short columns (Gardner and Nethercot, 2005), which is over-conservative for stocky columns. Of course, with the recent developments in nonlinear analysis based on the finite element method, this method can be used for more realistic predictions of the elasto-plastic behaviour of structures, including the plastic buckling. However, this numerical method is still considered to be too involved for a direct application in the design and assessment practice, and it does not provide significant insight into the main factors influencing the nonlinear response. Analytical models, on the other hand, address these two issues, and it is within this context that a new analytical model for the plastic buckling of stocky column will be developed in Chapter 3.

2.3 Plastic Buckling of Plates

2.3.1 Background

The theory of plate stability was first established in 1891 by Bryan (1891), who applied the energy criterion of stability to deal with the problem of elastic plate buckling. Later on, Timoshenko (1910; 1936) developed the stability principles for plates under various support conditions in the elastic range, from which the equation of flexural equilibrium governing the buckling of a plate under planar loading may be written as:

$$\frac{\partial^2 M_x}{\partial x^2} + 2\frac{\partial^2 M_{xy}}{\partial x \partial y} + \frac{\partial^2 M_y}{\partial y^2} = h\left(\sigma_x \frac{\partial^2 w}{\partial x^2} + \sigma_y \frac{\partial^2 w}{\partial y^2} + 2\tau_{xy}\frac{\partial^2 w}{\partial x \partial y}\right) \tag{2.2}$$

where “h” is the thickness of the plate, w is the transverse deflection, σ_x, σ_y and τ_{xy} are the planar normal and shear stresses, and M_x, M_y and M_{xy} are resultant bending/twisting moments, respectively. The expression in (2.2) is the governing differential equation for the behaviour of thin plates and is based on Kirchhoff’s assumption that the normals to the middle surface of a plate remain straight and

normal to the deflected middle surface (Kirchhoff, 1850). According to Kirchhoff's theory, the constitutive matrix relating the moments to the curvatures is given as:

$$\{M\} = [D]\{\kappa\} \Leftrightarrow \begin{Bmatrix} M_x \\ M_y \\ M_{xy} \end{Bmatrix} = \frac{Eh^3}{12(1-\nu^2)} \begin{bmatrix} 1 & \nu & 0 \\ \nu & 1 & 0 \\ 0 & 0 & 1-\nu \end{bmatrix} \begin{Bmatrix} \frac{\partial^2 w}{\partial x^2} \\ \frac{\partial^2 w}{\partial y^2} \\ \frac{\partial^2 w}{\partial x \partial y} \end{Bmatrix} \tag{2.3}$$

As a result, the critical elastic buckling stress of a simply-supported plate subject to compression along its longer edge "a" can be obtained as:

$$\sigma_{cr} = \frac{k\pi^2 E}{12(1-\nu^2)} \left(\frac{h}{b}\right)^2 \tag{2.4}$$

where E denotes the material Young's modulus, ν is Poisson's ratio, k is the plate instability coefficient which depends on the boundary conditions, and "b" is the width of the plate.

The first attempts to extend the theory of elastic plate bucking to the plastic buckling of stocky plates were made by Bleich (1924). He considered the plate as anisotropic in the plastic range and substituted a variable modulus of elasticity in the formulation of elastic critical stress. It was acknowledged that above the proportional limit, the modulus of elasticity is no longer constant but rather dependent on the stress-strain curve of the material under consideration.

On the topic of inelastic buckling of plates, Shrivastava and Bleich (1976) state: "The state of stress in columns, even during buckling, is essentially one-dimensional, so that the material behaviour is sufficiently described by the compressive stress-strain diagram and no complex theory of plasticity for multi-axial states of stress is needed. However, when a plate buckles the additional stresses are necessarily not uniaxial, even if the basic load is uniaxial. Any analysis of buckling must therefore be based on a law describing the relation between multidimensional stresses and strains."

Following the Engesser-von Karman methods for the inelastic buckling of columns, and with reference to the buckling of stocky plates beyond the proportional limit, numerous attempts have been made to develop the fundamental equations of the inelastic buckling of plates, such as:

1. Generalisation of Engesser-von Karman theory for columns to the plastic buckling of plates (Bleich, 1924;Timoshenko and Gere, 1961) which is obtained by simply replacing Young's modulus by the tangent or reduced modulus in the formulas for the elastic buckling of plates. This generalisation seems rather arbitrary since those theories were proposed in the case of a narrow strip simply-supported at its loaded edges and free on the longitudinal edges. The strip will consequently exhibit buckling curvatures only in one direction, but a plate which is restrained on one or both unloaded edges will undergo curvature in both directions; therefore, there is an evident difference between column buckling and plate buckling, leading to inaccuracy in this type of approach.
2. Development of Deformation Theory of Plasticity (Bijlaard, 1941;Budiansky, 1959;El-Ghazaly and Sherbourne, 1986;Hencky, 1924;Hutchinson and Neale, 1980;Ilyushin, 1947;Stowell, 1948), which only considers the initial and final states of stress, that is the history of the loading process is not considered, and adopts a secant stiffness for buckling assessment. Therefore, Deformation Theory is only valid for or near a proportional loading path, assuming that the stress components at all points also vary proportionally. A further detailed review of Deformation Theory will be undertaken in Section 2.3.3.
3. Development of Flow Theory of Plasticity, also known as Incremental Theory (Handelman and Prager, 1948;Neale, 1975;Onat and Drucker, 1953;Pearson, 1950;Prandtl, 1925;Reuss, 1930) in which the total strain not only depends on the state of stress but also on the load path. Hence, this theory can also deal with problems in which the stresses develop non-proportionally. Despite of its complexity, this theory offers a more accurate representation of the nonlinear material response of metals than Deformation Theory, yet its application to plastic buckling of plates using bifurcation analysis leads to grossly unrealistic results. A further detailed review of Incremental Theory will be undertaken in Section 2.3.4.

4. Development of a semi-rational plastic buckling method based on the generalised differential equation for plate buckling (Timoshenko, 1936), first presented by Lundquist (1939) who derived the buckling equation $\sigma_{cr} = \eta \frac{k\pi^2 E}{12\left(1-\nu^2\right)}\left(\frac{h}{b}\right)^2$ by modifying the coefficients for the bending and the twisting terms, in which $\eta = \left(\tau + 3\sqrt{\tau}\right)/4$ with $\tau = E_t/E$. This concept was subsequently improved by Bleich (1952) and is now widely used due to its simplicity. Similarly, Gerard (1945) presented his well-known Secant-Modulus Method which assumes that the buckling stress beyond the proportional limit is implicitly dependent on the stress-strain relations. Both semi-rational approaches will be discussed in more detail in Section 2.3.5.

While the Incremental Theory of plasticity is widely accepted to be consistent with the actual material response, the critical buckling loads obtained from the Deformation Theory show better agreement with the experimental results (Tugcu, 1991), a confounding outcome referred to as the "Plate Plastic Buckling Paradox". As a result, extensive research, including analytical/numerical modelling and physical testing, has been carried out to improve the current theories for plastic buckling analysis of plates considering different boundary conditions and various loading situations. Notwithstanding, there is still no generally applicable simplified method for plastic buckling analysis of plates, and while attempts have been made for its resolution (Becque, 2010), the Plate Plastic Buckling Paradox remains unresolved. Accordingly, a major aim of this work is to resolve this paradox with the development of simplified analytical models for plastic buckling of plates based on sound principles of mechanics.

2.3.2 Basic Principles of Theory of Plasticity

According to the plasticity theory, the material exhibits in the inelastic range strains which are the sum of reversible elastic strains and irreversible plastic strains. A material is called perfectly-plastic or, alternatively, work-hardening if the effective stress needed to induce plastic deformation remains constant or increases, respectively. Most engineering materials such as mild steel, aluminium and stainless steel exhibit work-hardening behaviour. The classical theory of plasticity exclusively dealt with the perfectly-plastic behaviour (Hill, 1950); however, because of the

increasing use of high strength steel and aluminium the plasticity theory studied in this thesis is concerned with the generalised theory considering work-hardening materials. Prior to yielding, the material is assumed to be elastic, but as the stresses continue to increase beyond the initial yield surface, the material enters the work-hardening zone (loading region), where both elastic and plastic deformations are induced. Considering typical uniaxial stress-strain curves (Figure 2.5a-b), a suitable approximation is often adopted to model the behaviour of material in a simplified and idealised manner (Figure 2.5c-d), and these uniaxial curves can then be adopted as a basis for generalisation to biaxial and triaxial stress conditions.

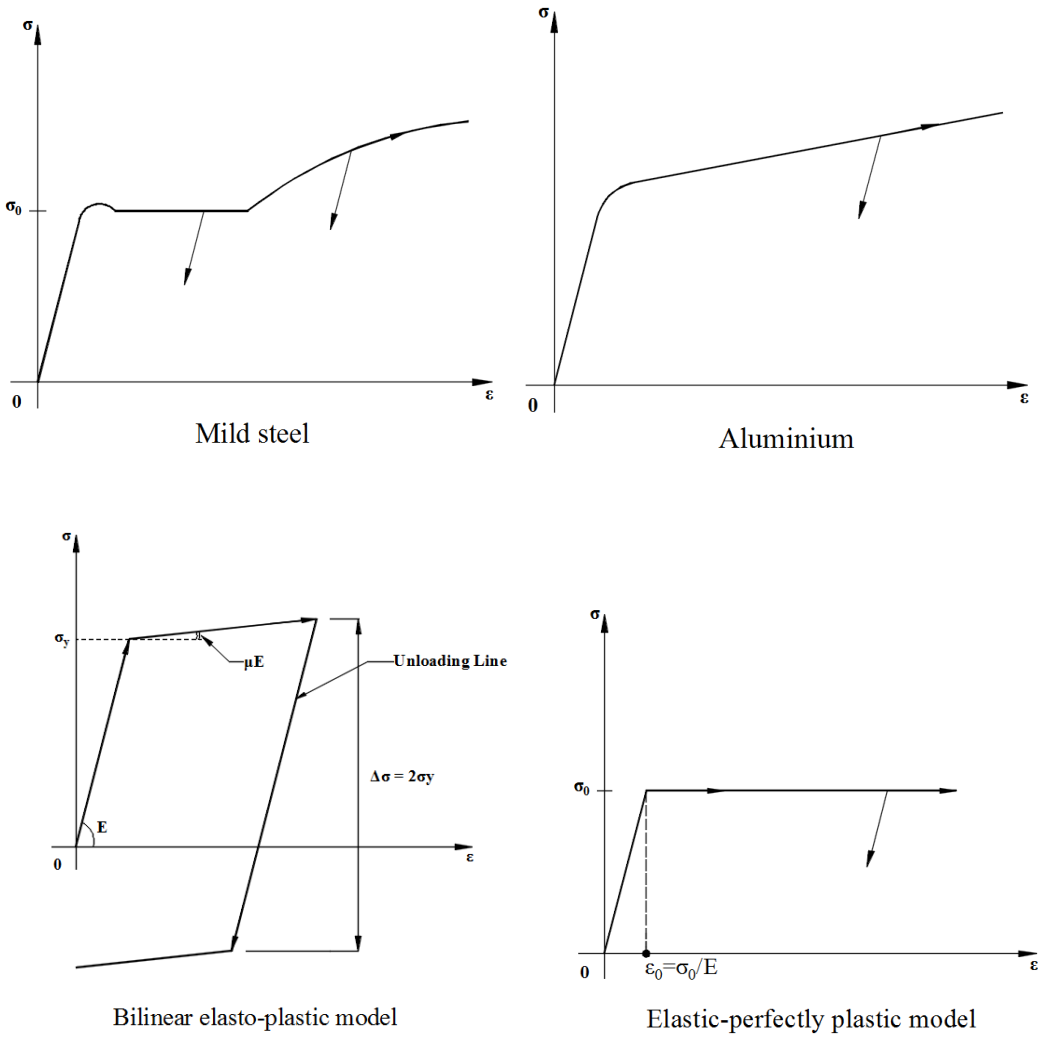

Figure 2.5. Stress-strain curves for mild steel, aluminium and idealised models

In generalising uniaxial plasticity theory to the biaxial and triaxial stress conditions, the concept of a "yield surface" is introduced in the stress space, as illustrated in Figure 2.6, which is defined by a relation of the form $f(\{\sigma\})=0$. Typically, a predictor stress state is obtained assuming elastic behaviour, which is accepted as the correct stress state if it lies within the yield surface. On the other hand, if $\{\sigma_e\}$ lies outside the yield surface, plastic deformations are introduced which correct the stress state back to the yield surface. Once on the yield surface, the material can experience elastic unloading or plastic loading, depending on whether the elastic predictor lies inside or outside the yield surface, respectively. Finally, with strain hardening, the yield surface can translate in accordance with the kinematic hardening theory (Prager, 1955, 1956), or it can expand in accordance with the isotropic hardening theory (Odqvist, 1933), where in both cases the change in the yield surface is related to the plastic strains.

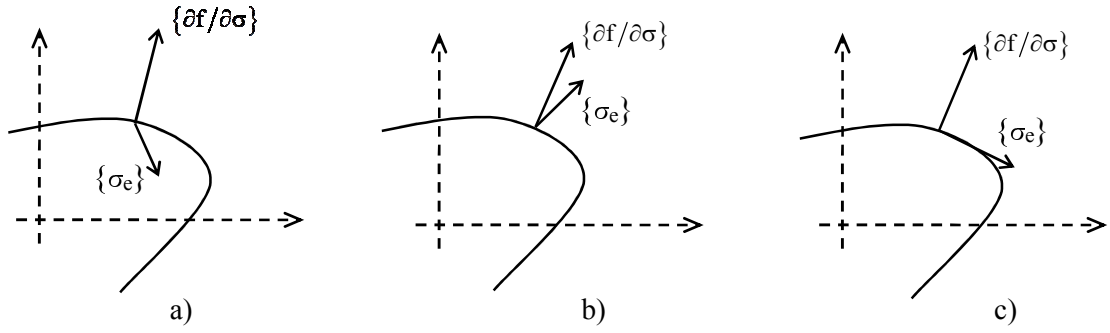

Figure 2.6. Elastic predictor stress rate with respect to yield surface: a) unloading, b) plastic loading and c) neutral loading

In applying plasticity theory to different materials, the main issues relate to the definition of the yield surface and its evolution with plastic deformations. For ductile materials such as mild steel, the onset of yielding does not depend on the volumetric part of the stress tensor (i.e. the mean stress), hence the yield surface can be formulated in terms of the von Mises yield criterion (von Mises, 1913), $f=J_2-c=0$, where J_2 is the second invariant of deviatoric stress $\left(J_2=\{s\}^T\{s\}\right)$, and c is a constant for non-hardening materials but varies with plastic strains in the case of an isotropic hardening (see Section 2.3.3 for more details). For a kinematic hardening, c is typically constant, but the deviatoric stress $\{s\}$ is evaluated with reference to a centre

of the yield surface that moves with the plastic deformation, though both isotropic and kinematic hardenings become similar for monotonic loading. Besides the definition of the yield surface and its evolution with strain hardening, a theory is required for relating the plastic strain components, where Deformation and Incremental Theories of plasticity are most common, as elaborated hereafter.

2.3.3 Deformation Theory of Plasticity

Roš and Eichinger (1932), Bijlaard (1941), Gerard (1945), Ilyushin (1947) and Stowell (1948) formulated rational theories for the stability of plates beyond the elastic limit which are based on the Deformation Theory of Plasticity. However, this theory (in its total form) was primarily formulated by Hencky (1924) to describe the constitutive relations for elastic-perfectly plastic materials and then by Nadai (1931) to illustrate the stress-strain relations for strain hardening material behaviour. Hencky suggested stress-strain relations in which the total strains are a function of only the total stresses without considering the effects of the stress history:

$$\left.\begin{aligned} \varepsilon_x &= \frac{1}{E_s}\left(\sigma_x - \nu\left(\sigma_y + \sigma_z\right)\right) \\ \varepsilon_y &= \frac{1}{E_s}\left(\sigma_y - \nu\left(\sigma_x + \sigma_z\right)\right) \\ \gamma_{xy} &= \frac{\tau_{xy}}{G_s} \end{aligned}\right\} \tag{2.5}$$

where E_s is the secant modulus which is the ratio of the effective stress to strain at any point on a stress-strain curve, ν is the Poisson's ratio, and $G_s = \frac{E_s}{2(1+\nu)}$ is the secant shear modulus.

Later on, the early total-strain theory was re-presented by the Russian researcher Ilyushin (1947) to consider the elasto-plastic stability of plates. Shortly afterwards, this theory was modified by Stowell (1948), who followed Shanley's proposition (1947) that elastic unloading does not occur during buckling and produced expressions for the plasticity factor η in $\sigma_{cr} = \eta \frac{k\pi^2 E}{12\left(1-\nu^2\right)}\left(\frac{h}{b}\right)^2$ relating to rectangular plates with different boundary conditions.

As previously mentioned, Deformation Theory is based on the total stress-strain relationship. In other words, the state of strain is uniquely determined by the state of stress as long as plastic strains continue to develop, which in turn can be expressed as $\{\varepsilon_p\} = \{\varepsilon\} - \{\varepsilon_e\} = f(\{\sigma\})$, f being only a function of the current stress, thus denoting the independency of the strain state from the load path. Clearly therefore, if Deformation Theory has a rational basis at all, it would be restricted to the material response under monotonic plastic loading.

According to Chen and Han (2007), J_2 Deformation Theory can be explained as follows. Under monotonic loading, it is assumed that:

1) the material is isotropic;

2) elastic strain is related to the stress through Hooke's law, while the plastic strain only consists of the deviatoric strain, with the volumetric plastic strain taken as zero;

3) the principal axes of strain and stress coincide; and

4) the ratio of the principal values of the plastic strains is identical to that of the deviatoric stresses, e.g. $\left(\frac{\varepsilon_1^p}{\varepsilon_2^p}\right) = \left(\frac{s_1}{s_2}\right)$.

From assumptions 3 and 4, the plastic strains can be related to the deviatoric stresses by $\{\varepsilon_p\} = \varphi\{s\}$ in which φ is a scalar function related to the material property (i.e. hardening function c in the yield rule) so that $\varphi = \varphi(J_2)$. In order to find the function φ, stress and strain intensities (also called effective stress and strain) are introduced as $\sigma_e = \sqrt{3J_2} = \sqrt{\frac{3}{2}\{s\}^T\{s\}}$ and $\varepsilon_{ep} = \sqrt{\frac{2}{3}\{\varepsilon_p\}^T\{\varepsilon_p\}}$.

In the case of a uniaxial compression ($\sigma_2=\sigma_3=0$, stresses in the y and z direction, respectively), the effective stress becomes $\sigma_e = \sigma_1$. Similarly, as a result of the plastic incompressibility condition $\varepsilon_2^p = \varepsilon_3^p = -0.5\varepsilon_1^p$, the effective strain reduces to

$\varepsilon_{ep} = \varepsilon_1^p$. Using the definitions of the effective stress and strain, the scalar φ can therefore be obtained from the uniaxial stress-strain relationship as $\varphi = \frac{3}{2}\frac{\varepsilon_{ep}}{\sigma_e} = \frac{3}{2}\left(\frac{1}{E_s} - \frac{1}{E}\right)$, where E_s is the secant stiffness at the effective uniaxial stress σ_e (Figure 2.7).

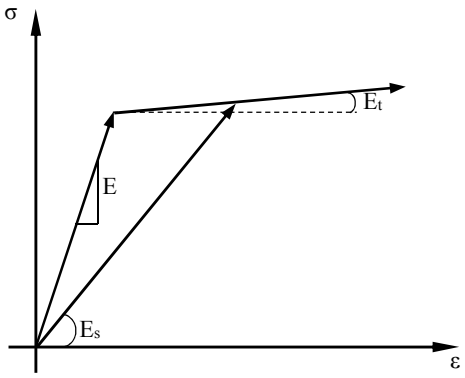

Figure 2.7 Stress-strain curve showing various moduli

In applying Deformation Theory to the plastic buckling of a plate subject to compressive stresses σ_x=-σ_1 and σ_y=-σ_2, the governing tangent modulus matrix $[E_t]$ can be derived from (2.5), allowing for the variation of E_s and G_s on the equivalent stress σ_e (Shrivastava, 1979;Durban and Zuckerman, 1999;Chakrabarty, 2000):

$$\left.\begin{aligned} \{d\sigma\} &= [E_t]\{d\varepsilon\} \\ d\sigma_x &= E(\alpha d\varepsilon_x + \beta d\varepsilon_y) \\ d\sigma_y &= E(\beta d\varepsilon_y + \gamma d\varepsilon_y) \\ d\tau_{xy} &= \frac{E}{2\nu + 3\frac{E}{E_s} - 1} d\gamma_{xy} \end{aligned}\right\} \qquad (2.6)$$

in which:

$$\left.\begin{aligned}
\alpha &= \frac{1}{\rho}\left(4-3\left(1-\frac{E_t}{E_s}\right)\frac{\sigma_1^2}{\sigma_e^2}\right)\\
\beta &= \frac{1}{\rho}\left(2-2(1-2\nu)\frac{E_t}{E}-3\left(1-\frac{E_t}{E_s}\right)\frac{\sigma_1\sigma_2}{\sigma_e^2}\right)\\
\gamma &= \frac{1}{\rho}\left(4-3\left(1-\frac{E_t}{E_s}\right)\frac{\sigma_2^2}{\sigma_e^2}\right)\\
\rho &= 3\frac{E}{E_s}+(1-2\nu)\left[2-(1-2\nu)\frac{E_t}{E}-3\left(1-\frac{E_t}{E_s}\right)\frac{\sigma_1\sigma_2}{\sigma_e^2}\right]
\end{aligned}\right\} \qquad (2.7)$$

where $E_s = \sigma_e/\varepsilon_{ep}$ (the secant modulus) and $E_t = d\sigma_e/d\varepsilon_p$ (the tangent modulus) are obtained from the material stress-strain curve.

With the availability of a tangent modulus matrix, Deformation Theory can be applied with the governing differential equation given by (2.2), but with the elastic constitutive matrix $12/h^3[D]$ replaced with $[E_t]$. Similar to the concept of the equivalent tangent-modulus in columns, it is assumed that all fibres are subject to plastic loading, hence no elastic unloading is considered upon buckling. Therefore, the above equations are potentially applicable only if $dJ_2>0$, but even in this case, the assumption that stress components increase in a constant ratio to each other is not realistic under buckling conditions. This is particularly true considering the different variation of stresses at the extreme fibres of the plate compared to the mid-plane stresses, where the difference becomes greater with increasing buckling deformations.

On the other hand, El-Ghazaly and Sherbourne (1986) employed Deformation Theory for the elasto-plastic buckling analysis of plates under non-proportional planar loading and non-proportional stresses. They utilised the modified Newton-Raphson technique and the initial stress method within a finite element formulation for the numerical solution of this nonlinear problem. It was shown that Deformation Theory in its incremental form can be applied in situations involving loading and reloading except for the case of elastic unloading which may occur in plasticity even under increasing load conditions. However, El-Ghazaly and Sherbourne believed that unloading only occurs when considerable plastic flow has taken place, and in plates under compression buckling occurs long before this late stage of plastic deformation.

Therefore, the authors recommended the application of Deformation Theory to analyse the inelastic buckling in the early and moderate stages of plastic deformation. Nevertheless, it is unclear why Deformation Theory should be employed in an incremental form for this type of problem in preference to Incremental Theory, given the inherent approximation arising from its assumption that stresses vary proportionally throughout the loading history.

2.3.4 Incremental Theory of Plasticity

The Incremental Theory of plasticity is widely regarded as the true plasticity theory (Prandtl, 1925;Reuss, 1930;Handelman and Prager, 1948;Pearson, 1950;Chakrabarty, 2000), where the increments of strain are related to the increments of stress. According to Jirasek and Bazant (2001), Incremental Theory is described as follows:

- the elastic limit of the material is defined by an initial yield surface, with the loading surface being expressed as a function of the current state of stress or strain and other parameters such as the plastic strain $\{\varepsilon_p\}$ and the hardening parameter K which defines the size of the yield surface $f(\{\sigma\},\{\varepsilon\},K)=0$.

Isotropic hardening (Odqvist, 1933) is denoted by $f(\{\sigma\})=\sigma_Y$ in which σ_Y is the size of the yield surface in Figure 2.8 and is a function of either one of the two quantities used to measure the degree of work-hardening:

- Plastic work per unit volume: $W^p = \int \{\sigma\}\{d\varepsilon\}$
- Equivalent plastic-strain increment: $d\varepsilon_{ep} = \sqrt{\frac{2}{3}\{d\varepsilon_p\}^T\{d\varepsilon_p\}}$

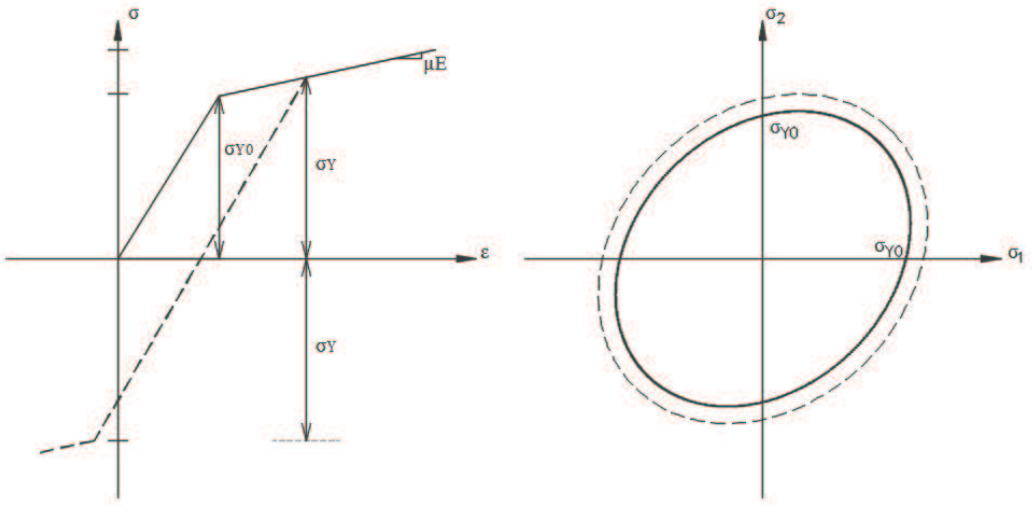

a. b.

Figure 2.8. Isotropic hardening: a) uniaxial stress-strain diagram, b) evolution of yield surface in biaxial stress plane

This type of hardening model is simple to use but it mainly applies to monotonic plastic loading. In other words, since the loading surface expands isotropically, the Bauschinger effect (Bauschinger, 1881) which represents induced directional anisotropy by plastic deformation could not be modelled. Therefore, the isotropic hardening rule does not lead to realistic results, for example, under cyclic loading.

On the other hand, the kinematic hardening rule assumes that the yield surface translates in the stress space, which also accounts for the Bauschinger effect as illustrated in Figure 2.8. The initial yield surface is expressed as $f\left(\{\sigma\}\right)=0$, while the equation of the subsequent loading surface has the form $f\left(\{\sigma\}-\{\alpha\}\right)=0$ in which $\{\alpha\}$ represents the total translation of the centre of the initial yield surface. In order to determine $\{\alpha\}$, Prager's (1955, 1956) hardening rule with $\{d\alpha\}=c\{d\varepsilon\}$ or Ziegler's (1959) hardening rule with $\{d\alpha\}=d\mu\left(\{\sigma\}-\{\alpha\}\right)$ are typically employed.

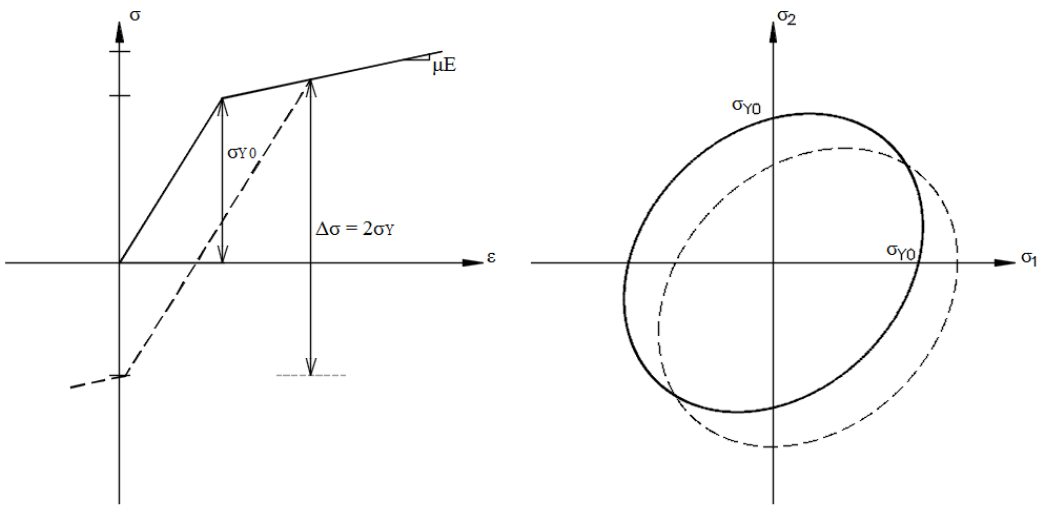

a. b.

Figure 2.9 Kinematic hardening a) uniaxial stress-strain diagram, b) evolution of yield surface in biaxial stress plane

More general hardening rules may combine isotropic and kinematic hardening, though in the present work isotropic hardening is considered for its simplicity and the fact that plastic buckling of plates involves mainly monotonic plastic loading without cyclic plasticity.

While in the Deformation Theory the total plastic strains are assumed to be proportional to the deviatoric stresses, a *flow rule* is utilised with Incremental Theory to define the incremental plastic strains. For metals, the "associated flow rule" is typically employed, where the incremental plastic strains are assumed to be normal to the yield surface at the current stress state, as defined by:

$$\{d\varepsilon_p\} = d\lambda \left\{\frac{\partial f}{\partial \sigma}\right\} \tag{2.8}$$

where $d\lambda$ is a positive scalar increment. A general constitutive equation for an elasto-plastic material which also exhibits strain hardening can be expressed as $\{d\sigma\} = [E_t]\{d\varepsilon\}$, where $[E_t]$ represents the tangent modulus matrix which depends on the load history of the material and the current state of the stress, and $\{d\varepsilon\}$ is the total

strain increment which consists of an elastic component $\{d\varepsilon_e\} = [E]^{-1}\{d\sigma\}$ and a plastic component $\{d\varepsilon_p\} = d\lambda\left\{\frac{\partial f}{\partial \sigma}\right\}$. Rewriting the elastic component of the strain increment in terms of total and plastic strain increments $\{d\varepsilon_e\} = \{d\varepsilon\} - \{d\varepsilon_p\}$, an expression for the total stress increment can be obtained $\{d\sigma\} = [E]\left(\{d\varepsilon\} - d\lambda\left\{\frac{\partial f}{\partial \sigma}\right\}\right)$. By calculating the value of dλ using the consistency condition df=0, since the stress state remains on the yield surface during plastic flow, the tangent modulus matrix can be fully determined.

A special case of the associated flow rule is the Prandtl-Reuss equation for J_2-plasticity (Prandtl, 1925;Reuss, 1930), where the increment of plastic strain vector is directed along the deviatoric stress vector. Therefore, the incremental constitutive relations based on the Prandtl-Reuss flow rule develop into (Chakrabarty, 2000;Handelman and Prager, 1948;Shrivastava and Bleich, 1976;Wang *et al.*, 2001):

$$\left.\begin{aligned} &\{d\sigma\} = [E_t]\{d\varepsilon\} \\ &d\sigma_x = E(\alpha d\varepsilon_x + \beta d\varepsilon_y) \\ &d\sigma_y = E(\beta d\varepsilon_y + \gamma d\varepsilon_y) \\ &d\tau_{xy} = G d\gamma_{xy} \end{aligned}\right\} \tag{2.9}$$

where:

$$\left.\begin{aligned} &\alpha = \frac{1}{\rho}\left(4 - 3\left(1 - \frac{E_t}{E}\right)\frac{\sigma_1^2}{\sigma_e^2}\right) \\ &\beta = \frac{1}{\rho}\left(2 - 2(1-2\nu)\frac{E_t}{E} - 3\left(1 - \frac{E_t}{E}\right)\frac{\sigma_1\sigma_2}{\sigma_e^2}\right) \\ &\gamma = \frac{1}{\rho}\left(4 - 3\left(1 - \frac{E_t}{E}\right)\frac{\sigma_2^2}{\sigma_e^2}\right) \\ &\rho = (5 - 4\nu) + (1-2\nu)^2\frac{E_t}{E} - 3(1-2\nu)\left(1 - \frac{E_t}{E}\right)\frac{\sigma_1\sigma_2}{\sigma_e^2} \\ &G = \frac{E}{2(1+\nu)} \end{aligned}\right\} \tag{2.10}$$

It is worth mentioning that (2.6) and (2.7) become identical to (2.9) and (2.10) if E_s is replaced by E. It is noted that the tangent shear modulus $G_t = d\tau_{xy} / d\gamma_{xy}$ resulting from the Incremental Theory is the elastic shear modulus $G = E/(2+2\nu)$, whereas a reduced shear modulus $G_t = E \Big/ \left(2\nu + 3\frac{E}{E_s} - 1 \right)$ is obtained in the Deformation Theory. This along with other differences in the tangent modulus matrix has significant influence on the plastic buckling predictions using the two theories, as elaborated in Section 2.3.6.

2.3.5 Bleich's Original Plate Buckling Theory

In the previous sections, alternative tangent modulus matrices governing the plastic material response, in accordance with the Deformation Theory and the Incremental Theory, were presented. Beside the questionable validity of using such a tangent modulus matrix for the out-of-plane flexural response, when it is derived on the basis of uniform planar stresses, its application in bifurcation analysis using the differential equation (2.2) is rather complicated. In this regard, Bleich (1952) argued that the expressions for the critical buckling stress of plates using the Deformation Theory as presented by Ilyushin and Stowell (see Section 2.3.3) are extremely involved as they contain both tangent modulus E_t and secant modulus E_s. As a simpler alternative, he presented a semi-rational equation which is associated with a more straightforward solution.

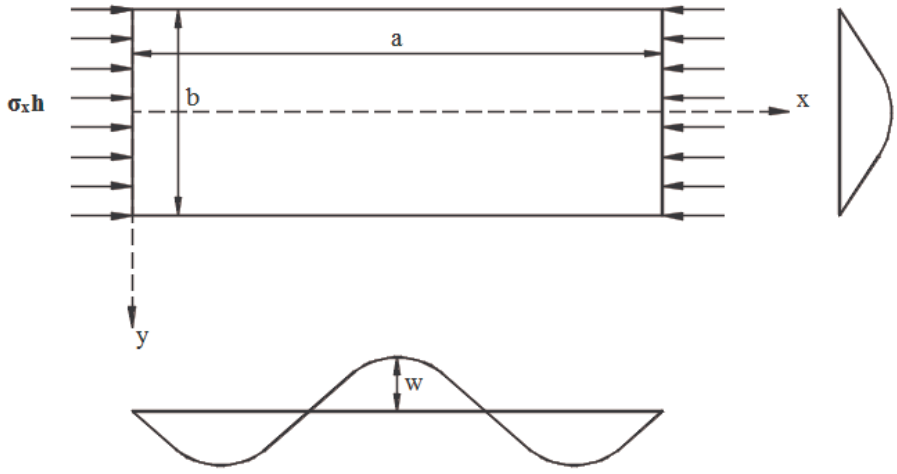

Figure 2.10 A flat simply-supported plate under a uniaxial loading (Bleich, 1952)

To illustrate Bleich's method, consider a flat rectangular plate of thickness "h" that is loaded on the two edges of length "b" perpendicular to the x-axis, as illustrated in Figure 2.10. The plate is simply-supported along its four edges for which the typical longitudinal and transverse deflections of the plate are depicted in Figure 2.10.

In the fundamental differential equation for the deflection w of a thin flat plate under the action of edge forces along its mid-plane (2.2), Bleich suggested that when σ_x exceeds the proportional limit, the tangent modulus E_t can be effective in the x-direction (loading direction) while the elastic Young's modulus E remains the same in the y-direction as there is no loading in that direction. Thus, the plate behaviour is assumed to be anisotropic after yielding has occurred. Therefore, the first term in the differential equation $\partial^2 M_x / \partial x^2$ which corresponds to bending of the plate strips along the loading direction ($\sigma_x \neq 0$), must be multiplied with $\tau = E_t / E$ when σ_{cr} exceeds the proportional limit. Similarly, the third term in that equation $\partial^2 M_y / \partial y^2$ will remain unchanged as there is no external loading in the y-direction ($\sigma_y = 0$) and the plate strips in the y-direction will not be subject to the planar stress. Finally, the middle term $\partial^2 M_{xy} / \partial x \partial y$ is associated with the distortion of plate due to the twisting moments and is therefore affected by the elasto-plastic characteristics associated with the planar shear deformation. Therefore, Bleich introduced a coefficient with a value between 1 and τ. Bleich (1952) stated that "We select somewhat arbitrarily the value $\sqrt{\tau}$ for the coefficient of the second term". He also adds that this plate theory must be regarded as a semi-rational theory, since the values of the critical buckling stress obtained from this theory can only be justified by comparison with the results from the experiments. As a result, the lowest buckling stress of an elasto-plastic plate can be found as:

$$\sigma_{cr} = \frac{k\sqrt{\tau}\pi^2 E}{12(1-\nu^2)}\left(\frac{h}{b}\right)^2 \tag{2.11}$$

According to Bleich's formula (2.11), the plastic buckling stress can be obtained by multiplying the elastic buckling stress by a so called "plasticity reduction factor" $\eta = \sqrt{E_t / E} = \sqrt{\tau}$. Although Bleich's theory yields predictions for the plastic buckling

stress of simply-supported plates which are in satisfactory agreement with the outcomes of the experiments, it cannot be considered as a correct theory of plastic buckling, mainly because his theory is not based on sound principles of mechanics of materials.

Similar to Bleich's approach, Gerard (1945) proposed a method using the secant modulus $E_s = \sigma/\varepsilon$ in the plate buckling equation (2.4) to predict the critical buckling stress of a simply-supported plate with one longitudinal unloaded edge free in the plastic range. This method is also not based on principles of mechanics of materials, and as such it suffers from similar shortcomings to Bleich's method.

2.3.6 Plate Plastic Buckling Paradox

As previously mentioned, a theory of plastic flow was initiated by Handelman and Prager (1948) which has since been accepted as the modern and valid theory of material plasticity. However, when used in the bifurcation analysis for the assessment of plastic buckling of plates, this theory has been shown to yield plate buckling predictions which are considerably greater than the test results (Pride and Heimerl, 1949), while the less acceptable Deformation Theory gave buckling loads in good agreement with the experimental results. This confounding outcome has since been referred to as the "Plate Plastic Buckling Paradox". In the last few decades, research efforts have been dedicated to resolve this paradox, as summarised hereafter.

Pearson (1950) improved the Incremental Theory by employing Shanley's concept of continuous loading (i.e. elastic unloading does not occur during buckling), but this did not significantly lower the predictions. A few years later, Onat and Drucker (1953) investigated the inelastic local plate buckling of cruciform columns and showed that if small initial imperfections are taken into account, the maximum supported load would reduce using the Incremental Theory to the prediction of the Deformation Theory. A few years later, Haaijer (1957) and Haaijer and Thurlimann (1958) studied inelastic buckling of plates in the strain hardening range using a reduced value for the shear modulus G_t. They used experimental results to determine the value of the tangent shear modulus and discovered an unusual reduction of G_t to 0.2G caused by the initial imperfections when using the Flow Theory. Later on,

Sewell (1964) investigated the sensitivity of the buckling loads to the variation of the direction of the normal to the yield surface and obtained somewhat lower predictions. Hutchinson and Budiansky (1974) confirmed the imperfection sensitivity of the buckling stress in plastic region investigated by Onat and Drucker. Neale (1975), Needleman and Tvergaard (1976) and Harding *et al.* (1977) examined the effect of initial geometric imperfections on the maximum supported load using J_2 Flow Theory and verified the imperfection sensitivity of its plastic buckling prediction. Up to now, imperfection sensitivity is a widely accepted explanation to the Plate Plastic Buckling Paradox; however, the way in which imperfections are effectively leading to a reduction in the effective tangent modulus matrix is yet to be resolved, especially in relation to the application in the analytical models.

Dawe and Grondin (1985) verified Haaijer and Thurlimann's work (1958), relating to the reduction of the tangent shear modulus in the plastic range, by conducting careful tests on the web and flange plate to investigate their inelastic buckling and came to a conclusion that the shear modulus reduces once the stress in the material exceeds its proportional limit. Gjelsvik and Lin (1987) studied the effect of friction acting on the loaded edges during tests and concluded that the stresses due to friction at the supports can effectively reduce the buckling stresses predicted by Flow Theory. However, it was argued that the amount of friction required for such a reduction is less than normally expected at the loaded edges of a real test (Tugcu, 1991). Shortly afterwards, Tuğcu (1991) showed that the presence of axial stresses in the load-free principal direction (i.e. biaxial loading) and in-plane shear stresses, caused by the testing procedure, can significantly reduce the values of buckling stresses predicted by Flow Theory.

Some researchers investigated the elasto-plastic buckling capacity of plates considering both plasticity theories; for instance, Shrivastava and Bleich (1979) considered the effects of the transverse shear on the inelastic buckling of plates and demonstrated that for the buckling of a plate supported on three sides, the correction due to the shear effects is generally larger for J_2 Incremental Theory than that for the Deformation Theory. Durban and Zuckerman (1999) performed a detailed parametric study on the elasto-plastic buckling of rectangular plates under uniform compression

combined with uniform tension (or compression) and again observed remarkable discrepancy between these two theories.

As can be noted from literature, most of the research carried out on resolving the Plate Plastic Buckling Paradox has been on modifying the shear modulus in the plastic range. Recently, a modification to J_2 Flow Theory has been proposed by Becque (2010), where he claimed that his method overcomes the "Plate Plastic Buckling Paradox" by determining the shear stiffness from second-order considerations, and he sought to verify his theory by collecting experimental data from the literature in a more recent article (Becque *et al.*, 2011). In his work, Becque investigated the local buckling of a flat plate without any initial imperfections and under a uniform axial loading, where a flow rule based on Hill's anisotropic yield criterion is employed. Chapter 5 discusses Becque's approach in more detail, and establishes more generally that a reduced shear modulus in the plastic range cannot on its own account for the overestimation of the plastic plate buckling resistance using Incremental Theory.

It is noticeable that despite the continuous efforts and remarkable developments in this field, the plastic buckling of plates continues to remain a paradox. However, it will be shown in this thesis that the "Plate Plastic Buckling Paradox" is resolved in the analytical models if the correct Incremental Theory of plasticity is applied with the consideration of the initial imperfections and the interaction between planar and flexural actions, leading to a considerably reduced effective tangent modulus compared to the conventional Incremental Theory. In Chapters 5 and 6, this argument will be substantiated through the verification of the results predicted by the Incremental Theory using a sophisticated nonlinear structural analysis programme ADAPTIC (Izzuddin, 1991).

2.4 Simplified Modelling and Design Codes

Most of structures such as ships, aircrafts and offshore platforms make extensive use of stiffened or unstiffened plates in their construction. These plated elements often experience significant planar compressive loading, and hence the ultimate strength of such plates is of a primary concern in their design. It is a well-known fact that a great amount of work has been devoted by researchers to the subject of collapse of

structures caused by either material yielding or structural instability (i.e. buckling) or a combination of both (i.e. inelastic buckling). The first type of failure is governed by the material yield strength whereas failures caused by structural instability depend on geometric nonlinearity.

For buckling analysis of complex structures, the nonlinear finite element (FE) analysis method is typically used with incremental loading to estimate the maximum resistance, accounting for both the geometric and material nonlinearity. Although the FE method offers the most sophisticated tool for the stability analysis of any type of structure, it can be computationally demanding, which renders its application in design and assessment practice prohibitively. Moreover, as a sophisticated numerical modelling tool, the FE method does not offer the required level of insight to resolve conceptual issues. This is evidenced by the fact that whilst the Plate Plastic Buckling Paradox has been attributed to the need for inclusion of imperfections in the Incremental Theory, the mechanism by which imperfections influence the effective tangent modulus of the Incremental Theory remains unclear. In this respect, simplified analytical modelling can play a dual role; firstly, these methods are more suited for practical applications, and secondly they furnish an enhanced understanding and appreciation of the main parameters influencing the nonlinear structural response (Izzuddin, 2008) .

From a design perspective, the prediction of the lowest load at which a structure becomes unstable is of particular interest, such load being dependent on the geometry and size of the structure, especially slenderness. Based on the latter, the structure may buckle elastically or collapse in the inelastic region beyond the yield point. For this reason, several attempts (Bleich, 1952;Gerard, 1945;Stowell, 1948) were made to formulate simplified models and methods for inelastic buckling analysis of structural elements such as columns, beams and plates. A brief review of some of the existing simplified methods proposed for buckling analysis of plates is provided hereafter.

Findings of most interest for practical purposes in this area are usually tabulated as values of the plasticity reduction factor η by which the elastic critical stress must be multiplied to give the critical stress in the inelastic range. As mentioned earlier, the

concept of effective modulus (ηE) for plates above the proportional limit was first put forward by Lundquist (1939) and then by Bleich (1952) who derived the buckling equation $\sigma_{cr} = \eta \frac{k\pi^2 E}{12\left(1-\nu^2\right)}\left(\frac{h}{b}\right)^2$ by modifying the coefficients for the bending and the twisting terms in the fundamental differential equation. However, after the introduction of Deformation Theory and Incremental Theory, this concept was much improved (Stowell, 1948). It must be emphasised that this concept is based on two major assumptions: "If the plate is uniformly loaded before buckling so that all material points are initially at the same stress state in the plastic range and if, in addition, buckling and increase in load are assumed to progress simultaneously, then the plate may be expected to remain in the purely plastic state in the early stages of buckling (Stowell, 1948)". Stowell's plate-buckling formulas are still being used for design purposes, for instance in design codes such as Eurocode 9 (Faella *et al.*, 2000). However, the values of η are limited to special cases of plates such as long flat rectangular plates simply-supported along two shorter/loaded edges while the two other sides can have any other boundary conditions.

As discussed in Section 2.3.5, Bleich's original theory in 1952 for calculating the plastic buckling stress of rectangular plates loaded longitudinally by compressive forces was developed mainly because Ilyushin-Stowell's Deformation Theory was extremely involved for the derivation of the design rules. His theory is still used for practical purposes, for instance in Eurocode 3 (Trahair *et al.*, 2008) where it is incorporated to obtain the buckling strength of stocky plates for which the calculated elastic buckling stress exceeds the yield stress. Yet, Bleich's theory can only be applied to plates subject to uniaxial loading.

Furthermore, Gerard (1945) proposed an analytical model in which the Young's modulus of elasticity is substituted in the elastic plate buckling equation by the secant modulus to predict the critical stress above the proportional limit, leading to $\sigma_{cr} = \frac{k\pi^2 E_s}{12\left(1-\nu^2\right)}\left(\frac{h}{b}\right)^2$. While this model was substantiated by means of tests performed on Z and channel sections, it suffers from previously noted shortcomings as a semi-rational model which cannot be applied reliably and more generally.

2.5 Summary and Conclusions

Because of the highly nonlinear nature of plastic buckling, including both geometric and material nonlinearity, models based on the FE method offer the most accurate predictions of plastic buckling resistance, accounting also for the presence of the initial imperfections. Despite this advantage, FE analysis is still considered to be overly demanding for the practical application, and it does not necessarily facilitate the resolution of the conceptual issues, such as the Plate Plastic Buckling Paradox. On the other hand, simplified analytical methods have the potential to yield considerable benefits in practice, including ease of use and reasonable estimates of the buckling load, and importantly to provide a better understanding of the main parameters influencing the plastic buckling response of structures based on cause and effect.

This chapter gives an overview of the current plastic buckling analysis methods of columns and plates. It was found that although significant research has already been carried out on the topic of plastic buckling analysis of such structures, effective simplified models founded on sound principles of structural mechanics remain largely absent. For this reason, the main focus of this research is to develop simplified buckling analysis methods and models for columns and plates taking account of both material and geometric nonlinearities. The main difficulty of the above objective is the fact that the material stiffness matrix for structures with material nonlinearity is not uniquely defined in the plastic range; that is the material stiffness for loading situation is different from that for unloading state (Izzuddin, 2007c). Therefore, it is necessary to define an appropriate tangent stiffness matrix founded on sound constitutive relations, taking into account the incremental nature of the buckling response. The literature review in this chapter has revealed that despite its complexity, Incremental Theory is widely regarded as the true plasticity theory, and should therefore be considered in the plastic buckling analysis. However, challenges must be addressed before Incremental Theory yields a realistic assessment of plastic buckling in plates, and hence achieve a final resolution of the Plate Plastic Buckling Paradox.

CHAPTER 3

An Analytical Model for Plastic Buckling of Columns

3.1 Introduction

While Euler's formula (Euler, 1744) provides very good predictions of the buckling strength of slender columns under a compressive axial force, there is still no single formula or a well-established analytical method to predict the buckling behaviour of stocky columns for which the axial buckling load exceeds the yield (i.e. squash) load. As previously reviewed in Chapter 2, it has been established that Engesser's tangent-modulus load $P_t = \pi^2 E_t I / L^2$ underestimates the maximum column buckling resistance. On the other hand, von Karman's reduced-modulus load $P_R = \pi^2 E_R I / L^2$, which assumes a constant axial force during buckling and accounts for strain reversal on the convex side of the buckled column, overestimates the column buckling resistance. It is worth noting that von Karman's reduced modulus is larger than Engesser's tangent modulus but smaller than the elastic modulus, hence $E_t < E_R < E$. Treating the reduced modulus load as the critical buckling load for elasto-plastic columns was questioned by Shanley who proved with his theory that the origin of the Column Paradox lies in the incorrect assumptions involved in the reduced-modulus theory (Shanley, 1946). Shanley also noted that since buckling starts at Engesser's load, the tangent-modulus equation should be used as a basis for determining the inelastic buckling strength of columns (Shanley, 1947). Hutchinson (1974) presented an asymptotic method for plastic buckling analysis of columns based on a simple Shanley column (i.e. simplified two-flange column as previously described in Chapter 2), which allows for the elastic unloading that initiates at the bifurcation point for a perfect column. His method, however, only gives accurate predictions of the maximum load when the latter is very close to Engesser's tangent-modulus load, since an approximate estimate of the maximum buckling load is found by truncating the series given in (2.1). In addition, his solutions become very complicated when the effect of initial imperfections is taken into account. In fact, Hutchinson (1974) admits that his method is not accurate over the full range of potential interest.

The main objective of this chapter is to illustrate the mechanics of the elasto-plastic buckling response of relatively stocky columns, where not only Euler's elastic buckling but also von Karman's reduced-modulus load is greater than the yield load, and where the maximum buckling capacity is significantly larger than Engesser's initial buckling load. For such columns, it can be easily shown that Engesser's tangent-modulus load is also greater than the yield load when the elasto-plastic stress-strain relationship is smooth, such as that of a Ramberg-Osgood model (1943), or it may take the yield load as a lower bound with a piecewise stress-strain relationship, such as the bilinear model generally adopted in the present work.

To this end, a simplified analytical model is proposed for plastic buckling of pin-ended stocky columns which not only offers more practical application than nonlinear finite element analysis, but also sheds significant light on the nature of the plastic buckling of columns. Supporting Shanley's theory, it will be shown in the first part of this chapter that under a monotonically increasing axial load, a stocky column starts to buckle at the Engesser load but remains stable as the load continues to increase. This increase is accounted for by the elastic unloading across the cross-section depth which spreads from the middle of the column towards its ends. In turn, this enables the column resistance to approach von Karman's reduced-modulus load, though this limit is not reached in reality, largely due to tensile yielding at the outer fibres of the convex side. The proposed analytical model considers the initiation of buckling in both perfect and imperfect stocky columns, commencing with elastic unloading over inner parts of the column accompanied by further plastification over the remaining parts, and limited by the onset of tensile yielding on the convex side.

The analytical model is initially applied to very stocky columns in which Engesser's load is significantly greater than the yield load, where both perfect and imperfect columns are considered. The applicability of the model to columns of intermediate stockiness is then demonstrated for perfect columns in which Engesser's load reduces to the yield load due to the slope discontinuity in the adopted bilinear stress-strain relationship, though as previously noted, von Karman's reduced modulus load is still greater that the yield load. It should be noted that there is a third category of stocky columns with relatively low stockiness for which both Engesser's and von Karman's loads are smaller than yield load. These columns typically reach their maximum buckling resistance at the yield load, and therefore they would not exhibit

any enhanced post-buckling response. For this reason, this type of column is excluded from the present scope.

The proposed model is distinguished by its adherence to the three fundamental principles of mechanics, namely compatibility, equilibrium and the constitutive law, which necessarily feature in the main threads of this chapter. Besides the possibility of practical application, the proposed model sheds light on the "Column Paradox", which is clearly disentangled with the correct application of the principles of nonlinear structural mechanics.

In this thesis, the following assumptions and considerations are made:

1. An idealised bilinear stress-strain curve with kinematic hardening is used.
2. A pin-ended column of a rectangular cross-section is considered.
3. The planar buckling response of the column is considered.
4. Prior to yielding the material is linear elastic.
5. The buckled mode shape of the column has a sinusoidal configuration.
6. Up to the point of strain reversal, the strain variation with applied loading over the whole column is monotonic.
7. According to Euler-Bernoulli hypothesis, plane sections remain plane and normal to the neutral axis.

The proposed analytical models have been implemented using Maple (Maplesoft), a mathematical computation engine with an intuitive user interface, and are applied to the plastic buckling problem considered in this thesis.

3.2 Perfect Stocky Columns

Most engineering materials such as mild steel, aluminium and stainless steel exhibit material plasticity at relatively high stress levels and subsequent work-hardening behaviour. Prior to yielding the material is assumed to be linear elastic, but beyond this range both elastic and irrecoverable plastic strains are induced (Figure 3.1a-b).

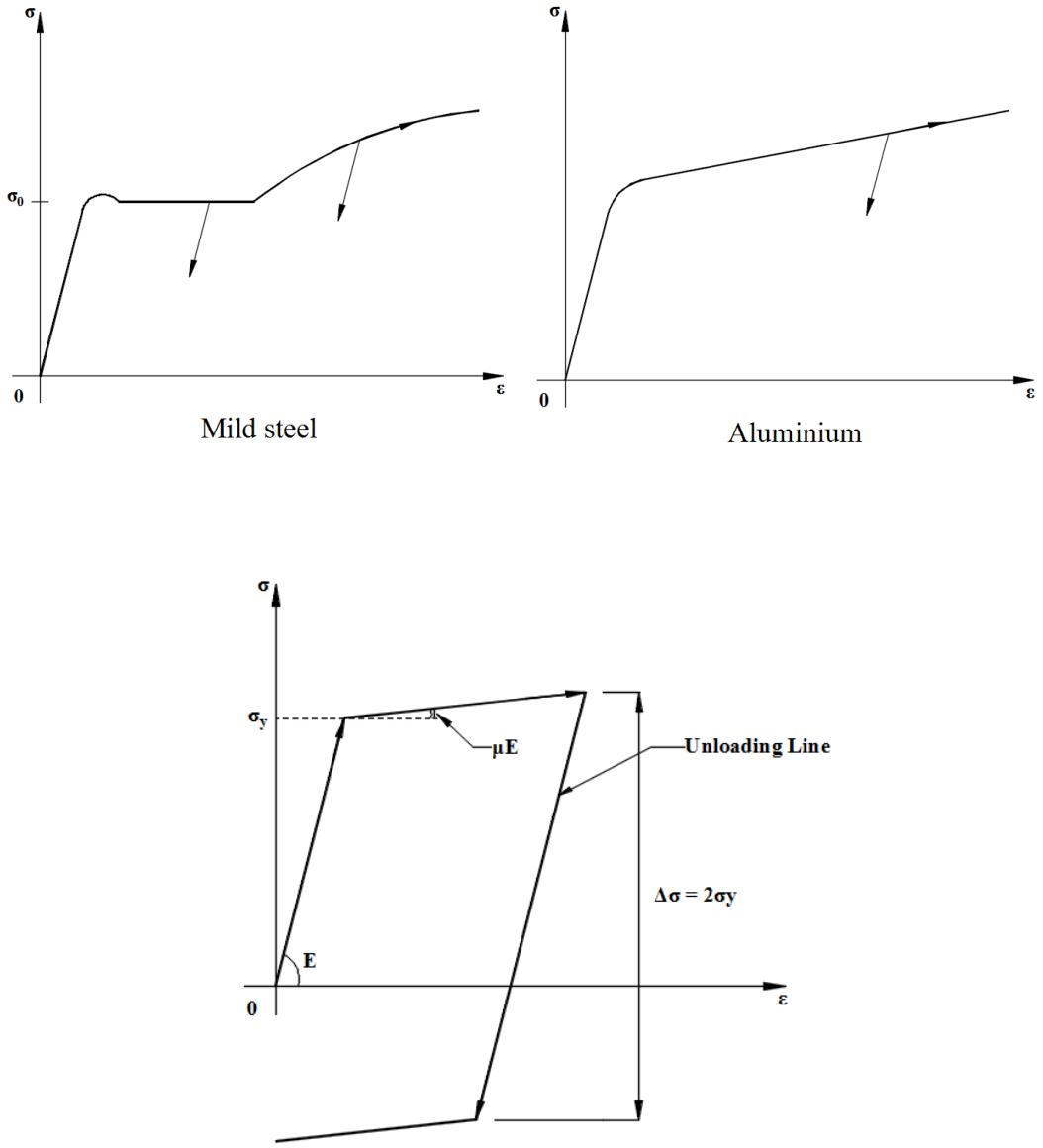

Figure 3.1 Typical stress-strain curves for a) mild steel, b) aluminium, and c) idealised bilinear relationship (Jirasek and Bazant, 2001)

A suitable approximation of the inelastic material response can be provided by a bilinear kinematic hardening law with a constant slope $E_t = d\sigma/d\varepsilon$ in the plastic range, which is adopted in the present work as it simplifies the consideration of material plasticity in the formulation of the analytical buckling models. As shown in Figure 3.1c, the bilinear material model is defined in terms of an elastic modulus E, yield strength σ_Y and a strain hardening parameter μ.

With the benefit of an idealised bilinear stress-strain curve, columns can be categorised into four classes depending on their slenderness ratios (λ=L/r, with $r = \sqrt{I/A}$ = radius of gyration of the cross-section). These are:

- Class 1: $\lambda < \pi\sqrt{E_t/\sigma_Y}$ representing very stocky columns for which Engesser's load is greater than the yield load $\left(P_t > P_Y\right)$;

- Class 2: $\pi\sqrt{E_t/\sigma_Y} < \lambda < \pi\sqrt{E_R/\sigma_Y}$ representing columns with intermediate stockiness for which Engesser's load is less than the yield load but von Karman's load is greater than the yield load $\left(P_t < P_Y < P_R\right)$, where the reduced modulus E_R is a function of E, E_t and the cross-section shape;

- Class 3: $\pi\sqrt{E_R/\sigma_Y} < \lambda < \pi\sqrt{E/\sigma_Y}$ representing columns with low stockiness for which von Karman's load is less than the yield load but Euler's load is greater than the yield load $\left(P_R < P_Y < P_E\right)$; and

- Class 4: $\lambda > \pi\sqrt{E/\sigma_Y}$ representing slender columns governed by elastic Euler buckling $\left(P_E < P_Y\right)$.

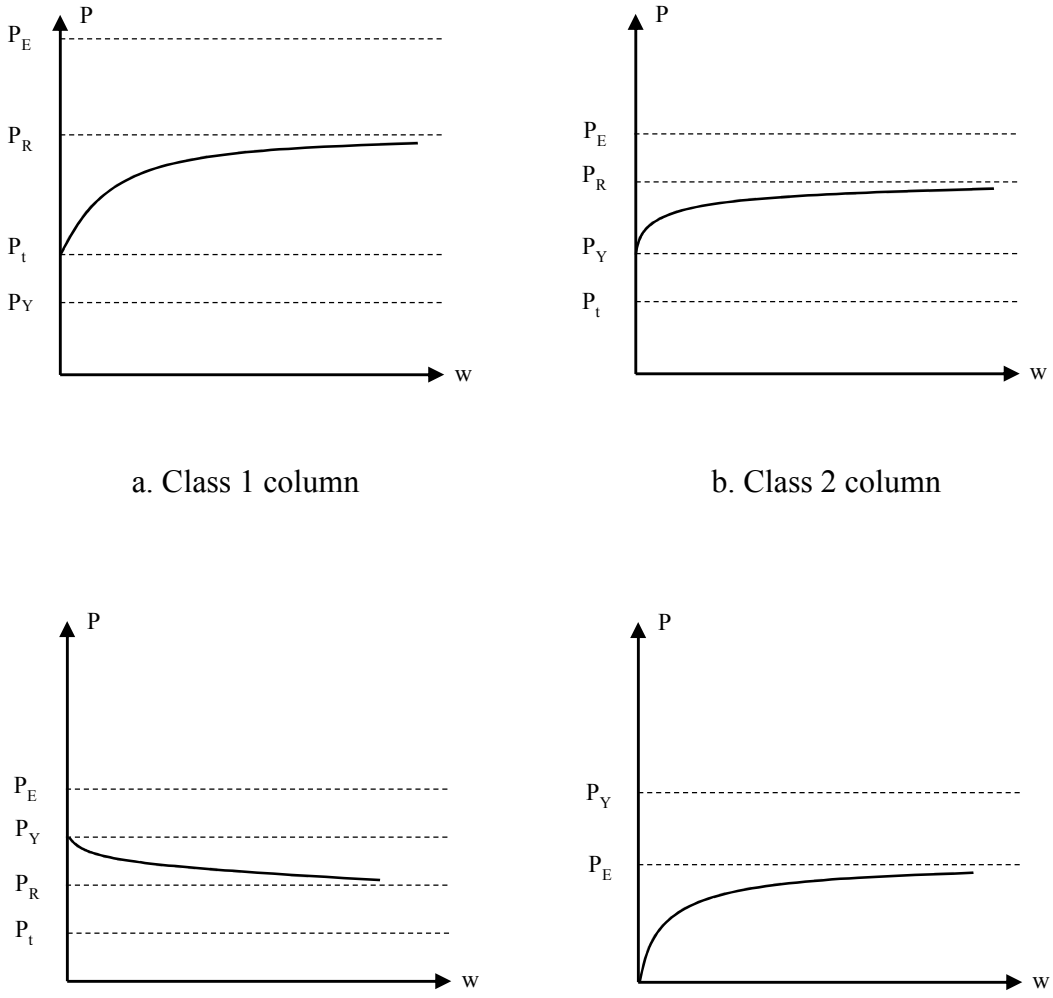

a. Class 1 column

b. Class 2 column

c. Class 3 column

d. Class 4 column

Figure 3.2 Four classes of slenderness according to a bilinear material model

This section is concerned with very stocky perfect columns (Class 1), thus the geometric and material properties of the model column in the illustrative examples are chosen to achieve slenderness in the desired range. The next section is concerned with imperfect columns of the same class, while the subsequent section deals with columns of intermediate stockiness (i.e. Class 2). The consideration of columns in Class 3 and Class 4 are outside the scope of the present work, since the maximum buckling resistance for both classes takes the yield load as an upper bound.

It is worth noting at this stage that the proposed analytical buckling model can, in principle, be amended to accommodate more sophisticated stress-strain relationships.

However, in such a case an iterative procedure would be required for determining the influence of the constitutive law on the generalised cross-sectional response. This is in contrast to the explicit treatment achieved in the present work, as presented in Section 3.2.3, which is made possible by the consideration of a bilinear stress-strain relationship.

3.2.1 Problem Definition

Consider a pin-ended column with a length "L" subject to an axial compressive load at the ends, as shown in Figure 3.3.

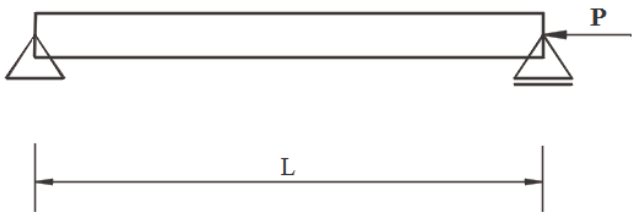

Figure 3.3 Perfect column under compressive load

Under a monotonically increasing load, it was acknowledged by Shanley's work that the column starts to buckle as the Engesser buckling load P_t is approached, and indeed it can be shown that a perfect column cannot develop equilibrium in an adjacent buckled state until the load equals P_t. Therefore, in order to capture the post-buckling response of a stocky column, the initial loading is assumed to be P_t at which the column is still straight. At the onset of buckling the stress distribution along the column is uniform and is equal to:

$$\sigma_t = \frac{P_t}{A} \tag{3.1}$$

At this point no unloading and lateral deflection have yet occurred. However, once the Engesser load is reached it is essential for the column to follow a bifurcating equilibrium path in which lateral deflections develop with increasing load. Increased loading is possible due to strain reversal that occurs on the convex side due to bending. As a result, for a general configuration along the post-buckling equilibrium path, the top fibre compressive stresses of all cross-sections within a distance x_e from the mid-length of the column are in an elastically unloaded state, as illustrated in Figure 3.4, where due to symmetry only half of the column is considered in the

analysis. In this zone, adopting the Euler-Bernoulli assumption of plane sections remaining plane, a reduced-modulus $\overline{E}$ is effectively obtained as a function of depth to the unloading zone y_e, while for the remaining length of the column $L/2-x_e$ the tangent-modulus E_t remains applicable. In this way, the spread of plasticity is accounted for over the cross-section depth and along the member length.

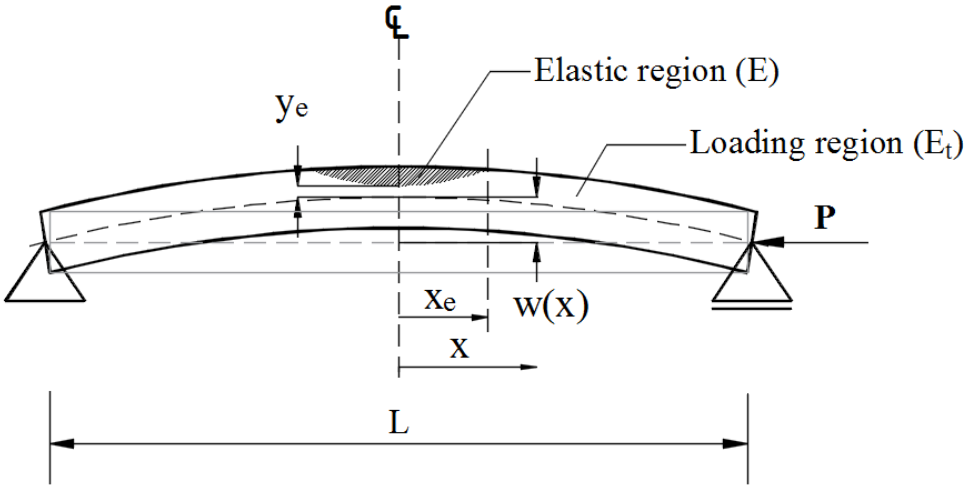

Figure 3.4 Column in deformed configuration

For an assumed buckling mode w(x), in order to find the depth of the unloading zone over any cross-section at location $0 \leq x < x_e$, the conditions of incremental axial equilibrium are considered. Once y_e is found, the equivalent modulus $\overline{E}$ over the cross-section is obtained by satisfying the constitutive law, and as a result the tangent material stiffness can be calculated. Along with the geometric stiffness, a linear eigenvalue problem can be solved for the instantaneous buckling load P_c (Figure 3.5), which has to be greater than the current load level for the column to remain in stable equilibrium.

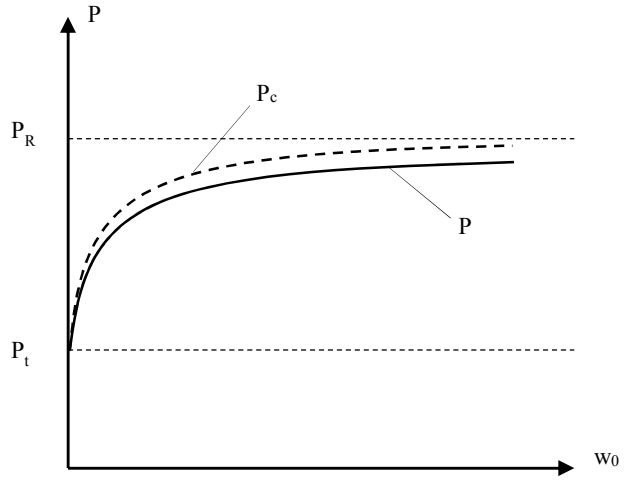

Figure 3.5 Instantaneous buckling load P_c

Finally, the incremental flexural equilibrium conditions are employed to relate the applied load P to the transverse buckling displacements, allowing for compatibility of curvatures with the assumed buckling mode. In this respect, the same buckling mode of the elastic column is considered for plastic buckling, which is only correct at the Engesser load level, where the equivalent modulus $\bar{E}$ is constant over the column length and equal to E_t. However, this assumption brings some inaccuracy at higher load levels due to partial elastic unloading, though as will be shown in subsequent comparisons the resulting approximation is still acceptable.

The approach briefly outlined above is detailed in the following sub-sections.

3.2.2 Incremental Axial Equilibrium Condition

For a perfect Class 1 stocky column, uniform plastification of the column cross-section occurs over the column length for loads in the range $P_Y \leq P \leq P_t$. However, when the load applied to the column exceeds P_t, the column starts to buckle along a stable bifurcating post-buckling path, and this is necessarily accompanied by elastic unloading around the middle part of the column on the convex side, such that the instantaneous buckling load is larger than the applied load. This region of elastic unloading is initiated at the column mid-length and spreads towards the supports as the load is increased in the range $P_t \leq P < P_R$. As previously noted, the von Karman reduced-modulus load P_R is an asymptotic limit that is not approached due to the development of tensile yielding on the convex side of the column after elastic unloading from compression.

Considering the column in a general buckled configuration, as shown in Figure 3.4, the incremental strain and stress distributions at the transition between the fully plastified and the partially unloaded parts of the column, $x=x_e$, is illustrated in Figure 3.6. Consideration is given here to a rectangular solid cross-section of width "b" and depth "h", though the proposed model can be easily extended to other cross-sectional shapes. Since at $x=x_e$ the top convex fibre is at the transition between elastic unloading and further plastic loading, the (infinitesimal) strain increment at the top fibre is $\delta\varepsilon_t=0$, and the increment of stresses over the full cross-section depth is related to the increment of strains by the tangent modulus E_t. Indeed, E_t also applies over the full cross-sections along part of the column which continues to be fully plastified, with $x_e<x\leq L/2$, except that for these cross-sections the top fibre incremental strains and stresses are non-zero (i.e. $\delta\varepsilon_t<0$).

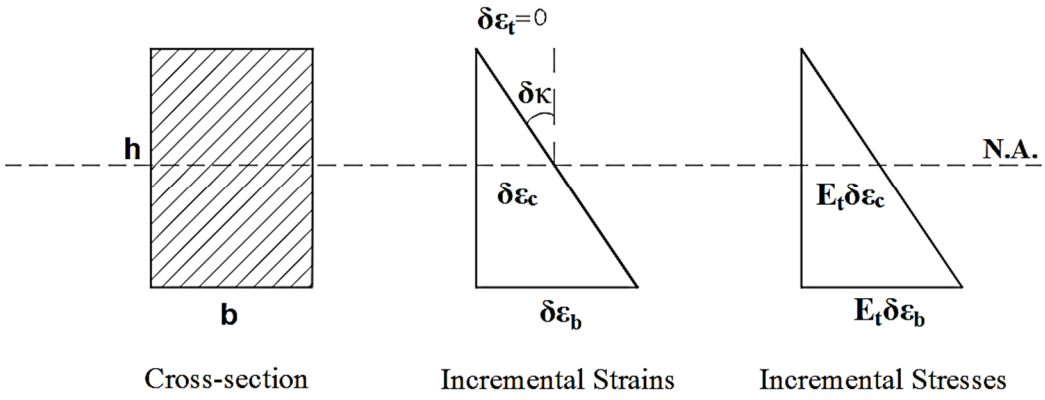

Figure 3.6 Linear incremental strain and stress distributions over cross-section at $x=x_e$

According to the Euler-Bernoulli assumption of plane sections remaining plane, the increment of axial force at $x=x_e$, δF_{x_e}, is easily obtained as:

$$\delta F_{x_e} = \delta\varepsilon_{c,x_e} E_t bh \tag{3.2}$$

According to the strain compatibility conditions, the increment of centroidal axial strain is related to the increment of curvature at $x=x_e$, $\delta\kappa_{x_e}$:

$$\delta\varepsilon_{t,x_e} = \delta\varepsilon_{c,x_e} - \frac{h}{2}\delta\kappa_{x_e} = 0 \Rightarrow \delta\varepsilon_{c,x_e} = \frac{h}{2}\delta\kappa_{x_e} \tag{3.3}$$

which leads to the following relationship between δF_{x_e} and $\delta\kappa_{x_e}$:

$$\delta F_{x_e} = \frac{bh^2}{2} E_t \delta\kappa_{x_e} \tag{3.4}$$

On the other hand, the incremental cross-sectional response in the region $0 \le x < x_e$ depends on both the elastic Young's modulus E and the tangent-modulus E_t, where the incremental strain and stress distributions are illustrated in Figure 3.7.

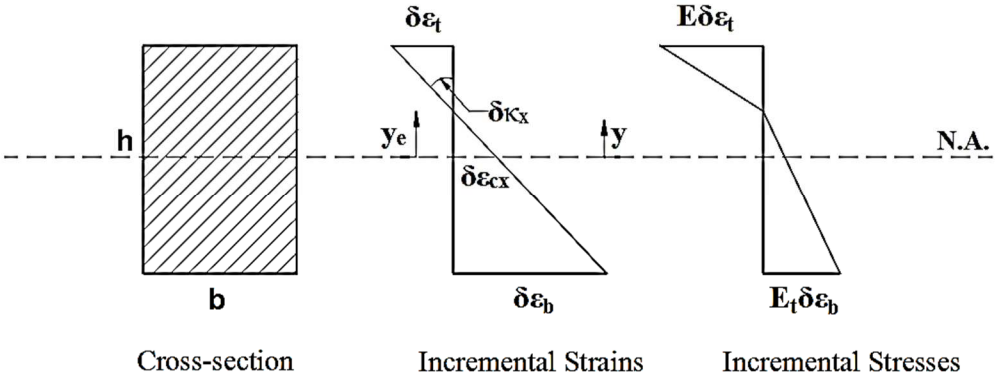

Figure 3.7 Incremental strain and stress distribution over cross-section at $0 \le x < x_e$

According to Figure 3.7 at $0 \le x < x_e$, the incremental strains $\delta\varepsilon_t$ and $\delta\varepsilon_b$ at the convex and concave faces of the column, respectively, can be related to the incremental curvature and the distance y_e of the instantaneous neutral axis from the centroidal reference line:

$$\delta\varepsilon_t = \left(y_e - \frac{h}{2}\right)\delta\kappa_x; \quad \delta\varepsilon_b = \left(y_e + \frac{h}{2}\right)\delta\kappa_x \tag{3.5}$$

thus the incremental axial force over the cross-section at $0 \le x < x_e$ is obtained as:

$$\delta F_x = \left[-E\left(y_e - \frac{h}{2}\right)^2 + E_t\left(y_e + \frac{h}{2}\right)^2\right]\frac{b\delta\kappa_x}{2} \tag{3.6}$$

Considering the condition of incremental axial equilibrium along the column length:

$$\delta F_x = \delta F_{x_e} \tag{3.7}$$

along with (3.4) and (3.6) enables y_e to be obtained in terms of x, over the range $0 \le x < x_e$, as follows:

$$y_e = \frac{h}{2}\left(\frac{E + E_t - 2\sqrt{E_t\left[E - (E - E_t)\left(\delta\kappa_{x_e} / \delta\kappa_x\right)\right]}}{(E - E_t)} \right) \tag{3.8}$$

where the ratio $\delta\kappa_{x_e} / \delta\kappa_x$ depends on x and x_e as determined by the second derivatives of the assumed mode :

$$\frac{\delta\kappa_{x_e}}{\delta\kappa_x} = \frac{w''(x_e)}{w''(x)} \tag{3.9}$$

It is worth noting that y_e becomes h/2 when $\delta\kappa_{x_e} / \delta\kappa_x = 1$, and it takes the value of the von Karman neutral axis $y_R = h/2 - h\sqrt{E_t}\Big/\left(\sqrt{E} + \sqrt{E_t}\right)$ when $\delta\kappa_{x_e} / \delta\kappa_x = 0$, as would be expected in both cases.

3.2.3 Cross-sectional Flexural Response

The constitutive law was used in the previous sub-section along with the conditions of compatibility and incremental axial equilibrium to relate the incremental axial force and curvature, and to establish the position of the instantaneous neutral axis y_e. Here, the constitutive law and conditions of compatibility are employed to establish the incremental flexural response for a cross-section at $0 \le x < x_e$ with a known y_e. Referring to Figure 3.7 the incremental stress at position y is given by:

$$\delta\sigma_x = \begin{cases} -E(y - y_e)\delta\kappa_x, & y > y_e \\ -E_t(y - y_e)\delta\kappa_x, & y \le y_e \end{cases} \tag{3.10}$$

hence, the incremental bending moment is obtained as.

$$\delta M = -\int_{-\frac{h}{2}}^{\frac{h}{2}} y\delta\sigma_x (bdy) = b\left(E\int_{y_e}^{\frac{h}{2}} y(y-y_e)dy + E_t\int_{-\frac{h}{2}}^{y_e} y(y-y_e)dy \right)\delta\kappa_x \tag{3.11}$$

With the tangential flexural response defined as follows:

$$\delta M = \overline{EI}\delta\kappa_x \tag{3.12}$$

the equivalent flexural modulus which varies over the unloaded region $0 \leq x < x_e$, is obtained from (3.11) as:

$$\overline{EI} = \frac{b}{24}\left(Eh^3 + 4Ey_e^3 - 3y_eEh^2 - 4E_ty_e^3 + E_th^3 + 3y_eE_th^2 \right) \tag{3.13}$$

Of course, for cross-sections outside the unloaded region $x > x_e$, which continue to be fully plastified, the effective flexural modulus is the tangent modulus $\overline{E} = E_t$.

It should be noted that the above expression is applicable to rectangular cross-sections, though generalisation to other cross-sectional shapes is possible. Moreover, by substituting either $y_e = h/2$ or $y_e = y_R = h/2 - h\sqrt{E_t}\Big/\left(\sqrt{E}+\sqrt{E_t}\right)$ in (3.13), $\bar{E}$ reduces to the tangent modulus E_t or the von Karman reduced modulus $E_R = 4EE_t/\left(\sqrt{E}+\sqrt{E_t}\right)^2$, respectively.

It is finally worth highlighting that the equivalent flexural stiffness $\bar{E}$ implicitly depends on both the location of the cross-section, x, and the extent of the unloaded region, x_e, by virtue of the explicit dependence of y_e on x and x_e. Since, x_e increases with applied loading in the post-buckling range, as will be shown later, $\bar{E}$ is not constant for an unloaded cross-section but varies along the post-buckling path.

3.2.4 Incremental Flexural Equilibrium Conditions

With the assumption of a dominant buckling mode, the incremental flexural equilibrium conditions can be derived from an analogy with a SDOF cantilever

column subject to an axial loading, as illustrated in Figure 3.8. This column is assumed to be rigid along its length but with a nonlinear rotational spring at its support. The total rotational equilibrium condition in the current known configuration at load P, accounting for geometric nonlinearity with small to moderate transverse displacements, is given by:

$$M = P w_0 \tag{3.14}$$

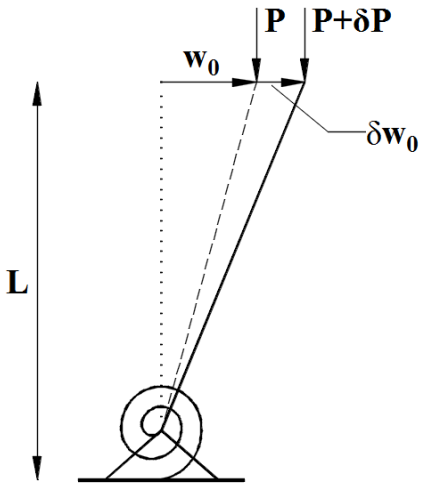

Figure 3.8 Cantilever column under a load P

The same condition in the next configuration at load P+δP, with an associated transverse deflection $w_0+\delta w_0$ at its free end is similarly given by:

$$M+\delta M = (P+\delta P)(w_0 + \delta w_0) \tag{3.15}$$

Therefore, the incremental equilibrium condition, assuming small increments, can be written as:

$$\delta M = P\delta w_0 + \delta P w_0 \equiv \left(P + w_0 \frac{\delta P}{\delta w_0} \right) \delta w_0 \tag{3.16}$$

On the other hand, an instantaneous buckling load P_c can be defined for this column, which represents the theoretical buckling load in the perfect configuration accounting for the influence of a varying rotational stiffness due to material nonlinearity.

Considering incremental equilibrium in the perfect configuration leads to the following expression for P_c:

$$P_c \delta w_0 = \delta M \Rightarrow P_c = \frac{\delta M}{\delta w_0} = \frac{\delta M}{\delta \theta_0 L} = \frac{k_e}{L} \tag{3.17}$$

where $\delta\theta$ is the incremental rotation in the spring, and k_e is its tangential rotational material stiffness.

Combining (3.16) and (3.17) leads to the following differential flexural equilibrium condition:

$$P_c = \left(P + w_0 \frac{\delta P}{\delta w_0} \right) \tag{3.18}$$

This expression can be readily applied to the more general plastic column buckling problem as an equivalent SDOF system with an assumed mode. In this case, P_c depends on the tangential material stiffness, which is in turn determined by the equivalent flexural modulus $\bar{E}$ over the column length, as discussed in the following sub-section.

Equation (3.18) sheds light on the nature of the buckling and post-buckling response of a perfect stocky column. At the initiation of buckling in the initial perfect configuration ($w_0=0$), the applied load is equal to the instantaneous buckling load ($P=P_c$). However, along the stable post-buckling path with increasing load ($w_0 \neq 0$, $\delta P/\delta w_0 > 0$), the instantaneous buckling load must exceed the applied load ($P<P_c$), the two becoming equal again only when the applied load has reached its maximum value ($\delta P/\delta w_0 = 0$).

3.2.5 Instantaneous Buckling Load P_c

The instantaneous buckling load P_c for the stocky column can be obtained by solving a simple linear eigenvalue problem, representing a reduced SDOF linear buckling condition in the undeformed configuration. In this respect, buckling occurs as a result of the singularity of the tangent stiffness (Izzuddin, 2007c), which consists of the

material stiffness matrix, which in this case varies with the spread of plasticity, and a geometric stiffness that depends on the axial force. For a general MDOF system, the tangent stiffness and its geometric and material components are all matrices. However, with an assumed buckling mode for the column problem, these reduce to single equivalent stiffness terms, which make the solution of the linear eigenvalue problem trivial. In this respect, and as previously noted, the elastic buckling mode is used for the plastic buckling problem, where with reference to Figure 3.4 and only taking half of column into consideration:

$$w(x) = w_0 \, \bar{w}(x); \;\; \bar{w}(x) = \cos\left(\frac{\pi x}{L}\right) \tag{3.19}$$

where $\bar{w}(x)$ is the normalised mode, and w_0 is the maximum transverse displacement at mid-length of the pin-ended column.

In the current analytical model, the Rotational Spring Analogy (Izzuddin, 2006;Izzuddin, 2007c) is employed for formulating the geometric stiffness, while the tangential material stiffness is obtained with due consideration for the spread of material plasticity. These are detailed in the following subsections, leading to the determination of P_c.

3.2.5.1 Geometric Stiffness

The Rotational Spring Analogy (RSA) was proposed by Izzuddin (2006) as a simplified approach for the formulation of the geometric stiffness matrix. To illustrate this approach, an axially loaded element which remains straight is first considered (Izzuddin, 2006), as shown in Figure 3.9. Considering that a compressive/tensile axial force has a destabilising/stabilising effect which leads to negative/positive geometric stiffness, an equivalent rotational spring can be placed along the element as a contribution to the geometric stiffness, and this can be treated using geometrically linear analysis principles based on first-order kinematics. The spring rotational stiffness is equal to the element axial force multiplied by the element length:

$$k_\rho = FL \tag{3.20}$$

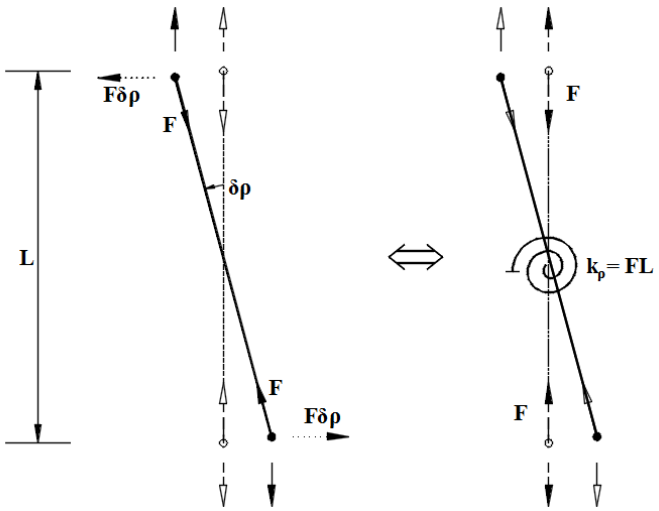

Figure 3.9 Equivalent geometric stiffness for straight element (Izzuddin, 2006)

If the element bends during buckling, the equivalent rotational springs will be uniformly distributed along the element length with a rotational stiffness equal to F (Figure 3.10).

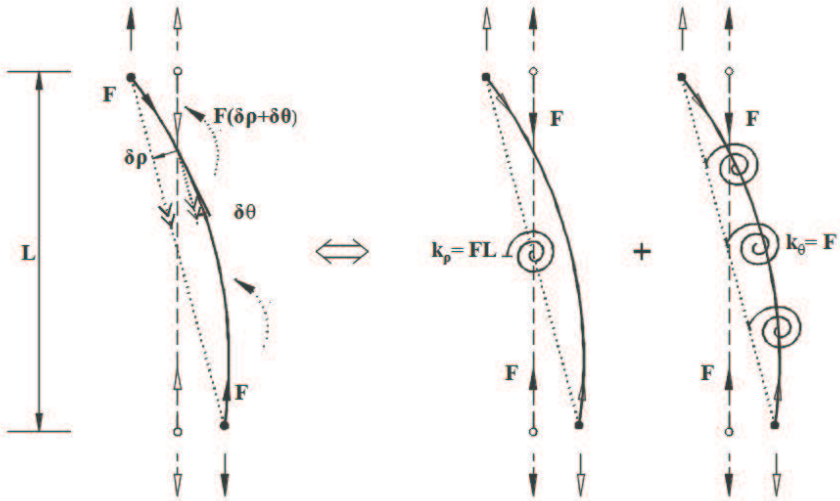

Figure 3.10 Equivalent geometric stiffness for bending element (Izzuddin, 2006)

Izzuddin provides several illustrative examples in his papers to demonstrate the simplicity and applications of his method in the buckling analysis of a range of structures, including columns, beams, frames and plates.

In applying the RSA to the buckling analysis of columns, the geometric stiffness is obtained from distributed equivalent rotational springs along the length of the column, with a rotation equal to the slope of the lateral buckling mode:

$$\theta = w'(x) = w_0 \bar{w}'(x) \tag{3.21}$$

To obtain the nominal geometric stiffness associated with a unit compressive axial load, the stiffness of the distributed equivalent rotational spring is taken as:

$$k_\theta = -1 \tag{3.22}$$

The SDOF geometric stiffness is thus obtained from linear analysis principles as:

$$k_g = \int_{-\frac{L}{2}}^{\frac{L}{2}} \bar{w}'(x)\, k_\theta \bar{w}'(x) dx = -2\int_0^{\frac{L}{2}} \left(\bar{w}'(x)\right)^2 dx \tag{3.23}$$

where $\bar{w}(x)$ is the normalised assumed buckling mode, as given by (3.19).

3.2.5.2 Material Stiffness

The tangential material stiffness k_e associated with the SDOF mode can be determined from well-known discretisation techniques based on the virtual work method as follows:

$$k_e = \int_{-\frac{L}{2}}^{\frac{L}{2}} \bar{w}''(x) \bar{E}I\, \bar{w}''(x) dx = 2\int_0^{\frac{L}{2}} \bar{E}I \left(\bar{w}''(x)\right)^2 dx \tag{3.24}$$

in which $\bar{w}''(x) = \partial^2 \bar{w} / \partial x^2$ is the curvature of the normalised buckling mode, and $\bar{E}$ is the effective modulus as given by (3.13). However, unlike the elastic buckling case where the effective modulus is the Young's modulus, for plastic buckling $\bar{E}$ is not constant along the column length, as previously discussed. Furthermore, considering that $\bar{E}$ reduces to E_t in the range $x \geq x_e$, the integration can be expressed as:

$$k_e = 2\left[\int_0^{x_e} \bar{E}I\left(\bar{w}''(x)\right)^2 dx + E_t I\int_{x_e}^{\frac{L}{2}} \left(\bar{w}''(x)\right)^2 dx\right] \tag{3.25}$$

Noting that $\bar{E}$ is a highly nonlinear function of x – as implied by (3.13), (3.8), (3.9) and (3.18) – the integration of the first term is best undertaken numerically or using a symbolic computation tool, while the second term can be easily obtained analytically.

Having determined the nominal geometric stiffness and the tangential material stiffness, the instantaneous buckling load can now be obtained from the singularity of the SDOF tangent stiffness k_t:

$$k_t = k_e + P_c k_g = 0 \Rightarrow P_c = -\frac{k_e}{k_g} \tag{3.26}$$

For verification purposes, substituting $\bar{E}$ with Young's modulus E, it can be easily shown that P_c reduces to the Euler buckling load for a pin-ended column:

$$k_e = \frac{\pi^4 EI}{2L^3};\quad k_g = -\frac{\pi^2}{2L} \Rightarrow P_c = -\frac{k_e}{k_g} = \frac{\pi^2 EI}{L^2} \tag{3.27}$$

3.2.6 Post-buckling Response and P_{max}

The previous components of the analytical model considering incremental axial and flexural equilibrium, along with the compatibility conditions and the constitutive law, are brought together here to trace the post-buckling path of the perfect stocky column. However, because of the highly nonlinear system of equations, coupled with a flexural equilibrium condition expressed in a differential form as in (3.18), a discrete solution procedure is required which must be carefully designed to avoid excessive iterations over several unknown parameters. Considering (3.18), it is noted that variable x_e alone determines not only P_c but also $\delta P/\delta w_0$, thus the discretisation process is based around varying x_e in small increments and applying a discrete form of (3.18) to solve for the corresponding increments in P and w_0.

With reference to Figure 3.11, it is assumed that the equilibrium state at step j is known, and that the next equilibrium state at step j+1 is being sought. An effective discretisation technique is proposed based on satisfying the differential flexural equilibrium condition of (3.18) for the averaged entities over the step, thus:

$$\frac{1}{2}\left(P_c^j + P_c^{j+1}\right) = \left(P^j + \frac{\Delta P^{j+1}}{2}\right) + \frac{1}{2}\left[\left(\frac{\delta P}{\delta w_0}\right)^j + \left(\frac{\delta P}{\delta w_0}\right)^{j+1}\right]\left(w_0{}^j + \frac{\Delta w_0{}^{j+1}}{2}\right) \tag{3.28}$$

With x_e^{j+1} given as the incremented parameter, all of the terms in the previous equation can be readily determined with the exception of ΔP^{j+1} and $\Delta w_0{}^{j+1}$. Since the following discrete equation relates these two unknown increments:

$$\Delta P^{j+1} = \frac{1}{2}\left[\left(\frac{\delta P}{\delta w_0}\right)^j + \left(\frac{\delta P}{\delta w_0}\right)^{j+1}\right]\Delta w_0{}^{j+1} \tag{3.29}$$

the discrete flexural equilibrium condition of (3.28) can now be expressed in terms of only $\Delta w_0{}^{j+1}$:

$$\frac{1}{2}\left(P_c^j + P_c^{j+1}\right) = P^j + \frac{1}{2}\left[\left(\frac{\delta P}{\delta w_0}\right)^j + \left(\frac{\delta P}{\delta w_0}\right)^{j+1}\right]\left(w_0{}^j + \Delta w_0{}^{j+1}\right) \tag{3.30}$$

which can thus be used to solve for $\Delta w_0{}^{j+1}$.

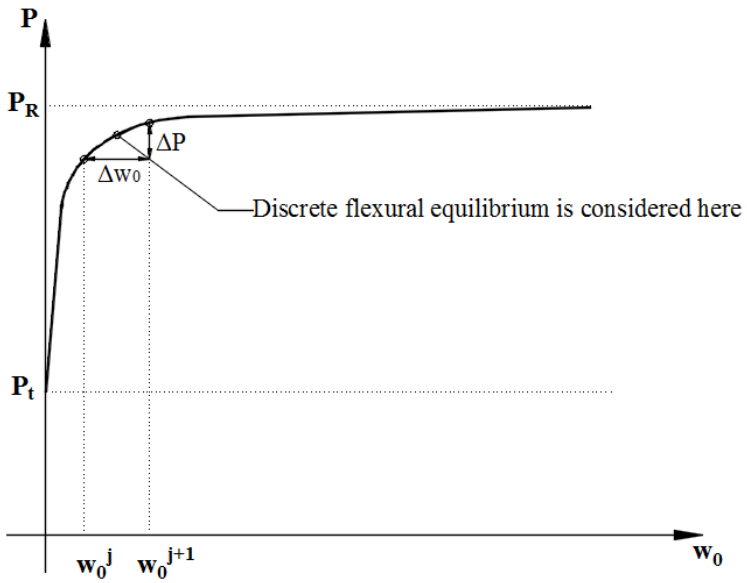

Figure 3.11 Illustration of a post-buckling load-deflection curve

As noted before, x_e determines P_c by obtaining the following: y_e for $0 \le x < x_e$ from (3.8) $\bar{E}$ from (3.13), k_e from (3.24), and P_c from (3.26), with k_g given independently of x_e by (3.23). Furthermore, x_e determines $\delta P/\delta w_0$ from (3.4), noting that $\delta P = -\delta F_{x_e}$, as follows:

$$\frac{\delta P}{\delta w_0} = -\frac{\delta F_{x_e}}{\delta w_0} = -\frac{\delta F_{x_e}}{\delta \kappa_{x_e}} \frac{\delta \kappa_{x_e}}{\delta w_0} \Rightarrow \frac{\delta P}{\delta w_0} = -\frac{E_t b h^2}{2} \bar{w}''(x_e) \tag{3.31}$$

At the start of buckling (j=1, $x_e^j = 0$), when the entire perfect column is at the state of pure compression ($\bar{E}=E_t$), the initial deflection w_0 is zero, the instantaneous buckling load P_c^j determined from (3.26) becomes identical to the tangent-modulus load P_t. The value of P^j is thus initialised to P_t, as this already satisfies incremental flexural equilibrium as given by (3.18), and $(\delta P/\delta w_0)^j$ is obtained from (3.31). Proceeding with the incremental solution with x_e^{j+1}, the values of P_c^{j+1} and $(\delta P/\delta w_0)^{j+1}$ are obtained as previously, hence Δw_0^{j+1} and ΔP^{j+1} are determined from (3.30) and (3.29), respectively. The values of P^{j+1} and w_0^{j+1} are updated to $P^j + \Delta P^{j+1}$ and $w_0^j + \Delta w_0^{j+1}$, respectively, and the incremental solution procedure proceeds to the

next step, enabling the post-buckling response of the perfect stocky column to be traced. However, due to tensile yielding at the outer fibre of the column cross-section in the middle region, the von Karman upper limit cannot be realised, and hence the maximum buckling load is attained within the range ($P_t<P_{max}<P_R$).

In order to assess the influence of tensile yielding along the convex side of the buckled column on its buckling resistance, consideration is given in the proposed analytical model to identify the equilibrium state along the post-buckling path where tensile yielding first occurs. Clearly, the level of loading associated with this state would be a lower bound on the maximum buckling resistance, since the instantaneous buckling load would continue to be greater than the applied load until significant tensile yielding has occurred in the middle convex region of the column.

To identify the first occurrence of tensile yielding, the value of stress at the mid-length top fibre σ_t is required. Initially, at the point of buckling, the column is in a state of pure compression, hence $\sigma_t^0 = P_t/(bh)$, where compressive stress is considered here to be positive. Once buckling occurs and strain reversal takes place, the stress at the extreme top fibre starts to decrease, where the corresponding increment can be obtained from the following discrete relationship:

$$\Delta\sigma_t^{j+1} = \frac{1}{2}\left[\left(\frac{\delta\sigma_t}{\delta w_0}\right)^j + \left(\frac{\delta\sigma_t}{\delta w_0}\right)^{j+1}\right]\Delta w_0^{\,j+1} \tag{3.32}$$

in which:

$$\frac{\delta\sigma_t}{\delta w_0} = \left(\frac{h}{2} - y_e\right) E\, w''(0) \tag{3.33}$$

evaluated at the column mid-length where x=0, noting that y_e depends on x_e and hence varies over the incremental steps. With reference to Figure 3.1, the tensile yielding of the extreme top fibre of the cross-section at x=0 is predicted at the end of the current increment (j+1) when the following condition is met:

$$\Delta\bar{\sigma}_t = \sigma_t^0 - \sigma_t^{j+1} \geq 2\sigma_Y \tag{3.34}$$

With the neglect of tensile yielding in the proposed analytical model, its predictions become less accurate as tensile yielding spreads on the convex side near the column mid-length. Accordingly, the load at first tensile yielding should be considered merely as a useful and informative lower bound on the maximum compressive buckling resistance of the stocky column.

The application of the proposed analytical model for buckling assessment of perfect stocky columns is illustrated in the flowchart of Figure 3.12.

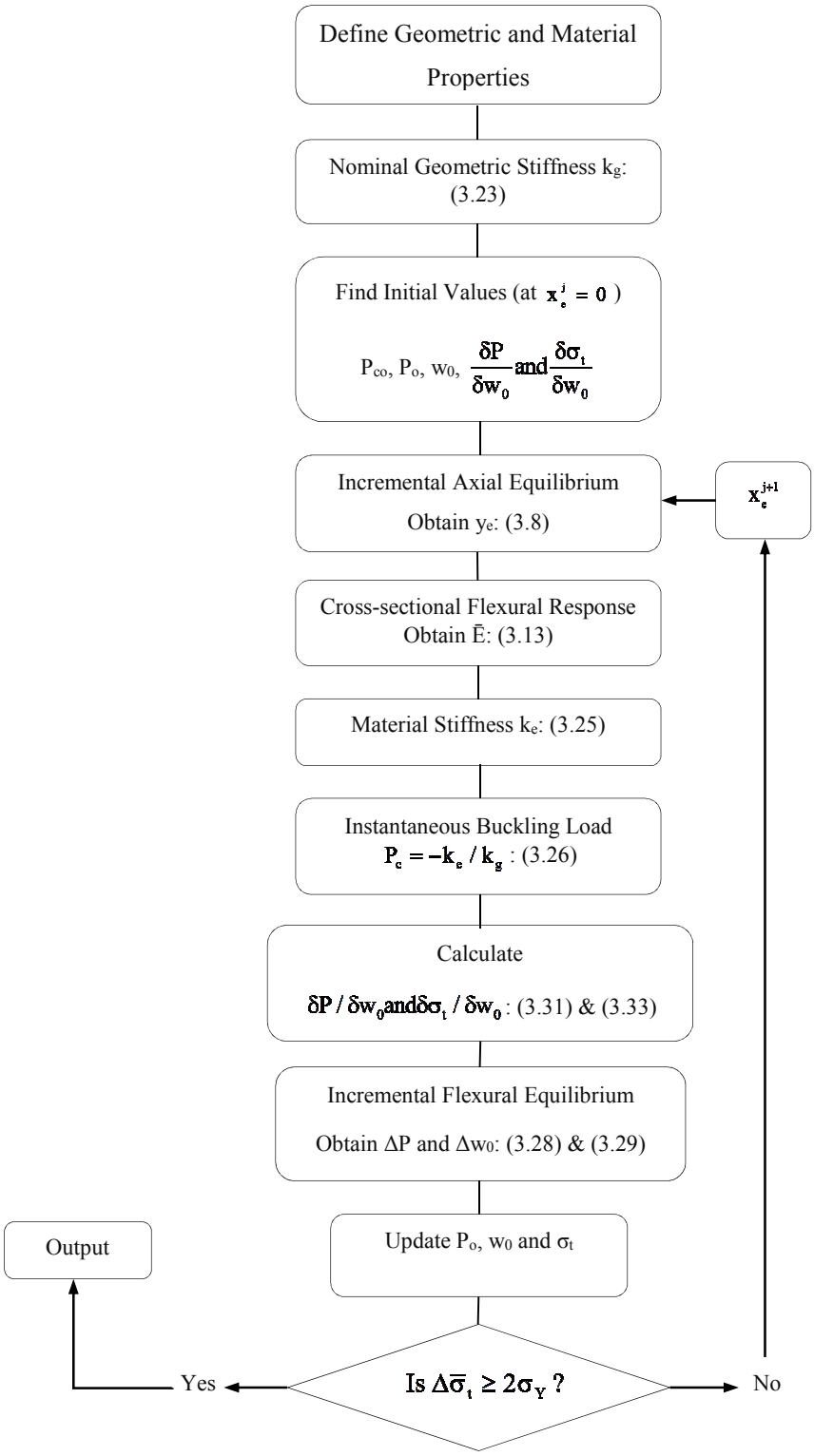

Figure 3.12 Flowchart of calculation

3.2.7 Results and Discussion

To verify the accuracy of the proposed model for plastic buckling of stocky columns and to illustrate its applicability, consider a pin-ended column with the following bilinear material model parameters (Figure 3.1c): $E=210\times10^9 N/m^2$, $E_t=4.2\times10^9 N/m^2$ ($\mu=0.02$), and $\sigma_Y=300\times10^6 N/m^2$, and with the following geometric characteristics (Figure 3.3 and Figure 3.6): L=600mm, b=100mm and h=200mm. Clearly for this column, the slenderness ratio $\lambda=L/r=10.4$ is less than $\pi\sqrt{E_t/\sigma_Y}=11.75$, which confirms that the column is a Class 1 stocky column.

The proposed model is applied to the above column with an incremental step $\Delta x_e = 0.6mm$, where a sample of results are provided in Table 3.1 and plotted in Figure 3.13 and Figure 3.14 (Note that the full results are plotted).

Table 3.1 Results of analytical model for perfect stocky column example

x_e(m)	w_0(m)	P(kN)	P_c(kN)	σ_t (N/m^2)	$\Delta\bar{\sigma}_t$ (N/m^2)
0	0	7676	7676	3.84×10^8	0
0.03	8.02×10^{-6}	7678	7680	3.84×10^8	3.61×10^4
0.06	0.000172	7715	7752	3.81×10^8	2.49×10^6
0.09	0.000894	7867	8051	3.60×10^8	2.35×10^7
0.12	0.002745	8228	8739	2.77×10^8	1.07×10^8
0.15	0.006506	8881	9940	4.67×10^8	3.37×10^8
0.18	0.013403	9902	11717	-4.87×10^8	8.71×10^8
0.21	0.02577	11370	14064	-1.64×10^9	2.03×10^9
0.24	0.049363	13401	16914	-4.21×10^9	4.59×10^9
0.27	0.106641	16297	20139	-1.13×10^{10}	1.17×10^{10}
0.3	2.214916	22931	23568	-3.10×10^{11}	3.10×10^{11}

Figure 3.13a shows the load-deflection response, with P characterising the applied load and P_c the instantaneous buckling load, where it is evident that P_c is greater than P while P increases at non-zero deflections, as noted in the previous section. The graphs also clearly demonstrate the initiation of the elasto-plastic buckling at the Engesser tangent-modulus load P_t and the subsequent increase of load P towards the von Karman double-modulus load P_R. With the assumption of a constant tangent-modulus E_t, it is interesting to note in Figure 3.13a that P_R represents an asymptote towards which P tends at very large lateral deflections, which confirms that the von

Karman reduced-modulus load is an upper bound on the column buckling resistance. Of course, this upper bound is never reached in reality because of tensile yielding, which as shown in Figure 3.13b is first initiated at a load P (9.4MN) that is significantly less than P_R (23.6MN).

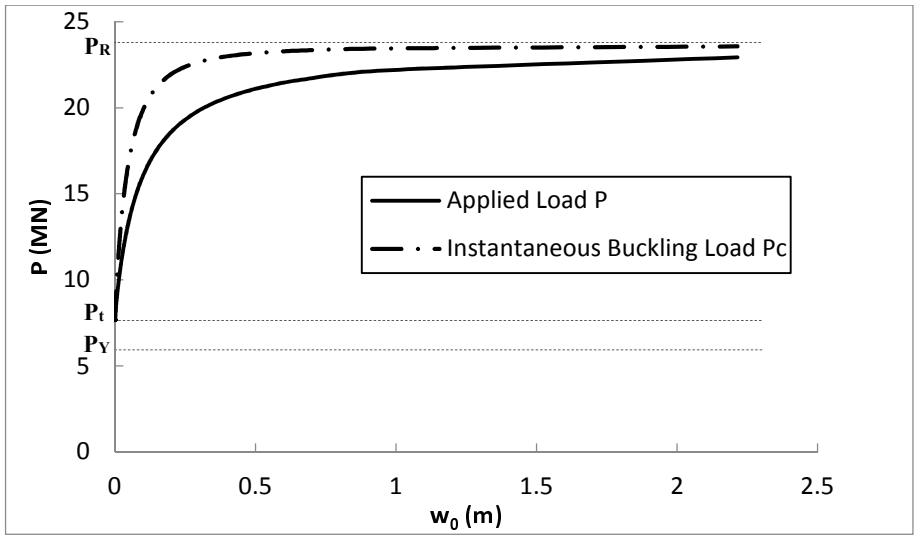

a. Load-deflection curve

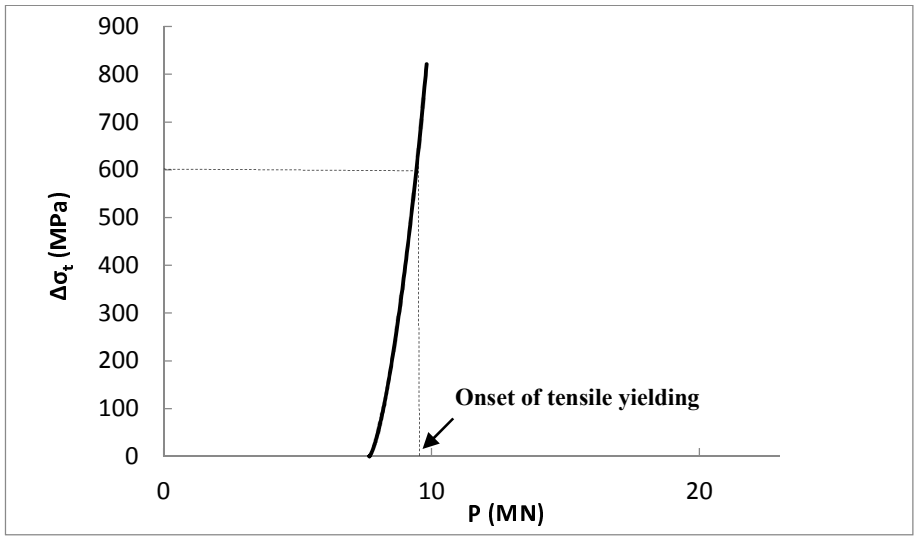

b. Initiation of tensile yielding

Figure 3.13 Elasto-plastic buckling response of perfect stocky column

Figure 3.14a shows the spread of elastic unloading across the depth at the column mid-length, denoted by $h_e = h/2 - y_e$, as it extends on the convex side in terms of x_e, with the dashed line indicating the point at which tensile yielding is initiated. There is a considerable amount of strain reversal taking place at the point of tensile

yielding, i.e. 7% of the column depth and 56% of the column length, leading to a lower bound on the maximum buckling load that is 23% greater than the Engesser tangent-modulus load (Figure 3.14b). The variation of the lateral displacement with x_e is shown in Figure 3.14c, which confirms that the column starts to buckle as soon as strain reversal has taken place (i.e. $x_e>0$). So far, this study has shown that the possible value of maximum load is considerably larger than P_t.

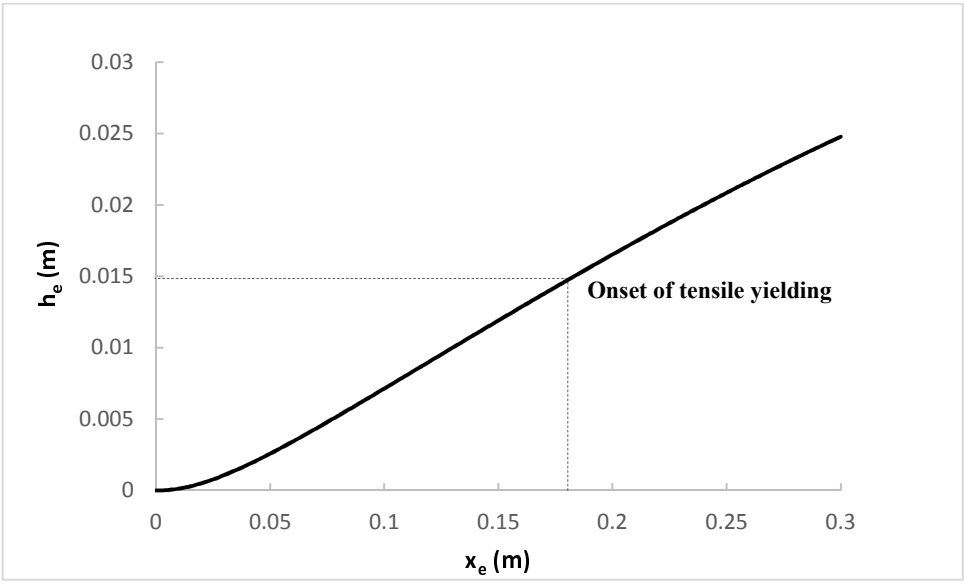

a. h_e

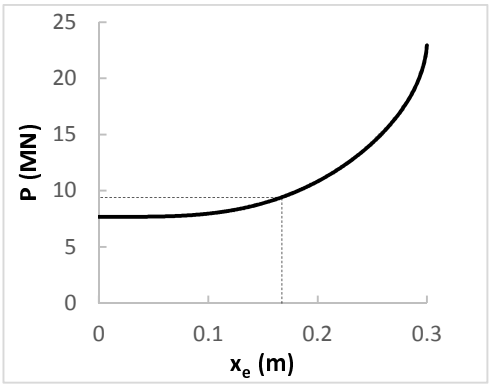

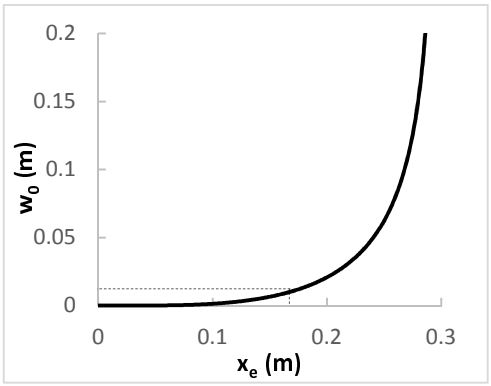

b. Applied load P c. Lateral deflection w_0

Figure 3.14 Results of analytical model with propagation of strain reversal

The proposed analytical model is verified against the nonlinear finite element program ADAPTIC (Izzuddin, 1991). Figure 3.15 compares the post-buckling response of the perfect column obtained from the proposed model against the numerical model obtained with ADAPTIC. The two load-deflection curves are

initially identical, with buckling initiating from the tangent-modulus load P_t and increasing towards the reduced-modulus load P_R; however, due to tensile yielding at the outer fibre of cross-section, the maximum buckling resistance P_{max} is closer to P_t than P_R according to ADAPTIC (since there are regions within column that tangent-modulus stress is not exceeded). A similar prediction is made in the analytical model considering the onset of tensile yielding, though there is clearly some reserve resistance in this range according to the ADAPTIC results as further tensile yielding develops. Leaving aside this issue, it is clear that the proposed model is very accurate within its intended scope, thus implying that the various assumptions made for the model development are accurate, including the consideration of the elastic buckling mode for the reduced SDOF model.

Further, if the tangent-modulus equation $P_t = \pi^2 E_t I / L^2$ is used as the basis for predicting the buckling strength of columns in the plastic range (Shanley's statement), the full buckling capacity of the column will not be exploited and hence this approach will lead to designs that are uneconomical.

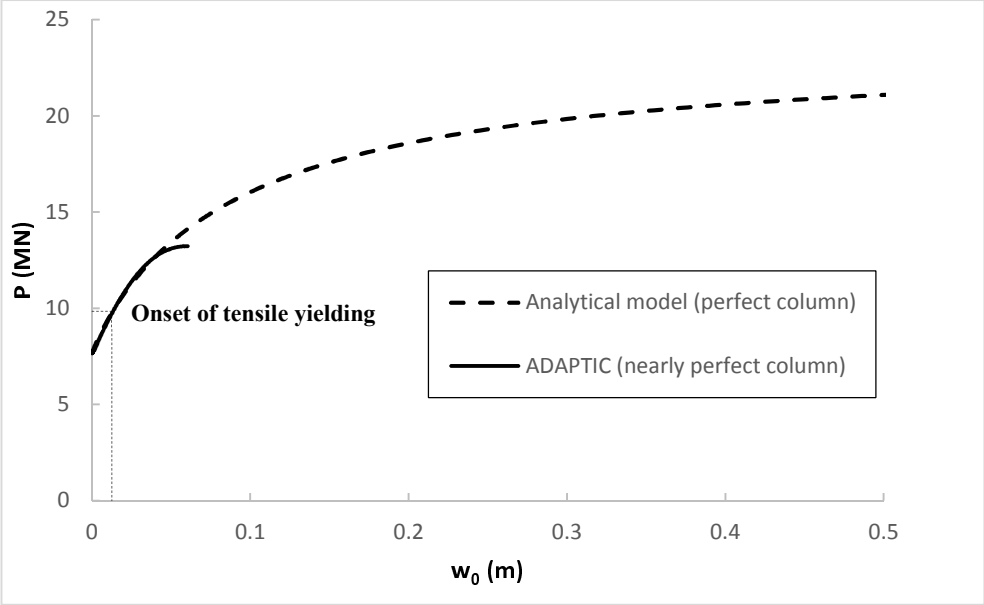

Figure 3.15 Comparison of analytical model against ADAPTIC

Comparison with Hutchinson's Model

Hutchinson's asymptotic model (Hutchinson, 1974) for the plastic buckling of a perfect column, as previously described in Chapter 2, finds an approximate estimate of the maximum buckling load after truncating the expansion (relating load to the column rotation) and using fractional powers, as follows: $P_{max} = P_t\left(1 + 4a_1^3 / \left(27a_2^2\right)\right)$ where $a_1 = 2L\left(9 / \left(\pi^2 I / L\right)\right)^{1/3}$ and $a_2 = -16/3\left(L/\pi\right)\left(L/I\right)^{1/3}\left(\sqrt{3E_t L / \left(\left(E - E_t\right)\left(I/L\right)^{1/3}\right)}\right)$.

Employing the same material and geometric properties of the perfect stocky column in this study, the Hutchinson's equation predicts a maximum load of P_{max}=54.7MN, which overestimates the buckling resistance obtained from ADAPTIC by four times; in fact, this prediction even exceeds the reduced-modulus load. Similarly when employing the DMV theory, the modified predicted value of maximum resistance of column (P_{max}=46.42MN) still over-predicts the numerical estimate by a large margin.

Therefore, as he had already stated (Hutchinson, 1974) this expansion is not accurate over the full range of interest. It is also important to note that, according to Hutchinson, the maximum buckling resistance of the column is given by an asymptotic formula rather than acknowledging the occurrence of tensile yielding at the outer fibre of the cross-section.

3.3 Imperfect Stocky Columns

Real structural members have imperfections in the form of out-of-straightness, which can influence the buckling and post-buckling response. In this section, the simplified analytical model presented in the previous section is extended to account for initial imperfections. This enables the investigation of imperfection sensitivity for plastic buckling of stocky columns, where amongst other findings a threshold imperfection level is established analytically and verified through comparisons against the results of nonlinear finite element analysis. It is shown that the post-buckling response of stocky columns is significantly affected by imperfections up to the threshold imperfection, beyond which the influence of imperfections is much reduced.

3.3.1 Imperfect Behaviour

The determination of the post-buckling response of a Class 1 stocky column becomes much more involved in the presence of imperfections. Firstly, in comparison with the perfect column case, the equilibrium state at which strain reversal, hence elastic unloading, starts is no longer the initial configuration but an amplified deformed configuration. Secondly, plastification does not spread uniformly over the column length; instead, it initiates at mid-length on the concave side at $P<P_Y$, spreads along this side to the pinned supports at $P=P_Y$, and then spreads along the convex side towards the column mid-length. The plastification reaches mid-length before strain reversal only for relatively small imperfections.

To establish the range of imperfections for which plastification proceeds to the column mid-length before strain reversal, consider a Class 1 pin-ended stocky column with a small imperfection amplitude w_{0i}, where the shape of imperfection is similar to the assumed buckling mode w(x) (Figure 3.4) as given by (3.19). The application of an axial load P induces an additional deflection w_0 and a corresponding bending moment at mid-length; assuming that the full column plastifies before strain reversal, M_0 can be obtained in the range of full plastification from the total cross-sectional flexural response:

$$M_0 = E_t I w''(0) = \frac{\pi^2 E_t I}{L^2} w_0 \equiv -P_t w_0 \tag{3.35}$$

where, as before, P_t is the Engesser tangent-modulus load.

On the other hand, the additional total deflection w_0 can be obtained in the same range as a magnification of the initial imperfection w_{0i} considering total flexural equilibrium, as expressed by Perry's rule (Timoshenko and Gere, 1961):

$$w_0 = \frac{w_{0i}}{\frac{P_t}{P} - 1} \tag{3.36}$$

where in this case P_t is the instantaneous buckling load, since the column is fully plastified.

Clearly, for the column to be fully plastified, the mid-length stress at the extreme top fibre must exceed the material yield strength, thus combining (3.35) and (3.36):

$$\sigma_{t0} = \frac{P}{A} + \frac{M_0}{S} = P\left(\frac{1}{A} - \frac{h}{2I}\frac{P_t w_{0i}}{P_t - P}\right) \geq \sigma_Y \tag{3.37}$$

When strain reversal takes place at the mid-length σ_{t0} becomes stationary with respect to the load P, which leads to the following condition when considering a column with a rectangular cross-section:

$$\frac{\delta\sigma_{t0}}{\delta P} = \frac{1}{A} - \frac{6P_c w_{0i}}{hA(P_t - P)}\left(1 + \frac{P}{(P_t - P)}\right) = 0 \tag{3.38}$$

Accordingly, the value of P at the onset of strain reversal is obtained from the solution of the above equation as:

$$P = P_t\left(1 - \sqrt{\frac{6w_{0i}}{h}}\right) \tag{3.39}$$

Note that the load P, at which strain reversal occurs at the mid-length, is now less than P_t while depending on the level of imperfection.

Of course, for strain reversal to initiate at the column mid-length, the yield condition of (3.37) must be satisfied at the value of P obtained in (3.39), which leads to the following condition on the imperfection amplitude for a rectangular cross-section:

$$w_{0i} \leq \left[w_{0i,max} = \frac{h}{6}\left(1 - \sqrt{\frac{P_Y}{P_c}}\right)^2 \right] \tag{3.40}$$

This defines a threshold imperfection amplitude $w_{0i,max}$ above which compressive plastification will only have spread partially towards the column mid-length when strain reversal occurs at the transition between the plastic and elastic zones along the convex side. The treatment of this case is discussed further in Section 3.3.3.

3.3.2 Small Imperfections

Initial imperfection amplitudes smaller than $w_{0i,max}$, as defined by (3.40), are categorised as 'small imperfections'. The procedure described in Section 3.2 for tracing the post-buckling response of a perfect stocky column still applies for an imperfect column with small imperfections, except that the starting equilibrium state is the one defined by P and the corresponding w_0 at the onset of strain reversal, as given by (3.39) and (3.36), respectively. A further important difference is that the incremental flexural equilibrium condition, as given by (3.18), must be amended with w_0 replaced by w_0+w_{0i} to allow for the initial imperfection.

Figure 3.16 illustrates the effect of small imperfections on the post-buckling behaviour of the same Class 1 stocky column considered in Section 3.2, for which the threshold imperfection is $w_{0i,max}$=0.45mm. It can be seen that a small initial imperfection w_{0i}=0.2mm can significantly reduce the buckling resistance, where the results for this case are compared in Table 3.2 to those of the perfect column and the imperfect column at the threshold imperfection. For w_{0i}=0.2mm, the onset of elastic unloading is marked at a load P_0 which is 8% lower than the Engesser tangent-modulus load P_t. Additionally, the load at the onset of tensile yielding, denoted by $\bar{P}_{max}$ as the lower bound on the maximum buckling resistance, has been reduced by 17% compared to the perfect column. The reduction in P_0 and $\bar{P}_{max}$ progresses marginally further with an increased imperfection up to the threshold amplitude $w_{0i}=w_{0i,max}$=0.45mm, but the effects of a further increase in imperfection beyond this threshold are much smaller as shown in the following sub-section.

Table 3.2 Influence of small initial imperfections on buckling resistance

w_{0i}(mm)	w_{0max}(m)	P_0(MN)	$\bar{P}_{max}$ (MN)
0.00	0.010	7.676	9.434
0.20	0.007	7.082	7.870
0.45	0.008	6.794	7.573

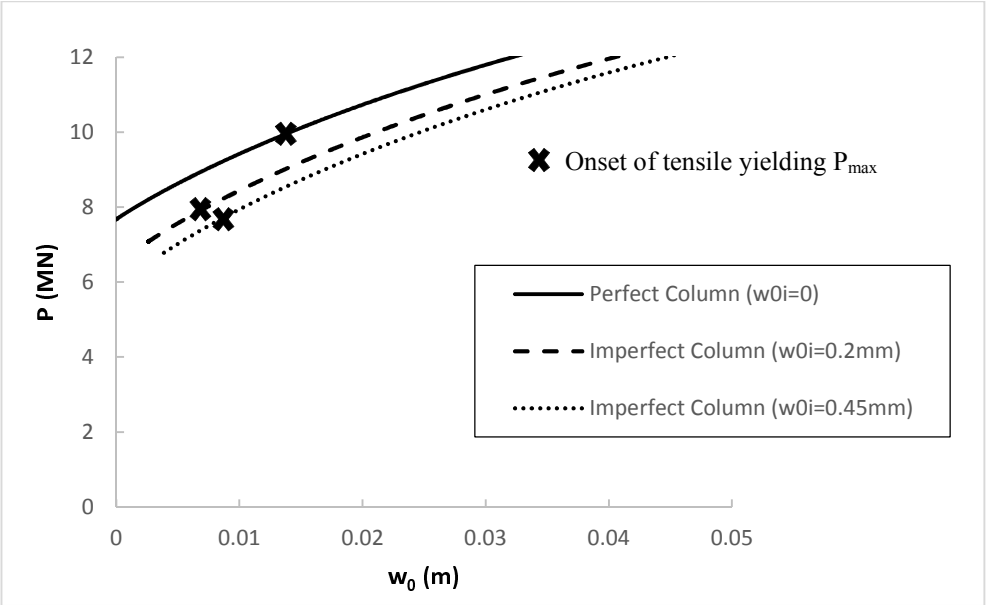

Figure 3.16 Effect of small imperfections on post-buckling response of Class 1 column

3.3.3 Large Imperfections

When the initial out-of-straightness of a Class 1 stocky column exceeds the threshold imperfection, as given by (3.40) for a rectangular cross-section, a different approach is required for determining the starting equilibrium state at the first strain reversal. In this case, full plastification of the column cross-section develops only partially towards the column mid-length, and strain reversal will occur at a location x_s defining the initial transition on the convex side between the plastic and elastic zones (Figure 3.17). Therefore, some parts along the convex side of the column within x_s from mid-length remain elastic, other parts within x_e from x_s initially become plastic and then unload, while the remaining cross-sections continue to be fully plastic.

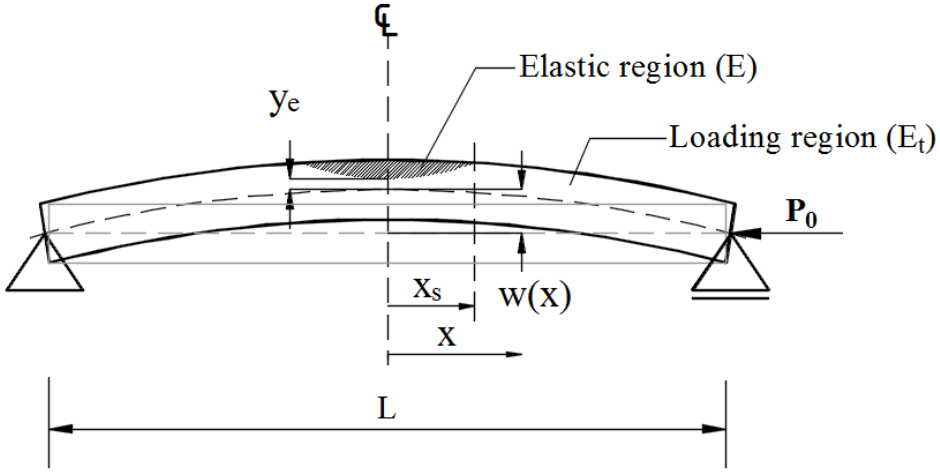

a. First occurrence of strain reversal

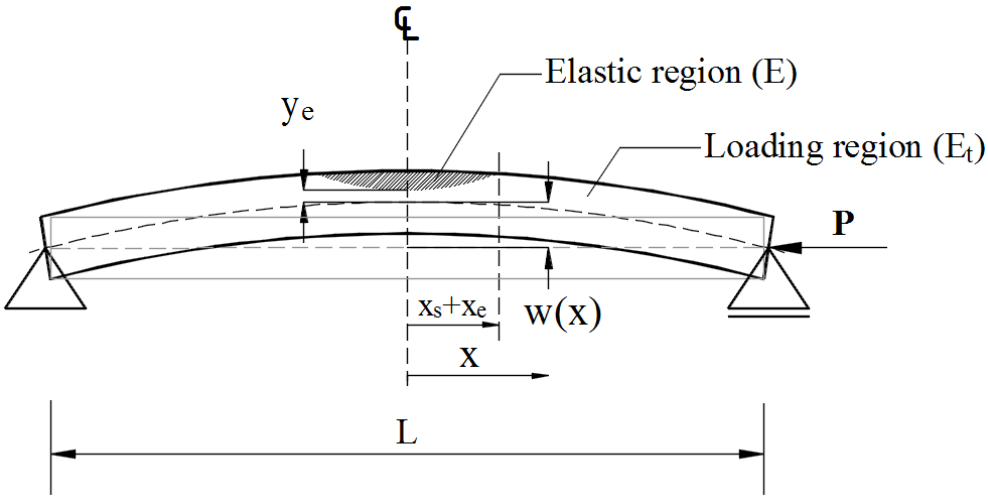

b. Spread of elastic unloading with increase of load

Figure 3.17 Column with a large initial imperfection

For a given initial imperfection $w_{0i}>w_{0i,max}$, the conditions of the total flexural equilibrium at the point of strain reversal allow x_s as well as the starting values of P and w_0 to be obtained as follows.

At $x=x_s$ where the cross-section is fully plastified, the bending moment is directly related to the curvature through the tangent modulus E_t:

$$M_s = E_t I\, w''(x_s) \tag{3.41}$$

In turn, w(x) depends on w_0, which is obtained at load P, in accordance with Perry's rule, from the total flexural equilibrium as an amplification of the initial imperfection w_{0i}:

$$w_0 = \frac{w_{0i}}{\frac{P_c}{P} - 1} \tag{3.42}$$

where P_c is the instantaneous buckling load, which can be shown to be identically obtained as in Section 3.2.5 with x_e taken as x_s. In this respect, assuming monotonic strain variation with applied loading over the whole column up to the point of strain reversal, the total strains and stresses follow the same incremental distribution as presented in Section 3.2.2. Accordingly, the associated material stiffness k_e represents the tangential flexural response, thus the corresponding P_c can be employed as in (3.42) to express the total flexural equilibrium.

A further condition at $x=x_s$ is that the stress at the top fibre induced by the combined bending moment and axial force is identical to the material yield strength, since this point is at the transition between plastic and elastic zones, thus:

$$\sigma_t = \frac{P}{A} + \frac{M_s}{S} = \sigma_Y \tag{3.43}$$

For a specific x_s, equations (3.41) to (3.43) can be combined to provide a quadratic equation in P:

$$P^2 - \left(P_c + P_Y + \frac{hA}{2} E_t \bar{w}''(x_s) w_{0i} \right) P + P_c P_Y = 0 \tag{3.44}$$

where as noted before P_c depends on x_s, and $\bar{w}(x)$ is given by (3.19). The above equation typically has two roots P which satisfy the equilibrium and yield conditions, but one repeated root when P represents the load at strain reversal. Accordingly, the

value of x_s at strain reversal can be obtained from the solution of the following equation:

$$\left(P_c + P_Y + \frac{hA}{2} E_t \bar{w}''(x_s) w_{0i} \right)^2 - 4 P_c P_Y = 0 \tag{3.45}$$

Clearly, this is a highly nonlinear equation, not least with P_c depending on x_s, which is therefore best solved numerically. Once x_s is determined, the corresponding value of P is obtained as $P = \sqrt{P_c P_Y}$ with w_0 established from (3.42), and these are then taken as the starting values for the proposed plastic buckling model, which can thus be applied in the same way as discussed in the previous sub-section.

Considering the same Class 1 stocky column example as before but now with an initial imperfection amplitude w_{0i}=1.0mm that exceeds the threshold imperfection, the value of x_s and the corresponding value of P are obtained as 106.1mm and 7.083MN, respectively. Proceeding with tracing the post-buckling response as in the case of small imperfections, the obtained results are provided in Table 3.3 and depicted in Figure 3.18. It is noticeable that $\bar{P}_{max}$ is barely affected by an increase in the amplitude of initial imperfection above the threshold level. Unlike the case of small imperfections where imperfection sensitivity of the elasto-plastic buckling response was evident, the case of large imperfections exceeding the obtained threshold exhibits hardly any imperfection sensitivity. One reasonable explanation is that due to large imperfections significant parts over the cross-section and along the length of the stocky column remain elastic during buckling, therefore the column behaves similar to an elastic slender column which does not display strong sensitivity to initial imperfections.

Table 3.3 Influence of a large imperfection on buckling loads

w_{0i}(mm)	w_{0max}(m)	P_0(MN)	$\bar{P}_{max}$ (MN)
0.00	0.010	7.676	9.434
0.45	0.008	6.794	7.573
1.00	0.008	7.083	7.544

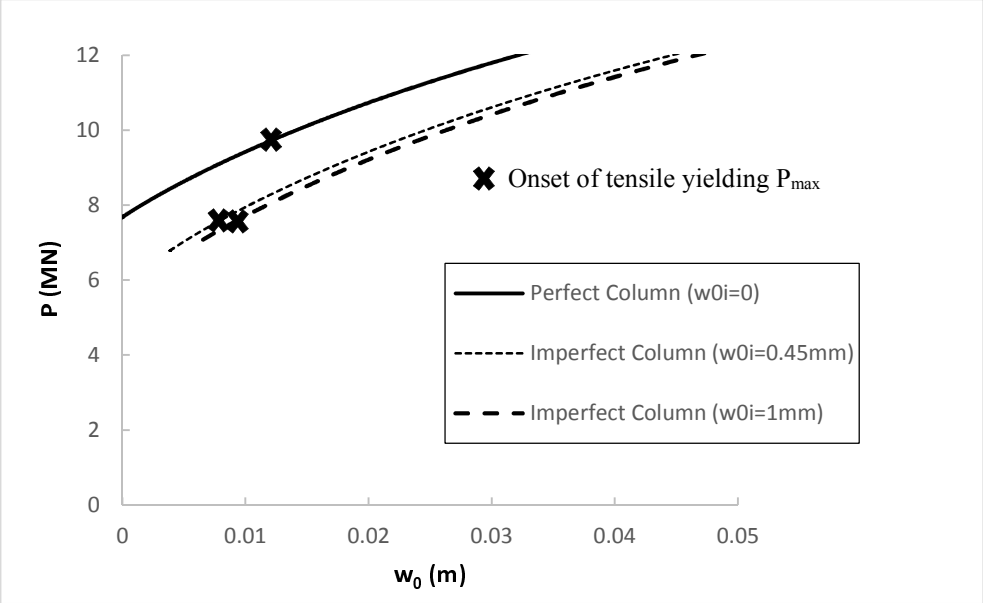

Figure 3.18 Effect of large imperfections on post-buckling response of Class 1 column

The outcomes of the proposed analytical model accounting for initial imperfections are verified against the results of the nonlinear finite element analysis program ADAPTIC (Izzuddin, 1991), as depicted in Figure 3.19 for small and large imperfection amplitudes. As in the case of the perfect stocky column, the comparison is favourable, where it is again evident that the point of first tensile yielding is a conservative lower bound on the maximum buckling resistance.

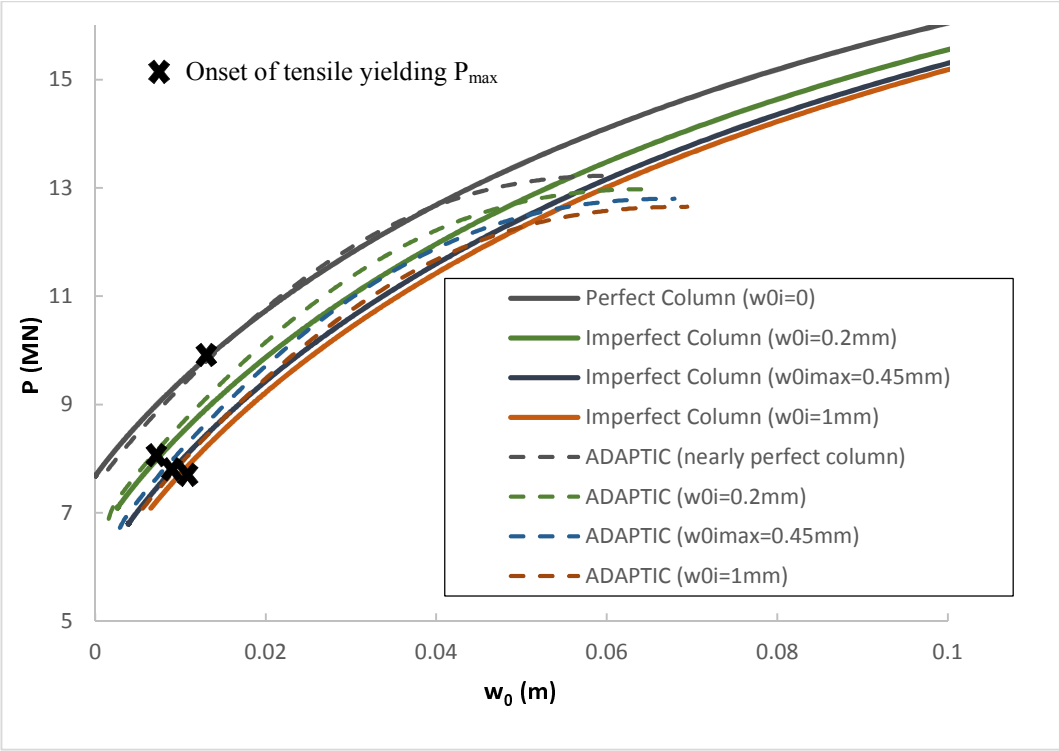

Figure 3.19 Comparison of results of analytical model and ADAPTIC

To investigate the effect of imperfections in further detail, the variation of the maximum buckling load P_{max}, as obtained from ADAPTIC with initial imperfections, is shown in Figure 3.20. Both the sensitivity of the buckling strength of Class 1 stocky columns to small imperfections and their insensitivity to large imperfections are even more apparent in this graph.

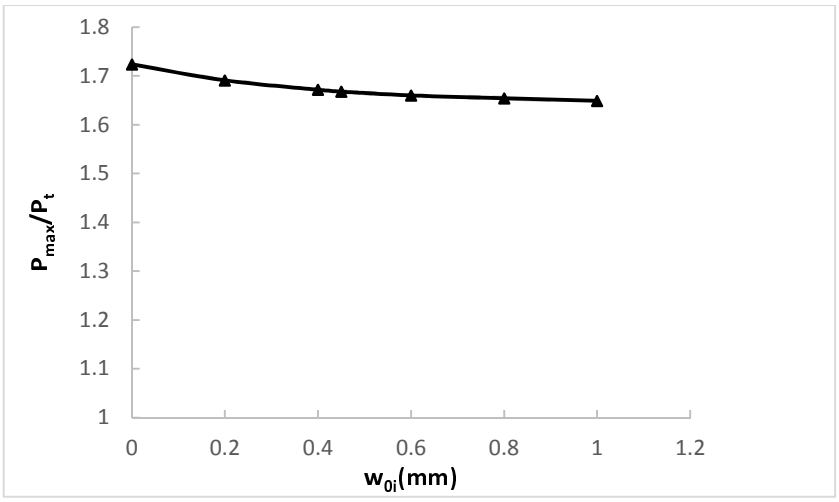

Figure 3.20 Imperfection sensitivity diagram (ADAPTIC results)

3.4 Columns with Intermediate Stockiness

The main focus of this chapter thus far has been set on the post-buckling and imperfection sensitivity of Class 1 stocky columns for which $P_t>P_Y$. This section is concerned with demonstrating the application of the proposed analytical model to Class 2 stocky columns for which $P_t<P_Y<P_R$, focussing on perfect columns. Since the perfect column is stocky, buckling must start at P_Y which then represents the effective Engesser tangent-modulus load, since at P_Y the tangent modulus for a bilinear stress strain relationship can be seen to take any value between E and E_t.

The proposed analytical model can be applied to Class 2 stocky columns following the same procedure as outlined in Section 3.2, except that strain reversal at the extreme top fibre of the cross-section does not initiate at the column mid-length but within a distance x_c from mid-length. This ensures that bifurcation is achieved at P_Y, with the load subsequently increasing towards the reduced-modulus load P_R.

For the perfect column under an initial load P_Y plastification is at the verge of initiation, but it only progresses partially over the column. In this respect, some parts along the top fibre of the column, within a distance x_c from the column mid-length (Figure 3.21), remain elastic. Other parts at a distance x_e+x_c from the column mid-length initially become plastic and then unload, while the remaining cross-sections continue to be fully plastic. Note the analogy between this case and Class 1 stocky columns with large imperfections (Figure 3.17 in Section 3.3.3), with a difference that this column is initially straight and has an initial buckling load equal to P_Y.

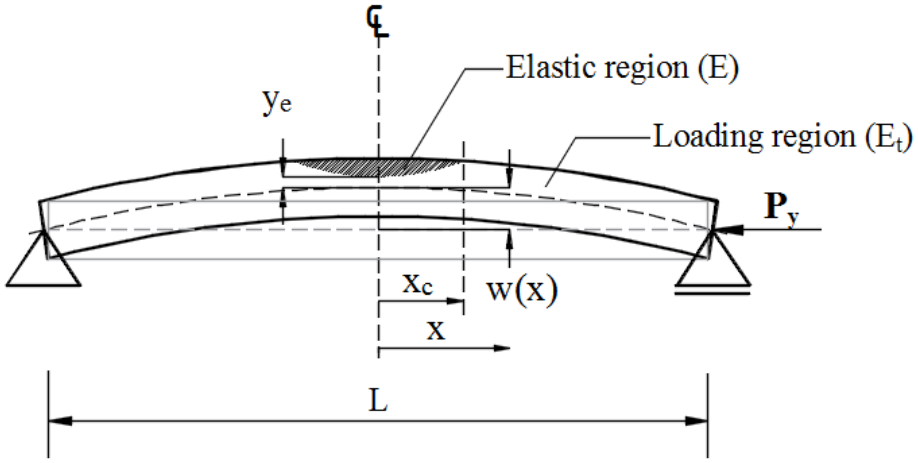

a. First occurrence of strain reversal

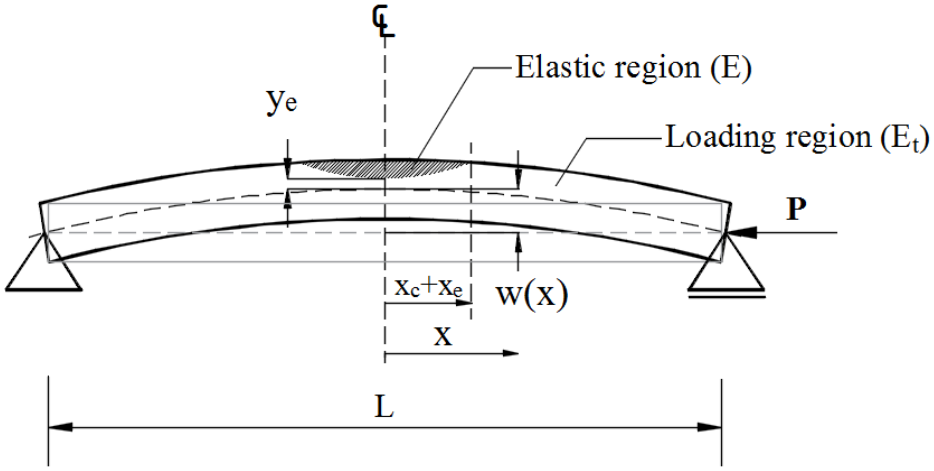

b. Spread of elastic unloading with increase of load

Figure 3.21 Stocky column with an intermediate slenderness ratio (Class 2)

To locate the point $x=x_c$ at which strain reversal takes place, the initial instantaneous buckling load P_c obtained from (3.26) must be equal to P_Y, thus:

$$P_c = -\frac{k_e}{k_g} = -\frac{\int_0^{x_c} \bar{E}I\left(\bar{w}''(x)\right)^2 dx + E_t I \int_{x_c}^{\frac{L}{2}} \left(\bar{w}''(x)\right)^2 dx}{\int_0^{\frac{L}{2}} \left(\bar{w}'(x)\right)^2 dx} = P_Y \qquad (3.46)$$

Since the above equation is highly nonlinear in x_c, a numerical solution procedure is required.

To illustrate the application of the proposed model to Class 2 perfect stocky columns, the previously considered column is investigated here but with a length L=1.0m, giving a slenderness ratio λ=L/r=17.3 which is greater than Engesser limit $\pi\sqrt{E_t/\sigma_Y} = 11.75$ but less than the von Karman limit $\pi\sqrt{E_R/\sigma_Y} = 20.6$. For this column, the solution of (3.46) predicts x_c=0.396m, thus initial elastic unloading at P_Y occurs relatively close to the supports. Figure 3.22 compares the post-buckling response predicted with the proposed analytical model against the results of ADAPTIC. Once again, the load-deflection curves associated with the analytical and numerical models are in close agreement. Furthermore, unlike very stocky columns, the onset of tensile yielding predicted in the proposed model at $\overline{P}_{max} = 6.3MN$ offers an excellent prediction of the maximum buckling capacity of 6.6MN obtained with ADAPTIC. It is worth noting, however, that the enhancement in the buckling resistance beyond the initial buckling load P_Y is rather marginal in this case, standing at around 10% (ADAPTIC).

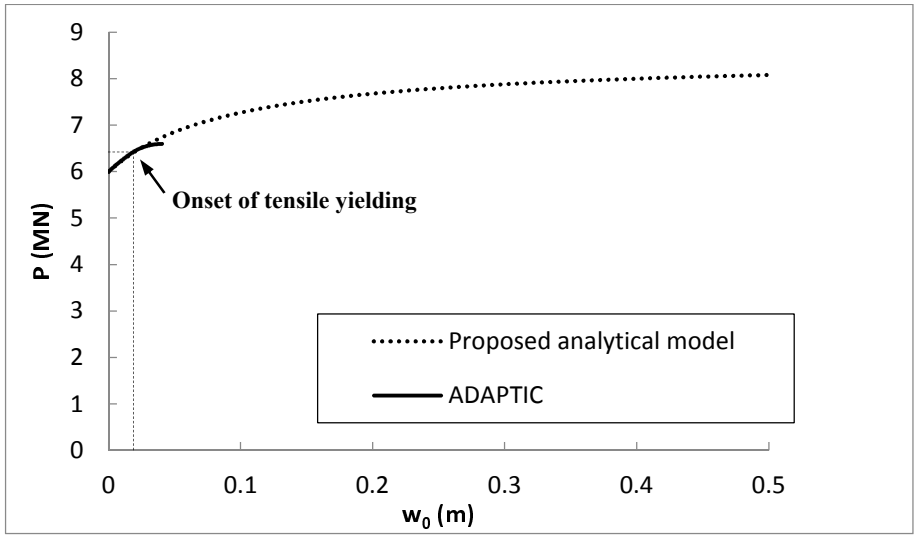

Figure 3.22 Response of Class 2 perfect stocky column

3.5 Conclusion

In this chapter, a simplified analytical model is presented for the plastic buckling of columns which captures the inelastic behaviour of stocky columns, and considers the mechanics of the initiation of buckling and the post-buckling response. This analytical SDOF model is based on the elastic buckling mode as an assumed mode, where the geometric stiffness is determined using the Rotational Spring Analogy, while the material stiffness is obtained with due consideration for the incremental spread of material plasticity. In addition, the model is derived for both cases of perfect and imperfect columns.

Besides ease of application, the developed analytical model provides insight into the initiation of plastic buckling at the Engesser tangent-modulus load and its subsequent increase towards the von Karman reduced-modulus load. It is also shown that the von Karman upper limit is typically not realised due to tensile yielding at the outer fibre of the column cross-section, where the onset of tensile yielding is shown to offer a reasonable lower bound on the maximum buckling resistance. It is therefore contended that the proposed analytical model sheds new light on the "Column Paradox" by showing that the plastic buckling response of stocky columns is captured using sound principles of mechanics. Most importantly, it seems that the acknowledgement of tensile yielding at the outer fibre of the column cross-section has not yet been perceived in the previous research work.

Furthermore, considering Class 1 stocky columns, a threshold level of imperfection is established from the developed model, beyond which it is shown that the plastic post-buckling response is barely affected by a further increase in the out-of-straightness. These findings are verified against the results of nonlinear finite element analysis using ADAPTIC, highlighting the important benefits of analytical models for direct application and enhanced understanding of plastic buckling.

Finally, the simplified analytical model is employed to predict the post-buckling behaviour of Class 2 stocky columns, for which buckling initiates at the yield load. For such columns, the onset of tensile yield offers a close approximation of the maximum buckling resistance, though compared to Class 1 stocky columns the enhancement in the maximum buckling resistance compared to the initial buckling load diminishes as P_Y approaches P_R.

CHAPTER 4

Comparison of Plastic Buckling in Columns and Plates

4.1 Introduction

Similar to the plastic buckling of columns, where Euler's elastic buckling load expression is used with a tangent-modulus E_t to obtain Engesser's buckling load or with a reduced-modulus E_R to attain von Karman's buckling load, there have been attempts (Bleich, 1924;Gerard, 1945;Timoshenko, 1936) to utilise an effective or reduced modulus of elasticity into the formulas for the elastic bucking load of plates to approximate their plastic buckling resistance. However, this generalization seems rather arbitrary, since the buckling of columns involves a one-way deformation mode dominated by uniaxial stresses, while on the other hand the buckling of plates that are supported on four edges involves a two-way mode with biaxial stress interactions. As a result, a rather complex theory of plasticity is required to capture the post-buckling behaviour of stocky plates.

The following question then arises: "*If an approach based on a tangent-modulus or a reduced-modulus were to be employed in a simplified model for plastic buckling analysis of plates, would it offer lower and upper bound predictions, respectively, as in the case of columns (see Chapter 3)?*". In order to answer this question, a detailed numerical parametric study of the plastic buckling response of stocky columns and stocky plates is undertaken using ADAPTIC (Izzuddin, 1991). This study seeks to investigate the similarities and differences in the buckling behaviour of plates and columns in the plastic range, and will therefore serve as the starting point for assessing existing analytical models for plastic buckling of plates and the development of a new analytical model, as presented in Chapters 5 and 6.

In addition, this chapter investigates the sensitivity of the post-buckling behaviour of columns and plates to geometric properties, such as the slenderness ratio and initial

geometric imperfections, and material properties, such as the yield strength and strain hardening. The primary objective of this study is to identify the main parameters influencing the plastic buckling of columns and plates, and to establish whether there are clear grounds for adopting similar assumptions in the formulation of related analytical models.

4.2 Influence of Slenderness

It was noted in the previous chapter that stocky columns, where the Euler buckling load is greater than the yield load ($P_E > P_Y$), can be categorised into three classes according to their slenderness ratio $\lambda = L/r$: Class 1 with $\lambda < \pi\sqrt{E_t/\sigma_Y}$, Class 2 with $\pi\sqrt{E_t/\sigma_Y} < \lambda < \pi\sqrt{E_R/\sigma_Y}$, and Class 3 with $\pi\sqrt{E_R/\sigma_Y} < \lambda < \pi\sqrt{E/\sigma_Y}$. In order to make comparisons between the plastic buckling of stocky columns and plates, three plates with equivalent slenderness to the corresponding columns in the above three categories are considered, where the equivalent slenderness implies identical ratios of elastic buckling load to yield load P_E/P_Y.

The parametric study is undertaken using ADAPTIC (Izzuddin, 1991), where the Incremental Theory of Plasticity is utilised for both the 1D beam-column elements and the 2D shell elements, allowing for the spread of material plasticity over the cross-section depth/plate thickness and over the 1D element length/2D element area. Furthermore, initial imperfections are required by the nonlinear solution procedure employed in ADAPTIC in order to trace the post-buckling equilibrium path.

A bilinear idealisation of the stress-strain response with a yield strength σ_Y=300MPa and a strain hardening parameter μ=2% is used here. The model columns have a depth h=0.2m and a width b=0.1mm, and are pin-ended. According to the class of column, as noted before, three different slenderness ratios λ=10.4, 17.3 and 26 are selected, for which L=0.6m, 1.0m and 1.5m, corresponding to Classes 1, 2 and 3, respectively. On the other hand, simply-supported square plates are considered with length and width a=b=2.4m. To draw comparisons between columns and plates of similar slenderness, three different b/h ratios are chosen with equivalent slenderness of b/h=6.3, 10.4 and 24, for which h=0.38m, 0.23m and 0.1m, respectively. Figure 4.1 illustrates the geometric configuration and boundary conditions for the

considered columns and plates. It is important to note that all columns are restrained against out-of-plane buckling, and all plates are simply supported and allowed to pull-in along the four edges. Furthermore, only uniaxial loading is considered for the plates ($N_x \neq 0$, $N_y = 0$) in the current parametric study, thus excluding biaxial loading that is not applicable to columns. Finally, a sinusoidal initial imperfection with a maximum amplitude $w_{0i}=b/10000$ (for plates) and $w_{0i}=L/10000$ (for columns), to simulate a nearly perfect structure, is considered.

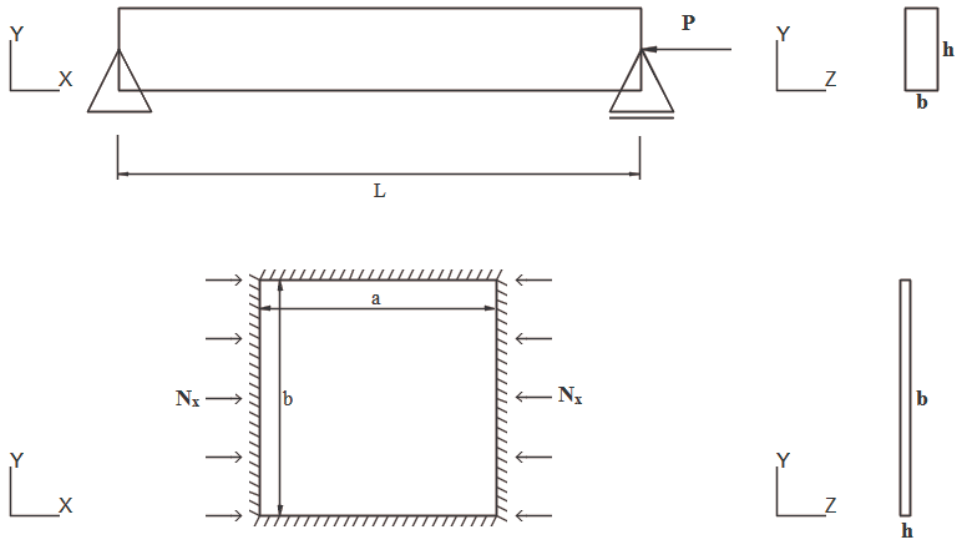

Figure 4.1 Pin-ended column and simply-supported plate

For the case of column, a detailed elasto-plastic model using a cubic elasto-plastic element cbp2 is chosen to perform the analysis (Izzuddin and Elnashai, 1993), where a mesh of 600 elements is used to model a single column. Based on the uniaxial material response, this model can accurately model the spread of plasticity over the cross-section using a fibre approach, where 40 layers/monitoring areas are employed over each cross-section. On the other hand, 9-noded quadrilateral shell elements csv9 (Izzuddin, 2007a;Li *et al.*, 2008) are utilised to model the plate, where a mesh of 24×24 elements is utilised, and 10 integration points are employed over the thickness to model the spread of plasticity. The buckling responses of both structural elements are shown in Figure 4.2a-b, where the loading is normalised with respect to the yield load P_Y.

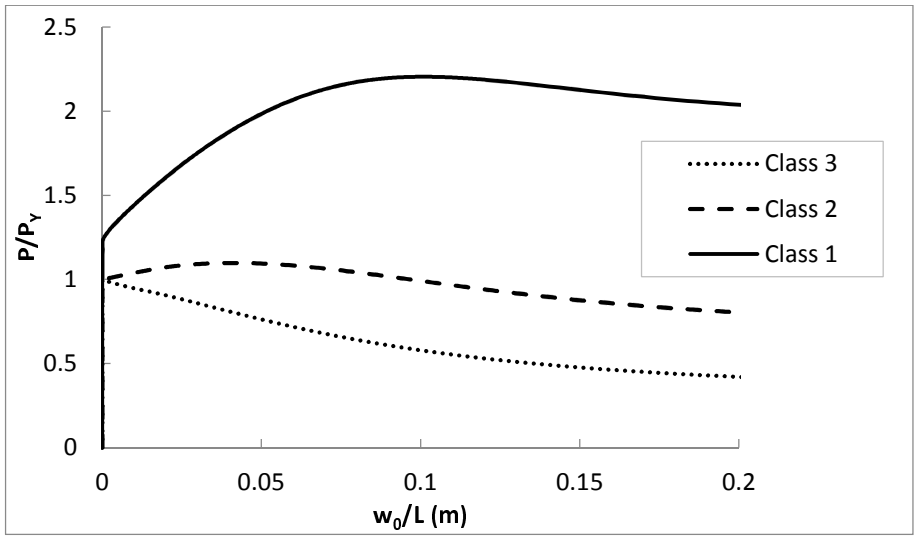

a. Buckling response of stocky columns

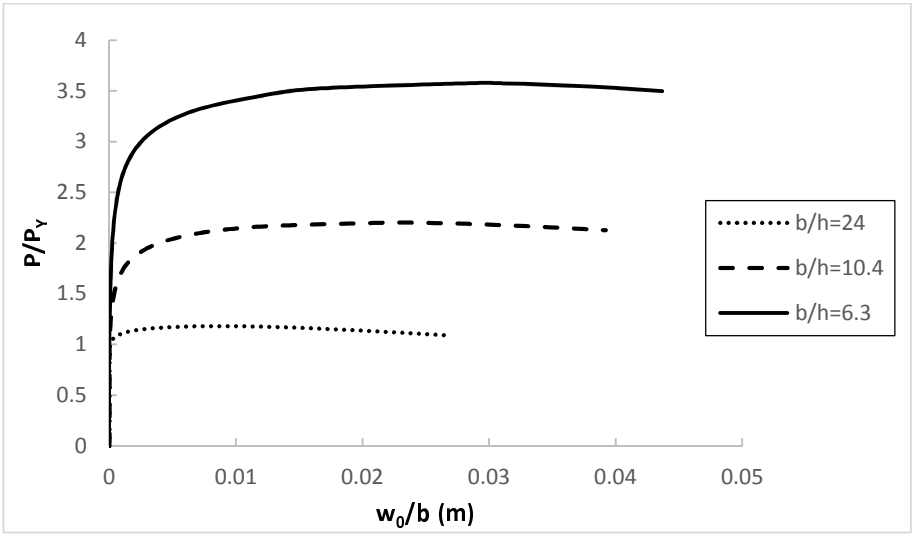

b. Buckling response of stocky plates

Figure 4.2 Influence of slenderness on buckling response of stocky columns and plates

The results reveal some general similarities but also significant differences in the nature of the buckling responses for the two types of structural element. As expected, both stocky plates and columns do not exhibit buckling deflections up to the yield load, and the subsequent deflections up to the point of maximum buckling resistance are relatively small. An interesting difference is that the stocky plates resist much larger loads compared to columns of equivalent slenderness, which may be attributed to the enhanced material stiffness in the plastic range arising for plates under biaxial buckling deformations. However, as elaborated in Chapter 6, the determination of the appropriate material stiffness for stocky plates is not as straightforward as for

columns, since even an Engesser load with a tangent-modulus matrix obtained from the Theory of Plasticity typically overestimates the maximum buckling resistance. Other similarities and differences in the buckling responses of columns and plates are discussed in detail hereafter for each slenderness class.

Class 1 Column with λ=10.4 vs. Plate with b/h=6.3

In line with the findings of Chapter 3, the considered Class 1 stocky column (λ=10.4) starts to buckle at the Engesser load P_t, which is approximately 30% greater than the yield load P_Y, as shown in Figure 4.2a. At this point, elastic unloading takes place on the convex face of column, and the axial load continues to increase until a maximum load P_{max} which is 70% greater than P_t. However, for the plate with equivalent slenderness (b/h=6.3), buckling evidently starts from the yield load P_Y, as illustrated in Figure 4.2b. Compared to the case of column, the load increases gradually until it reaches P_{max} which is 250% greater than P_Y.

The key points of this comparison are as follows:

- The Engesser load for the plate is obtained using the 3x3 tangent modulus matrix from the conventional Incremental Plasticity Theory with the elastic shear modulus ($P_t=76P_Y$) or even with a zero tangent shear modulus ($P_t=48P_Y$) as an alternative value, as shown in Chapter 6, where it is demonstrated that the plate Engesser load is remarkably larger than its ultimate buckling capacity ($P_{max}=3.6P_Y$). Since the plate Engesser load is greater than that of the column ($1.3P_Y$), then it is clear that the effective biaxial plastic material modulus for the governing biaxial deformation mode is greater than the uniaxial plastic modulus.

- The fact that the buckling of plate initiates at P_Y and not at the Engesser load implies that the effective biaxial tangent modulus is initially much less at P_Y than what is obtained from the conventional Incremental Theory even with a zero tangent shear modulus and less than the uniaxial tangent modulus with 2% hardening value governing the column buckling problem.

- While buckling is initiated at a lower relative load compared to the column, the maximum buckling resistance is relatively higher in comparison.

- These features for the plate buckling are realised without elastic unloading (as will be verified in Chapters 5/6), which highlights the complex variation in the effective material modulus at different levels of loading. Further investigation of the mechanics underlying this variation will be undertaken in the following chapters.

Class 2 Column with λ=17.3 vs. Plate with b/h=10.4

Both columns and plates of intermediate stockiness start to buckle at their corresponding yield load P_Y. At this point, strain reversal takes place on the outer fibres of the column middle region, and the load continues to increase towards the reduced-modulus load but is limited by tensile yielding at the outer fibre as discussed in Chapter 3. Analogous to the buckling of the previous stockier plates, the current plate reaches its maximum capacity at a relatively small buckling deflection, with a significant increase in resistance beyond P_Y. On the other hand, the maximum load of the column with intermediate stockiness is only slightly greater than P_Y, as previously elaborated in Chapter 3.

Class 3 Column with λ=26 vs. Plate with b/h=24

As expected, the Class 3 column buckles at P_Y, and the post-buckling resistance is vanishes, thus P_Y is also the maximum buckling capacity. On the other hand, a plate with equivalent slenderness still exhibits a marginal increase in the post-buckling resistance, and clearly provides a more ductile response compared to the column.

Summary

In the above, the post-buckling responses of stocky columns and plates have been compared considering different slenderness ratios for a specific yield strength, strain hardening and initial imperfection. It has been observed that plates always start buckling at P_Y regardless of their slenderness, whereas the onset of column buckling is at the Engesser load, which could either be P_Y or P_t depending on the column

slenderness ratio. The comparisons have shown some similarities between column and plate buckling, where the increase in buckling resistance compared to the initial buckling load is clearly inversely related to slenderness. However, in relation to the question previously posed in Section 4.1, there are clear differences in relation to the adequacy of the tangent-modulus and reduced-modulus buckling loads as lower and upper bounds on the maximum buckling resistance. While these bounds are applicable to the buckling assessment of Class 1 and 2 stocky columns, even the tangent-modulus plate buckling load obtained from the conventional Incremental Theory is much higher than its maximum buckling load. Clearly, therefore, a reduced-modulus theory would provide even larger and less realistic predictions of the maximum buckling resistance of the stocky plates. This highlights the need for further investigation of the mechanics underlying plastic buckling of stocky plates, where it is evident that the issue of continuous variation in the tangent material response with loading over the plastic range is central to the development of any related analytical model.

4.3 Influence of Yield Strength

It was shown in the previous section that the onset of buckling occurs at yield load for both stocky plates and columns, except for Class 1 columns where buckling initiates at the Engesser load. Therefore, it would be informative to investigate the effects of material yield strength on the initial buckling load, the post-buckling response and particularly on the maximum load P_{max}. Numerical analyses are carried out for the same model plates and columns investigated in the previous section but for an additional yield strength f_Y=240MPa. The corresponding load-deflection curves are plotted as dashed lines in Figure 4.3, where the applied load is normalised with respect to the yield load corresponding to f_Y=240MPa.

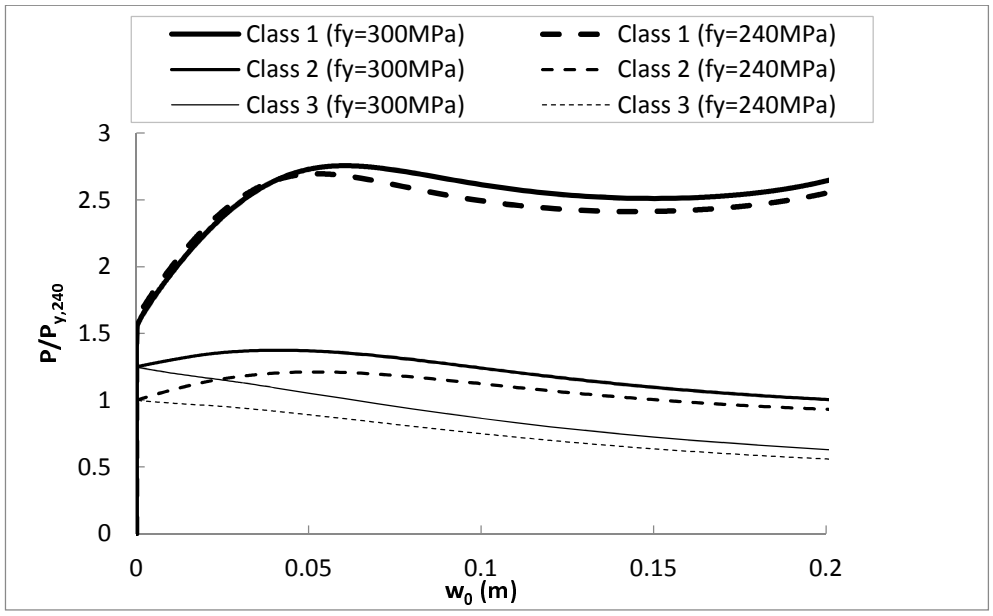

a. Buckling response of stocky columns with different yield strengths

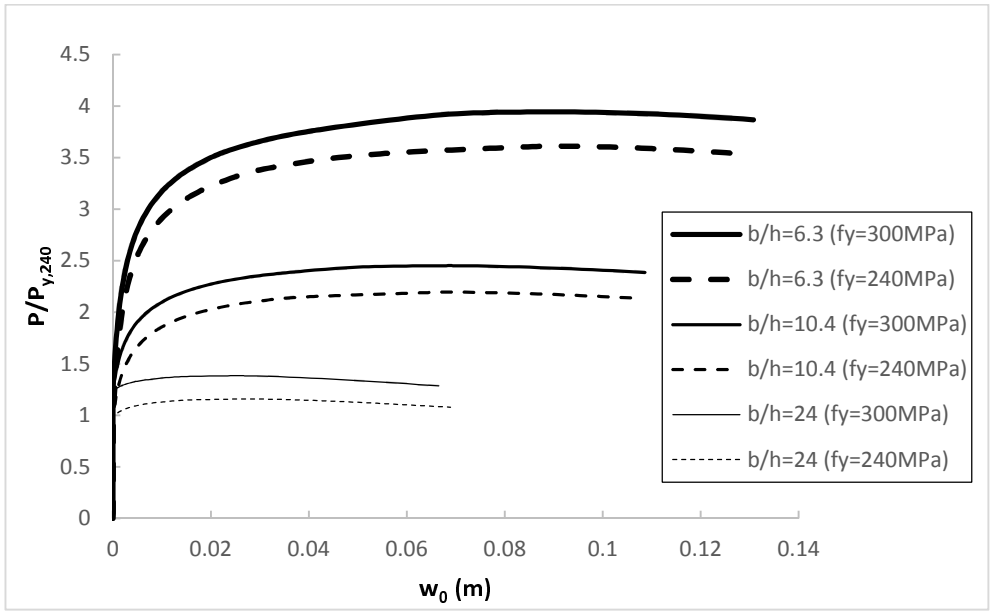

b. Buckling response of stocky plates with different yield strengths

Figure 4.3 Influence of yield strength on buckling response of stocky columns and plates

From Figure 4.3a, it can be seen that the change in yield strength hardly affects the initial buckling load of Class 1 columns with λ=10.4. This is consistent with the fact that very stocky columns start to buckle at the tangent-modulus load P_t which is greater than the yield load and independent of the yield strength. However, the

maximum load is slightly reduced using a lower grade steel, which is attributed to earlier tensile yielding.

On the other hand, the initial buckling loads of the Class 2 and 3 columns, with λ=17.3 and 26, respectively, are both P_Y and thus determined by the yield strength. While the same influence is realised in relation to the maximum buckling capacity of the Class 3 column, the maximum capacity of the Class 2 column is less influenced by the yield strength.

In comparison with the columns, the initial buckling load and maximum buckling resistance of the stocky plates are directly influenced by the yield strength, regardless of slenderness. This again highlights a basic difference in that the effective tangent material modulus for plates not only varies with loading but is also influence by the yield strength.

4.4 Influence of Strain Hardening

In order to assess the influence of strain hardening on the buckling response of stocky columns and plates, different hardening parameters μ=1%, 2% and 4% are considered for the bilinear material model with a yield strength of 300MPa. The results for the Class 1 and 2 column and the corresponding plates of equivalent slenderness are presented in Figure 4.4 and Figure 4.5, respectively. It can be seen that the plastic buckling response of both columns and plates is highly sensitive to strain hardening, as reflected in the material tangent modulus E_t.

Considering the column results in Figure 4.4a, it is clear that strain hardening does not affect the initial buckling load for λ=17.3, at least in the considered range of μ, since the original Class 2 column with μ=2% remains Class 2 but with μ=4% and becomes Class 3 with μ=1%, all of which buckle initially at P_Y. However, strain hardening affects the maximum buckling capacity of the Class 2 columns, as it has a direct effect on the reduced-modulus von Karman load. On the other hand, for λ=10.4 (Figure 4.4b), strain hardening has a direct influence on both the initial and maximum buckling loads. Since the columns with μ=2% and 4% are Class 1, thus they buckle at Engesser tangent-modulus load, while the column with μ=1% is Class 2 and buckles initially at P_Y. Furthermore, it is clear from Figure 4.4 that the

influence of strain hardening on the maximum load is greater for the stockier column, where the maximum load is almost proportional to strain hardening.

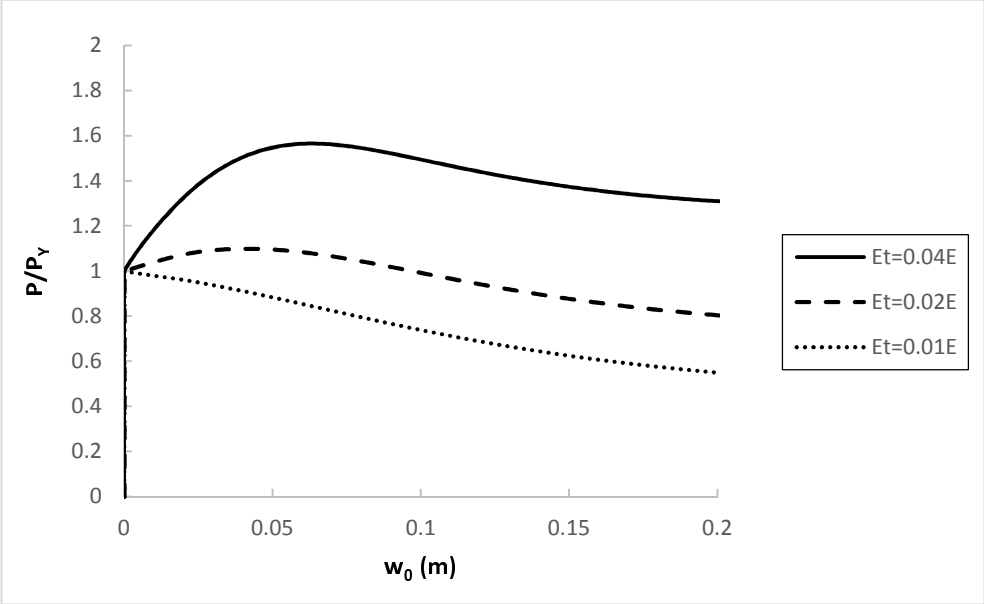

a. λ=17.3

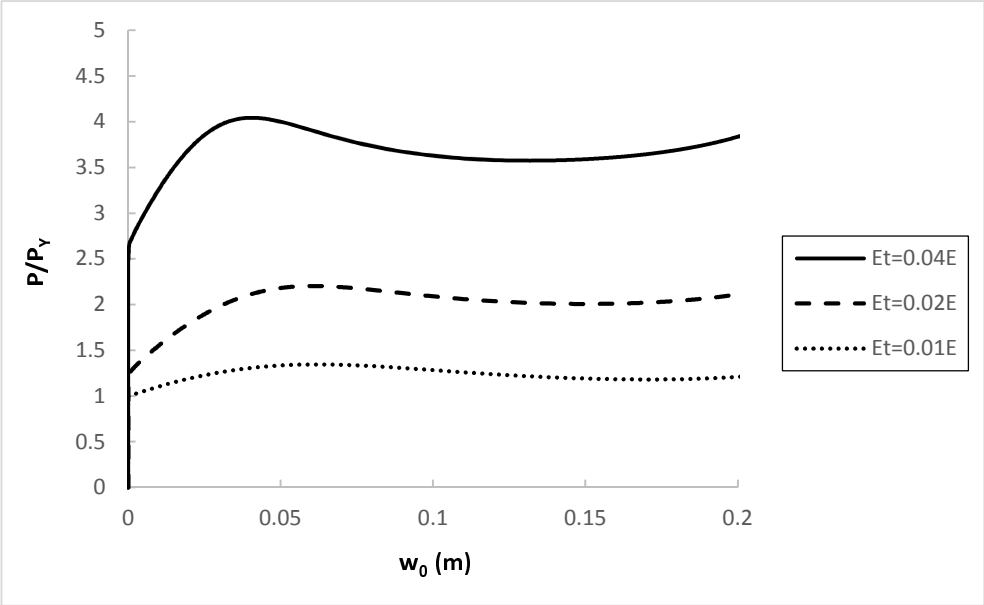

b. λ=10.4

Figure 4.4 Influence of strain hardening on buckling response of stocky columns

Figure 4.5 shows the influence of strain hardening on the buckling response of stocky plates, where it is clear that the initial buckling load is not affected by the change in strain hardening, as this is the yield load regardless of slenderness. However, the maximum buckling strength is evidently influenced by strain

hardening, though the impact is not as drastic as in the case of the Class 1 stocky column (λ=10.4). Nevertheless, similar to plastic column buckling, the influence of strain hardening is greater for the stockier plate (b/h=6.3).

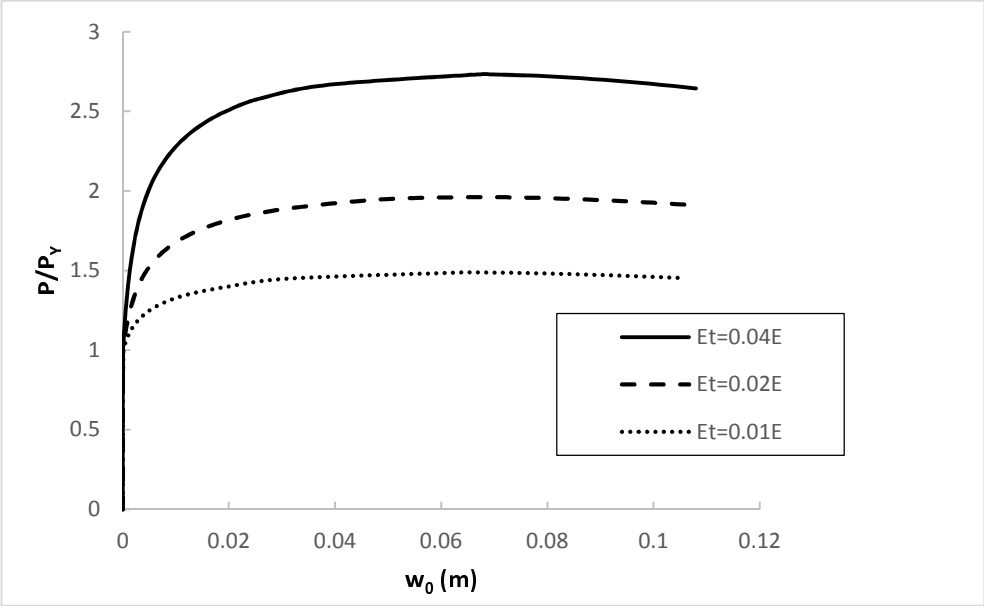

a. b/h=10.4

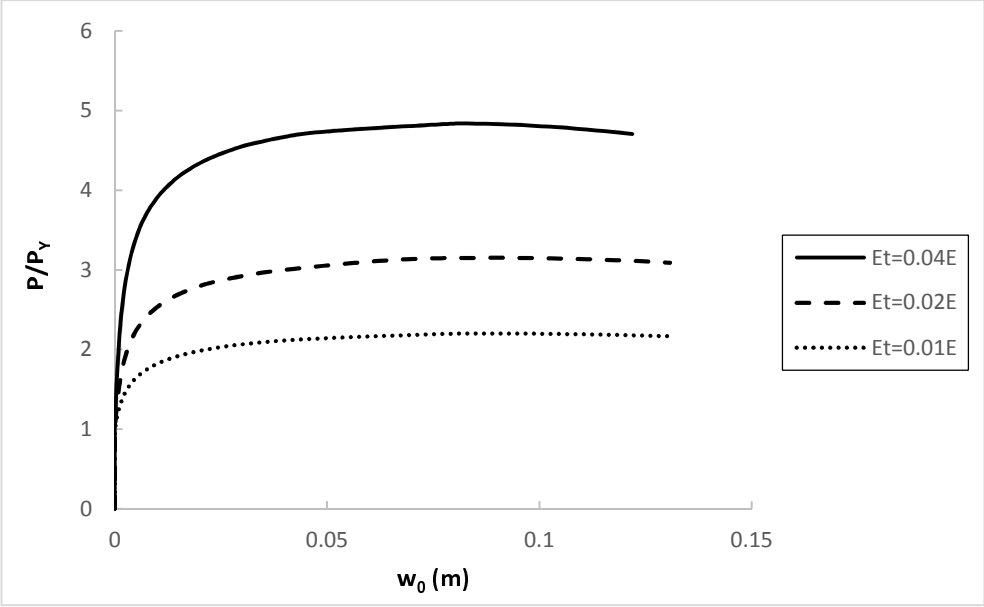

b. b/h=6.3

Figure 4.5 Influence of strain hardening on buckling response of stocky plates

4.5 Imperfection Sensitivity

The inevitable presence of initial geometric imperfections in structural elements can have an important impact on their buckling response. In the previous chapter, the

effect of imperfections on the post-buckling behaviour of Class 1 stocky columns (λ=10.4) was studied using the proposed analytical model, and the model predictions were verified against the numerical results of ADAPTIC. It was also shown that there exists a threshold level of imperfection for Class 1 columns beyond which further increase in the amplitude of imperfection hardly affects the post-buckling response. A similar imperfection sensitivity study is carried out here using ADAPTIC for a stocky plate with equivalent slenderness (b/h=6.3) in search for the existence of a similar threshold imperfection.

To investigate the imperfection sensitivity of the stocky plate, various imperfection amplitudes w_{0i}= b/8000, b/4000, b/2000, b/1000, b/500 and b/250 are considered. As previously noted, the geometric imperfection is modelled assuming a half-wave sinusoidal shape with a maximum amplitude of w_{0i} in the centre of the plate. Figure 4.6 illustrates the effect of imperfections on the plastic buckling response of the stocky plate.

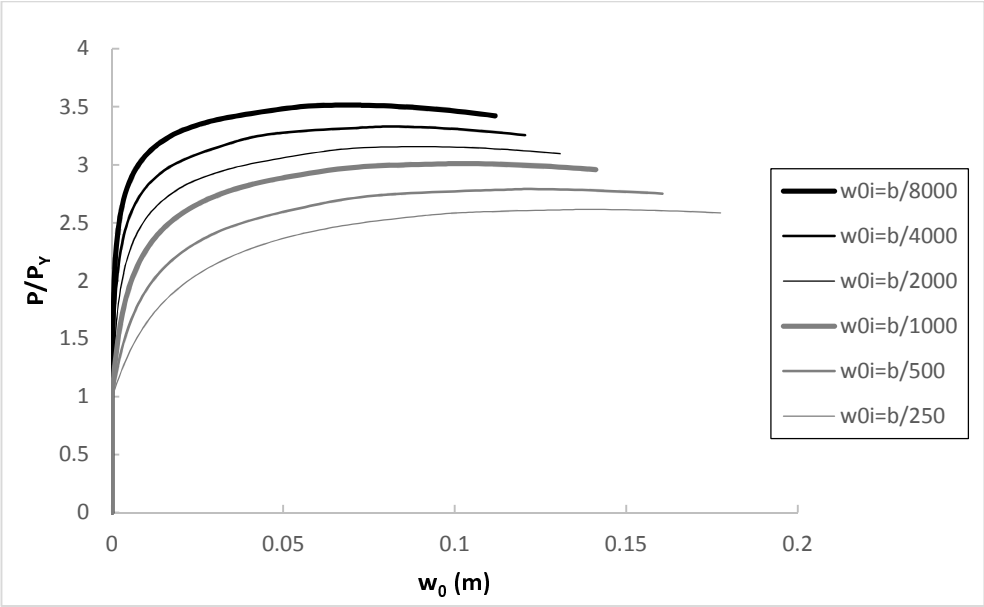

Figure 4.6 Influence of initial imperfections on buckling response of stocky plate (b/h=6.3)

The inclusion of imperfections clearly has a significant influence on the buckling response of plates including the maximum buckling capacity, where the buckling resistance continues to reduce with increasing levels of imperfection. Compared to the response of the equivalent stocky column (λ=10.4), obtained using ADAPTIC

and presented in Figure 4.7, the plate exhibits considerable sensitivity to the amplitude of initial imperfection. As can be noted from Figure 4.7, the load at which buckling starts for a Class 1 stocky column is also affected by imperfection, as captured by the analytical model presented in Chapter 3.

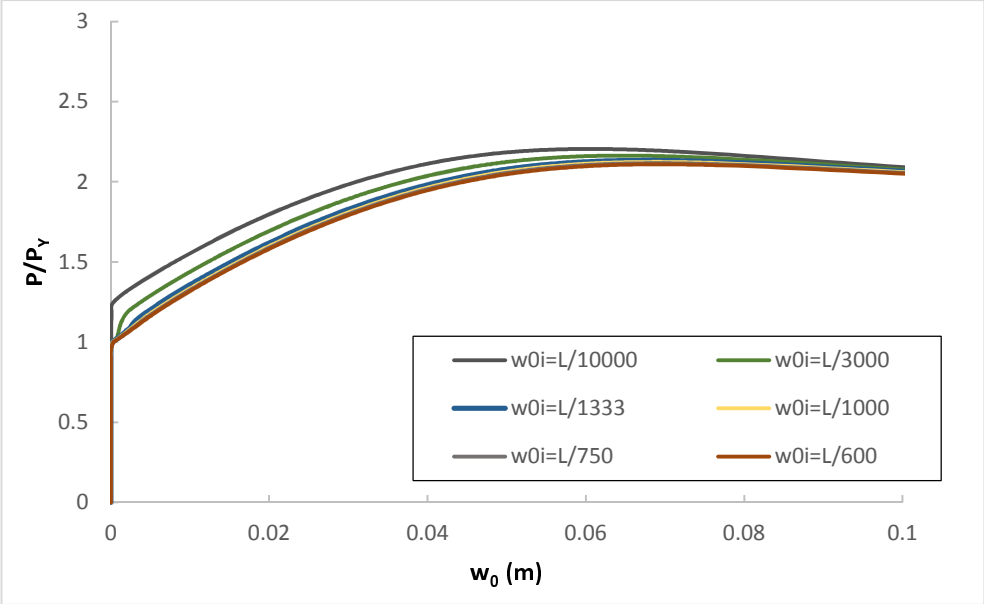

Figure 4.7 Influence of initial imperfections on buckling response of stocky column (λ=10.4)

Importantly, there does not appear to be a threshold imperfection for stocky plates as observed for the equivalent stocky column, for which the threshold is $w_{0i,max}$=L/1333. To clearly demonstrate this, imperfection sensitivity diagrams are produced in Figure 4.8 where maximum buckling loads P_{max} are plotted against the corresponding amplitudes of imperfection. As can be seen, the imperfection sensitivity is stronger for the plate than for the column with equivalent slenderness. Displaying a high sensitivity to the initial imperfections for inelastic plates may be due to the fact that there is no elastic unloading during buckling unlike the case of inelastic columns where buckling is accompanied with strain reversal.

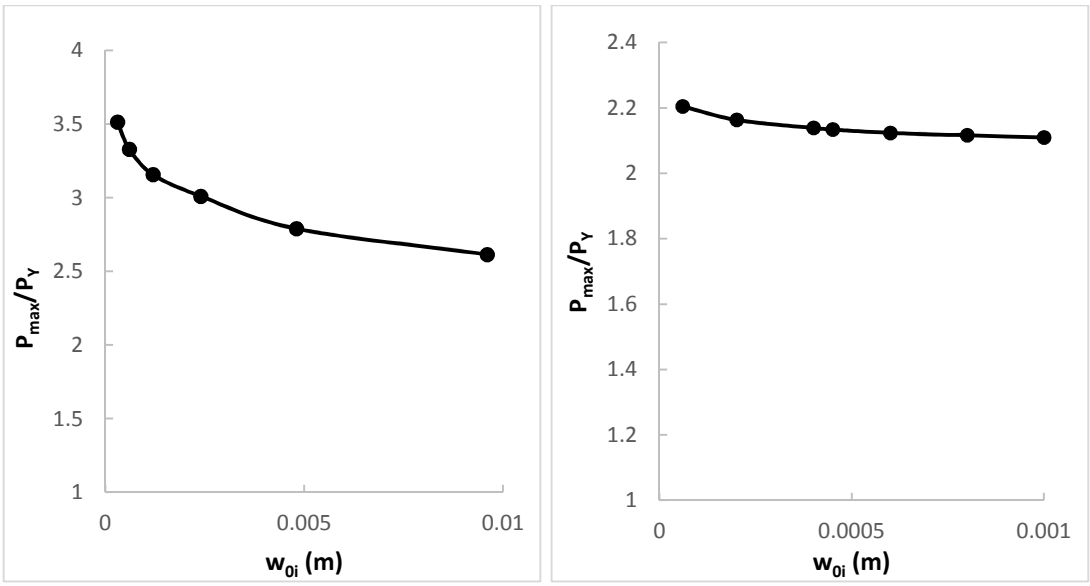

a. Plate with b/h=6.3 b. Column with λ=10.4

Figure 4.8 Imperfection sensitivity of stocky plate and column

4.6 Conclusions

This chapter has presented a comparative parametric study of the plastic buckling response, from initiation of buckling to the maximum buckling resistance, between stocky columns and plates using the nonlinear analysis program ADAPTIC. The influence of parameters such as slenderness ratio, material yield strength, strain hardening and initial imperfection has been considered. The comparative study of these two structural elements has confirmed that principles of mechanics governing the plastic buckling of plates are not a simple extension of those principles previously identified in Chapter 3 for the plastic buckling of columns. In particular, the role of the Engesser load as a lower bound on the maximum buckling resistance is put into question. It appears that, unlike columns, the plastic buckling of plates is governed by an effective tangent material modulus which starts relatively small at the yield load and increases with loading, but never reaches the level predicted by the conventional Incremental Theory of Plasticity. Accordingly, the buckling of plates is always initiated at the yield load, and the subsequent enhancement in the maximum buckling resistance, as also influenced by both the yield strength and strain hardening, is typically greater for plates than for columns of equivalent slenderness.

Moreover, it has been shown that a threshold imperfection, which was previously identified for Class 1 stocky columns, is notably absent for stocky plates.

The differences noted above in the plastic buckling response of columns and plates are mainly attributed to the biaxial nature of the deformations induced in the buckling of plates supported on four edges. This implies the need for a more sophisticated treatment of plastic plate buckling compared to columns, and sets the scene for the challenges to be addressed in the following chapters.

CHAPTER 5

On the Plate Plastic Buckling Paradox

5.1 Introduction

In Chapter 2, the two well-known theories of plasticity (i.e. Deformation Theory and Incremental Theory) were discussed in detail. It was shown that although Incremental Theory accords better with the accepted principles of plasticity than Deformation Theory, it predicts critical buckling stresses for plates which are significantly higher than those obtained from Deformation Theory. In addition, the test results obtained from experiments performed on simply-supported plates (Pride and Heimerl, 1949) are in good agreement with the predictions of the less correct Deformation Theory. In the last few decades, many efforts have been devoted to solving what is thus known as "Plate Plastic Buckling Paradox" (see Chapter 2), yet there is still a debate surrounding this issue.

One of the few attempts (Haaijer, 1957;Haaijer and Thurlimann, 1958;Shrivastava and Bleich, 1976;Dawe and Grondin, 1985), as mentioned in the literature review, to resolve the Plate Plastic Buckling Paradox involves the amendment of the shear modulus in the plastic region (G_t). A recent paper by Becque (2010), based on the Flow Theory of Plasticity, establishes an equation for plastic shear stiffness to avoid the paradox. He claims that the origin of the "Plate Plastic Buckling Paradox" is in the incorrect modelling of the shear stiffness in the Incremental Theory, which in turn is due to the incorrect assumption that the plate undergoes plastic deformations only in the longitudinal x- and transverse y-directions, with incremental plastic shear deformations excluded at the onset of buckling (Becque, 2010). However, it will be demonstrated here that his approach is not founded on sound principles of mechanics, and therefore it is also incorrect.

On this topic, a detailed analysis, both numerical and analytical, has been performed and a rational explanation for the plastic buckling paradox is presented. Gaining

insight into what actually happens in the course of elasto-plastic buckling of plates not only puts an end to the plastic buckling paradox but can also offer reliable predictions for the inelastic buckling of structures.

5.2 Becque's Explanation

Recently, a modification to J_2 Flow Theory has been proposed by Becque (2010) where it is claimed that this method can overcome the "Plate Plastic Buckling Paradox" by determining the shear stiffness from second-order considerations. In his work, Becque investigated the local buckling of a flat plate without any initial imperfections and under uniform axial loading (Figure 5.1), where a flow rule based on Hill's anisotropic yield criterion is employed. Becque (2010) puts forward his method applied to plates loaded in one direction σ_x as follows.

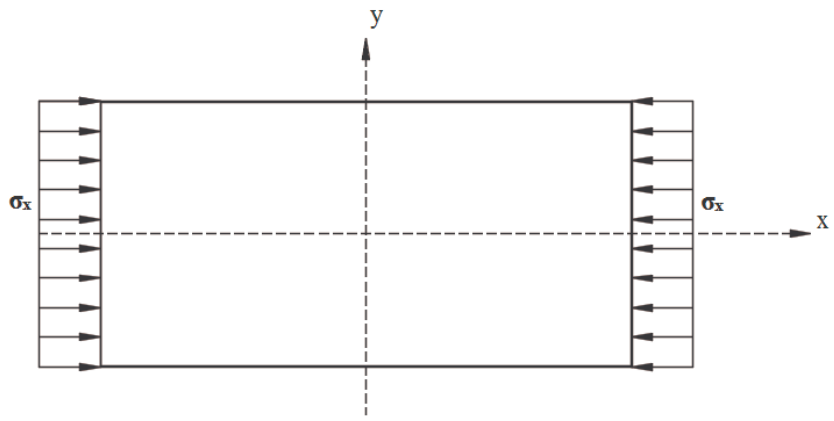

Figure 5.1 Plate under uniform axial loading (Becque, 2010)

According to the associated flow rule and the von Mises yield criterion, the ratio of the plastic strain in the principal y-direction to the plastic strain in the principal x-direction at the point of buckling is:

$$\frac{\dot{\varepsilon}_{p,y}}{\dot{\varepsilon}_{p,x}} = k = -\frac{1}{2} \tag{5.1}$$

Note that Becque uses "·" to indicate increments.

From the material stress-strain curve the following relations can be determined:

$$\dot{\varepsilon} = \dot{\varepsilon}_{el} + \dot{\varepsilon}_{p} \tag{5.2}$$

$$\frac{\dot{\sigma}}{E_t} = \frac{\dot{\sigma}}{E} + \frac{\dot{\sigma}}{E_p} \tag{5.3}$$

where E is the initial modulus and E_t is the tangent modulus and E_p relates the plastic strain increments to the plastic stress:

$$\dot{\sigma} = E_p \dot{\varepsilon}_p \tag{5.4}$$

so that:

$$\frac{1}{E_p} = \frac{1}{E_t} - \frac{1}{E} \tag{5.5}$$

Becque states that under the load increment corresponding to $\dot{\sigma}_x$, the plate buckles out of its initial flat shape and undergoes a shear deformation. Next, Mohr's circle is used to find the plastic shear strain increments along the inclined planes (Figure 5.2) so that a relationship could be established between the plastic component of the shear strain θ_p and the principal plastic strain increment $\dot{\varepsilon}_p$ associated with the load increment $\dot{\sigma}_x$:

$$\theta_p = \frac{(1-k)}{2} \dot{\varepsilon}_{p,x} \sin\theta \tag{5.6}$$

where $\theta = \theta_e + \theta_p$

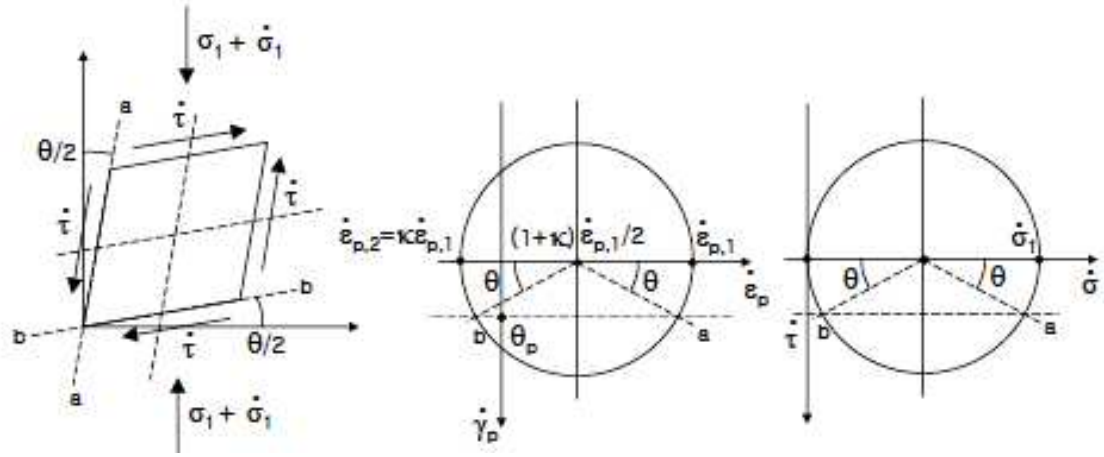

Figure 5.2 Mohr's circles of plastic strain and stress increments (Becque, 2010)

Comment: The application of Mohr's circle to find the associated plastic shear strain increment is not rational, since this is obtained by multiplying the increment of plastic strain $\dot{\varepsilon}_{p,x}$ with an infinitesimal rotation which leads to a zero value of θ_p.

Becque carries on with his argument as follows:

Since $\dot{\varepsilon}_{p,x} = \frac{\dot{\sigma}_x}{E_p}$ then:

$$\theta_p = \frac{(1-k)}{2}\frac{\dot{\sigma}_x}{E_p}\sin\theta \tag{5.7}$$

Using Mohr's circle the shear stress can be determined as a result of an increase in the axial stress $\dot{\sigma}_x$:

$$\dot{\tau} = \frac{\dot{\sigma}_x}{2}\sin\theta \tag{5.8}$$

Combining the elastic $(\theta_{el} = \tau / G)$ and the plastic components of the shear strain increment, a modified shear modulus can be adapted for the inelastic buckling of plates (ν is the Poisson's ratio):

$$\dot{\tau} = \bar{G}\theta = \frac{E_t E}{(1+k+2\nu)E_t + (1-k)E}\theta \tag{5.9}$$

Comment: As can be noted, $\bar{G}$ is directly proportional to E_t which indicates that in case of an elastic-perfectly plastic material model (i.e. E_t=0), $\bar{G}$ becomes practically zero. However, the latter cannot be correct since in the Incremental Theory based on the associated flow rule, when an element is loaded uniaxially up to the yield point and then loaded in shear (i.e. constant axial load) its incremental response to applied shear is elastic.

The main point is that Becque's $\bar{G}$ expresses the variation of the shear stress τ with shear strain θ in an arbitrarily inclined reference system, for increments of plastic strain in the original system that do not include plastic shear strain. It does not inform the variation of shear stress with shear strain when the incremental deformations in the original reference system include shear strain.

In addition to his incorrect derivation of the plastic shear modulus, Becque presents the incremental stress-strain relations as follows:

$$\dot{\varepsilon}_x = \dot{\varepsilon}_{el,x} + \dot{\varepsilon}_{p,x} = (\frac{\dot{\sigma}_x}{E} - \nu\frac{\dot{\sigma}_y}{E}) + \frac{\dot{\sigma}_x}{E_p} = \frac{\dot{\sigma}_x}{E_t} - \nu\frac{\dot{\sigma}_y}{E} \tag{5.10}$$

$$\dot{\varepsilon}_y = \dot{\varepsilon}_{el,y} + \dot{\varepsilon}_{p,y} = (\frac{\dot{\sigma}_y}{E} - \nu\frac{\dot{\sigma}_x}{E}) + \kappa\frac{\dot{\sigma}_x}{E_p} = \frac{\dot{\sigma}_y}{E} + \dot{\sigma}_x(\frac{\kappa}{E_t} - \frac{\nu+\kappa}{E}) \tag{5.11}$$

As can be noticed, he does not take the influence of $\dot{\sigma}_y$ on $\dot{\varepsilon}_{p,x}$ into account, which is incorrect given that buckling induces biaxial bending stresses. Furthermore, this assumption leads to an asymmetric tangent stiffness matrix, which does not accord with the outcome of the theory of plasticity. Yet, Becque carries on solving the classical differential equation, describing the buckling of elastic plates, but with different coefficients to allow for plastic buckling, including the influence of his modified shear modulus. As a result, Becque establishes a formula to estimate the lowest inelastic buckling load for a long simply-supported plates under axial thrust. By introducing a variable number of half-waves m of the sinusoidal buckling mode

over the plate length "a" in the direction of loading, with a single half-wave over the plate width "b", he establishes that the optimal longitudinal half-wave length associated with the lowest plastic buckling load is much smaller than the transverse half-wave length "b", as expressed by:

$$\frac{a}{m} = \sqrt[4]{\frac{E_t}{E}}b \tag{5.12}$$

However, it will be shown in Chapter 7 that this outcome is incorrect, which casts further doubts on the validity of Becque's shear modulus and his effective tangent modulus matrix used for plastic buckling analysis of plates.

Based on the above arguments, Becque's proposed method cannot be considered as a valid method for obtaining the inelastic local plate buckling mainly because it is not based on sound principles of mechanics. As such, Becque's explanation of the plastic buckling paradox is not considered to be credible.

5.3 On the Reduction in Shear Stiffness

5.3.1 Description of Problem

Previous studies have suggested that, unlike Incremental Theory which considers a constant elastic shear stiffness G for plate buckling, the shear stiffness reduces with an increase in load when stresses exceed the material yield strength (See Chapter 2). To investigate the accuracy of this hypothesis, numerical analysis using the nonlinear finite element analysis program ADAPTIC (Izzuddin, 1991) has been undertaken on a simply supported plate subject to uniaxial loading. The outcomes of the numerical analysis are then considered in conjunction with a comprehensive analytical study to shed important light on the Plate Plastic Buckling Paradox.

5.3.2 Reduction of Shear Stiffness

Consider a square flat plate of length a = b = 2.4m and thickness h, loaded in-plane with a uniform uniaxial compressive load P, as illustrated in Figure 5.3. The plate is simply-supported along its four edges, and a slenderness ratio (b/h=20) is chosen for a stocky plate to induce plastic buckling.

A detailed elasto-plastic analysis of this stocky plate is performed using ADAPTIC (Izzuddin, 1991), specifically the 9-noded shell element (Izzuddin and Li, 2004;Izzuddin, 2007a). This element accounts for geometric nonlinearity, and it employs material models for steel based on the incremental theory of plasticity, where the spread of plasticity over the plate area and thickness is incorporated. Moreover, with the ability to consider other factors such as geometric imperfection, influence of transverse shear deformation for thick plates and the pull-in effects, this element provides a rigorous simulation of inelastic plate buckling problems.

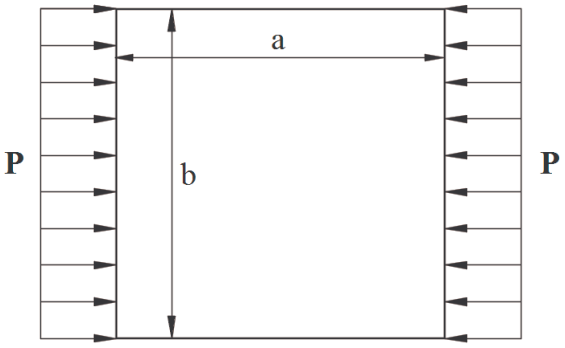

Figure 5.3 Square plate under uniform axial loading

To ensure accuracy of analysis in the plastic range, the plate is discretised into a mesh of 24×24 9-noded shell elements, with 10 integration points used over the thickness of the plate to model the associated spread of plasticity. A bilinear material model is selected with the properties provided in Table 5.1.

Table 5.1 Properties of bilinear material model

Properties	**Values (dimensions)**
Modulus of Elasticity E	210×10^9 (N/m^2)
Poisson ratio ν	0.3
Yield Strength σ_Y	300×10^6 (N/m^2)
Strain-hardening $\mu = E_t/E$	0.02
Elastic Shear Modulus $G=E/(2+2\nu)$	8.077×10^{10} (N/m^2)

The plate is assumed to have an initial sinusoidal imperfect geometry (i.e. a half-wave length in both x- and y-direction such as the buckling mode of an elastic eigenvalue problem) for which the maximum magnitude is taken as (w_{0i} = b/1000).

The plate is proportionally loaded in the x-direction at its mid-plane according to a load factor ($\rho=P/P_Y$), where P_Y is the load at yield, switching between load and displacement control whilst tracing the transverse displacement w_0 along the equilibrium path in the pre- and post-buckling stages.

After performing the analysis, three elements are selected from three different locations over the plate domain for further inspection (i.e. near corner, centre and intermediate), as illustrated in Figure 5.4. In addition to post-buckling response, increments of twisting moment ΔM_{xy} and twisting curvature $\Delta\kappa_{xy}$ are extracted from the results file to establish the effective tangent shear modulus G_t:

$$G_t = \left(\frac{12}{h^3}\right)\frac{\Delta M_{xy}}{\Delta\kappa_{xy}} \tag{5.13}$$

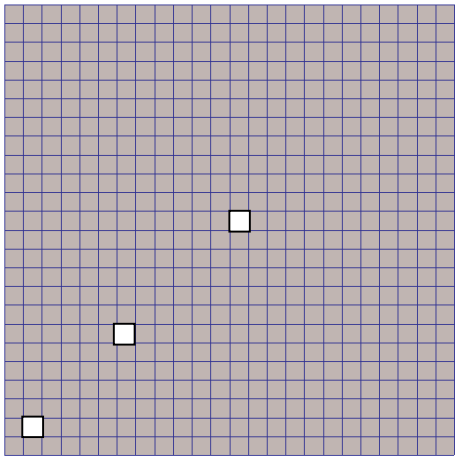

Figure 5.4 Finite elements selected at various locations over plate

The load-transverse deflection response of the plate is shown in Figure 5.5. The onset of buckling occurs at the yield point ($P_Y = 8.64\times10^7$N) beyond which the plate starts to exhibit significant transverse displacement, indicating the onset of buckling. The plate continues to sustain more load till it reaches its maximum buckling load

($P_{max}=1.0\times10^{8}$N), which is then followed by load reduction at moderate displacements ($w_0\approx h/3$ where h=0.12m).

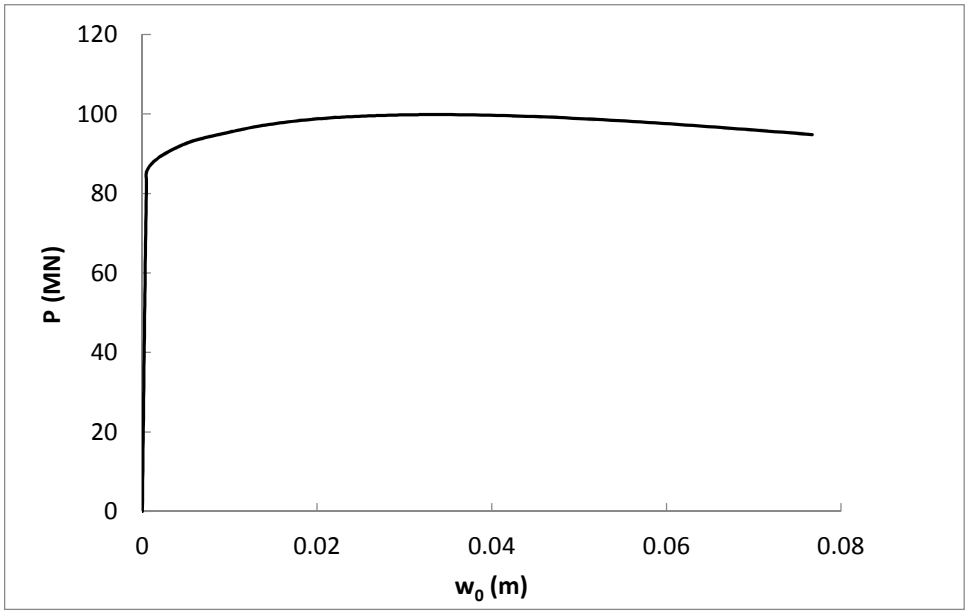

Figure 5.5 Buckling response of a square plate (b/h=20)

Figure 5.6 illustrates the values of the effective tangent shear stiffness with the increase in load/displacement. As can be noted from Figure 5.6, up to the yield point, the tangent shear stiffness is constant and equal to the initial elastic shear modulus ($G = 8.077\times10^{10}$). However, G_t drops dramatically once the load exceeds P_Y up to a point beyond which it largely remains constant. This numerical investigation clearly ascertains the inadequacy of methods assuming that the tangent shear stiffness remains equal to the elastic value in the inelastic range, as is the case with Incremental Theory for example.

To explain this phenomenon in application of plastic buckling, and to point out the shortcomings of the Incremental Theory of Plasticity, the behaviour of a plate element under combined (normal/shear) stresses is studied using an analytical model.

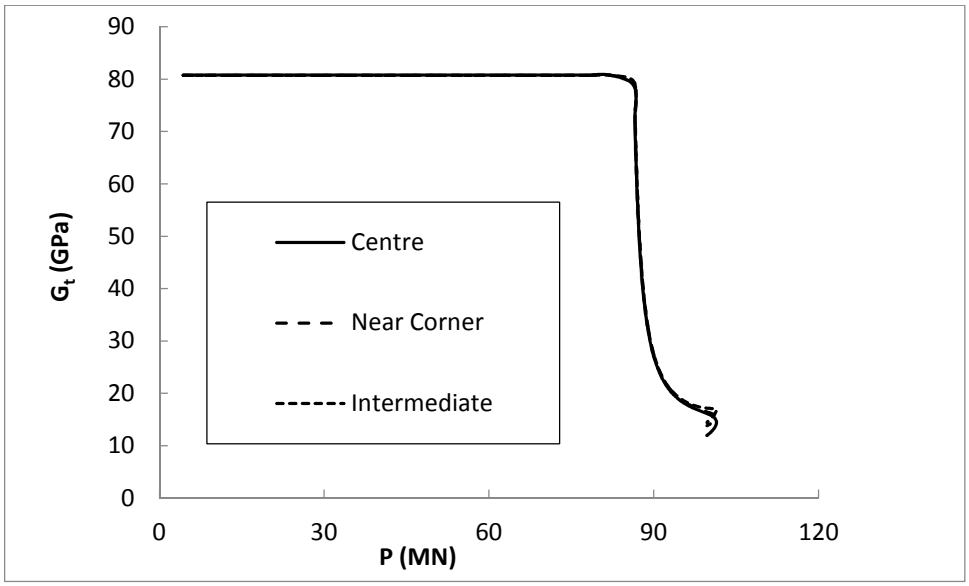

a. Shear modulus G_t versus applied load P

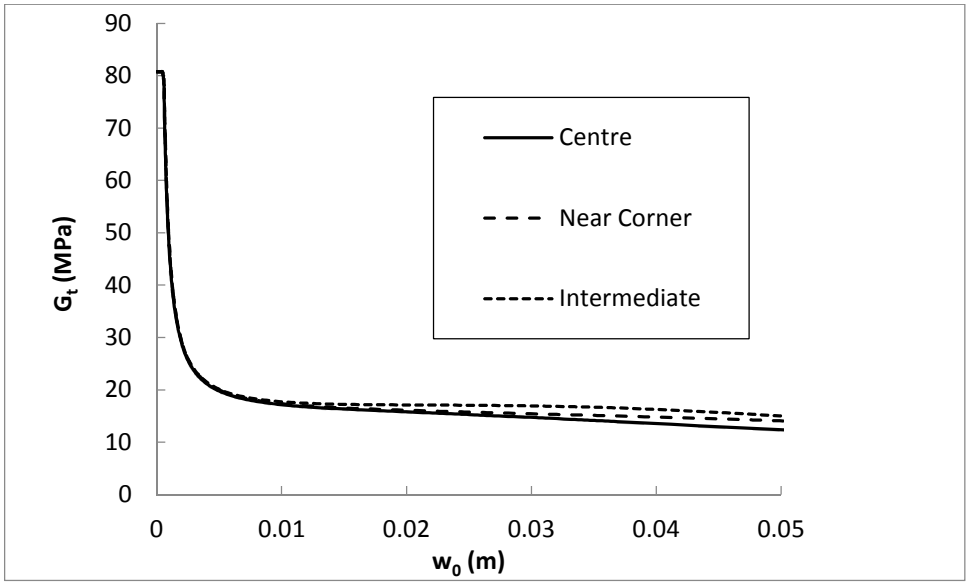

b. Shear modulus G_t versus transverse displacement w_0

Figure 5.6 Variation of shear stiffness with applied load and transverse displacement

5.3.3 Analytical Investigation of Tangent Shear Stiffness Reduction

In this section, the changing magnitude of the tangent shear stiffness is monitored for an element sustaining only normal stress σ_x and shear stress τ_{xy} under the action of corresponding strains, considering plasticity theory with both isotropic and kinematic hardening.

In accordance with the associated flow rule, and the implementation details of von Mises plasticity by Izzuddin and Lloyd Smith (1996), an analytical procedure is

established such that for given normal and shear strain increments $\left(\Delta\varepsilon_x, \Delta\gamma_{xy}\right)$, the stress state $\left(\sigma_x, \tau_{xy}\right)$ corresponding to the strains $\left(\varepsilon_x, \gamma_{xy}\right)$ is obtained from previous values $\left(\sigma_{x0}, \tau_{xy0}\right)$.

The interaction between normal stress σ_x and shear stress τ_{xy} is expressed by the von Mises yield criterion, assuming isotropic hardening, as follows:

$$f\left(\sigma_x, \tau_{xy}, \varepsilon_p\right) = \sqrt{\sigma_x^2 + 3\tau_{xy}^2} - \sigma_0 = 0 \tag{5.14}$$

where:

$$\sigma_0 = \begin{cases} \sigma_Y + H\lambda, \Delta\lambda \le 0 \\ \sigma_Y + H\left(\lambda + \Delta\lambda\right), \text{otherwise} \end{cases} \tag{5.15}$$

with H as hardening modulus $H = EE_t/\left(E + E_t\right)$, σ_0 the current value of yield stress and ε_p the accumulated plastic strain presented in terms of λ.

For the given strain increments the elastic stress state (i.e. elastic predictors) is evaluated as:

$$\begin{pmatrix} \sigma_{xe} \\ \tau_{xye} \end{pmatrix} = \begin{pmatrix} \sigma_{x0} \\ \tau_{xy0} \end{pmatrix} + \begin{bmatrix} E & 0 \\ 0 & G \end{bmatrix} \begin{pmatrix} \Delta\varepsilon_x \\ \Delta\gamma_{xy} \end{pmatrix} \tag{5.16}$$

where E is the Young's modulus and G is the elastic shear modulus. At the first step $\left(\sigma_{x0}, \tau_{xy0}\right)$ is the initial stress state.

Putting the elastic stresses back into the von Mises equation we can find out whether the current stress state exceeds the yield surface with $\sigma_0 = \sigma_0^o = \sigma_Y + H\lambda$. If the solution lies within the yield surface, the actual response is elastic; however, if the elastic estimation of the stress state exceeds the yield surface, plastic strain increments $\left(\Delta\varepsilon_x^p, \Delta\gamma_{xy}^p\right)$ are then applied to bring the stress state back to the interaction surface:

$$\begin{pmatrix}\sigma_x\\ \tau_{xy}\end{pmatrix}=\begin{pmatrix}\sigma_{xe}\\ \tau_{xye}\end{pmatrix}-\begin{bmatrix}E & 0\\ 0 & G\end{bmatrix}\begin{pmatrix}\Delta\varepsilon_x^p\\ \Delta\gamma_{xy}^p\end{pmatrix} \tag{5.17}$$

where:

$$\begin{pmatrix}\Delta\varepsilon_x^p\\ \Delta\gamma_{xy}^p\end{pmatrix}=\Delta\lambda\begin{pmatrix}\dfrac{\partial f}{\partial\sigma_x}\\ \dfrac{\partial f}{\partial\tau_{xy}}\end{pmatrix} \tag{5.18}$$

with $\Delta\lambda$ a positive multiplier for the incremental plastic strain and $\{N\}=\langle\partial f/\partial\sigma_x \quad \partial f/\partial\tau_{xy}\rangle^T$ the current normal.

As a result, the above simultaneous equations can be solved for $\Delta\lambda$ using an iterative method, such as the Newton-Raphson method. For the next step, the current values of the stress state (σ_{x0},τ_{xy0}), σ_0^o and λ are updated to (σ_x,τ_{xy}), σ_0 and $\lambda+\Delta\lambda$, respectively.

In order to appreciate how the tangent shear stiffness is varying after the plate has reached its yield limit, the consistent tangent-modulus matrix $[E_t]$ is calculated at the start and at the end of the step from the following expression (Izzuddin and Smith, 1996):

$$[E_t]=[R]^{-1}[E]\left([I]-\frac{\beta\{N\}\{N\}^T[R]^{-1}[E]}{\beta\{N\}^T[R]^{-1}[E]\{N\}+H}\right) \tag{5.19}$$

with:

$$[E]=\begin{bmatrix}E & 0\\ 0 & G\end{bmatrix}$$

$$[R] = \begin{bmatrix} 1 + \dfrac{E\Delta\lambda}{\sigma_0} & 0 \\ 0 & 1 + \dfrac{3G\Delta\lambda}{\sigma_0} \end{bmatrix}$$

$$\beta = \frac{\sigma_0{}^{o}}{\sigma_0}$$

$$\{N\} = \begin{pmatrix} \dfrac{\partial f}{\partial \sigma_x} \\ \dfrac{\partial f}{\partial \tau_{xy}} \end{pmatrix}$$

The increments in normal and shear stress over the step can then be obtained as:

$$\begin{pmatrix} \Delta\sigma_x \\ \Delta\tau_{xy} \end{pmatrix} = [E_t] \begin{pmatrix} \Delta\varepsilon_x \\ \Delta\gamma_{xy} \end{pmatrix} \tag{5.20}$$

Accordingly, the effective tangent shear modulus in plastic region G_t is determined as the aggregate of the second row of $[E_t]$:

$$G_t = \frac{E_{t2,1}\Delta\varepsilon_x + E_{t2,2}\Delta\gamma_{xy}}{\Delta\gamma_{xy}} \tag{5.21}$$

G_t as given by the above equation, expresses the effective tangent shear stiffness representing the variation of τ_{xy} with γ_{xy} in the presence of simultaneous ε_x. This draws parallel with plastic plate buckling where the variation of M_{xy} with κ_{xy}, which contributes to the flexural plate stiffness, arises under the simultaneous action of applied axial loading and a significant corresponding planar strain ε_x.

Outcomes of model application

The following outcomes are noted:

1. Applying shear strains γ_{xy} in different proportions of the normal strain ε_x (ratio = $\Delta\gamma_{xy}/\Delta\varepsilon_x$ in Figure 5.7) leads to different shear stresses for the same ε_x, but identical values for the same $\gamma_{xy,}$ implying identical effective tangent shear modulus G_t or secant shear modulus G_s for the same ε_x (Figure 5.8).

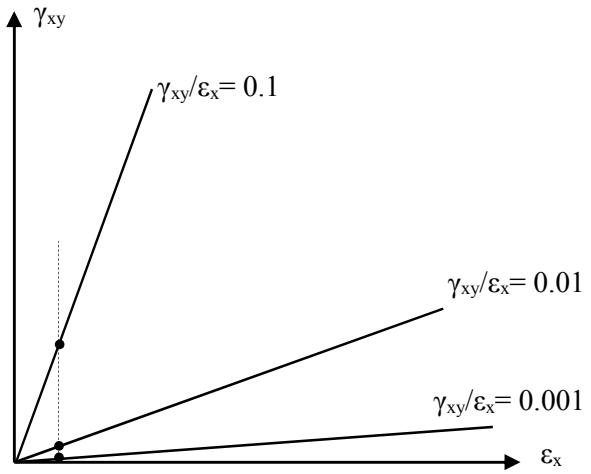

Figure 5.7 Ratios of shear strains γ_{xy} to normal strain ε_x

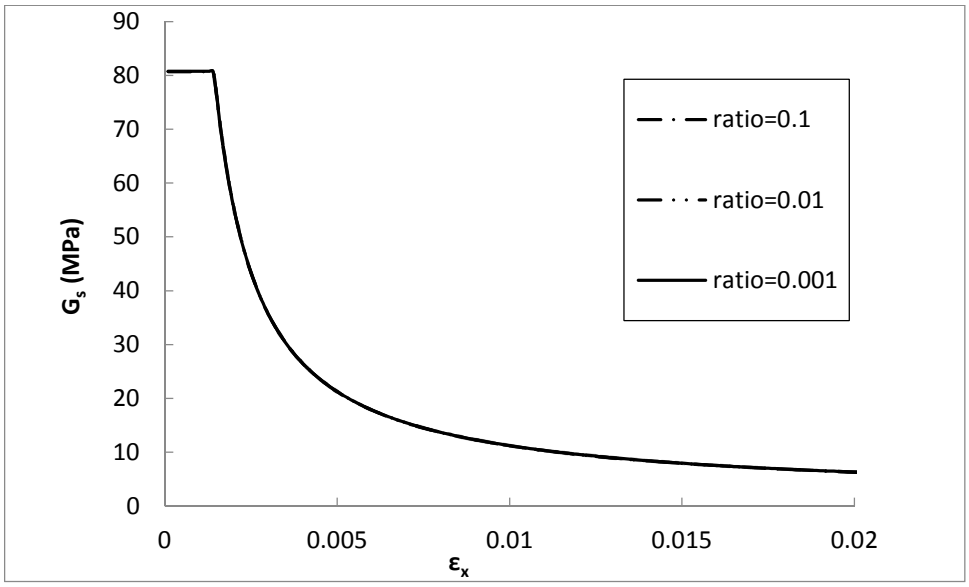

Figure 5.8 Secant shear modulus with increase in plastic deformation

2. For the purpose of this study three different scenarios have been considered (Figure 5.9): Case 1 where the initial stress state is randomly chosen somewhere

inside the interaction surface (in this case $\sigma_{x0}=0$, $\tau_{xy0}=0$), Case 2 for which the increments of strains are started from an initial state on the interaction surface ($\sigma_{x0}=299$MPa, $\tau_{xy0}=1$kPa) where the normal {N} is proportional to the ratio of applied shear/normal strain $\Delta\gamma_{xy}/\Delta\varepsilon_x$, and Case 3 for which the increments of strains are started from an initial state on the interaction surface where the shear stress is zero and the normal stress is the yield ($\sigma_{x0}=\sigma_y$, $\tau_{xy0}=0$). To appreciate the significance of G_t for the three cases a τ_{xy}–γ_{xy} curve has been produced, as depicted in Figure 5.10.

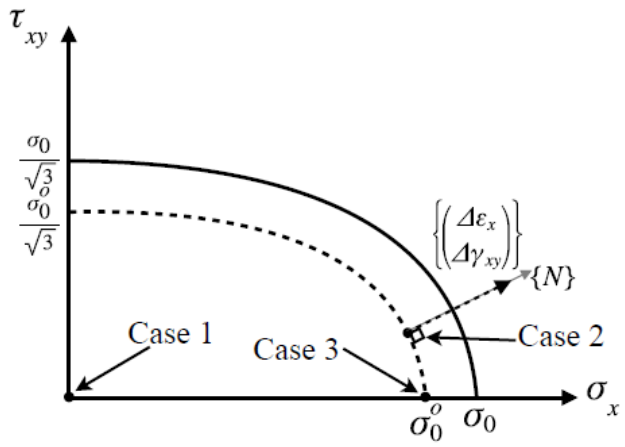

Figure 5.9 Initial stress state (σ_{x0}, τ_{xy0}) for three different scenarios

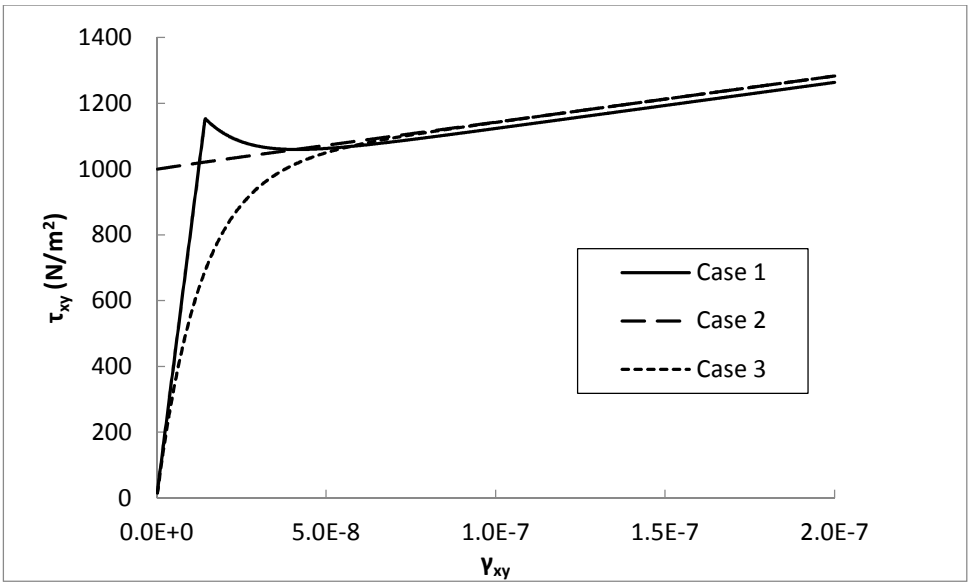

Figure 5.10 τ_{xy}–γ_{xy} curve for three cases (Isotropic Hardening)

As can be noted in Case 1, up to the yield there is a linear relation between τ_{xy} and γ_{xy} with G as the shear modulus. However, thereafter the shear stress remains largely around the yield value, dropping initially then increasing according to the plastic strain hardening modulus. In Case 2, the shear stress increases from the start in accordance with the hardening modulus, rather than the initial elastic shear modulus. On the other hand, in Case 3, the shear stress rises more rapidly, initially with a tangent shear modulus equal to G and then becomes asymptotic to the hardening curve with the reduced modulus G_t.

3. Clearly, the effective tangent shear modulus depends on the current stress state (more specifically the current normal {N}) and how the current ratio of shear to normal strain increment is related to the components of {N}. If this ratio is proportional to the components of {N}, then the tangent shear modulus is the hardening modulus. On the other hand, if it is different, the shear stress may increase or decrease depending on which side of {N} the strain increment vector is. This is reflected in the second row of $[E_t]$ where a relatively large ε_x can offset the influence of γ_{xy} leading to an increment $\Delta\tau_{xy}$ which is very different from what is implied by the diagonal term $E_{t2,2}$.
4. The outcome of this study is that the Incremental Theory is correct, but that consideration must be given to the current stress state (including the influence of small shear stress values) and the actual relative increment of shear/normal strains in order to establish the effective shear modulus G_t, which would then represent the aggregate effect of the second row of $[E_t]$.

The above deduction is also true for a material model utilising kinematic hardening, where for the uniaxial monotonic response both isotropic and kinematic hardening generally do not differ, as illustrated in Figure 5.11 for Case 3.

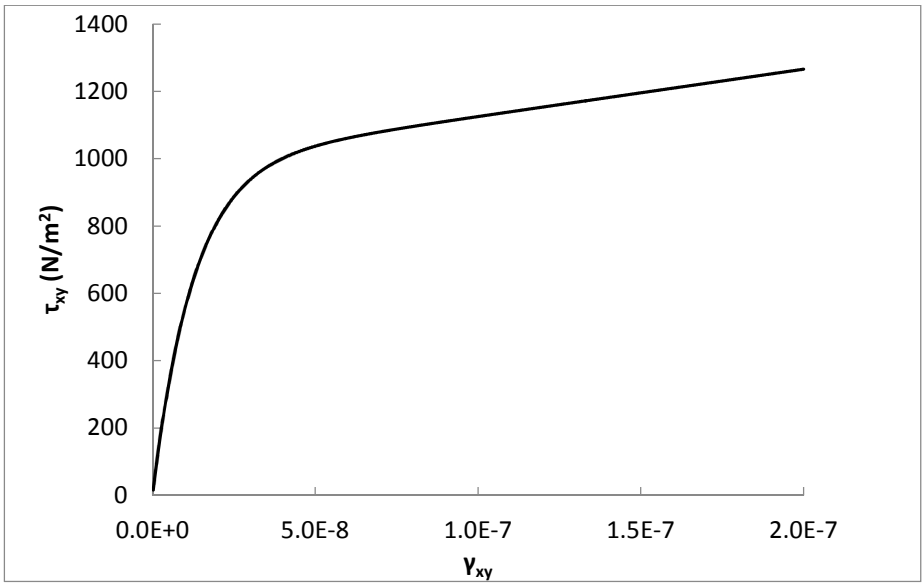

Figure 5.11 τ_{xy}–γ_{xy} curve for Case 3 (Kinematic Hardening)

5.4 Discussion and Conclusions

In this chapter it has been verified, both numerically and analytically, that by applying a uniform stress σ_x producing significant plastic axial deformation, and regardless of the relative magnitude of accompanying shear deformation, the shear stiffness G_t drops immediately after σ_x has reached the material yield strength.

With regard to the plate buckling problem these findings raise interesting prospects. A widespread belief reflected in common approaches to plastic plate buckling is that the coupling between the bending components of the 3×3 [E_{tb}] (i.e. the top left 2×2 submatrix, the consistent tangent stiffness matrix presented in Chapter 2) used to determine the instantaneous buckling load P_c is correctly determined from the conventional Incremental Theory of Plasticity. Hence, focus has been on utilising $E_{tb3,3}$ which reflects the tangent shear modulus G_t, though suggested approaches have either been empirical or not based on sound principles of mechanics. A main outcome of this chapter is that the effective G_t can be obtained from principles of incremental plasticity, though it must be determined with due consideration of the increment in the shear strain and the relatively large increment of the normal strain, typically dominated by the mid-plane strain since curvatures at the onset of buckling are relatively small.

Further to the resolution in this chapter of the mechanics leading to the reduction of G_t, the next chapter will question the widely accepted notion that the reduction in G_t alone accounts for the inaccuracy of the Incremental Theory. Towards this end, an analytical model for elasto-plastic buckling analysis of plates will be proposed founded on the present findings, generalised to consider other pertinent issues, and applied to gain further insight into the plastic buckling of plates and the associated paradox.

CHAPTER 6

Analytical Models for Plastic Buckling of Square Plates

6.1 Introduction

In Chapter 3, an analytical model was presented for elasto-plastic buckling analysis of short columns. Compared to a simply-supported column, a uniaxially loaded square plate that is simply-supported on its four edges exhibits a characteristically different buckling response, not least in relation to the elastic buckling load which is much greater than that of a corresponding column with the same width and depth/span ratio. Accordingly, stocky plates can have significantly larger slenderness ratios compared to stocky columns. Another distinguishing feature for stocky plate buckling is that the tangent modulus continuously varies after the attainment of the yield load, leading to the initiation of buckling at yield, while the buckling of relatively stocky columns is initiated at the Engesser load which can be larger than the yield load.

An analytical model is developed in this chapter for the buckling analysis of stocky plates, which is aimed at enhancing the understanding of plastic plate buckling and resolving the related Plastic Buckling Paradox. Initially, the findings of the previous chapter on the reduction of tangent shear stiffness are used to establish the tangent modulus matrix as a modification to that obtained from the conventional Incremental Theory, so as to establish whether this modification alone can account for the inaccuracy of the Incremental Theory. It is subsequently shown that although this modification leads to buckling loads which are lower than those obtained from the conventional Incremental Theory, significant discrepancies are still observed compared to the more accurate plastic buckling response obtained from detailed nonlinear finite element analysis. Accordingly, the possible sources of these

discrepancies are investigated with a view to addressing the shortcomings of this initial analytical model based on a modified tangent shear modulus.

Towards the end of this chapter, a revised form of the proposed analytical model is formulated. This model takes full account of the tangent modulus matrix leading to buckling load predictions in close agreement with the numerical outcomes of nonlinear finite element analysis. Imperfection sensitivity and the possibility of elastic unloading are also considered. Furthermore, in comparing the new analytical model to the existing methods of plastic plate buckling analysis, consideration is given to square plates with various slenderness ratios, with the aim of resolving the Plastic Buckling Paradox of plates once and for all.

It is worth noting that the main objective of this chapter is to develop a method of obtaining the plastic buckling capacity of simply-supported square plates on the basis of an assumed buckling mode consisting of a single half-wave in each of the two planar directions. At this stage, it is not suggested that this mode governs the plastic buckling capacity of square plates, where further consideration of the influence of the buckling mode and associated modal imperfections will be investigated in the next chapter.

6.2 Analytical Model Based on Modified Tangent Shear Modulus

6.2.1 Description of Problem

Consider a square plate of length “a” and thickness “h” loaded in-plane with a uniform uniaxial compressive load N_x (in this case $N_x=P/a$ and $N_y=0$), as illustrated in Figure 6.1. The transverse edges at x=0 and x=a are simply-supported, while the longitudinal edges at y=0 and y=a can take any variation of boundary conditions. However, the main focus in this chapter will be on square plates simply-supported along the four sides.

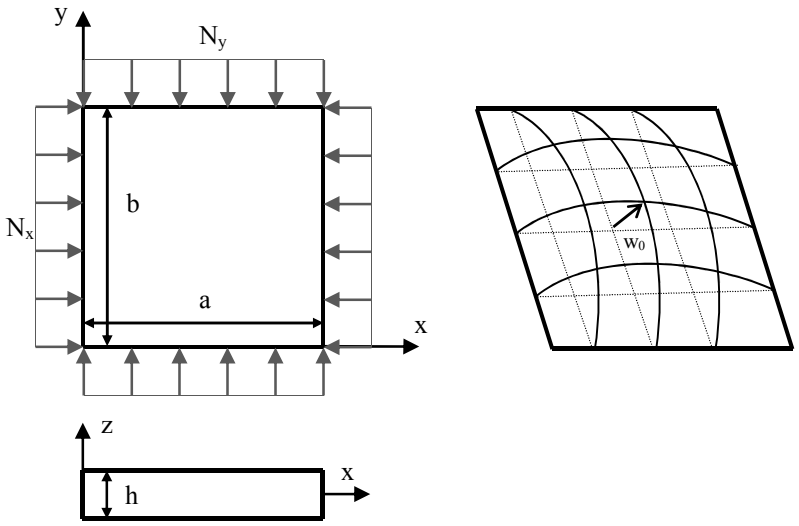

Figure 6.1 Square plate under uniform compression

A sinusoidal buckling mode is assumed as follows:

$$w(x,y) = w_0 \bar{w}(x,y);\ \ \bar{w}(x,y) = \sin(\frac{m\pi x}{a})\sin(\frac{n\pi y}{b}) \tag{6.1}$$

where m and n are the number of half-waves in x- and y-directions, respectively, and are taken as m=n=1 for the square plate. This assumed mode satisfies both the kinematic and static boundary conditions for a simply-supported square plate.

Starting from an imperfect sinusoidal configuration, which accords with the assumed buckling mode given by (6.1), the plate is assumed to remain elastic for loading up to the yield load P_Y. Hence, an initial equilibrium state at P_Y is determined from an amplified elastic response with reference to the elastic buckling load P_{cr}. In this approach allowing for the modification of only the tangent shear modulus G_t, the buckling response of the plate is revised by modifying the twisting component $E_{tb3,3}$ of the tangent modulus matrix $[E_{tb}]$ obtained from the conventional Incremental Theory of plasticity. To trace the post-buckling response of the plate, the increment of transverse displacement Δw_0 is determined for successive load increments ΔP. In this respect, it is assumed that the plate is sufficiently stocky for all fibres to remain plastified (i.e. no elastic unloading) as the load P is increased.

For the purpose of tracing the post-buckling response of the plate, the equation of incremental bending equilibrium is utilised to obtain the increment of displacement Δw_0 in terms of ΔP, where w_0 and Δw_0 henceforth refer to the maximum transverse displacement and the increment of transverse displacement, respectively, at the centre of the plate. This in turn requires the determination of the instantaneous buckling load P_c, which is obtained for the assumed mode using the Rotational Spring Analogy (Izzuddin, 2006).

6.2.2 Incremental Bending Equilibrium Condition

Similar to the column buckling problem, the increment of transverse displacement Δw_0 can be obtained from incremental equilibrium of a generalised SDOF system, as illustrated in Figure 6.2 for a simple cantilever column problem. Considering the flexurally rigid column to have a rotational spring at its bottom support, with an initial imperfection w_{0i} at its free end, the rotational equilibrium condition is given by:

$$M = P(w_0 + w_{0i}) \tag{6.2}$$

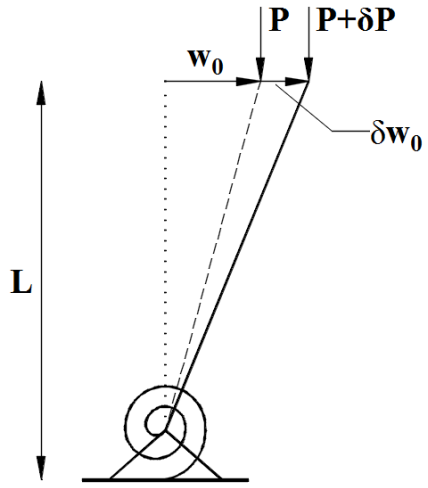

Figure 6.2 Rotational equilibrium for straight element

Applying this condition to a successive equilibrium state with a load increment ΔP and an associated incremental displacement Δw_0 leads to:

$$M + \Delta M = (P + \Delta P)(w_0 + w_{0i} + \Delta w_0) \tag{6.3}$$

Assuming sufficiently small increments, thus ignoring the second-order terms, the above equation can be expressed in an incremental form and simplified in the range of small to moderate displacements to:

$$P_c = P + \frac{\Delta P}{\Delta w_0}\left(w_{0i} + w_0\right) \tag{6.4}$$

where $P_c = \Delta M/\Delta w_0$ is the instantaneous buckling load (see Chapter 3, section 3.2.4 for more details). By analogy with the cantilever column, this is the equation of incremental equilibrium for a plate which relates ΔP and the increment in the modal amplitude Δw_0. However, in contrast to the analytical model presented in Chapter 3 for the plastic buckling of columns, the above equation of incremental equilibrium can only be applied in a forward manner using values at the start of the step.

The increment of transverse displacement Δw_0 associated with the load increment ΔP is thus obtained from:

$$\Delta w_0 = \frac{\left(w_{0i} + w_0\right)\Delta P}{P_c - P} \tag{6.5}$$

where w_{0i} is the initial imperfection amplitude at the centre of the plate.

As shown in the parametric studies of Chapter 4, the plate starts to buckle as the load approaches the yield load P_Y. Therefore, in order to capture the post-buckling response of a stocky plate, the initial loading is assumed to be $P=P_Y$ up to which the plate is assumed to behave elastically. At this point, applying Perry's rule (Timoshenko and Gere, 1961), w_0 is the amplified initial displacement associated with load P due to initial bending moments:

$$w_0 = \frac{w_{0i}P}{P_{cr} - P} \tag{6.6}$$

where P_{cr} is the elastic critical buckling load of the square plate:

$$P_{cr} = \frac{4\pi^2 E h^3}{12a\left(1-\nu^2\right)} \tag{6.7}$$

Starting from this initial equilibrium state, the incremental condition of (6.5) is used to determine the increment of transverse displacement Δw_0 associated with the load step ΔP, which is then followed by an update of the corresponding entities before the application of the next step increment. This incremental process requires the determination of the instantaneous buckling load P_c, which in turn depends on the geometric stiffness and the tangent modulus matrix for bending deformations, as presented in the following section.

6.2.3 Instantaneous Buckling Load

The instantaneous buckling load P_c corresponds to a level of loading which, if applied in the current deformed configuration, results in a negative geometric stiffness matrix $[K_G]$ that overcomes the positive definite tangent material stiffness matrix $[K_E]$, leading to a singular overall tangent stiffness matrix $[K_T]$ (Izzuddin, 2007c). This shares a similar notion of the elastic buckling load, where the singularity condition of $[K_T]$ can be derived from variational energy principles (Bazant and Cedolin, 1991;Crisfield, 1991). In the context of the current plastic plate buckling problem, $[K_G]$ is proportional to the loading in view of the assumption of small to moderate displacements, though P_c changes during incremental loading due to a changing $[K_E]$.

Considering the plate under proportional loads consisting of nominal loading N_x (N_y=0 in this case) subject to a load factor ρ, the instantaneous buckling load factor can be obtained from the singularity condition of $[K_T]$:

$$[K_T] = [K_E] + \rho[K_G] \tag{6.8}$$

where $[K_G]$ is the geometric stiffness matrix associated with the nominal loading N_x. This corresponds to the solution of the linear eigenvalue problem:

$$[K_T]\{U\} = \left([K_E] + \rho[K_G]\right)\{U\} = 0 \qquad \left(\{U\} \neq \{0\}, \rho = \rho_c\right) \tag{6.9}$$

in which {U} is the associated buckling mode.

An approximate solution of the MDOF problem is obtained with an assumed mode {U}, where the instantaneous buckling load factor is then determined from:

$$\rho_c = -\frac{\{U\}^T[K_E]\{U\}}{\{U\}^T[K_G]\{U\}} = -\frac{k_e}{k_g} \tag{6.10}$$

in which k_e and k_g represent equivalent SDOF tangential material and nominal geometric stiffness terms, respectively. For the plate problem under consideration, the sinusoidal mode employed in (6.1) will be employed for determining k_g and k_e, as elaborated next.

6.2.4 Geometric Stiffness

The equivalent SDOF geometric stiffness can be easily obtained using the Rotational Spring Analogy (RSA) proposed by Izzuddin (2007c). Assuming that the planar stresses remain uniform and in proportion to the applied loading, the geometric stiffness is obtained from two sets of equivalent rotational springs distributed over the plate area, with rotations equal to the slopes of the lateral buckling mode w (Izzuddin, 2006):

$$\{\theta\} = \begin{Bmatrix} \frac{\partial w}{\partial x} \\ \frac{\partial w}{\partial y} \end{Bmatrix} = \{T_\theta\}\{U\} \tag{6.11}$$

considering (6.1) for the SDOF mode implying $\{U\}=w_0$, and

$$\{T_\theta\} = \begin{Bmatrix} \frac{\partial \bar{w}}{\partial x} \\ \frac{\partial \bar{w}}{\partial y} \end{Bmatrix} = \begin{Bmatrix} \frac{m\pi}{a}\cos\frac{m\pi x}{a}\sin\frac{n\pi y}{b} \\ \frac{n\pi}{b}\sin\frac{m\pi x}{a}\cos\frac{n\pi y}{b} \end{Bmatrix} \tag{6.12}$$

The stiffness of the equivalent rotational springs is in turn related to the internal planar resultant forces, which are assumed to be equal to the applied loading:

$$[k_\theta] = \begin{bmatrix} -N_x & 0 \\ 0 & -N_y \end{bmatrix} \tag{6.13}$$

where the nominal load is taken to be the same as the yield load (i.e. $N_x = \sigma_Y h$ and $N_y = 0$).

Therefore, the corresponding equivalent geometric stiffness becomes:

$$k_g = \iint \{T_\theta\}^T [k_\theta] \{T_\theta\} dA \tag{6.14}$$

6.2.5 Material Stiffness

The main difficulty when developing an analytical model for the plastic buckling analysis of plates is the fact that the tangent material stiffness appears to be continuously varying from the onset of buckling at the yield load, as demonstrated in Chapter 4, which is attributed to complex interactions of biaxial stresses. As discussed in Chapter 2, Incremental Plasticity Theory offers a more sound representation of the inelastic response of metals compared to the Deformation Theory, yet its use in bifurcation analysis leads to much more unrealistic predictions of the plastic buckling loads. Here, a modified Incremental Theory is considered for the analytical model in which the tangent shear modulus, effective for the twisting curvatures in the buckling deformations, is evaluated with due consideration of the significant planar plastic strains in the loading direction. This follows on from the suggestions of previous researchers (Haaijer, 1957;Haaijer and Thurlimann, 1958;Shrivastava and Bleich, 1976;Dawe and Grondin, 1985), where the shortcomings of Incremental Theory were attributed to a reduced tangent shear modulus G_t, but contrasts with Becque's method (Becque, 2010) in that G_t is determined from sound principles of the mechanics of materials.

Using standard discretisation principles, the material stiffness k_e can be determined as follows:

$$k_e = \iint \{B\}^T [D_{ep}] \{B\} dA \tag{6.15}$$

where the three generalised strains are expressed in:

$$\{B\} = \frac{1}{w_0}\begin{Bmatrix} \kappa_x \\ \kappa_y \\ \kappa_{xy} \end{Bmatrix} = \begin{Bmatrix} \dfrac{\partial^2 \bar{w}}{\partial x^2} \\ \dfrac{\partial^2 \bar{w}}{\partial y^2} \\ 2\dfrac{\partial^2 \bar{w}}{\partial x \partial y} \end{Bmatrix} \tag{6.16}$$

and $\left[D_{ep}\right] = \left(h^3/12\right)\left[E_{tb}\right]$ is the flexural tangent modulus matrix, with $[E_{tb}]$ representing the governing tangent modulus matrix allowing for interactions between biaxial planar stresses and strains.

Clearly, the above assumes that there is no variation in $[E_{tb}]$ over the thickness of the plate, which is potentially realistic when the curvatures associated with buckling deformations are relatively small, in which case plastic strains are dominated by the values at the plate mid-plane. For a simply supported plate subject to a normal edge loading, this is largely true for the normal plastic strains ($\varepsilon_x^p, \varepsilon_y^p$) but not the plastic shear strains γ_{xy}^p, since the resultant planar shear force is zero. Assuming that the mid-plane plastic strains are related to the planar stress resultants, the mid-plane γ_{xy}^p would be zero, while relatively small γ_{xy}^p arise away from the mid-plane as a result of the incremental twisting buckling curvatures.

Therefore, considering the incremental biaxial constitutive law as given by:

$$\{\delta\sigma\} = [E_{tb}]\{\delta\varepsilon\} \tag{6.17}$$

with an uncoupled normal/shear material response:

$$\left[E_{tb}\right] = \begin{bmatrix} E_{tb1,1} & E_{tb1,2} & 0 \\ E_{tb2,1} & E_{tb2,2} & 0 \\ 0 & 0 & E_{tb3,3} \end{bmatrix} \tag{6.18}$$

it would be realistic to consider the top left 2×2 sub-matrix to be determined for the averaged normal planar stresses ($\sigma_x = N_x/h, \sigma_y = 0$). On the other hand, $E_{tb3,3}$,

which represents a modified tangent shear modulus G_t, would be determined with due consideration of the large values of the planar normal plastic strains $(\varepsilon_x^p, \varepsilon_y^p)$ relative to the plastic shear strains γ_{xy}^p.

Considering first the top left 2×2 sub-matrix $[E_{tb}]$, with reference to Figure 6.3, the terms obtained from the Incremental Theory are given by (Chakrabarty, 2000;Wang et al., 2001):

$$E_{tb1,1} = \frac{E\left(4 - \frac{3\left(1-\frac{E_t}{E}\right)\sigma_x^2}{\sigma_e^2}\right)}{(5-4\nu) - \frac{(1-2\nu)^2 E_t}{E} - \frac{3(1-2\nu)\left(1-\frac{E_t}{E}\right)\sigma_x\sigma_y}{\sigma_e^2}} \tag{6.19}$$

$$E_{tb1,2} = E_{tb2,1} = \frac{E\left(2 - 2(1-2\nu)\frac{E_t}{E} - \frac{3\left(1-\frac{E_t}{E}\right)\sigma_x\sigma_y}{\sigma_e^2}\right)}{(5-4\nu) - \frac{(1-2\nu)^2 E_t}{E} - \frac{3(1-2\nu)\left(1-\frac{E_t}{E}\right)\sigma_x\sigma_y}{\sigma_e^2}} \tag{6.20}$$

$$E_{tb2,2} = \frac{E\left(4 - \frac{3\left(\frac{E_t}{E}\right)\sigma_y^2}{\sigma_e^2}\right)}{(5-4\nu) - \frac{(1-2\nu)^2 E_t}{E} - \frac{3(1-2\nu)\left(1-\frac{E_t}{E}\right)\sigma_x\sigma_y}{\sigma_e^2}} \tag{6.21}$$

in which $\sigma_x = N_x / h$ and $\sigma_y = 0$ in x-and y-direction, respectively, and the equivalent stress σ_e is based on the von Mises yield criterion:

$$\sigma_e = \sqrt{\sigma_x^2 + \sigma_y^2 - \sigma_x.\sigma_y} \tag{6.22}$$

As noted previously, the use of Incremental Theory in plastic bifurcation analysis of perfect plates leads to $E_{tb3,3}$ which is the same as the elastic shear modulus G. However, when considering plates with small imperfections, $E_{tb3,3}$ is not only different from G once the load exceeds P_Y but can become a significantly reduced tangent shear modulus G_t, as illustrated in Chapter 5 for a biaxial stress state. Indeed, it was demonstrated that the effective tangent shear modulus G_t could be obtained from principles of incremental plasticity, provided due consideration is given to the increment in the shear strain and the relatively large increment of the normal strain, as detailed previously in Section 5.2.3. To this end, the value of G_t at the start of an incremental step entering into the evaluation of the material stiffness k_e, and hence P_c as required for (6.5), is determined as follows.

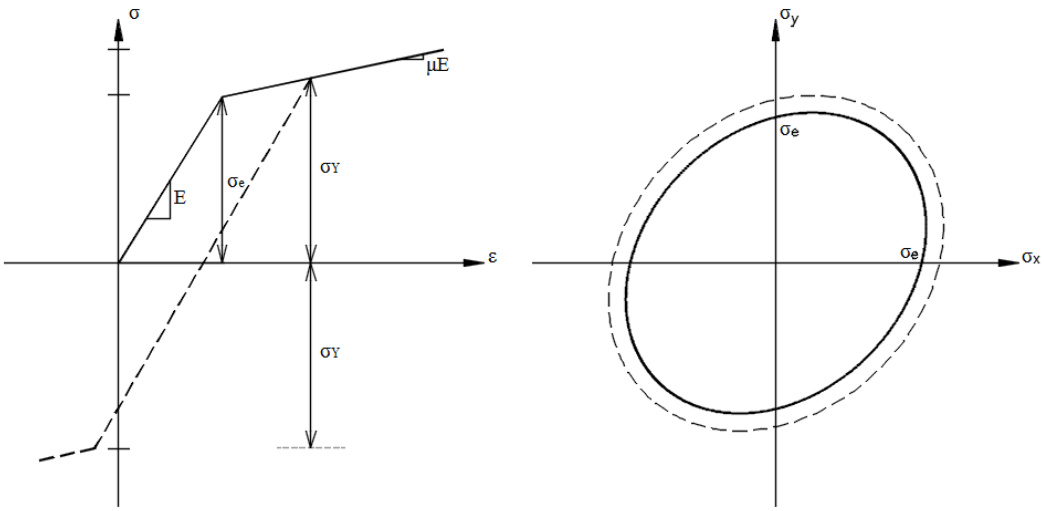

a) uniaxial stress-strain diagram b) yield surface for biaxial stress state

Figure 6.3 Biaxial elasto-plastic response with isotropic hardening

Up to the yield point, the plate is assumed to be elastic and is initially in an equilibrium state with $P=P_Y$. This is determined from the total amplified equilibrium using P_c established from $[E_{tb}]$ with $E_{tb3,3}$ taken as the elastic shear modulus G; which is justified on the basis of negligible plastic strains at this point. However, once the yield load is exceeded, P_c as determined from (6.10) and (6.15) is related to the unknown $E_{tb3,3}$ representing G_t over the incremental step.

Following the study in Chapter 5, which showed that the tangent/secant shear modulus remains unchanged for different small ratios of incremental shear and normal strains ($\Delta\gamma_{xy}/\Delta\varepsilon_x$), the effective shear modulus G_t (hence $E_{tb3,3}$) is taken to be the same for all the points over the plate. Therefore, G_t is determined as the aggregate of the second row of $[E_t]$, as given by (5.21), referring to a single location over the plate and considering the shear stress τ_{xy} with the normal stress σ_x and the corresponding strain increments $\Delta\gamma_{xy}$ and $\Delta\varepsilon_x$. Considering (5.20) and (5.21), G_t is therefore obtained as:

$$G_t = E_{t2,2} + \frac{E_{t2,1}}{E_{t1,1}}\left(\frac{\Delta\sigma_x}{\Delta\gamma_{xy}} - E_{t1,2}\right) \tag{6.23}$$

where $\Delta\gamma_{xy}$ is obtained at a specific location from the increment of buckling displacement Δw_0:

$$\Delta\gamma_{xy} = -2z\frac{\partial^2 \bar{w}}{\partial x \partial y}\Delta w_0 \tag{6.24}$$

and $\Delta\sigma_x$ is taken as the average increment over the plate thickness, which is assumed to be uniform over the plate area and thus obtained from the planar equilibrium in terms of ΔP:

$$\Delta\sigma_x = \frac{\Delta P}{bh} \tag{6.25}$$

In anticipation of subsequent developments of the analytical model where the tangent modulus matrix $[E_{tb}]$, hence $[D_{ep}]$, varies nonlinearly over the plate domain, the integration of the equivalent material stiffness over the area of the plate is approximated using Gaussian quadrature:

$$k_e = \int \{B\}^T [D_{ep}]\{B\} dA \simeq \sum_{i=1}^{n} w_i \{B\}^T [D_{ep}]\{B\}_{(x_i, y_i)} \tag{6.26}$$

where n is the number of Gauss points, (x_i, y_i) denotes the location of Gauss point i, and w_i represents the corresponding weighting factor.

In this case, 2×2 Gaussian quadrature over the whole plate area produces sufficiently accurate results, as demonstrated later. Due to symmetry, a quarter model of the plate may be considered (Figure 6.4) to obtain k_e and hence P_c, where the associated Gauss station $(x_1, y_1) = \left(a\left(1-\sqrt{3}/3\right)/2, b\left(1-\sqrt{3}/3\right)/2\right)$ and w_1=ab/4. Although for more accurate numerical integration more Gauss points over the area of the plate could be employed, the choice of one Gauss point in a quarter model leads to a simpler and more efficient analytical model.

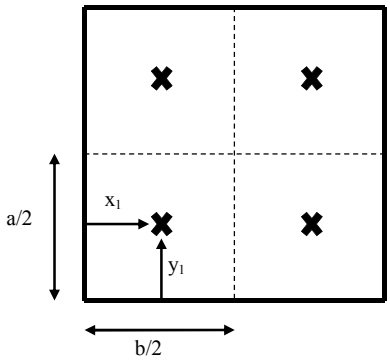

Figure 6.4 Location of Gauss points over the plate

6.2.6 Method of Analysis

Considering the dependence of k_e on the current stress state at a specific reference point and the ratio $\Delta\sigma_x/\Delta\gamma_{xy}$ according to (6.23), it is clear that the effective tangent material modulus depends on the relative values of ΔP and Δw_0, even in the absence of any elastic unloading. This is in contrast with the plastic column buckling problem, where a fully plastified cross-section with a bilinear elasto-plastic material model has a constant effective tangent modulus $E_t = \mu E$, and it highlights the complexities arising from the biaxial interaction in plastic buckling of plates. As a result, P_c depends on ΔP and Δw_0, and along with the equation of incremental equilibrium given by (6.5)this presents a set of nonlinear simultaneous equations which can be solved iteratively for Δw_0 and P_c given a specific load increment ΔP.

Referring to the square plate in Figure 6.1, the analysis is started from the yield load $P=P_Y$, where the reference point in the plate is in a state of stress $\left(\sigma_{x0} = \sigma_Y, \sigma_{y0} = 0, \tau_{xy0} = G\gamma_{xy0}\right)$. The initial shear strain is $\gamma_{xy0} = -2zw_0\left(\partial^2 \bar{w} / \partial x \partial y\right)$ obtained at the reference point location, with w_0 taken as the amplified deflection of

the elastic plate. Starting from this configuration, the value of Δw_0 associated with a given ΔP is obtained iteratively as above, following which the values of P, w_0 and the reference stress state $\left(\sigma_{x0}, \sigma_{y0}, \tau_{xy0}\right)$ are updated for the next increment, where for the case of loading in the x-direction only:

$$\Delta\sigma_{x0} = \frac{\Delta P}{bh}; \quad \Delta\sigma_{y0} = 0; \quad \Delta\tau_{xy0} = G_t \Delta\gamma_{xy0} = G_t\left(-2z\frac{\partial^2 \bar{w}}{\partial x\, \partial y}\Delta w_0\right) \tag{6.27}$$

This allows the determination of the load-deflection response and the maximum buckling resistance P_{max} as the limit point on this post-buckling equilibrium path.

6.2.7 Results and Discussion

Consider a simply supported square plate as in Figure 6.1 with length a=b=2.4m, thickness h=b/20=120mm, and initial imperfection amplitude w_{0i}=b/1000. The material properties associated with a bilinear elasto-plastic material model (Figure 6.3) are $\sigma_Y = 300\times10^6\,\mathrm{N/m^2}$, $E = 2.1\times10^{11}\,\mathrm{N/m^2}$, $\mu = 2\%, \nu = 0.3$, $G = E/(2+2\nu) = 8.077\times10^{10}\,\mathrm{N/m^2}$. Figure 6.5 illustrates the post-buckling response of the plate associated with three different methods: i) the analytical model based on Incremental Theory with a modified G_t, as presented above, ii) the same model but using the conventional Incremental Theory, thus G_t=G, and iii) the numerical predictions from nonlinear finite element analysis using ADAPTIC (Izzuddin, 1991).

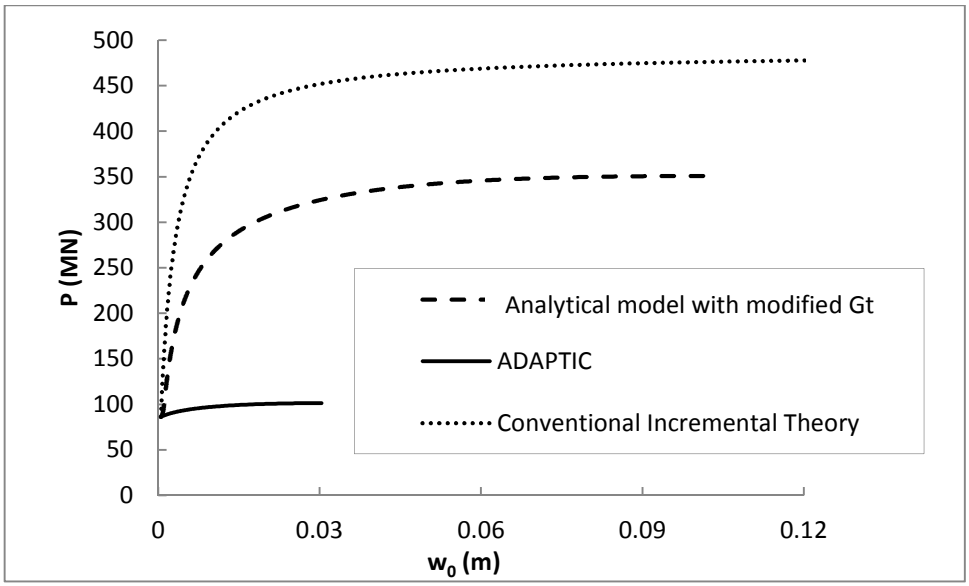

Figure 6.5 Post-buckling response of a square plate (b/h=20, w_{0i}=b/1000)

As can be noted from both the numerical and analytical analyses, the plate starts to buckle at P_Y. Although a substantial reduction in the P-w response of the plate can be observed by incorporating a reduced tangent shear modulus in the conventional Incremental Theory, this still significantly overestimates the more realistic nonlinear finite element predictions of ADAPTIC.

It is worth noting that while imperfections are considered in the above results, it is shown later that an imperfection level of w_{0i}=b/1000 does not result in a significant reduction in P_{max} to the extent of accounting for the major discrepancy between the numerical and analytical results.

To gain further insight into the predictions of the analytical model with a modified G_t compared to previous models, the values of P_{max} are computed for a plate slenderness b/h=20 and compared in Table 6.1.

Table 6.1 Maximum buckling loads P_{max} in (MN)

Bleich's Theory	Conventional Incremental Theory	Deformation Theory	Analytical modified G_t	Becque's Method	ADAPTIC
86.4	487	95.4	351	235	101

Reduction of G_t (from 8.077×10^{10} to 2.954×10^{10} N/m^2) in the inelastic range has lowered the maximum bucking load obtained from the conventional Incremental Theory by nearly 40%, nevertheless the resulting P_{max} still considerably overestimates the result of ADAPTIC. Even a further reduction of G_t to zero, does not improve the buckling load prediction significantly, resulting in a large value of P_{max} of 296 MN.

It is also worth noting that in the above results, the predictions from Becque's model (Becque, 2010) are obtained with a number of half waves m=1 in the direction of loading for consistency with the current analytical model and the observed buckling mode obtained with ADAPTIC, where the influence of shorter wave lengths is investigated in the next chapter. Clearly, for such a case P_{max} obtained with Becque's tangent modulus matrix is even smaller than that predicted by the conventional Incremental Theory with G_t=0; this confirms again that his asymmetric tangent stiffness matrix does not accord with the theory of plasticity and does not present, as he claims, a mere modification associated with the tangent shear modulus.

Noting that the finite elements in ADAPTIC employ constitutive relations based on the Incremental Theory of plasticity, the above results from the analytical model confirm that a reduced shear modulus on its own does not account for the reduction in the plastic buckling load of plates. In order to explain this significant discrepancy, some of the underlying factors that may influence the plastic buckling behaviour are examined. Firstly the kinematics of both numerical and analytical models are compared at three different locations over the plate, referring specifically to the curvatures which are obtained in the analytical model from:

$$\{\Delta\kappa\} = \Delta w_0 \begin{Bmatrix} \dfrac{\partial^2 \bar{w}}{\partial x^2} \\ \dfrac{\partial^2 \bar{w}}{\partial y^2} \\ 2\dfrac{\partial^2 \bar{w}}{\partial x \partial y} \end{Bmatrix} \tag{6.28}$$

It has been observed that for the same increment in transverse displacement Δw_0, there is a good agreement between the curvatures, which implies a reasonable

correspondence between the single assumed mode and the effective mode obtained with ADAPTIC in the elasto-plastic range (Figure 6.6).

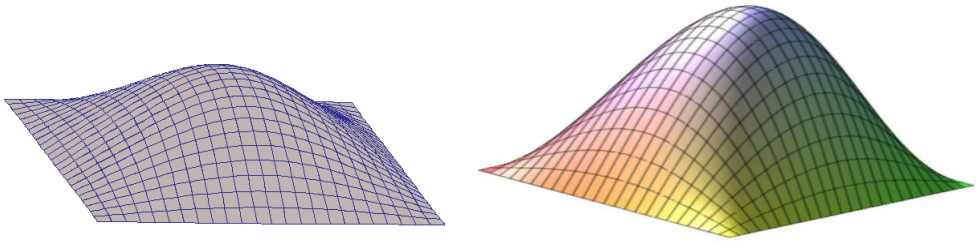

ADAPTIC Analytical Model

Figure 6.6 Deformed shape of plate at P_{max}

Next, the generalised bending stresses $\{\Delta M\}$ corresponding to the generalised curvature strains $\{\Delta\kappa\}$ are inspected by means of introducing a single measure as an indicative value for the tangential bending stiffness η:

$$\eta = \frac{\{\Delta M\}^T \{\Delta\kappa\}}{\{\Delta\kappa\}^T \{\Delta\kappa\}} \tag{6.29}$$

where in the analytical model:

$$\{\Delta M\} = \left[D_{ep} \right] \{\Delta\kappa\} \tag{6.30}$$

The values of η are calculated for the three methods previously considered and are presented in Figure 6.7. Clearly, the representative values of the tangential stiffness matrix calculated from the conventional Incremental Theory are significantly higher than those obtained from ADAPTIC. Modifying the conventional Incremental Theory with a reduced G_t has resulted in a reduction of η but the values are still large, noting that even G_t=0 leads to a large η=5.67MN/m^2. It can therefore be argued that it is the entire tangent stiffness matrix $[E_{tb}]$, utilised in the analytical model, that is responsible for overestimating the buckling resistance and not simply the twisting shear component.

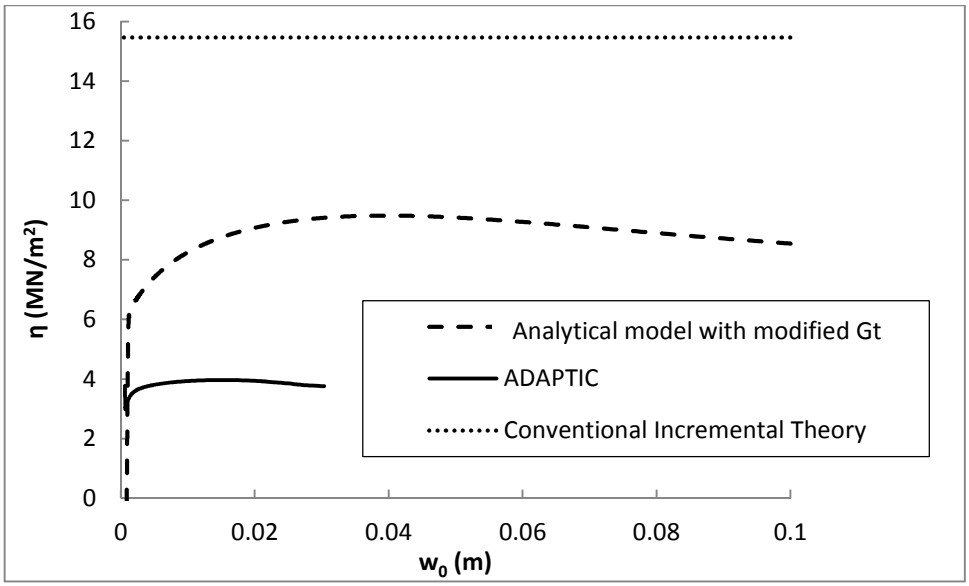

Figure 6.7 Variation of η with w_0

The current approach merely considers the reduction of G_t in $[E_{tb}]$, having assumed that the bending components in $[E_{tb}]$ were correctly determined. However, to assess the correctness of the latter the same single measure is recalculated excluding the shear/twisting component:

$$\eta_1 = \frac{\Delta M_x \Delta \kappa_x + \Delta M_y \Delta \kappa_y}{\Delta \kappa_x^{\,2} + \Delta \kappa_y^{\,2} + \Delta \kappa_{xy}^{\,2}} \tag{6.31}$$

The corresponding variation of η_1 is plotted in Figure 6.8. It is evident that the bending components of $[E_{tb}]$ associated with the conventional Incremental Theory are much higher than those used in ADAPTIC. By comparing Figure 6.7 and Figure 6.8, it is interesting to note that the ratio by which the values of η are larger is very similar to that observed by the values of η_1 which evidently questions the widely accepted perception on lowering the maximum buckling loads by merely taking account of the reduction in G_t.

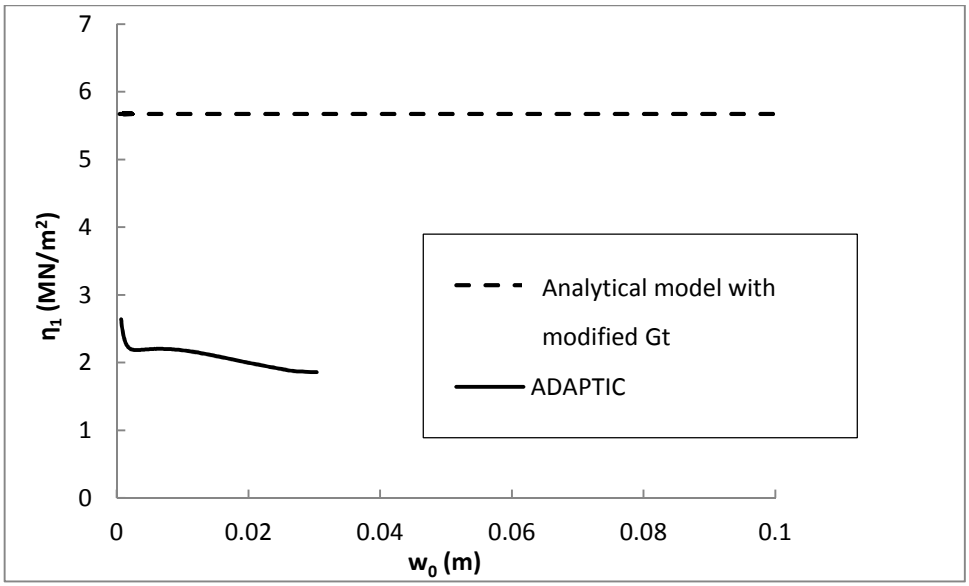

Figure 6.8 Variation of η_1 with w_0

Concluding remarks

Up to this point, a simplified analytical model has been presented for predicting the post-buckling response of a stocky simply supported square plate subject to a uniaxial loading. This model employs the stress-strain relations based on the conventional Incremental Plasticity Theory, except for the tangent shear modulus G_t which is modified with due consideration of the increment in the shear strain and the relatively large increment of the normal strain. However, the above study has demonstrated that the reduction in G_t alone does not account for the fundamental deficiency of Incremental Theory. In the following section, this simplified model will be enhanced to account for the variation of the full flexural tangent modulus matrix, where two alternative methods are proposed for evaluating the through-thickness generalised response: i) A Linear Stress Model, and ii) a Linear Strain Model.

6.3 Proposed Analytical Model

6.3.1 Introduction

It has been shown in the previous section that a biaxial flexural modulus matrix based on the Incremental Plasticity Theory with a modified shear modulus for the twisting response still does not represent the plastic buckling of stocky plates adequately. Indeed, it was demonstrated that not only is the twisting generalised

response affected but also the bending response represented by the upper left 2×2 submatrix of $[E_{tb}]$. This suggests that the full 3×3 flexural modulus matrix $[D_{ep}]$ is influenced by planar plastic deformations under the action of the applied planar load.

The most effective way to address these interactions is to consider through-thickness discretisation of the plate, which is commonly applied in nonlinear finite element analysis using several integration points over the thickness. However, besides the computational demands of this approach to through-thickness discretisation, the analytical model would lose some of its conceptual benefits if the flexural tangent modulus is obtained using such a numerical procedure. Instead, two simplified approaches are considered in the proposed analytical model, namely i) a Linear Stress approach where the stresses/strains are sampled at the mid-plane and at one extreme fibre, and ii) a Linear Strain approach where the stresses/strains are sampled at the mid-plane and at the two extreme fibres. Following the presentation of the two approaches and their incorporation into the proposed model, a comparative study is undertaken against the results of the nonlinear finite element analysis for a range of initial imperfections and plate slenderness ratios. In this respect, the aim is to establish whether the Plate Plastic Buckling Paradox could indeed be attributed to the aforementioned influences on the full 3×3 flexural modulus matrix $[D_{ep}]$.

6.3.2 Linear Stress Model

This approach is founded on the assumption of a linear distribution of stress over the thickness of the plate, with stresses and strains effectively sampled at the mid-plane and the compressive fibre on the concave side of the buckled plate.

The stress-strain relations follow the von Mises J_2-Flow Theory of Plasticity, hence the consistent tangent modulus matrix at the material point level for a plastic stress state can be obtained at the start of the incremental step from the following expression (Crisfield, 1991;Izzuddin and Smith, 1996):

$$[E_t] = [E]\left([I] - \frac{\{N\}\{N\}^T[E]}{\{N\}^T[E]\{N\} + H} \right) \tag{6.32}$$

with:

$$H = \frac{\mu}{\mu + 1} \tag{6.33}$$

$$[E] = \frac{E}{1-\nu^2}\begin{bmatrix} 1 & \nu & 0 \\ \nu & 1 & 0 \\ 0 & 0 & \frac{1-\nu}{2} \end{bmatrix} \tag{6.34}$$

$$\{N\} = \begin{pmatrix} \frac{\partial f}{\partial \sigma_x} \\ \frac{\partial f}{\partial \sigma_y} \\ \frac{\partial f}{\partial \tau_{xy}} \end{pmatrix} = \begin{pmatrix} \frac{2\sigma_x - \sigma_y}{2\sigma_0} \\ \frac{2\sigma_y - \sigma_x}{2\sigma_0} \\ \frac{3\tau_{xy}}{\sigma_0} \end{pmatrix} \tag{6.35}$$

where μ is the hardening parameter of the bilinear elasto-plastic material law (Figure 6.3), and σ_0 is the current yield strength.

Noting that elastic unloading is not a major consideration for plastic buckling of plates, as demonstrated in Section 6.4, isotropic hardening is considered instead of kinematic hardening for simplicity, where the components of a plastic stress state satisfy the following von Mises yield condition:

$$\sigma_0 = \sqrt{\sigma_x^2 + \sigma_y^2 - \sigma_x\sigma_y + 3\tau_{xy}^2} \tag{6.36}$$

As can be noted, the tangent modulus matrix for a plastic stress state depends on the current stress state (σ_x, σ_y, τ_{xy}) and the current value of yield strength σ_0.

For a specific point on the plate, small increments of stress and strain can be related by the tangent modulus matrix:

$$\{\Delta\sigma\} = [E_t]\{\Delta\varepsilon\} \tag{6.37}$$

For a point away from the mid-plane, the incremental strains are further given by:

$$\{\Delta\varepsilon\} = \{\Delta\varepsilon_m\} + \{\Delta\varepsilon_f\} \Rightarrow \begin{Bmatrix} \Delta\varepsilon_x \\ \Delta\varepsilon_y \\ \Delta\gamma_{xy} \end{Bmatrix} = \begin{Bmatrix} \Delta\varepsilon_{xm} \\ \Delta\varepsilon_{ym} \\ \Delta\gamma_{xym} \end{Bmatrix} + \begin{Bmatrix} \Delta\varepsilon_{xf} \\ \Delta\varepsilon_{yf} \\ \Delta\gamma_{xyf} \end{Bmatrix} \tag{6.38}$$

where $\{\Delta\varepsilon_m\}$ is the increment of mid-plane strains and $\{\Delta\varepsilon_f\}$ is the increment of flexure-related strains. The latter is defined in terms of the increment of curvatures:

$$\{\Delta\varepsilon_f\} = z\{\Delta\kappa\} \text{ with } -\frac{h}{2} \le z \le \frac{h}{2} \tag{6.39}$$

where $\{\Delta\kappa\}$ is related to Δw_0 according to (6.28).

With the assumption of linear stress variation over the thickness, and assuming further that there is no variation in the planar stress resultants over the plate area, the increment of mid-plane stresses can be related to the load increment as follows:

$$\{\Delta\sigma_m\} = \frac{1}{h}\begin{Bmatrix} \Delta N_x \\ \Delta N_y \\ \Delta N_{xy} \end{Bmatrix} \tag{6.40}$$

where, for the case of the increments of a uniaxial loading in the x-direction,:

$$\begin{Bmatrix} \Delta N_x \\ \Delta N_y \\ \Delta N_{xy} \end{Bmatrix} = \begin{Bmatrix} \Delta P/b \\ 0 \\ 0 \end{Bmatrix} \tag{6.41}$$

Accordingly, the increment of mid-plane strains $\{\Delta\varepsilon_m\}$ can be obtained from:

$$\{\Delta\varepsilon_m\} = [E_{t,m}]^{-1}\{\Delta\sigma_m\} \tag{6.42}$$

where $[E_{t,m}]$ is obtained from (6.32) for the mid-plane stresses $\{\sigma_m\}$ at the start of the step, which for the uniaxial loading case are $\langle \sigma_x \quad \sigma_y \quad \tau_{xy} \rangle^T = \langle P/bh \quad 0 \quad 0 \rangle^T$, with the current yield strength given by (6.36).

In addition to the mid-plane, the strains and stresses are sampled at the concave side of the buckled plate, which is the bottom fibre (z= –h/2) for an upward buckling mode. With the initial response up to the yield load assumed to be elastic, the initial stress state at the bottom fibre is obtained as follows:

$$\{\sigma_b\} = \begin{Bmatrix} \sigma_Y \\ 0 \\ 0 \end{Bmatrix} - \frac{h}{2}[E]\{\kappa\} \tag{6.43}$$

where $\{\kappa\}$ is the curvature associated with w_0 as the initial amplified deflection, given by (6.16) for $P=P_Y$. Clearly, the initial $\{\sigma_b\}$ exceeds the yield surface by a small amount depending on imperfection, though this small discrepancy is considered acceptable for the starting point of the model's application.

The proposed approach seeks to evaluate the increment of stress at the bottom fibre $\{\Delta\sigma_b\}$ for a specific increment of curvatures $\{\Delta\kappa\}$, hence Δw_0, in the presence of the increment of mid-plane strains $\{\Delta\varepsilon_m\}$ as determined by (6.42), as follows:

$$\{\Delta\sigma_b\} = [E_{t,b}]\{\Delta\varepsilon_b\} = [E_{t,b}]\left(\{\Delta\varepsilon_m\} - \frac{h}{2}\{\Delta\kappa\}\right) \tag{6.44}$$

where $[E_{t,b}]$ is obtained from (6.32) for the bottom fibre stresses $\{\sigma_b\}$ at the start of the step, and $\{\Delta\kappa\}$ is related to Δw_0 according to (6.28).

With the stresses assumed to vary linearly over the thickness, as shown in Figure 6.9a, the increment in the generalised bending stresses is obtained for a specific increment of $\{\Delta\kappa\}$ as follows:

$$\{\Delta M\} = \int_{-\frac{h}{2}}^{\frac{h}{2}} z\left(\{\Delta\sigma_b\} - \{\Delta\sigma_m\}\right)\left(\frac{z}{-h/2}\right)dz = \left(\{\Delta\sigma_m\} - \{\Delta\sigma_b\}\right)\frac{h^2}{6} \tag{6.45}$$

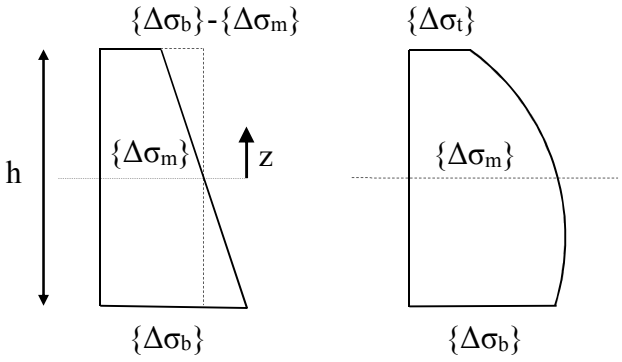

a. Linear Stress Model b. Linear Strain Model

Figure 6.9 Linear and quadratic distribution of stress over thickness

Therefore, for a specific Δw_0, $\{\Delta\kappa\}$ hence $\{\Delta\sigma_b\}$ and $\{\Delta M\}$ can be determined from (6.28), (6.44) and (6.45), respectively, and this determines the equivalent material tangent stiffness parameter according to (6.29). For small increments, the variation of $\{\Delta M\}$ with $\{\Delta\kappa\}$ reflects the flexural tangent modulus $[D_{ep}]$, hence it can be easily shown that the tangent material stiffness previously given by (6.26) becomes:

$$k_e = \int \{B\}^T \eta \{B\} dA \simeq \sum_{i=1}^{n} w_i \{B\}^T \eta \{B\}_{(x_i, y_i)} \tag{6.46}$$

Note that the proposed simplified approach does not require the explicit evaluation of the full 3×3 $[D_{ep}]$ but incorporates its influence implicitly via the evaluation of η.

For a specific load increment ΔP, k_e obtained from the proposed Linear Stress model depends on Δw_0, as above, hence the instantaneous buckling load P_c also depends on Δw_0. Therefore, the model application proceeds in the same way as discussed in Section 6.2.6 for the analytical model with a modified G_t, where P_c and Δw_0 are determined iteratively for the current incremental step. Once convergence is

achieved, P, w_0 and $\{\sigma_b\}$ are updated with their respective increments before proceeding to the next incremental step.

Remarks

It is noted that the tangent flexural modulus $[D_{ep}]$, as reflected in η, is influenced by the different tangent modulus matrices $[E_t]$ at the mid-plane and bottom extreme fibres, which are in turn determined by gradually diverging stress states at these two locations. In this respect, it is clear that the use of a constant tangent modulus matrix $[E_{tb}]$ for the flexural response, as considered in the previous plastic buckling theories, is inconsistent with the mechanics of buckling in plates with imperfections. Indeed, this effect is responsible for the interaction between flexural and axial actions, and could be a key factor for the significant inaccuracy observed in the previous analytical model utilising Incremental Theory with a modified shear modulus.

It is also worth mentioning that assumption of a linear stress variation over the plate thickness does not accord in the plastic range with the kinematics of thin plates in which the total strain is assumed to vary linearly over the thickness. In this respect, the proposed Linear Stress model, while satisfying the incremental planar and flexural equilibrium conditions, is rather weak on compatibility, which is only satisfied at the mid-plane and the bottom extreme fibre. To assess the significance of this issue, a so-called Linear Strain model is also considered in the next section, where stronger compatibility is considered by sampling strains at three points over the thickness, and utilising a quadratic distribution for the stresses in the incremental planar and flexural equilibrium conditions.

6.3.3 Linear Strain Model

In this model, the strains are sampled at three positions over the thickness, at the mid-plane and the two extreme fibres, in accordance with the kinematic assumption of linear strain distribution over the thickness, and the corresponding stresses are interpolated quadratically over the thickness (Figure 6.9b). Accordingly, the initial state of stress is obtained at the three corresponding points over the thickness similar to (6.43):

$$\{\sigma_m\} = \begin{Bmatrix} \sigma_Y \\ 0 \\ 0 \end{Bmatrix}; \quad \{\sigma_t\} = \{\sigma_m\} + \frac{h}{2}[E]\{\kappa\}; \quad \{\sigma_b\} = \{\sigma_m\} - \frac{h}{2}[E]\{\kappa\} \tag{6.47}$$

where, as before, $\{\kappa\}$ is the curvature associated with the amplified imperfection assuming an initially elastic response.

The tangent flexural modulus parameter η is obtained in a similar manner to the previous Linear Stress model, with the exception that the incremental planar strains $\{\Delta\varepsilon_m\}$ and curvatures $\{\Delta\kappa\}$ are now coupled in the conditions of incremental planar equilibrium, hence $\{\Delta\varepsilon_m\}$ cannot be determined independently of $\{\Delta\kappa\}$ as in the Linear Stress model. Instead, $\{\Delta\varepsilon_m\}$ is obtained as part of the iterative procedure seeking the values of P_c and $\{\Delta w_0\}$, as discussed for the Linear Stress model where, at every iteration, $\{\Delta\kappa\}$ would be known.

With the increments of strain at the two extreme fibres given by:

$$\{\Delta\varepsilon_t\} = \{\Delta\varepsilon_m\} + \frac{h}{2}\{\Delta\kappa\}; \quad \{\Delta\varepsilon_b\} = \{\Delta\varepsilon_m\} - \frac{h}{2}\{\Delta\kappa\} \tag{6.48}$$

the incremental stresses at the three sampled locations, $\{\Delta\sigma_m\}$, $\{\Delta\sigma_b\}$ and $\{\Delta\sigma_t\}$, are effectively determined in terms of $\{\Delta\varepsilon_m\}$ and $\{\Delta\kappa\}$ using the respective tangent modulus matrices $[E_t]$ at the start of the incremental step:

$$\{\Delta\sigma_{t\backslash b}\} = [E_{t,t\backslash b}]\left(\{\Delta\varepsilon_m\} \pm \frac{h}{2}\{\Delta\kappa\}\right); \quad \{\Delta\sigma_m\} = [E_{t,m}]\{\Delta\varepsilon_m\} \tag{6.49}$$

With the assumption of a quadratic stress distribution, the incremental stresses are obtained over the thickness:

$$\{\Delta\sigma\} = 2\left(\{\Delta\sigma_t\} + \{\Delta\sigma_b\} - 2\{\Delta\sigma_m\}\right)\left(\frac{z}{h}\right)^2 + \left(\{\Delta\sigma_t\} - \{\Delta\sigma_b\}\right)\frac{z}{h} + \{\Delta\sigma_m\} \tag{6.50}$$

thus also effectively determined by $\{\Delta\varepsilon_m\}$ and $\{\Delta\kappa\}$.

Noting the conditions of incremental planar equilibrium:

$$\int_{-\frac{h}{2}}^{\frac{h}{2}} \{\Delta\sigma\}\, dz = \begin{Bmatrix} \Delta N_x \\ \Delta N_y \\ \Delta N_{xy} \end{Bmatrix} \Rightarrow \{\Delta\sigma_t\} + 4\{\Delta\sigma_m\} + \{\Delta\sigma_b\} = \frac{6}{h} \begin{Bmatrix} \Delta N_x \\ \Delta N_y \\ \Delta N_{xy} \end{Bmatrix} \tag{6.51}$$

with the incremental stress resultants given by (6.41) for a uniaxial loading in the x-direction, $\{\Delta\varepsilon_m\}$ can be obtained for a specific $\{\Delta\kappa\}$ from:

$$\left([E_{t,t}] + 4[E_{t,m}] + [E_{t,b}]\right)\{\Delta\varepsilon_m\} = \frac{6}{h} \begin{Bmatrix} \Delta N_x \\ \Delta N_y \\ \Delta N_{xy} \end{Bmatrix} - \frac{h}{2}\left([E_{t,t}] - [E_{t,b}]\right)\{\Delta\kappa\} \tag{6.52}$$

Thus for a specific $\{\Delta\kappa\}$, the incremental bending/twisting moments can be determined from:

$$\{\Delta M\} = \int_{-\frac{h}{2}}^{\frac{h}{2}} z\{\Delta\sigma\}\, dz = \left(\{\Delta\sigma_t\} - \{\Delta\sigma_b\}\right)\frac{h^2}{12} \tag{6.53}$$

which resembles the corresponding expression in (6.45) for the Linear Stress model.

With $\{\Delta M\}$ associated with $\{\Delta\kappa\}$ determined as above, the application of the Linear Strain model proceeds in a similar manner to the Linear Stress model, as presented in the previous section, where at every incremental step iterations are undertaken to establish P_c and Δw_0 that satisfy the expressions of the instantaneous buckling load and the conditions of the incremental flexural equilibrium. The plate maximum buckling resistance P_{max} is obtained when the criterion $\Delta P/\Delta w_0 \approx 0$ is satisfied.

A flowchart representing the application procedure of both the Linear Stress and Linear Strain models is presented in Figure 6.10.

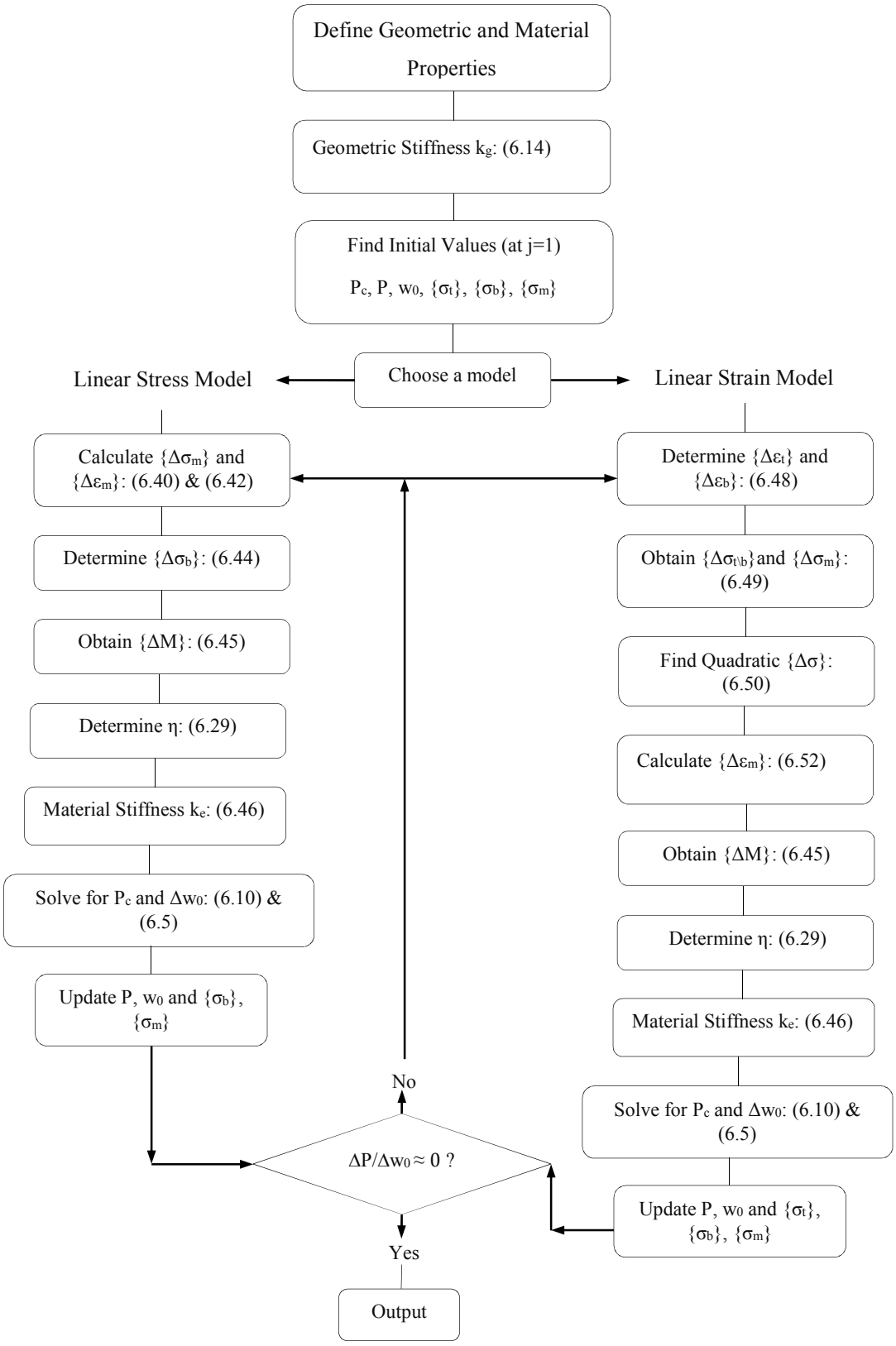

Figure 6.10 Flowchart of calculation

6.3.4 Results and Comparisons

As with the analytical model based on the Incremental Theory with a modified shear modulus, the equivalent tangent material stiffness k_e is evaluated numerically from (6.46) using Gaussian quadrature while the geometric stiffness k_g is obtained analytically from (6.14). It is noted that when k_e is evaluated using one integration point over a quarter model of the plate, both approaches underestimate the prediction of the elastic critical buckling load by nearly 9%. In other words, one Gauss point per quarter model may not be adequate to estimate the correct value of k_e, hence the buckling response. In this respect, a comparative study will be subsequently undertaken to establish the influence of enhanced numerical integration with more Gauss points.

6.3.4.1 Post-buckling Response

The post-buckling responses of a simply-supported stocky square plate, with the same geometric and material properties considered previously in Section 6.2.7, are obtained using the Linear Stress and Linear Strain models with 1 Gauss point over a quarter model, and are compared to the numerical results of ADAPTIC in Figure 6.11.

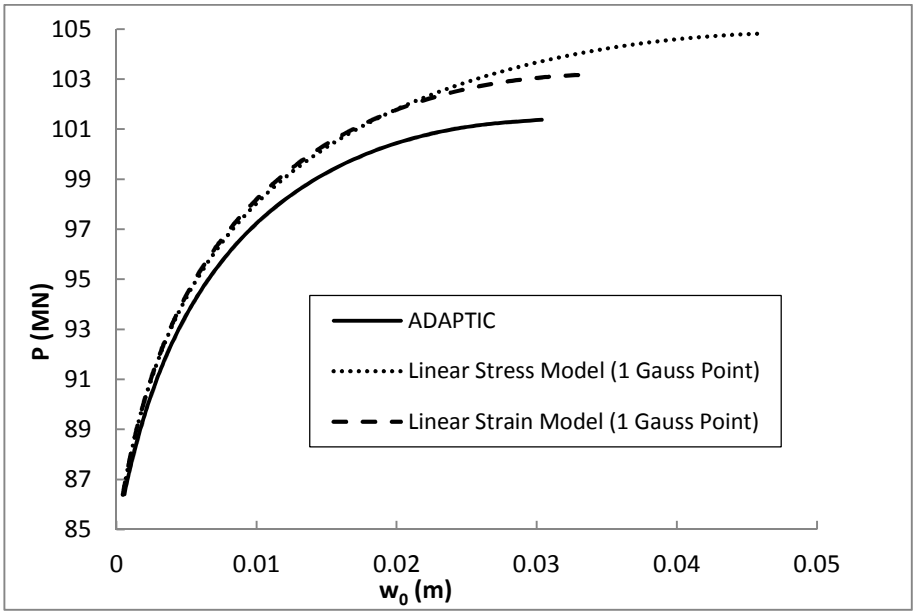

Figure 6.11 Post-buckling response of stocky square plate with b/h=20 and w_{0i}=b/1000

It is strikingly clear that the two proposed Linear Stress and Linear Strain models offer an excellent comparison against the results of ADAPTIC in terms of the initial post-buckling response and the maximum buckling resistance, which is predicted to within 3.4% and 1.8% by the two respective models. A comparison against Incremental Theory with and without a reduced shear modulus is presented in Table 6.2. Considering that the analytical model based on the Incremental Theory with a reduced shear modulus overestimated the buckling resistance by over 250% as previously shown in Figure 6.5, the success of the two proposed analytical models becomes evident. Moreover, this reaffirms the contention of this work that the reduced plastic buckling capacity of stocky plates cannot be attributed merely to a reduced tangent shear modulus, rather it can only be explained if the interactions between the planar and flexural actions are considered in the plastic range. It is therefore contended that this offers the first rational and mechanics-based explanation of the Plate Plastic Buckling Paradox.

Table 6.2 Comparison of P_{max} (MN)

b/h	P_Y	Linear Stress Model	Linear Strain Model	ADAPTIC	Incremental Theory	Incremental Theory with Modified G_t
20	86.4	105	103	101	487	351

Considering the results in Figure 6.10, there are some differences between the predictions of the Linear Stress and Linear Strain models, notably the displacement corresponding to the maximum buckling resistance. This is of course attributed to the different effective stress distributions considered by the two models. However, with the discrepancy in the maximum buckling resistance being rather small, this suggests that the assumption of a linear stress variation over the thickness, even in the plastic range, is reasonable. This is particularly interesting, since the Linear Stress model is much simpler to apply than the Linear Strain model.

To shed further light on the reduction in the plastic buckling resistance with the two proposed models, a comparison of the tangential flexural stiffness parameter η as obtained from the different models is undertaken in Figure 6.12. It is evident that the flexural tangent modulus matrix $[D_{ep}]$, as reflected by η, is greatly improved. The

values of η from ADAPTIC are slightly greater than those of the proposed analytical models, which is somewhat at odds with the fact that the post-buckling resistance from the analytical models overestimates that from ADAPTIC.

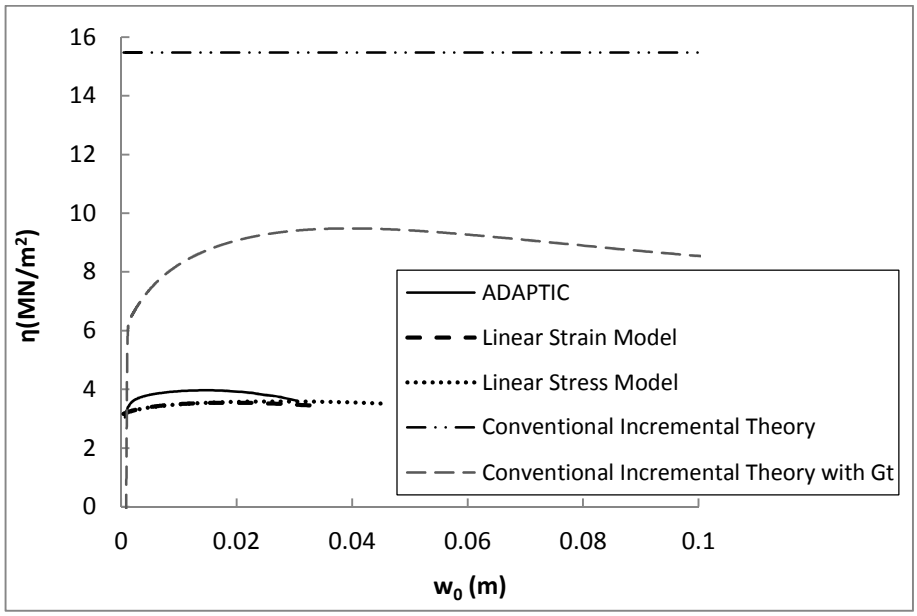

Figure 6.12 η-w curves for simply-supported square plate, b/h=20 and w_{0i}=b/1000

The slight discrepancy in the values of η obtained from the analytical models and ADAPTIC is attributed to the following approximations and assumptions:

- A SDOF buckling mode is assumed for the analytical models, while ADAPTIC employs a more accurate MDOF discretisation. This can lead to a discrepancy in the curvatures between the analytical and finite element models.
- The true stress distribution over the plate thickness, captured with ADAPTIC using several through-thickness integration points, may not be accurately represented by the linear and quadratic stress distributions assumed for the two analytical models.
- The planar resultant stresses may vary over the domain, which is captured with ADAPTIC, while a uniform distribution is assumed in the proposed analytical models.

Despite the fact that the analytical models underestimate η in comparison with ADAPTIC, the buckling resistance is overestimated. This is mainly attributed to the

numerical integration in the analytical models with only one Gauss point, where it is possible that η is subject to significant variation over the plate area. To shed further light on this issue, the results from the analytical models are obtained with 4×4 Gauss points over the whole plate domain, or 2×2 Gauss points over a quarter model with the coordinates and weighting factors given by:

$(x_1, y_1) = (0.06943a, 0.06943b)$ with $w_1 = 0.34785$
$(x_2, y_2) = (0.33001a, 0.06943b)$ with $w_2 = 0.65214$
$(x_3, y_3) = (0.33001a, 0.33001b)$ with $w_3 = 0.65214$
$(x_4, y_4) = (0.06943a, 0.33001b)$ with $w_4 = 0.34785$

Interestingly, the elastic buckling load of the plate is obtained with the increased number of Gauss points to an improved accuracy of around 0.03%. However, the predictions of the proposed analytical models relating to the plastic buckling response have become slightly worse compared to the results of ADAPTIC, as illustrated by the comparisons in Figure 6.13.

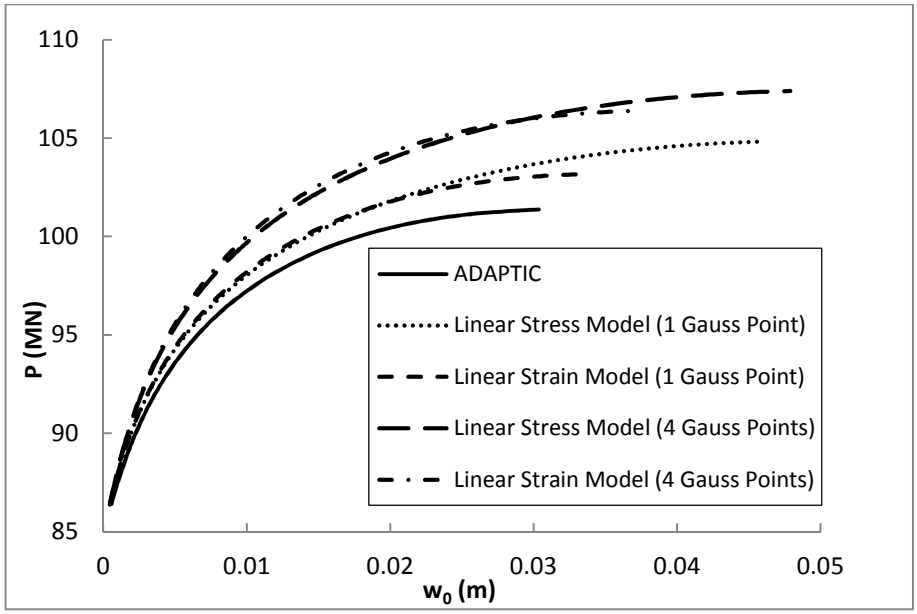

Figure 6.13 Post-buckling response with 2×2 Gauss Points, b/h=20 and w_{0i}=b/1000

Notwithstanding, the reduction in accuracy with more Gauss points, which is mainly attributed to the SDOF buckling mode assumed in the analytical models, the comparison of η at the Gauss point locations in Figure 6.14 confirms that the flexural

stiffness varies significantly over the plate domain. This raises further questions on the adequacy of previous analytical methods, in which it was assumed that plastic buckling of plates may be treated as a bifurcation problem similar to elastic buckling but using a uniform and modified tangent flexural stiffness. Importantly, it is clear that the proposed analytical model captures the variation of the tangent flexural stiffness over the plate very well, and that its slight overestimation of the maximum buckling resistance can be attributed to the overestimation of η; particularly at Locations 2 and 4.

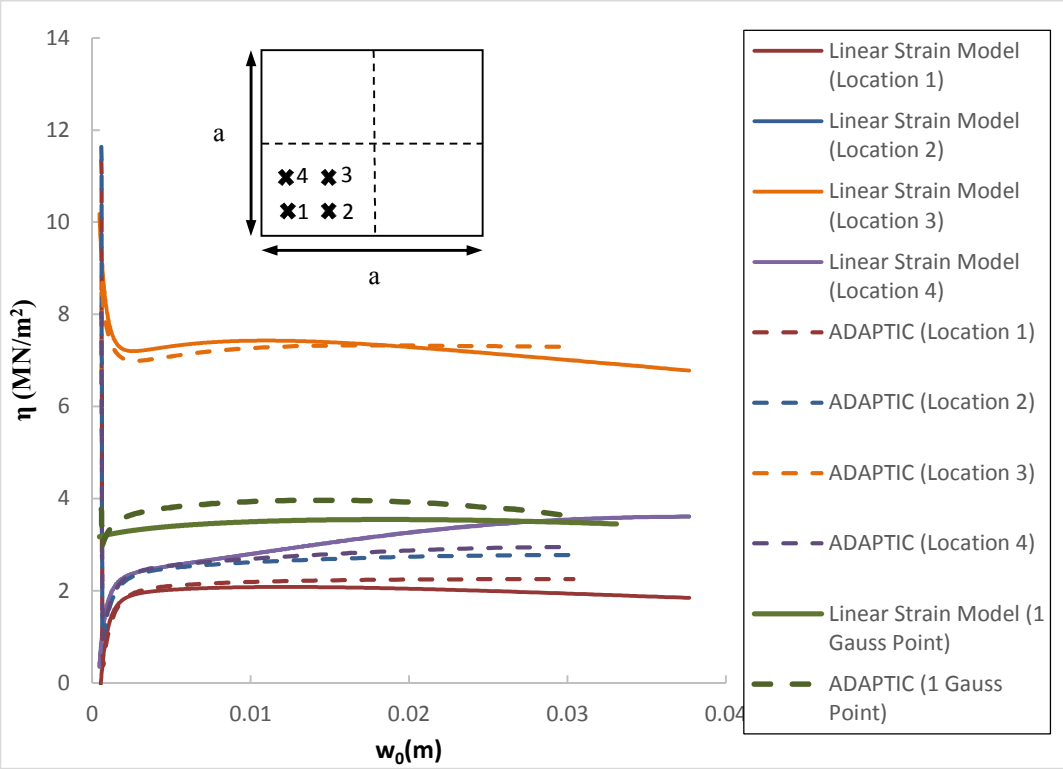

Figure 6.14 η-w curves evaluated at Gauss point locations in a quarter model

In the following sub-sections, the two proposed analytical models are verified further in comparison with ADAPTIC considering different levels of imperfection and plate slenderness, and comparisons are finally made against the results of previous methods.

6.3.4.2 Imperfection Sensitivity

The sensitivity of the plastic buckling response of a stocky plate to geometric imperfections is investigated here, where consideration is given to different

imperfection amplitudes: w_{0i}= b/2000, b/1000, b/500 and b/250. As before, the mode of imperfection is taken to be identical to the assumed buckling mode. The post-buckling response of the stocky plate with b/h=20 for different imperfections is shown in Figure 6.15, where the predictions of the two proposed analytical models are compared against the results of ADAPTIC.

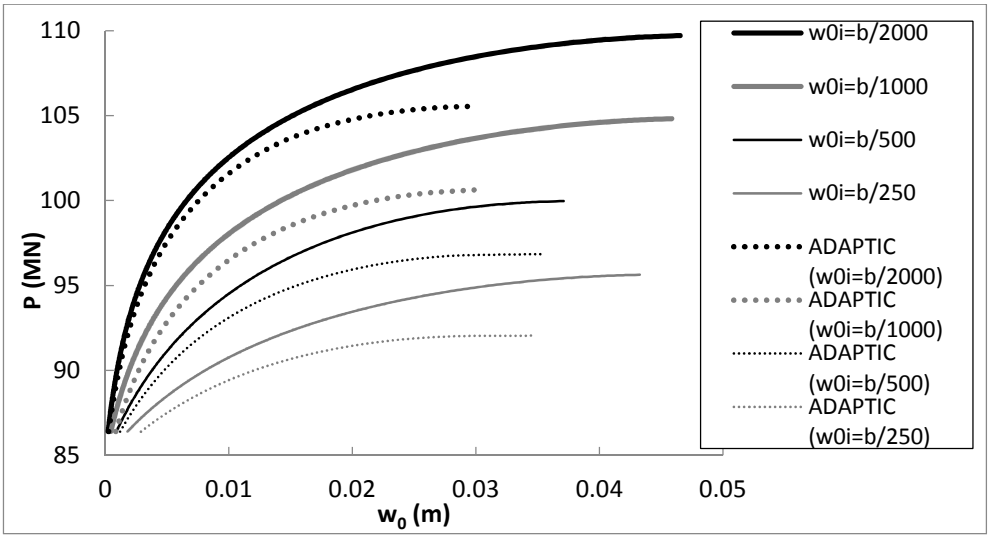

a. Linear Stress model

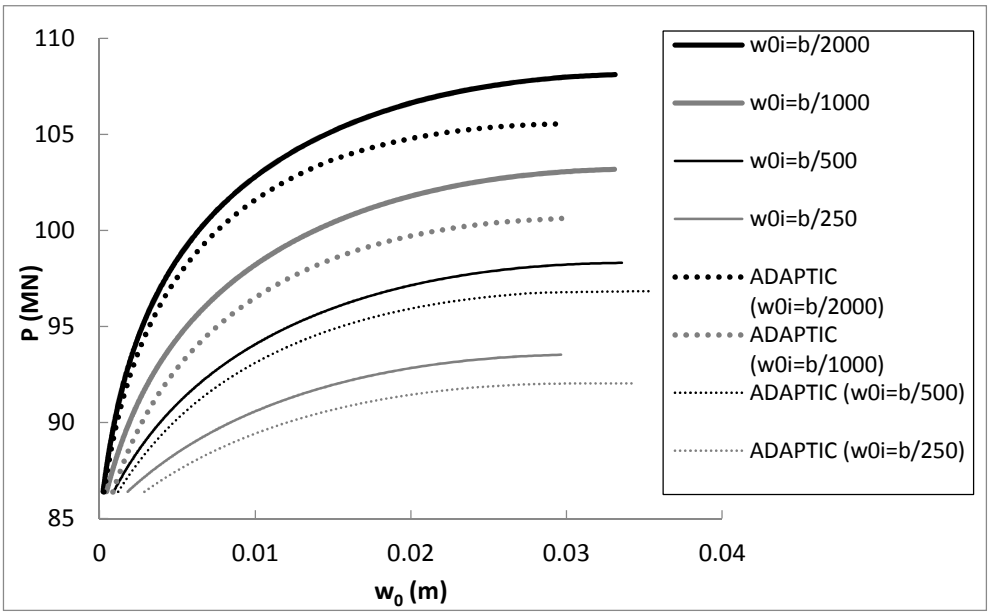

b. Linear Strain model

Figure 6.15 Influence of imperfection on plastic buckling response of stocky plate (b/h=20)

The results demonstrate that the Linear Stress and Linear Strain models provide good predictions of the maximum buckling capacity to well within 7% for all levels of imperfection. Moreover, it is generally observed that increasing imperfection reduces the post-buckling response, which is consistently predicted by the analytical models and ADAPTIC. Similar sensitivity analysis was also performed for less stocky plates (b/h=25, 30, 35) but not shown here, where it was found out that stockier plates are more susceptible to imperfection.

6.3.4.3 Effect of Slenderness

Consideration is given here to the effect of plate slenderness on the plastic buckling response, maintaining a low level of imperfection of w_{0i}=b/2000, where the results are presented in Figure 6.16 for a range of b/h ratios achieved by modifying the thickness h. The stockier plates exhibit increased resistance, as expected, and also an enhanced maximum plastic buckling resistance in relation to the initial buckling load at yield. The buckling resistances obtained from the two proposed analytical models agree well with the predictions of ADAPTIC to within 9%, where the discrepancy is greater for the stockier plates. This may be attributed to the presence of transverse shear deformation in relatively thick plates, which is accounted for in ADAPTIC but not in the analytical models.

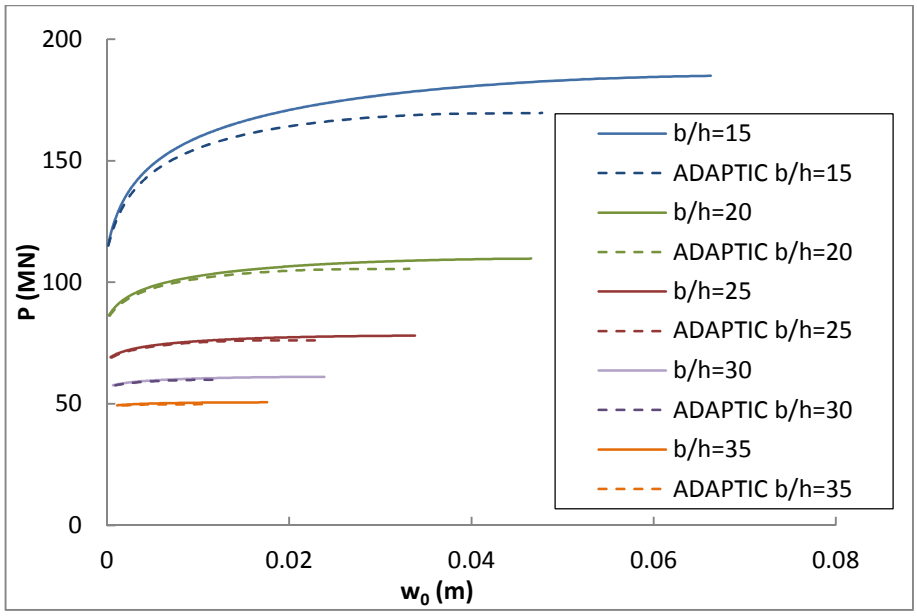

a. Linear Stress model

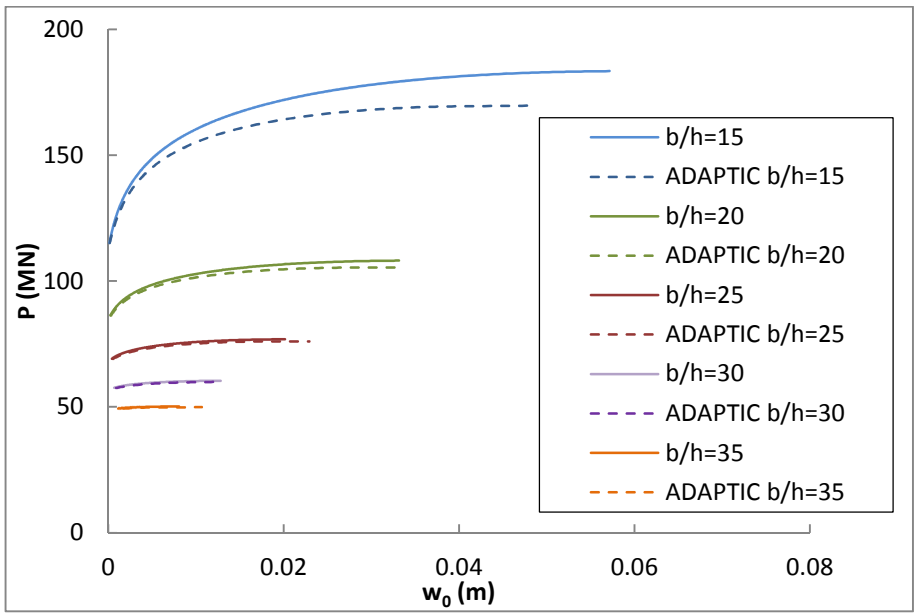

b. Linear Strain model

Figure 6.16 Influence of slenderness on plastic buckling response of an imperfect plate (w_{0i}=b/2000)

6.3.4.4 Comparisons with Previous Methods

As already evident from the previous comparisons, it is clear that the Plate Plastic Buckling Paradox is mainly due to the fact that no consideration was given in the previous approaches to the plastic interaction between planar and flexural actions.

Indeed, it has been shown that consideration of this interaction with established principles of material plasticity in the proposed analytical models effectively resolves this paradox. This is further highlighted by comparing the maximum buckling resistance obtained from the proposed analytical models against the predictions of previous methods, namely i) conventional Incremental Theory, ii) Deformation Theory, iii) Bleich's semi-rational equation, and iv) Becque's approach (with m=1), where the results are presented in Table 6.3 and Figure 6.17 for various b/h ratios. Except for ADAPTIC and the proposed analytical models, none of the aforementioned approaches consider the influence of initial imperfections, hence a small imperfection w_{0i}=b/2000 is considered for comparison purposes.

Table 6.3 Maximum buckling resistance (in MN) for imperfect stocky plate (w_{0i}=b/2000)

b/h	P_Y	P_{ce}	Conventional Incremental Theory	Deformation Theory	Analytical Model		ADAPTIC	Bleich's Theory	Becque's Approach
					Linear Stress	Linear Strain			
60	28.80	20.25	20.25	20.25	20.25	20.25	20.25	20.25	20.25
50	34.60	34.98	34.98	34.98	34.98	34.98	34.85	34.98	34.98
40	43.20	68.33	60.88	43.59	43.45	43.30	43.09	43.20	43.20
35	49.40	102.00	90.87	50.28	50.60	50.17	49.88	49.40	49.40
30	57.60	162.00	144.30	59.52	61.10	60.38	60.00	57.60	69.60
25	69.10	279.90	249.40	73.20	78.02	76.87	76.16	69.12	120.31
20	86.40	546.60	487.00	95.44	109.70	108.11	105.50	86.40	235.20
15	115.20	1296.00	1154.40	139.00	185.00	183.00	170.00	183.24	557.03

It is also interesting to compare the predictions of different methods of finding the maximum buckling load for simply-supported square plates using load-slenderness curves, Figure 6.17.

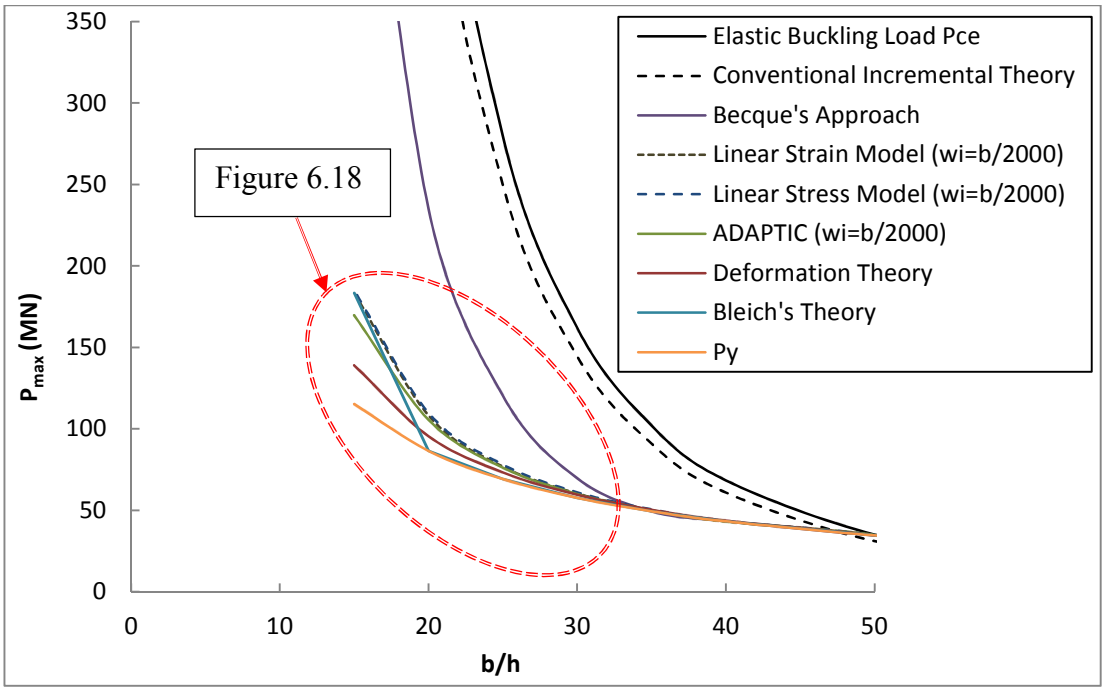

Figure 6.17 Comparison of maximum plate buckling resistance predicted by various methods

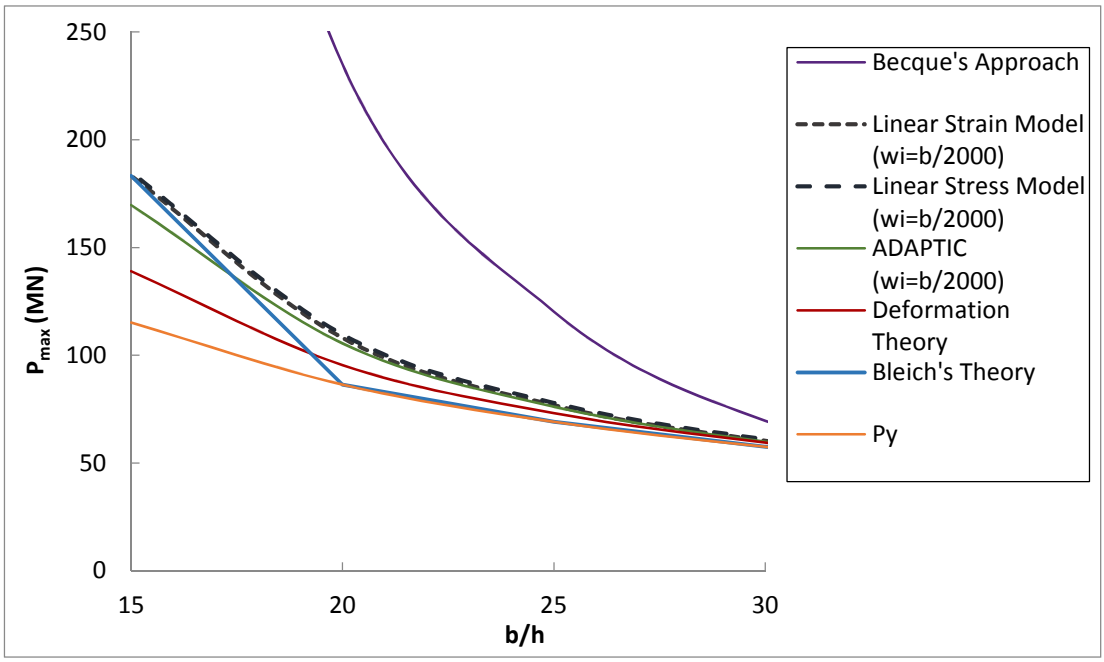

Figure 6.18 Zoomed-in area in Figure 6.17

With the same material properties used for all methods, Figure 6.17 shows that the various predictions of the plate buckling resistance P_{max} are bounded from below by the yield load P_Y and from above by the elastic buckling load P_{ce} , as expected.

Beyond a slenderness ratio of around b/h=30 (i.e. an 80mm thickness), all methods except for the conventional Incremental Theory predict P_{max} close to the yield load P_Y. However, for stockier plates P_{max} becomes greater than P_Y, and the difference between the various methods becomes more significant. It is evident that the conventional Incremental Theory followed by Becque's method with a single half-wave (m=1) overestimate the plastic buckling significantly in comparison with the results of ADAPTIC. On the other hand, Deformation Theory generally predicts a buckling resistance for stocky plates which is smaller compared to all the other methods and becomes increasingly inaccurate for stockier plates. Evidently, the proposed analytical models founded on the accepted principles of incremental plasticity, but with a modified flexural tangent modulus that accounts for the interaction with the planar actions, provide greatly improved prediction of P_{max} compared to previous methods and particularly the conventional Incremental Theory.

6.4 Elastic Unloading

It is well established that local elastic unloading may occur in structures sustaining plastic deformation even under increasing load. In accordance with the theory of plasticity, plastic loading is maintained for a material point that is already plastic only if the non-zero incremental plastic deformations required to keep the stress state on the yield surface are in the direction of the outward normal to the same surface. Otherwise, no further plastic deformations occur, and the stress state moves inside the yield surface.

In order to investigate whether elastic unloading occurs in the plastic buckling of stocky plates, consideration is given to the material points on the convex surface (z=h/2) at Gauss point locations. With reference to Figure 6.19, the condition of elastic unloading can be expressed in terms of the incremental stresses $\{\Delta\sigma_t\}$ and the normal $\{N\}$ to the yield surface at the current stress state $\{\sigma_t\}$:

$$\{N\}^T\{\Delta\sigma_t\} < 0 \Leftrightarrow \text{elastic unloading} \tag{6.54}$$

In the Linear Strain model, $\{\Delta\sigma_t\}$, hence $\{\sigma_t\}$, is already evaluated for the through-thickness discretisation, while for the Linear Stress model, $\{\Delta\sigma_t\}$ is obtained from the incremental stresses at the bottom fibre and the mid-plane as follows:

$$\{\Delta\sigma_t\} = 2\{\Delta\sigma_m\} - \{\Delta\sigma_b\} \tag{6.55}$$

Careful investigation of the results from the two analytical models has shown that there is no elastic unloading at the Gauss points throughout the plastic buckling response up to the maximum buckling resistance. This highlights another significant difference between the plastic buckling of plates and columns, where elastic unloading occurs for columns in the early stages of plastic buckling.

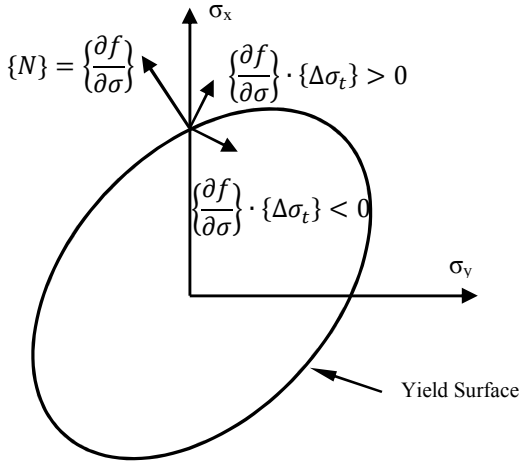

Figure 6.19 Criterion for elastic unloading

6.5 Discussion and Conclusions

As discussed in Chapter 2, constitutive relations based on the Incremental Plasticity Theory using the associated flow rule are widely accepted to represent the mechanics of materials undergoing plastic deformations. Yet, the direct application of these relations in the plastic buckling of stocky plates was shown to provide significant overestimation of the plastic buckling resistance in comparison with the less sound Deformation Theory, leading to the Plate Plastic Buckling Paradox. In this chapter, two simplified analytical models have been proposed for simply-supported square plates subject to a uniaxial loading, which employ Incremental Theory but recognise the important influence of the interaction between planar and flexural actions. Through verification against the results of nonlinear finite element analysis, it has been confirmed that the proposed analytical models provide a notable improvement over other simplified methods that are empirical or irrational, and importantly offer

the definitive explanation regarding the inaccuracy of the conventional buckling approach based on the Incremental Theory as well as the associated Plastic Buckling Paradox.

To gain further insight into the predictions of different simplified buckling methods, the associated tangent modulus matrix $[E_t]$ is evaluated for each of these methods at their maximum predicted buckling resistance, where for comparison purposes the previously investigated square plate with b/h=20 and an initial imperfection w_{0i}=b/2000 is considered:

Deformation Theory ($P_{max}=0.95\times10^8$N)

$$[E_t]=\begin{bmatrix} 1.590\times10^{10} & 2.359\times10^{10} & 0 \\ 2.359\times10^{10} & 4.755\times10^{10} & 0 \\ 0 & 0 & 1.275\times10^{10} \end{bmatrix}$$

Conventional Incremental Theory ($P_{max}=4.87\times10^8$N)

$$[E_t]=\begin{bmatrix} 5.863\times10^{10} & 1.097\times10^{11} & 0 \\ 1.097\times10^{11} & 2.212\times10^{11} & 0 \\ 0 & 0 & 8.077\times10^{10} \end{bmatrix}$$

Conventional Incremental Theory with a reduced G_t ($P_{max}=3.51\times10^8$N)

$$[E_t]=\begin{bmatrix} 5.863\times10^{10} & 1.097\times10^{11} & 0 \\ 1.097\times10^{11} & 2.212\times10^{11} & 0 \\ 0 & 0 & 2.954\times10^{10} \end{bmatrix}$$

Becque's Approach ($P_{max}=2.35\times10^8$N)

$$[E_t]=\begin{bmatrix} 4.934\times10^{9} & 1.480\times10^{9} & 0 \\ 1.224\times10^{11} & 2.467\times10^{11} & 0 \\ 0 & 0 & 2.759\times10^{9} \end{bmatrix}$$

Linear Stress model ($P_{max}=1.097\times10^8$N)

At mid-plane:

$$\left[E_{t,m}\right]=\begin{bmatrix} 5.863\times10^{10} & 1.097\times10^{11} & 0 \\ 1.097\times10^{11} & 2.212\times10^{11} & 0 \\ 0 & 0 & 8.077\times10^{10} \end{bmatrix}$$

At bottom fibre:

$$\left[E_{t,b}\right]=\begin{bmatrix} 7.268\times10^{10} & 2.595\times10^{10} & 6.111\times10^{10} \\ 2.595\times10^{10} & 2.189\times10^{11} & 1.673\times10^{10} \\ 6.111\times10^{10} & 1.673\times10^{10} & 5.715\times10^{10} \end{bmatrix}$$

Linear Strain model ($P_{max}=1.081\times10^{8}N$)

At top fibre:

$$\left[E_{t,t}\right]=\begin{bmatrix} 1.227\times10^{11} & 1.327\times10^{11} & -3.073\times10^{10} \\ 1.327\times10^{11} & 1.934\times10^{11} & 1.807\times10^{10} \\ -3.073\times10^{10} & 1.807\times10^{10} & 7.203\times10^{10} \end{bmatrix}$$

At mid-plane:

$$\left[E_{t,m}\right]=\begin{bmatrix} 5.770\times10^{10} & 1.089\times10^{11} & 1.332\times10^{9} \\ 1.089\times10^{11} & 2.217\times10^{11} & -3.050\times10^{8} \\ 1.332\times10^{9} & -3.050\times10^{8} & 8.076\times10^{10} \end{bmatrix}$$

At bottom fibre:

$$\left[E_{t,b}\right]=\begin{bmatrix} 4.181\times10^{10} & 6.518\times10^{10} & 3.714\times10^{10} \\ 6.518\times10^{10} & 2.307\times10^{11} & 7.965\times10^{8} \\ 3.714\times10^{10} & 7.965\times10^{8} & 7.347\times10^{10} \end{bmatrix}$$

Clearly, $[E_t]$ varies over the thickness with the proposed Linear Stress and Linear Strain models, which is attributed to the different stress states over the thickness. This is illustrated for the Linear Stress model in Figure 6.20, where a graphical

representation is provided of the associated stress states relative to the yield surface in the (σ_x,σ_y) and (σ_x,τ_{xy}) spaces.

Comparing the [E_t] matrices corresponding to the conventional Incremental Theory and Deformation Theory, it is evident that the diagonal terms of the former are much larger than those of the latter, which is mainly responsible for the unrealistically large buckling resistance of the Incremental Theory.

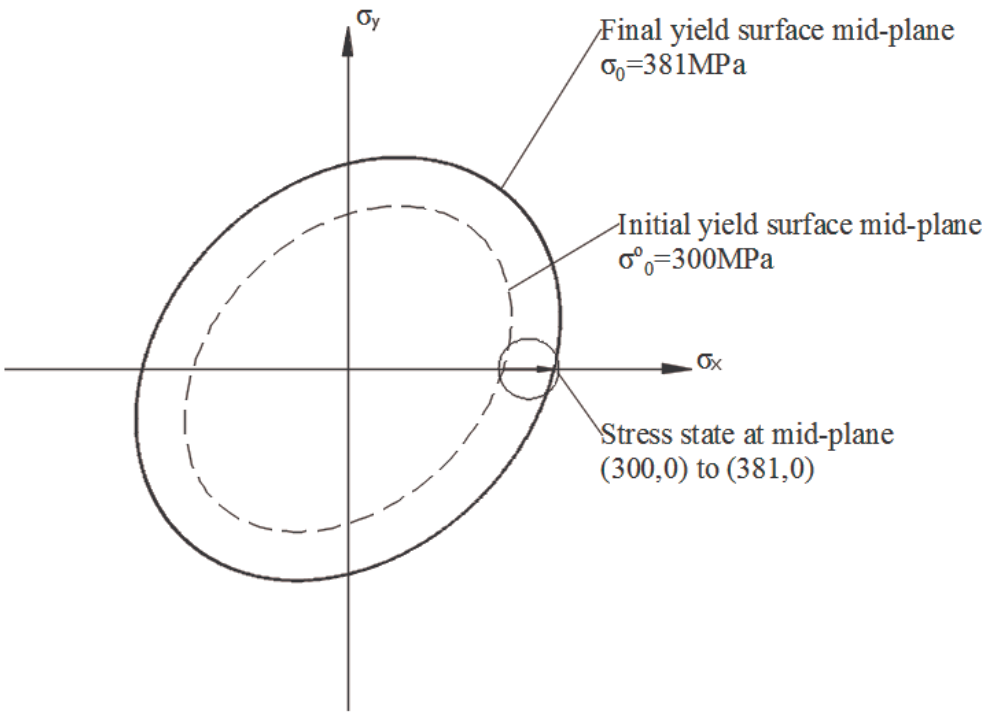

a. Hardening in (σ_x,σ_y) space

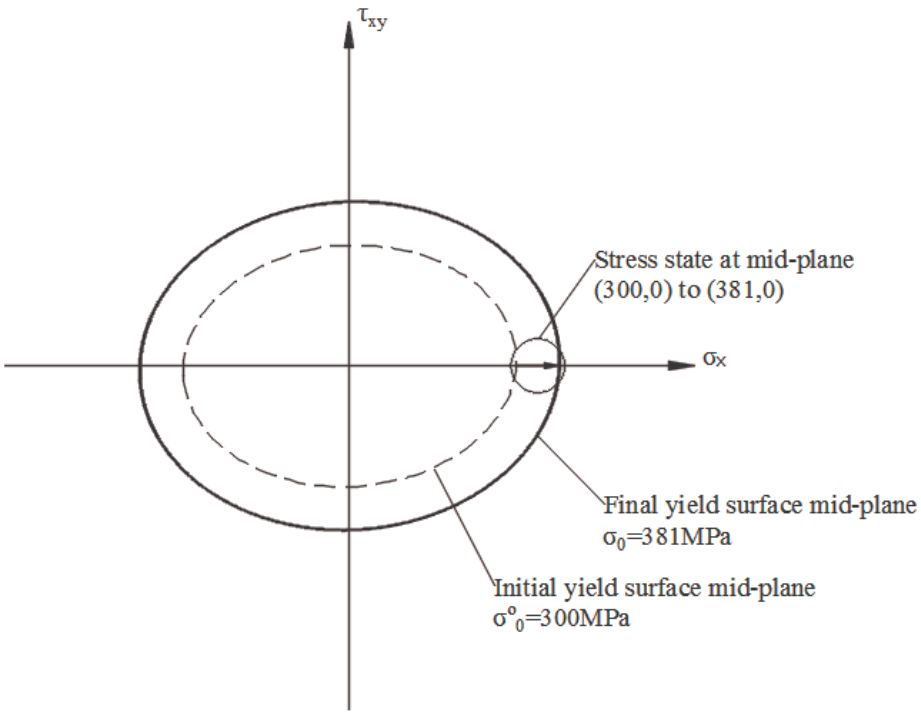

b. Hardening in (σ_x,τ_{xy}) space

Figure 6.20 Mid-plane initial and final stress states at Gauss point (Linear Stress model)

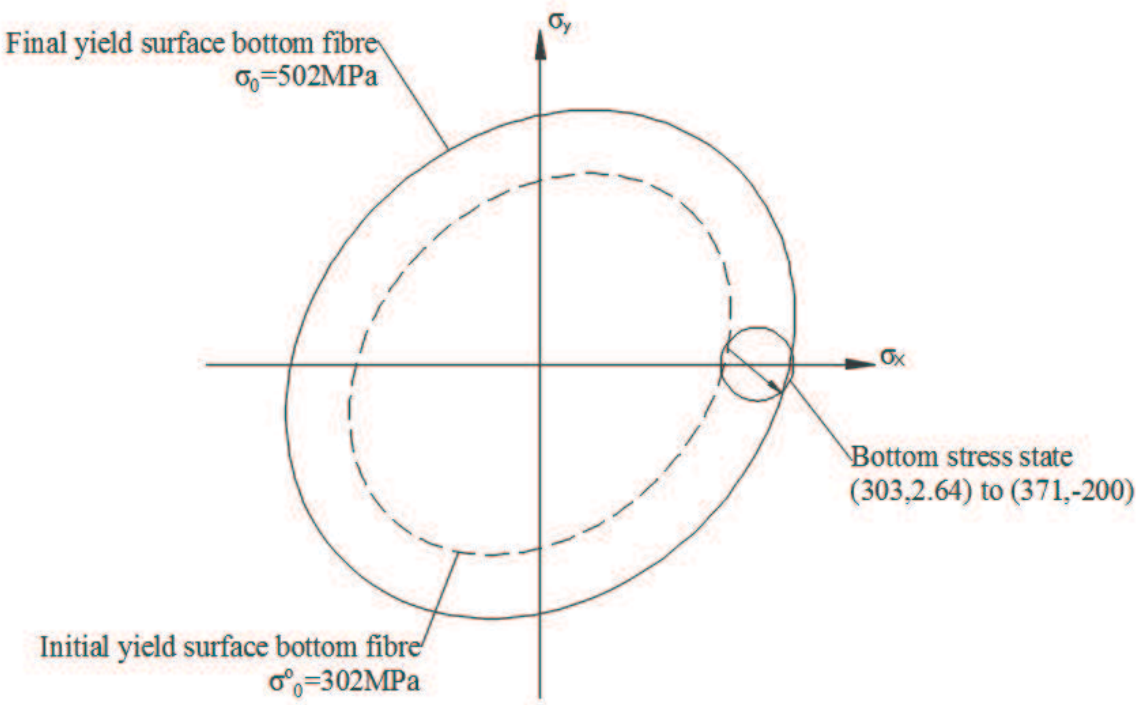

a. Hardening in (σ_x,σ_y) space

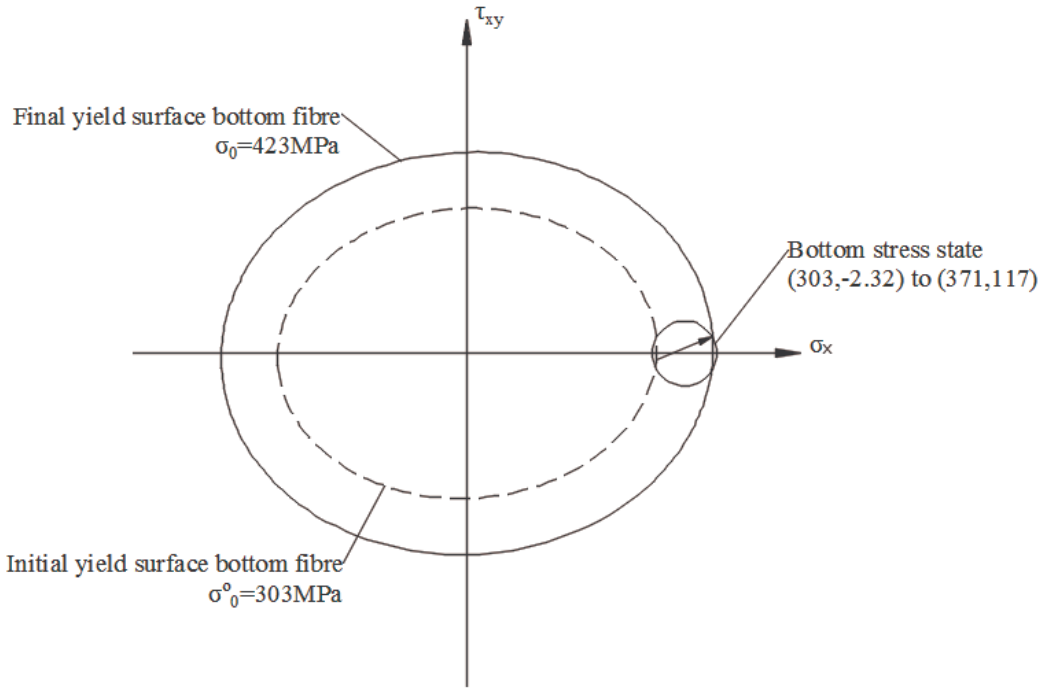

b. Hardening in (σ_x,τ_{xy}) space

Figure 6.21 Bottom fibre initial and final stress states at Gauss point (Linear Stress model)

Considering the proposed analytical models, $[E_t]$ at mid-plane for the Linear Stress model is identical to that of the conventional Incremental Theory, and that is almost the same at the mid-plane for the Linear Strain model. However, it is evident that utilising an $[E_t]$ associated with the stress state at mid-plane, regardless of whether the tangent shear modulus G_t is modified to any value in the range [0, G], leads to a significant overestimation of P_{max}. Thus, it is confirmed that a realistic determination of the buckling resistance requires additional information about the distribution of stresses and the associated variation of $[E_t]$ over the thickness.

The variation of $[E_t]$ over the thickness has important implications about the dependence of the incremental moments $\{\Delta M\}$ not only on the incremental curvatures $\{\Delta\kappa\}$ but also on the incremental mid-plane strains $\{\Delta\varepsilon_m\}$, which is completely ignored in the previous analytical methods. To elaborate, considering (6.44) and (6.45) for the Linear Stress model, $\{\Delta M\}$ is effectively related to both $\{\Delta\kappa\}$ and $\{\Delta\varepsilon_m\}$ as follows:

$$\{\Delta M\} = \frac{h^3}{12}\left[E_{t,b}\right]\{\Delta\kappa\} - \frac{h^2}{6}\left(\left[E_{t,b}\right] - \left[E_{t,m}\right]\right)\{\Delta\varepsilon_m\} \tag{6.56}$$

The first term multiplying $\{\Delta\kappa\}$ is the only term considered by the previous simplified methods of plate buckling analysis. Considering the specific numerical values of $[E_{t,m}]$ and $[E_{t,b}]$ provided above for the Linear Stress model, it is evident that $[E_{t,b}]$ is comparable to $[E_{t,m}]$, thus it is this significant negative second term that would account for a reduction in $\{\Delta M\}$ and hence the associated tangent modulus parameter η.

With the resolution of the Plate Plastic Buckling Paradox, the two proposed analytical models offer a valuable tool for assessing and gaining insight into factors that influence the plastic buckling of stocky plates. Such factors, including the buckling mode, plate aspect ratio, biaxial loading and material properties are considered in the next chapter.

CHAPTER 7

Parametric and Application Studies

7.1 Introduction

Steel plates as structural components have a wide range of application including construction (buildings, bridges, etc.), shipbuilding, offshore structures, and military applications, to name but a few. In most cases, moderately thick steel, aluminium or stainless steel plates are utilised, for which the compressive resistance can be much greater than the yield limit due to strain hardening. Yet, in some applications, such as the design of plated steel beams, the compressive strength of stocky plates is limited to the yield strength (Standards, 2006), which could be attributed to the lack of a sound analytical model for plastic buckling of plates.

The main focus in Chapter 6 was to present two variants of a simplified model for predicting the plastic buckling resistance of simply-supported square plates under uniform uniaxial compression. The buckling mode and initial imperfection were assumed to have the shape of the critical elastic buckling mode, characterised by one half-wave in the two planar directions. The first part of this chapter considers the further application of the proposed model to square plates, investigating the effects of imperfection amplitude w_{0i}, buckling mode (i.e. number of half-waves m in the direction of loading), strain-hardening, and biaxial loading. On the other hand, the second part is concerned with the application of the analytical model to the plastic buckling of rectangular plates, ranging from infinitely long plates, loaded longitudinally along the short edge, to wide plates, loaded transversely along the long edge.

Given its simplicity and demonstrable accuracy, as shown in Chapter 6, the Linear Stress model is considered in this chapter for the application studies in preference to the Linear Strain model, with numerical integration performed using 2×2 Gauss points over the whole domain (i.e. 1 Gauss point over a quarter model). However, in

some specific cases where the accuracy of this basic model may be in question, the Linear Strain model and/or 4×4 Gauss points over the whole plate are considered. Furthermore, for all cases, the issue of elastic unloading is monitored and reported.

Whereas the parametric study undertaken in Chapter 4 was centred around variations of a default square plate configuration with a slenderness b/h=20, this chapter considers a stockier default plate configuration with b/h=15. This is firstly to enrich the previously obtained parametric results of Chapter 6 with further information on the influence of imperfection, and secondly to make the focus of the current study on the stockier plates which have a significantly enhanced resistance compared to the yield strength. Aside from this shift in slenderness ratio, the default configuration is similar to that used in Chapter 6, unless specifically stated otherwise.

7.2 Square Plates

7.2.1 Influence of Initial Imperfections

This section supplements the parametric investigation of Chapter 6, which centred around simply-supported square plates with b/h=20, where consideration is given here to a similar plate but with the default stockier configuration for which b/h=15.

As before, imperfections are considered in the governing buckling mode:

$$w(x,y) = w_0 \sin\left(\frac{m\pi x}{a}\right)\sin\left(\frac{n\pi y}{b}\right) \tag{7.1}$$

where the amplitude of the imperfection is denoted by w_{0i}. Assuming a single mode for a square plate (i.e. m=n=1), the variation of the buckling response with w_{0i} is presented in Figure 7.1. It is clear that the level of imperfection no matter how small has a significant effect on the maximum buckling resistance, which highlights the importance of including imperfection in the assessment of plastic buckling of stocky plates. An interesting point to note here is that other existing simplified methods of plastic plate buckling completely ignore the influence of initial imperfections.

Compared to the numerical predictions, the error of the analytical model is limited to a maximum of 9% achieved with the smallest considered imperfection w_{0i}=b/2000,

and this error reduces to 4% for the largest imperfection w_{0i}=b/250. These results are particularly encouraging, since practical imperfections specified in design codes (Standards, 2005) tend to be around w_{0i}=b/300 or b/200.

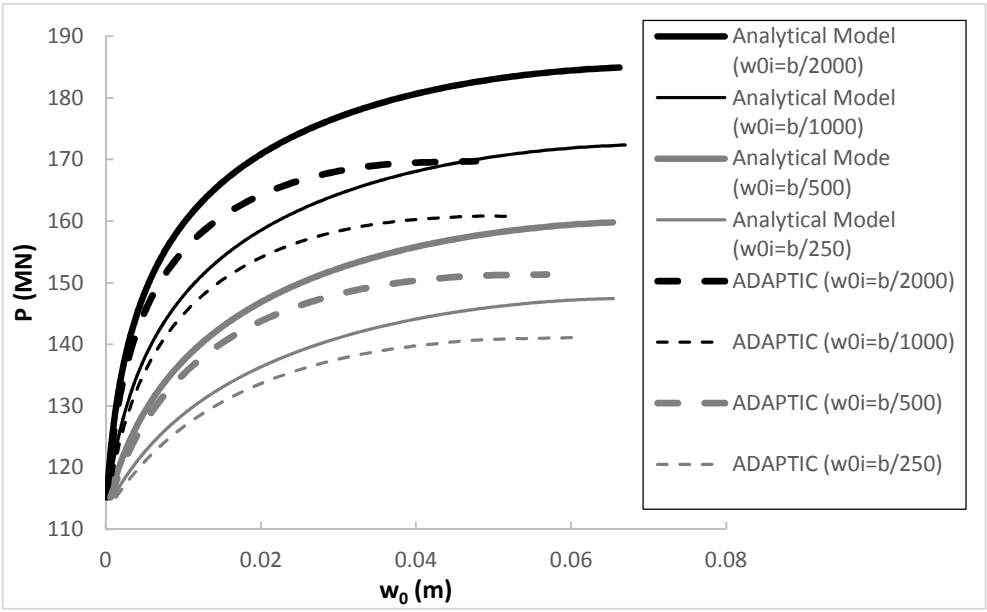

Figure 7.1 Effect of initial imperfection on buckling response of a square plate (b/h=15)

7.2.2 Effect of Buckling Mode

In applying Becque's modified tangent modulus matrix (Becque, 2010) to an infinitely long simply-supported plate of width "b", his solution implied an understated outcome that the governing plastic buckling mode consists of a transverse half-wave length equal to "b" and a much shorter longitudinal half-wave length equal to b/m with m=2.7. When considering Becque's method for a simply-supported square plate, the governing plastic buckling mode would be as described by (7.1) but with n=1 and m=3.

Up to this point, the proposed analytical models have been applied to simply-supported square plates with a mode consisting of single half-waves in both directions, that is m=n=1, where imperfection of a similar shape is assumed. When including such an imperfection in the nonlinear finite element models of ADAPTIC, the buckling deformations appeared to follow a similar shape to the original sinusoidal imperfection with m=n=1. However, imperfections are arbitrary in reality, and it is therefore conceivable that for different imperfection shapes, plastic buckling

may be governed by a shorter longitudinal wave-length as implied by Becque's method.

To investigate this potentially important issue, different imperfection shapes are considered in the numerical simulations of a simply-supported plate under a uniaxial loading using ADAPTIC. These imperfection shapes correspond to the general mode given by (7.1) with n=1, but with alternative values of m=1, 2 or 3, where the maximum amplitude of imperfection is taken as (a/m)/500. It is also worth noting that the analytical models can be directly applied for such cases considering a plate sub-structure with width "b" and length a/m, given that the full plate is simply supported.

The final deflected shapes obtained with ADAPTIC are illustrated in Figure 7.2, noting that the case with short longitudinal imperfection wave-length (m=3) has clearly induced a longer wave component in the final deflected shape, which suggests that m=3 does not correspond to the lowest plastic buckling mode. This is further confirmed in the results of Figure 7.3 and Table 7.1, where the results of ADAPTIC and the proposed analytical model are comparable and show that a single half-wave in the longitudinal direction (m=1) indeed represents the governing plastic buckling mode. While the proposed analytical model is accurate and its predictions are within 6% of the numerical results of ADAPTIC, the lowest buckling load predicted by Becque's model with m=3 has an error of over 100% in comparison with the minimum buckling load of ADAPTIC with m=1. This casts further doubts over Becque's model (Becque, 2010), where it appears that an incorrect tangent modulus matrix leads to an incorrect prediction of the governing plastic buckling mode. This is of course leaving aside the issue that the bifurcation analysis of perfect plates, as in the previous simplified models including Becque's method, is in fact inadequate for predicting the plastic buckling resistance of plates, as highlighted in the previous chapter.

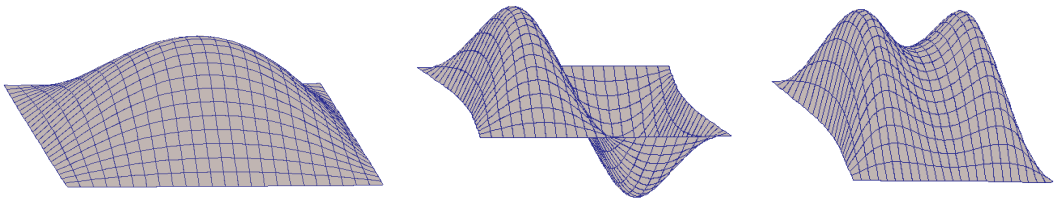

m=1 m=2 m=3

Figure 7.2 Deformation modes in ADAPTIC

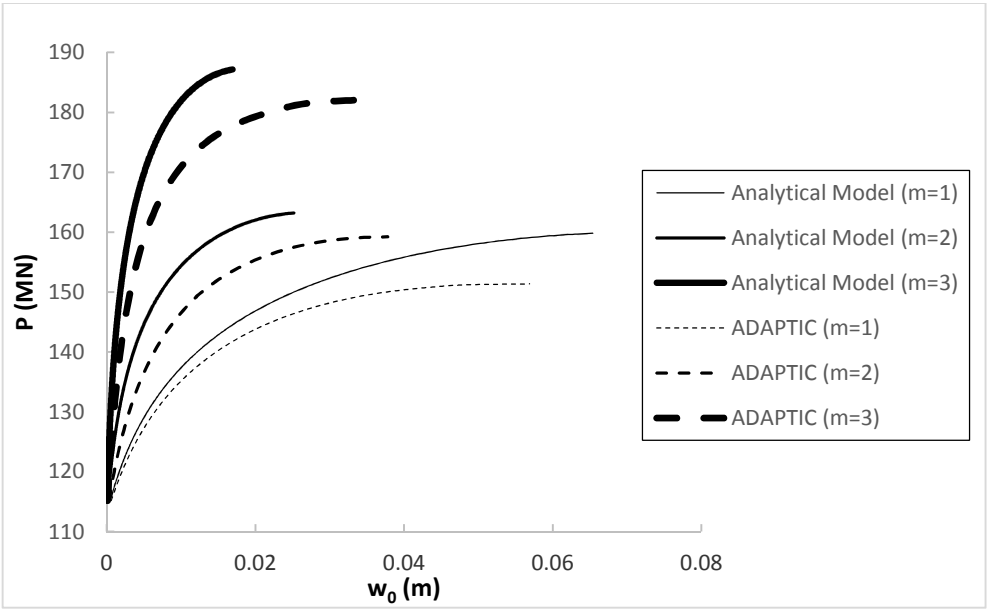

Figure 7.3 Influence of buckling mode on buckling response of square plate (b/h=15)

Table 7.1 Comparison of analytical predictions and numerical results for inelastic square plate (MN)

Square Plate (b/h=15, w_{0i}=(b/m)/500, P_Y=115.2MN)			
m	**ADAPTIC**	**Linear Stress model**	**Becque's method**
	P_{max}	**P_{max}**	**P_{max}**
1	151.18	159.8	557.04
2	159.22	163.2	318.09
3	182.18	187.16	304.62

7.2.3 Influence of Strain Hardening

A bilinear stress-strain relationship has been used in the development of the proposed analytical models as a practical idealisation of the nonlinear elasto-plastic stress-strain response of metals including steel. According to this bilinear relationship, a constant tangent modulus $E_t = \mu E$ is considered in the plastic range, where thus far the application of the proposed model has been limited to a strain-hardening level of μ=2%. Therefore, this section investigates the influence of different strain hardening levels with μ=1%, 2% and 4%, as illustrated in Figure 7.4.

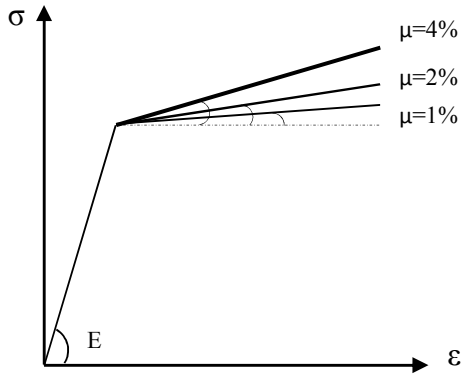

Figure 7.4 Idealised bilinear stress-strain curve with different strain hardening parameters

Figure 7.5 illustrates the influence of the strain hardening parameter on the plastic buckling response of the square plate, highlighting again the accuracy of the predictions of the analytical model, with a maximum error below 8% compared to the numerical results. As confirmed in the numerical parametric study of Chapter 4, strain-hardening does not influence the initiation of buckling, which occurs at the yield load, but can significantly affect the maximum buckling resistance.

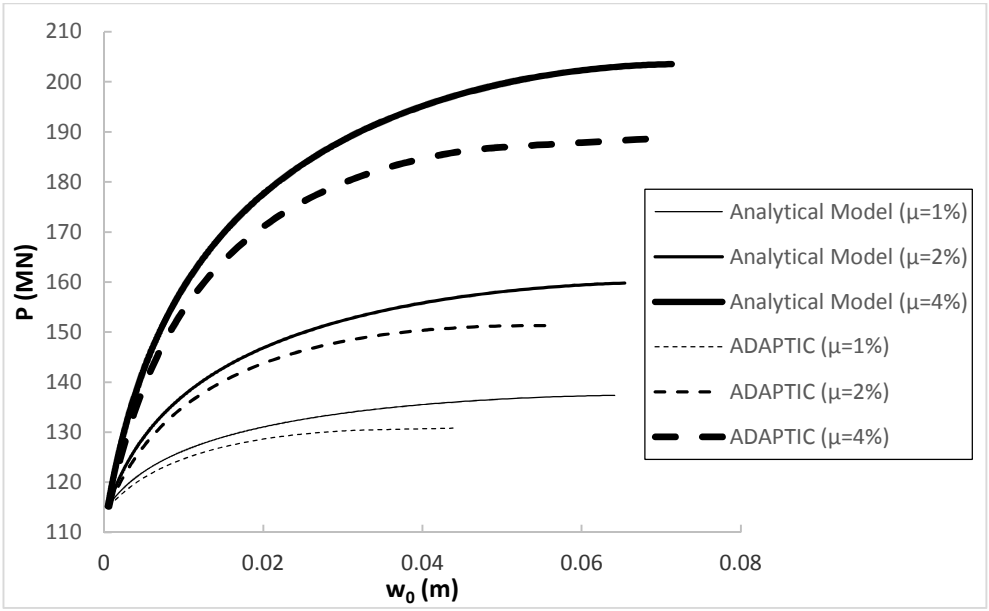

Figure 7.5 Effect of strain hardening on buckling response of square plate (b/h=15)

7.2.4 Influence of Biaxial Loading

There are numerous situation in practice where plates are subjected to biaxial loading scenarios which can induce buckling. This section considers the influence of biaxial loading on the plastic buckling response of square plates using the proposed analytical models, with verification against that numerical results of ADAPTIC.

7.2.4.1 Adjustments to Analytical Model

The methodology and procedure of tracing the post-buckling response and obtaining the maximum buckling resistance are virtually identical to those outlined in the previous chapter, except for some minor adjustments. Consider for this purpose the simply-supported square plate, as shown in Figure 7.6, to be subjected to a uniform compressive force N_x in the x-direction and a uniform compressive/tensile force $N_y=\beta N_x$ in the y-direction, with $\beta<0$ denoting tensile N_y and $\beta=1$ corresponding to equi-biaxial compression.

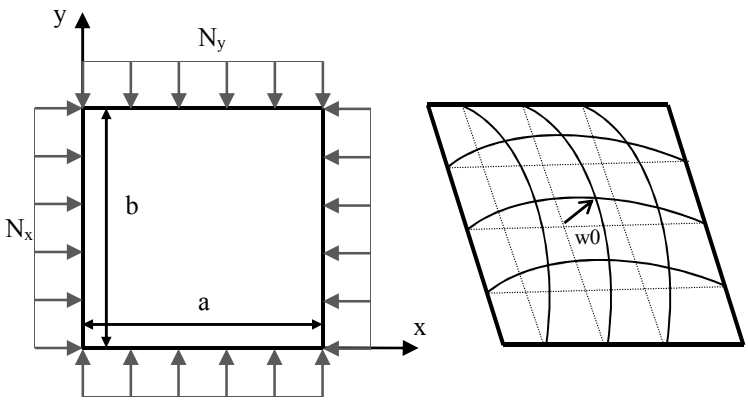

Figure 7.6 Square plate with thickness h under biaxial loading

Following the conclusion of Section 7.2.2, the governing buckling mode is assumed to consist of one half-wave in each direction, as given by (7.1) with m=n=1, which is also assumed for the shape of initial imperfection.

Under the biaxial loading which induces uniform stresses σ_x and σ_y in the x- and y-direction, respectively, yielding occurs at a different σ_x compared to the uniaxial loading case, in accordance with the von Mises yield criterion:

$$\sigma_Y = \sqrt{\sigma_x^2 - \sigma_x \sigma_y + \sigma_y^2} = \sigma_x \sqrt{1 - \beta + \beta^2} \tag{7.2}$$

Taking the load in the x-direction ($P=N_x b$) as the reference loading entity, yielding occurs at a new load given by:

$$P_Y = \frac{\sigma_Y bh}{\sqrt{1-\beta+\beta^2}} \tag{7.3}$$

which is then used as the starting point for the model application.

As a result of applying a planar biaxial loading to the plate, the equivalent geometric stiffness obtained from the Rotational Spring Analogy according to (6.14) is modified by the presence of N_y, increasing in negative magnitude for compressive N_y (i.e. $\beta>0$).

Finally, it was acknowledged that formulation of the incremental constitutive relations requires information of the current normal and the increments of stress. Under a biaxial loading, the initial stress state at the mid-plane becomes:

$$\{\sigma_m\} = \{\sigma_Y, \beta\sigma_Y, 0\} \tag{7.4}$$

and the incremental mid-plane stresses for the Linear Stress model are modified to:

$$\{\Delta\sigma_m\} = \frac{\Delta P}{b\,h}\langle 1 \quad \beta \quad 0\rangle^T \tag{7.5}$$

while the incremental planar stress resultants for the Linear Strain model become:

$$\langle \Delta N_x \quad \Delta N_y \quad \Delta N_{xy} \rangle^T = \frac{\Delta P}{b}\langle 1 \quad \beta \quad 0\rangle^T \tag{7.6}$$

Aside from these minor modifications, the application of the proposed analytical models proceeds along similar lines for a biaxial loading as for the uniaxial case.

7.2.4.2 Results and Discussion

In order to have an objective assessment of the influence of a biaxial loading, as determined by β, on the maximum buckling resistance, the ratio of the elastic buckling load to the yield load P_{ce}/P_Y is kept constant, which is achieved by varying "h" with β. Accordingly, in the presented results, the plate slenderness b/h varies with β, while the amplitude of initial imperfection is fixed at w_{0i}=b/500.

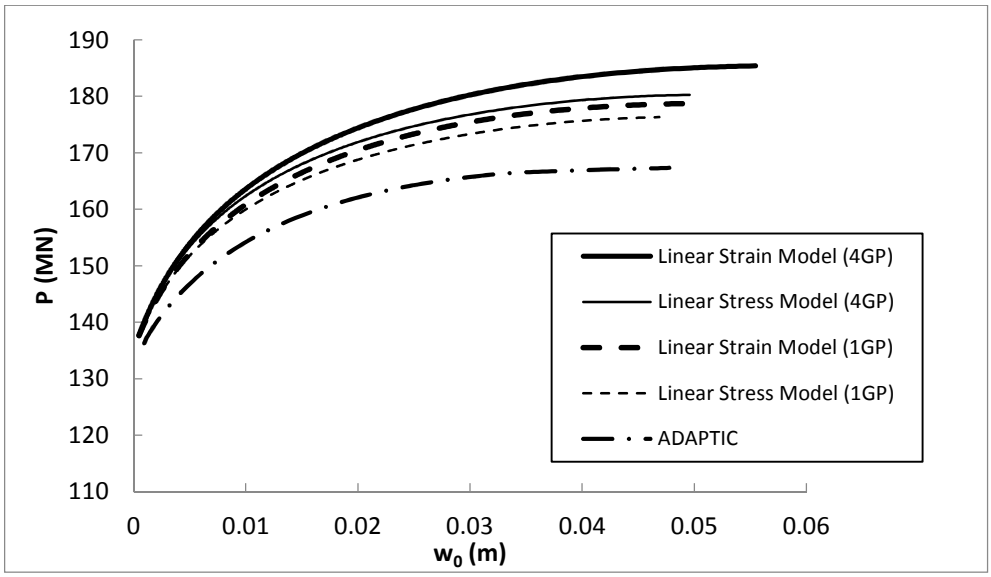

a. β= 20%, b/h=13.7

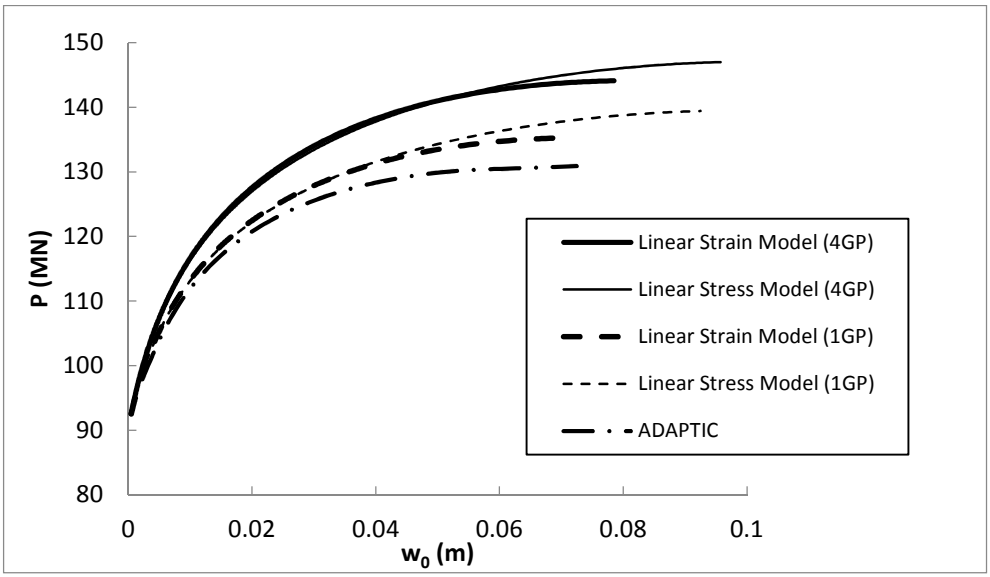

b. β= -20%, b/h=16.8

Figure 7.7 Buckling response of square plate subject to biaxial loading

The plastic buckling response of the square plate subject to a biaxial compression/compression and compression/tension (β=±20%) is provided in Figure 7.7. In both cases, the Linear Stress and Linear Strain models capture the influence of a biaxial loading well. In this respect, both models predict a reduced enhancement in the buckling resistance beyond the initial yield load for compression/compression (β=20%) compared to compression/tension (β=-20%), which is also confirmed by the results of ADAPTIC. There is a marginal discrepancy

of around 6% between the analytical model results and those of ADAPTIC, which cannot be attributed to the numerical integration with only one Gauss point over a quarter model, as evident from the results using four Gauss points. Such errors are therefore attributed to the approximation of the through thickness stress distribution and/or the assumed buckling mode.

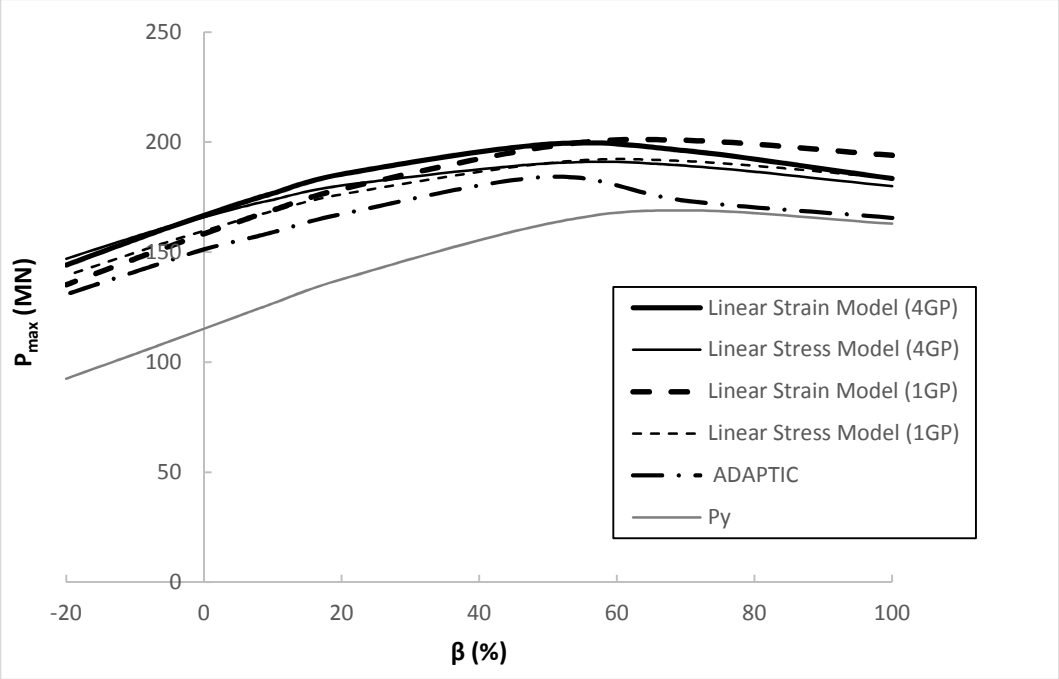

Figure 7.8 Influence of biaxial loading parameter β on maximum buckling resistance

Figure 7.8 shows the influence of β on the maximum buckling resistance P_{max} obtained both numerically and analytically, where the yield load P_Y is also included for comparison purposes. It is interesting that the maximum buckling resistance, as predicted numerically and analytically, follows a similar trend of variation with β to the yield load, but to a smaller extent. As noted before, this implies a greater enhancement over the yield strength under a compression/tension loading scenario ($\beta<0$) compared to a compression/compression one ($\beta>0$). Furthermore, beyond $\beta=50\%$, the discrepancy between the analytical predictions and numerical results becomes greater, which may be attributed as before to the approximation of the through-thickness stress distribution and/or the assumed buckling mode.

It is worth noting that in all these analyses, no elastic unloading was observed, except for the equi-biaxial compression loading case (β=100%), where elastic unloading was detected at the Gauss point nearest to the centre of the plate for loading close to the maximum resistance. The results from ADAPTIC, however, confirm that this elastic unloading has no significant influence on the subsequent maximum buckling resistance.

Table 7.2 presents the maximum buckling resistance predicted with the proposed Linear Stress and Linear Strain models using 1 and 4 Gauss points per quarter model, where again the shortcomings of the conventional Incremental Theory are evident.

Table 7.2 Comparison of maximum buckling resistance (MN) under biaxial loading

				ADAPTIC	**Linear Stress Model**		**Linear Strain Model**		**Conv. Incremental Theory**
β (%)	**b/h**	**P_Y**	**P_{ce}**	**P_{max}**	**P_{max} (1GP)**	**P_{max} (4GP)**	**P_{max} (1GP)**	**P_{max} (4GP)**	**P_{max}**
20	13.69	137.69	1548.66	167.38	176.36	180.27	178.73	185.40	1247.90
-20	16.77	92.53	1040.73	130.90	139.44	147.01	135.29	144.13	985.25

7.3 Rectangular Plates

Consideration is given in this section to infinitely long plates loaded along the two short edges, rectangular plates with typical aspect ratios, and wide plates loaded along the two long edges.

7.3.1 Infinitely Long Plates

Prediction of the buckling loads of long rectangular plates is of practical importance in structural design since it can provide insight to the buckling behaviour of various types of structures such as stiffened panels.

Consider an infinitely long rectangular plate simply-supported along its four edges and compressed in the longitudinal direction by a uniformly distributed load N_x. When the plate buckles, it has the tendency to buckle in a number of half-waves in the direction of loading, hence it becomes similar to a plate sub-panel of length "a" supported by transverse stiffeners, as illustrated in Figure 7.9. The question arises

then as to the optimal half-wavelength “a” that would correspond to the lowest maximum buckling resistance. Bazant and Cedolin (1991) state that the lowest elastic buckling load for a long plate occurs when the half-wavelength “a” is as close to the width “b” as possible. Having established in Section 7.2.1 the significance of imperfections for plastic plate buckling, it is important that the question of the critical wavelength is considered with a consistent level of imperfection.

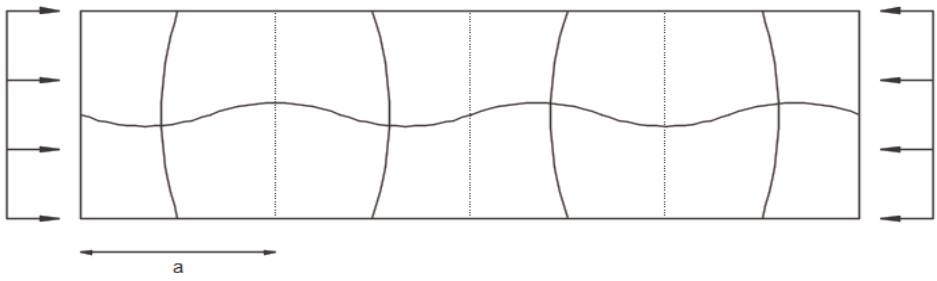

Figure 7.9 Buckling mode of an infinitely long plate

In undertaking this investigation, the width of the plate is kept to b=2.4m as before, with a slenderness b/h=15, and the length of the sub-panel “a” is varied. To ensure the consistency of imperfections between the different configurations, the imperfection amplitude is taken as w_{0i}=a/500 for a<b and w_{0i}=b/500 for a≥b. For each considered configuration, the maximum buckling load P_{max} is obtained using the Linear Stress model and ADAPTIC, where the results for different half-wavelengths “a” are depicted in Figure 7.10. It is worth noting that the ADAPTIC results are obtained from models in which the edges of the sub-panel are kept straight so as to ensure the satisfaction of compatibility when considered with adjacent sub-panels in the infinitely long plate.

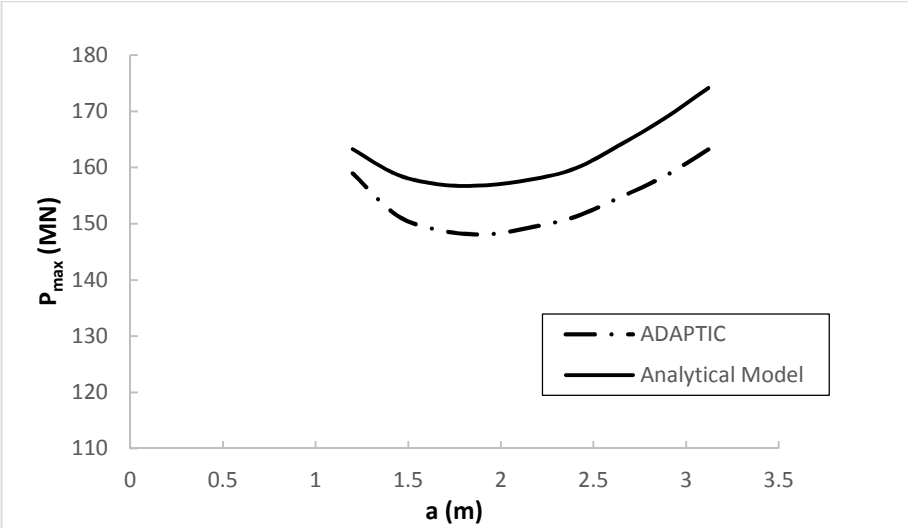

Figure 7.10 Critical value of half-wavelength for infinitely long plate (b=2.4m, b/h=15)

It is clear from the results in Figure 7.10 that the critical half-wavelength for the considered plate, as predicted by both numerical and analytical models, is a=1.92m. This suggests that plastic buckling of long plates is characterised by slightly shorter wavelengths compared to elastic buckling, but certainly nowhere as short as suggested in Becque's method (2010) which predicts a=0.9m. It is also worth noting that the discrepancy between the analytical model and the numerical results of ADAPTIC relating to P_{max} is again less than 6%.

7.3.2 Influence of Plate Aspect Ratio

The previous section has shown that an infinitely long stocky plate loaded in the longitudinal direction is effectively similar to a plate with an aspect ratio a/b=0.8. This section investigates the influence of the actual aspect ratio in rectangular simply-supported stocky plates subject to uniaxial loading, where consideration is first given to an aspect ratio a/b=1.5, for which the governing buckling mode may be associated with one or two longitudinal half-wavelengths (i.e. m=1 or m=2).

To trace the post-buckling response of the plate and to obtain its maximum inelastic buckling capacity, similar material properties have been employed as before with the following geometric properties: Length a=3.6m, width b=2.4m, thickness h=b/15=160mm.

To investigate the governing buckling mode, alternative initial imperfection shapes are considered with ADAPTIC, as depicted in Figure 7.11(a-c). The first two imperfection shapes in Figure 7.11(a-b) correspond directly to the possible buckling modes, with amplitudes w_{0i}=b/500 and w_{0i}=(a/m)/500, where the imperfection amplitude is realistically reduced for the shorter wavelength. On the other hand, the third imperfection shape in Figure 7.11(c) is a direct sum of the first two imperfection shapes, with the aim of establishing whether the governing mode is maintained under the more realistic scenario of combined modal imperfections. Furthermore, the case of two longitudinal half-waves (m=2) is considered with a full model of the whole plate, as in Figure 7.11(b), and alternatively with a half model with w_{0i}=a/1000 considering the edges to remain straight, as in Figure 7.11(d), so as to confirm whether the half model with the considered boundary conditions is realistic over the full range of buckling response.

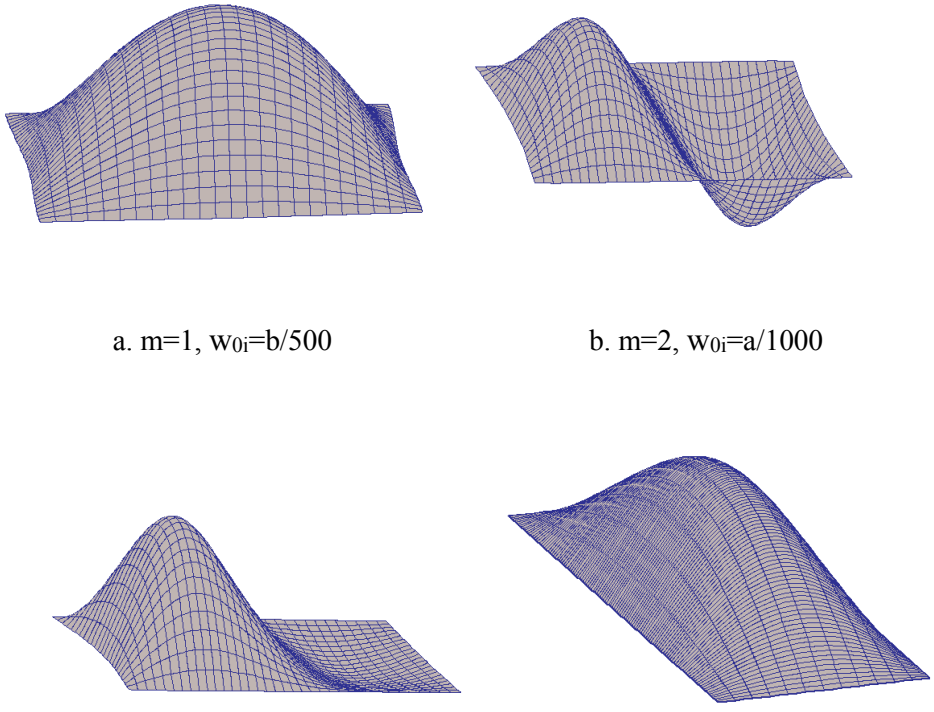

a. m=1, w_{0i}=b/500 b. m=2, w_{0i}=a/1000

c. Combined mode (a + b) d. Half model with straight edges

Figure 7.11 Buckling deformed shapes obtained with ADAPTIC

The buckling response obtained with ADAPTIC for the different models is presented in Figure 7.12, where it is clear that for the considered aspect ratio a/b=1.5 the governing buckling mode consists of two longitudinal half-waves (m=2), whether it is considered with the related or combined imperfections. Moreover, it is evident that the half model with the suggested boundary conditions predicts virtually identical results to the full model.

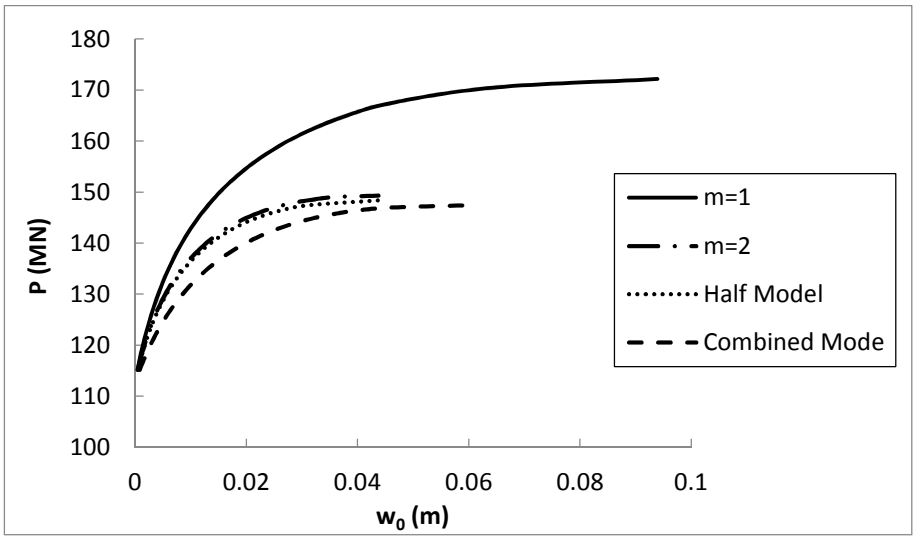

Figure 7.12 Buckling response predicted by ADAPTIC for rectangular plate (a/b=1.5)

Figure 7.13 compares the plastic buckling response of the rectangular plate predicted by the proposed analytical model, considering half the plate similar to Figure 7.11(d), against the numerical finite element predictions of ADAPTIC. A generally favourable comparison is achieved, where the maximum discrepancy of the Linear Stress model using numerical integration with one Gauss point over a quarter model is around 5.5%.

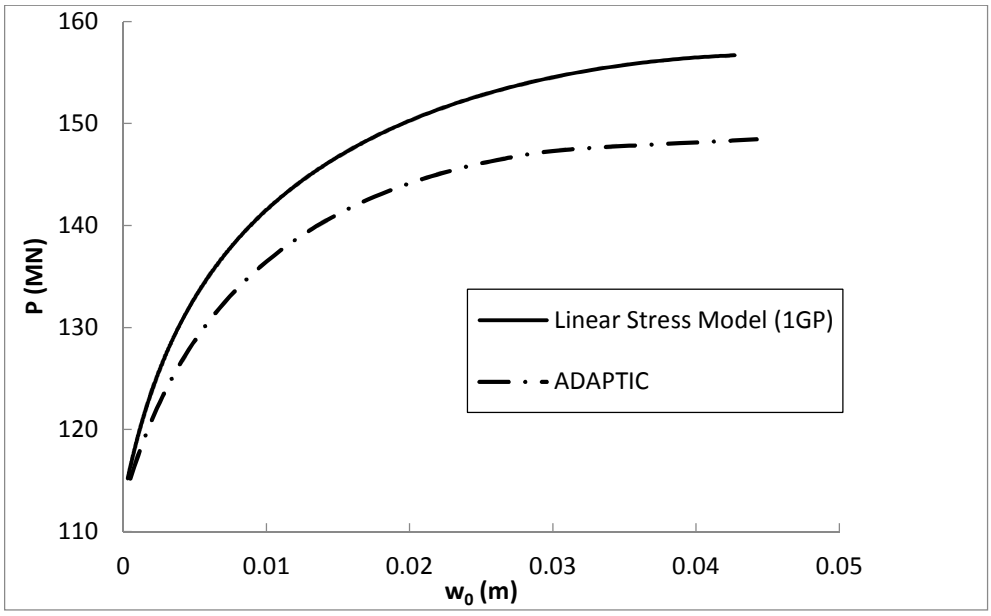

Figure 7.13 Buckling response of a rectangular plate (a/b=1.5)

To assess the influence of different plate aspect ratios on both the plastic buckling response and the maximum buckling resistance, two additional plate lengths "a" are considered with the corresponding aspect ratios a/b=0.5 and 1.0, where the imperfection amplitude is w_{0i}=a/500. Considering that both additional aspect ratios are associated with a governing buckling mode that consists of a single longitudinal half-wave (m=1), the proposed analytical model is applied to the whole plate for these cases, where the results for all three aspect ratios, including a/b=1.5, are compared to the numerical results of ADAPTIC in Figure 7.14. Again, the maximum buckling resistance predicted by the analytical model compares to the prediction of ADPAPTIC to within 5.5% for all aspect ratios, where it is evident that the smaller the aspect ratio the greater the maximum buckling capacity of the plate.

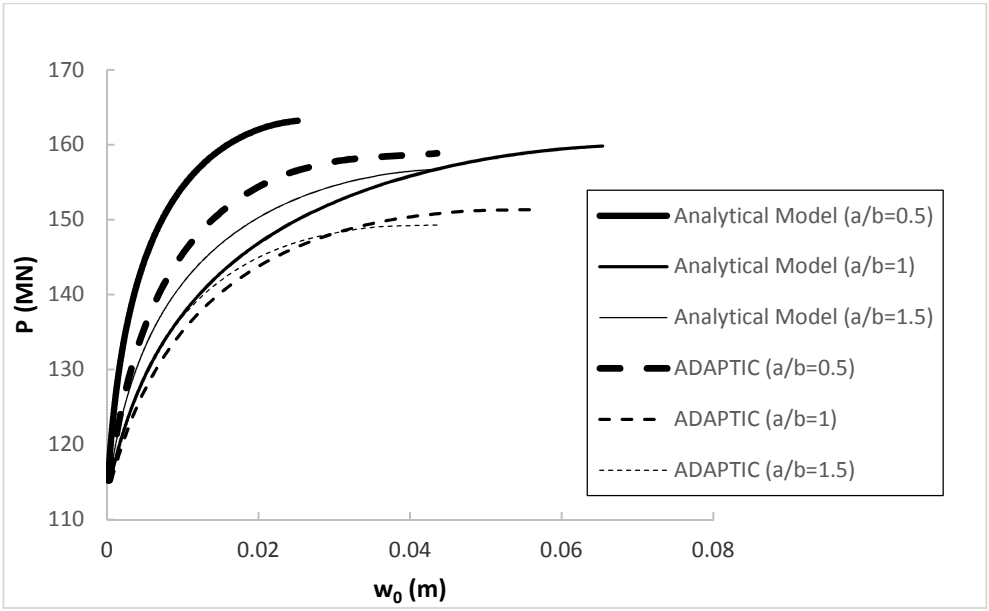

Figure 7.14 Influence of aspect ratio on plastic buckling of plate with different aspect ratios

It is finally worth comparing the influence of aspect ratio on the buckling resistance obtained from the proposed analytical models with the results of other existing methods of analysis, as given in Table 7.3. According to Becque (2010), the optimal number of half-waves for aspect ratios a/b=0.5, 1.0 and 1.5 is m=1, 3 and 4, respectively. This contradicts the findings of the proposed analytical models, with m=1, 1 and 2, respectively, which are confirmed by the numerical results of ADAPTIC. While significant improvement is achieved with the proposed analytical models compared to the other simplified methods, it is worth noting that none of the existing methods account for initial imperfections, which as demonstrated previously is of critical importance for the plastic buckling of plates.

Table 7.3 Comparison of buckling loads (MN) for rectangular plate of different aspect ratios

a/b	P_Y	P_{ce}	ADAPTIC	Conv. Incremental Theory	Deformation Theory	Linear Stress Model	Linear Strain Model	Becque's Method
0.5	115.2	2591.4	158.9	1168.4	142.8	163.2	173.4	318.1
1.0	115.2	1295.7	151.4	1154.4	139.4	159.8	158.4	304.6
1.5	115.2	1405.9	149.3	1082.5	137.8	158.7	159.0	301.8

7.3.3 Wide Plates

Consideration is given here to rectangular plates that are relatively short in the direction of compressive loading ($b/a \gg 1$), where the governing buckling mode consists of a single half-wave in both directions. In this respect, consider a simply-supported rectangular plate with an aspect ratio $a/b=0.1$ which is loaded on its two long edges by a uniformly distributed load N_x, as shown in Figure 7.15. Since the maximum curvature of the buckling mode is in the direction of loading, the slenderness of the plate is defined in terms of the shorter edge length "a", where a slenderness ratio $a/h=7$ is considered with an initial imperfection amplitude $w_{0i}=a/500$.

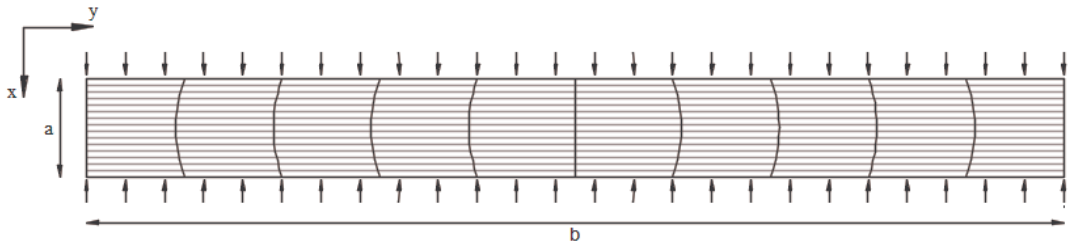

Figure 7.15 Simply-supported wide plate subjected to uniaxial compression

It has been found that the Linear Stress model requires in this case four Gauss points per quarter model for a reasonably accurate prediction of the buckling load resistance. On the other hand, the Linear Strain model achieves a good prediction with only one Gauss point. Figure 7.16 presents the buckling response of the wide plate obtained from the proposed analytical model and ADAPTIC. There is a general good agreement between the predictions of Linear Strain model and the numerical results of ADAPTIC while the Linear Stress model using four Gauss points overestimates the maximum buckling resistance by only 4%.

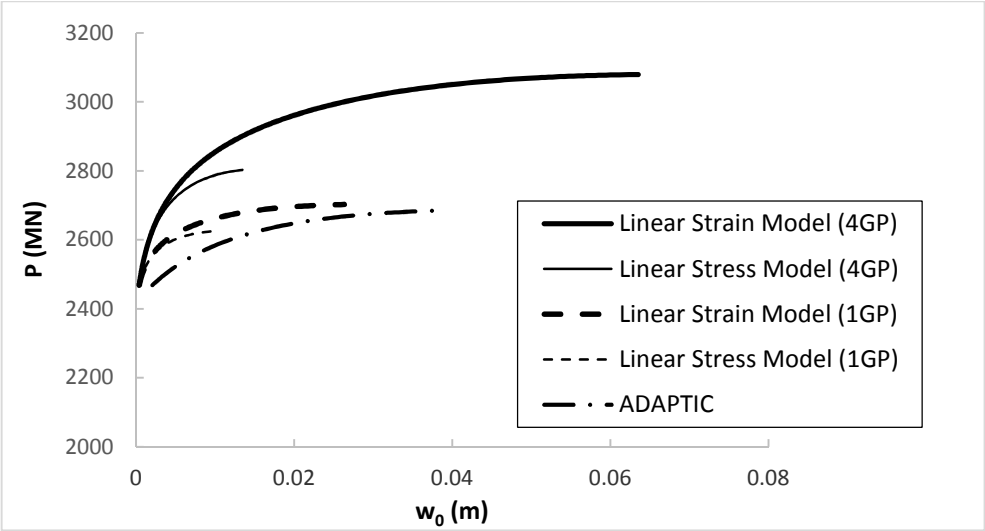

Figure 7.16 Buckling response of a wide plate (a/b=0.1)

It is worth noting that the overestimation of the plastic buckling resistance by the analytical models could be attributed to the assumed mode becoming less accurate for wide plates and also to the non-uniform planar stress resultants as the wide plate tends to take more load near the short edges. The former has been verified by investigating the plate kinematics, where the plate curvatures obtained from ADAPTIC show a discrepancy of up to 15% in comparison with the assumed curvatures at Gauss point locations for the same level of buckling deformation. This is also borne out by the comparison of the final deformed configuration obtained with ADAPTIC and the buckling mode assumed for the analytical models, as depicted in Figure 7.17.

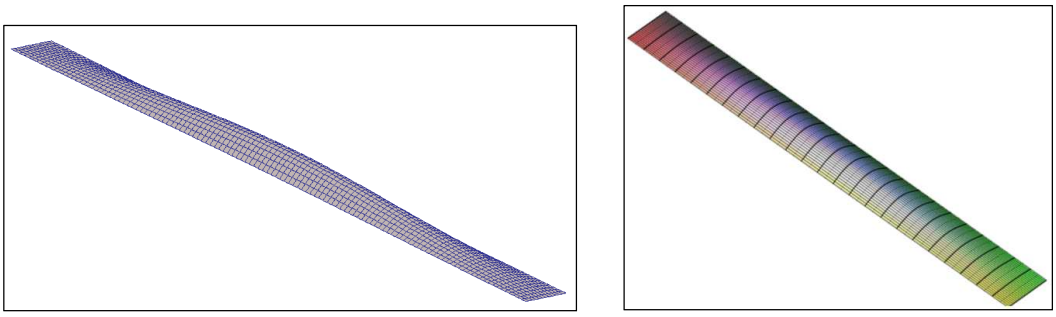

a. ADAPTIC b. Analytical Model

Figure 7.17 Deformed shape from ADAPTIC compared to assumed buckling mode

7.4 Conclusions

In Chapter 6, a simplified analytical model was proposed, with two the so-called Linear Stress and Linear Strain variants, for predicting the plastic buckling response of stocky simply-supported square plates subject to a uniaxial planar loading. In this chapter, it is shown that the model can be easily generalised to deal with biaxial loading conditions, the influence of the buckling mode shape, and rectangular plates of different aspect ratios. To verify the accuracy of the analytical model solutions, the results of the model are compared against the corresponding outcomes of the rigorous nonlinear finite element analysis. For all the considered variations in geometric properties and boundary conditions, the proposed analytical model is shown to provide reasonably accurate estimates of the maximum buckling resistance, which reinforces the resolution provided in Chapter 6 for the Plate Plastic Buckling Paradox. In addition to these benefits, an important feature of the proposed model is the simple concept of plastic buckling analysis that it provides; besides facilitating the enhanced understanding of plastic buckling, this feature can facilitate the development of simplified design-oriented procedures for the plastic buckling assessment of plated structures.

Based on the parametric and application studies undertaken in this chapter, the following conclusions can be drawn:

1. Unlike the plastic buckling of stocky columns, the plastic buckling of stocky plates is remarkably sensitive to the level of initial imperfection. This underscores the shortcomings of the previous simplified methods for the plastic buckling analysis, in which imperfection is completely ignored.
2. Contrary to the implicit findings of Becque's method, the governing buckling mode for a simply-supported long stocky plate has a longitudinal half-wavelength of approximately 0.8 rather than 0.4 times the plate width.
3. It is verified that strain-hardening influences the plastic buckling resistance of the stocky plates, but to a lesser extent compared to its influence on stocky columns as observed in Chapters 3 and 4.
4. The application of a biaxial loading to stocky plates has a similar influence on the plastic buckling resistance as on the yield strength, though the

enhancement of buckling resistance over the yield strength is greater with a compressive/tensile loading compared to compressive/compressive loading.

5. For uniaxially loaded plates, a greater length to width aspect ratio leads to a smaller maximum buckling resistance for a level of imperfection proportional to the shorter planar dimension.

CHAPTER 8

Summary and Conclusion

8.1 Summary

Extensive studies have been carried out over many decades on the topic of plastic buckling in search for a realistic assessment of the ultimate buckling capacity of structures. Indeed, the story of the inelastic buckling formula of a column has a continuity of over a century, and it can be traced back to the fact that Euler formula over-predicted the critical buckling load of a stocky column. Despite the huge amount of studies on this topic, plastic buckling behaviour of columns still attracts the attention of many researches particularly in developing analytical models that would be much more practical for the design application. To date, the most successful analytical methods that have been established for plastic buckling of columns have a rather limited range of applicability (i.e. columns of relatively low stockiness and/or considering very small imperfections) and are based on a simplified rigid bar/column assumption, and neglect the spread of plasticity along the column length.

On the topic of inelastic buckling of plates, analogous analytical solutions to the tangent-modulus load for the columns have been obtained for the maximum buckling load of plates. However, due to the multi-axial stress state in the plates, a different approach was required, and as a result two main theories of plasticity, namely Deformation Theory and Incremental Theory, were adopted to deal with the constitutive relations in the plastic range. However, as noted in Chapter 2, it was discovered that the more mathematically correct Incremental Theory consistently overestimated the buckling loads observed in tests, whereas the predictions of the less accepted Deformation Theory were in good agreement with the test results, a confounding outcome that has since been known as the Plate Plastic Buckling Paradox. Despite numerous investigations to resolve this paradox, so far no single method or explanation has been offered founded on the sound principles of mechanics. In the absence of accurate and versatile analytical models, an accurate

solution for the elasto-plastic buckling problems can be obtained with detailed numerical methods such as the finite element (FE) method. However, despite its accuracy and generality, FE modelling poses considerable computational demands that are often prohibitive in practice, and it does not offer sufficient insight as with the analytical models to enhance understanding and to resolve such conceptual issues as the Plate Plastic Buckling Paradox.

In this context, simplified analytical models for the plastic buckling of columns and plates have been developed in this thesis which are in accordance with the widely accepted principles of mechanics of materials. These analytical models are mainly intended to illustrate the mechanics of the plastic buckling response of stocky columns and plates, starting from the point of buckling initiation and considering the post-buckling response. In these models, the Rotational Spring Analogy is used for formulating the geometric stiffness matrix, whereas the material stiffness matrix is obtained with due consideration for the incremental spread of material plasticity. In addition to establishing some key features of the plastic buckling, the imperfection sensitivity in the plastic range is also investigated for the two types of structural component. The outcomes of the analytical models have been verified against the results of the nonlinear finite element analysis program ADAPTIC, where the important benefits of the analytical models for a direct application and an enhanced understanding of the plastic buckling have been highlighted.

8.2 Plastic Buckling of Columns

For the case of stocky columns, an analytical model has been presented in Chapter 3 which captures their plastic buckling behaviour from the initiation of buckling to the maximum resistance, through incremental tracing of the post-buckling response. The model is developed for both initially perfect and imperfect columns, providing insight into the initiation of the plastic buckling at the Engesser tangent-modulus load and its subsequent increase towards the von Karman reduced-modulus load. However, it is demonstrated in the present work that this upper limit is not realised due to tensile yielding taking place at the outer fibre of the column cross-section. The onset of tensile yielding has been shown to offer a reasonable lower bound on the maximum buckling resistance of Class 1 stocky columns, as verified by means of a numerical analysis run by ADAPTIC. It is also worth highlighting that this finding is not acknowledged in the existing simplified methods.

The analytical model was initially developed for the case of very stocky (Class 1) columns, where the Engesser tangent-modulus load is greater than the yield load. When employing the model for Class 2 columns of an intermediate slenderness, for which the buckling starts at the yield load and the enhancement of the maximum bucking load compared to the initial buckling load is marginal, it has been shown that the onset of tensile yielding offers a close approximation of the maximum buckling resistance.

With the aid of the proposed analytical model, imperfection sensitivity of very stocky columns has also been investigated, and as a result a threshold level of imperfection is established beyond which it has been shown that the plastic post-buckling response is barely affected by a further increase in the level of imperfection. One reasonable explanation is that due to large imperfections significant parts over the cross-section and along the length of the stocky column remain elastic during buckling, therefore the column behaves similar to an elastic slender column which does not display strong sensitivity to initial imperfections.

Within the scope of the thesis (i.e. assuming a buckling mode, considering an idealised bilinear material model, and assuming a monotonic strain variation up to the point of strain reversal) the analytical model established here has succeeded to determine the correct plastic response from the initiation of buckling to the maximum buckling resistance of both perfect and imperfect stocky columns.

8.3 Plastic Buckling of Plates

Having established a successful simplified model for the plastic buckling analysis of stocky columns, the question arose as to whether similar notions could be used to develop an analytical model for the plastic buckling of plates leading to similar conclusions. To answer this question, Chapter 4 presented a comparative parametric study of the plastic buckling response between stocky columns and plates using the nonlinear finite element analysis ADAPTIC. The comparative study of these two types of structural element has confirmed that the principles governing the plastic buckling of plates are not a simple extension of those principles previously identified in Chapter 3 for the plastic buckling of columns. In particular, the role of the

Engesser load as a lower bound on the maximum buckling resistance is put into question. Furthermore, the crucial influence of the initial imperfections on the plastic bucking resistance of plates, which contrasts with their limited influence in the case of columns, is confirmed.

The differences noted in the plastic buckling response of columns and plates in Chapter 4 (e.g. the plastic buckling of plates is governed by an effective tangent material modulus which starts relatively small at the yield load and increases with loading, but never reaches the level predicted by the Conventional Incremental Theory of Plasticity) are mainly attributed to the biaxial nature of the deformations induced in the buckling of plates supported on four edges. This indicated the need for a more sophisticated treatment of the plastic plate buckling compared to columns, as presented in Chapter 5 and 6.

It was mentioned in the literature review that one of the few attempts to resolve the Plastic Buckling Paradox of plates involved the amendment of the shear modulus in the plastic region. It has been indeed verified in Chapter 5, both numerically and analytically, that by applying a uniform normal stress producing significant plastic deformation, and regardless of the relative magnitude of the accompanying shear deformation, the shear stiffness drops immediately after the stress has reached the material yield strength. However, further to the resolution of the mechanics leading to the reduction of the plastic shear modulus, Chapter 6 questioned the widely accepted notion that this reduction alone accounts for the inaccuracy of the Incremental Theory.

In Chapter 6, two simplified analytical models, namely Linear Stress and Linear Strain models, have been proposed for simply-supported square plates subject to a uniaxial loading, which employ the Incremental Theory but recognise the important influence of the interaction between planar and flexural actions. Through verification against the results of the nonlinear finite element analysis, it has been confirmed that the proposed analytical models provide a notable improvement over other simplified methods that are empirical or irrational, and importantly offer the definitive resolution of the Plate Plastic Buckling Paradox and the associated explanation for the inaccuracy of the conventional buckling approach based on the Incremental

Theory. It has been further shown that utilising a tangent modulus matrix associated with the stress state at the mid-plane, regardless of whether the tangent shear modulus is modified to any value in the range [0, G], leads to a significant overestimation of the maximum buckling resistance. Thus, it has been confirmed that a realistic determination of the plastic buckling resistance in plates requires additional information about the distribution of stresses and the associated variation of the tangent modulus matrix over the thickness.

With the resolution of the Plate Plastic Buckling Paradox, the two proposed analytical models have been shown to offer a valuable tool for assessing and gaining insight into factors that influence the plastic buckling of stocky plates. In Chapter 7, it has been demonstrated that both models can be easily generalised to deal with the biaxial loading condition, the influence of buckling mode shape, and rectangular plates of different aspect ratios, and that they provide accurate solutions compared against the corresponding outcomes of the rigorous nonlinear finite element analysis. Importantly, it has also been shown that the governing buckling mode for square/long simply-supported stocky plates under longitudinal loading does not consist of short longitudinal waves, as predicted in recent analytical models, but of a half-wavelength approximately equal to 80% of the plate width.

This work has demonstrated that the simplified analytical models in the nonlinear structural analysis, which in the present context deal with the plastic buckling of columns and plates, can be extremely beneficial, as they enhance the understanding of complex conceptual issues and the factors influencing the nonlinear response. In particular, provided the models are founded on sound principles of mechanics, it is possible to identify which approximations may be made while still achieving reasonably accurate solutions compared to the more detailed numerical methods. This sheds invaluable light on the important factors governing the structural response, enabling the resolution of any paradoxes, besides facilitating application in practice due to the relative ease of use.

8.4 Future Work and Recommendations

In literature review of Chapter 2, the shortcomings of existing simplified methods for the plastic buckling analysis of columns and plates and the corresponding paradoxes

were highlighted. It is contended that this thesis has succeeded in developing representative analytical models for plastic buckling of stocky columns and plates, which also resolve the long-standing paradoxes. However, by their very nature, these analytical models are based on some simplifying assumptions, and would therefore require further extension and generalisation for wider application.

The analytical models proposed in the course of this thesis have been founded on specific geometric and material properties. In the case of columns, a rectangular cross-section has been assumed, and thus future work may consider the extension of the analytical model to other cross-section shapes. Furthermore, in both cases of columns and plates, a bilinear elasto-plastic material model has been assumed, primarily to aid in the resolution of the paradoxes without introducing additional uncertainty in the comparisons between the simplified analytical models and the nonlinear FE models. Therefore, further work on the analytical model development may consider more general elasto-plastic stress-strain relations, such as a Ramberg-Osgood and a trilinear model. The main difficulty of employing a nonlinear material model is that due to the dependency of E_t on the current stress state which is yet to be found an iterative procedure becomes essential.

For both columns and plates, the plastic buckling mode was assumed to have a similar sinusoidal configuration to the elastic buckling mode, though this is clearly a simplifying assumption. Therefore, future work may consider the investigation of the approximation involved, particularly if the analytical models are extended to deal with different support conditions. In this respect, the stocky columns considered in this work have been pin-ended, though future work could be devoted to adjusting the analytical model to deal with various boundary conditions. However, not only the buckling mode would need to be modified, but the consideration of more zones of elastic unloading would be required (e.g. near the middle and the supports for a fixed-ended column), which would increase the number of parameters to be solved for incrementally in the analytical model.

The analytical model presented in Chapter 6 for the plastic buckling of simply-supported square plates was elaborated further in Chapter 7 to rectangular plates and biaxial loading. However, there is scope for further extension of this simplified

model to account for plates of arbitrary shapes subject to various support conditions. The main requirement for this extension would be a suitable choice of a buckling mode that is reasonable and satisfies the boundary conditions. The analytical model may also be enhanced to consider the plastic buckling of a stocky plate under a non-uniform uniaxial/biaxial loading. Together with the consideration of plates of arbitrary shapes, this would pave the way for a simplified modelling of the plastic buckling in more challenging structural forms, such as cellular beams.

References

BAUSCHINGER, J. 1881. Uber die Veranderung der Elastizitatsgrenze und des Elastizitatsmoduls verschiedener Metalle. *Civilingenieur*, 289-348.

BAZANT, Z. P. & CEDOLIN, L. 1991. *Stability of structures,* New York, Dover.

BECQUE, J. 2010. Inelastic Plate Buckling. *Journal of Engineering Mechanics,* 136, 1123-1130.

BECQUE, J., LATHOURAKIS, P. & JONES, R. 2011. Experimental verification of an inelastic plate theory based on plastic flow theory. *Thin-Walled Structures,* 49, 1563-1572.

BIJLAARD, P. P. 1941. Theory of the plastic stability of thin plates *Publications of the International Association of Bridge and Structural Engineering,* VI.

BLEICH, F. 1924. Theorie und Berechnung der eiseren Brucken. *Julius Springer*.

BLEICH, F. 1952. *Buckling strength of metal structures,* New York, McGraw-Hill Book Co., Inc.

BRYAN, G. H. 1891. On the stability of a plane plate with thrusts in its own plane with applications to the buckling of the sides of a ship. 22, 54-67.

BUDIANSKY, B. 1959. A reassessment of deformation theory of plasticity *Journal of Applied Mechanics,* 26, 259-264.

CAMOTIM, D. & ROORDA, J. 1985. On the effect of residual stresses in the plastic buckling of columns- A model study *CSME,* 33.

CAMOTIM, D. & ROORDA, J. 1993. Plastic buckling with residual stresses- 1. Postbifurcation behaviour. *Dynamic and Stability of Systems,* 8.

CHAKRABARTY, J. 2000. *Applied Plasticity,* New York, Springer.

CHEN, W. F. & HAN, D. J. 2007. *Plasticity for Structural Engineers*, J. Ross Publishing Classics.

CHRISTENSEN, C. D. & BYSKOV, E. 2008. Advanced postbuckling and imperfection sensitivity of the elastic-plastic Shanley-Hutchinson model Column. *Journal of Mechanics of Materials and Structures,* 3.

CONSIDERE, A. 1891. Resistance des pieces comprimees. *Congres international des procedes de construction,* 3.

CRISFIELD, M. A. 1991. *Nonlinear finite element analysis of solids and structures,* Chichester, Wiley.

DAWE, J. L. & GRONDIN, G. Y. 1985. Inelastic buckling of steel plates. *ASCE,* 111.

DONNELL, L. H. 1933. Stability of thin walled tubes under torsion. *Report No. 479.* Washington DC: NACA.

DUBERG, J. E. & WILDER, T. W. 1952. Inelastic column behaviour. *National Advisory Commitee for Aeronautics, Report No. 1072*.

DURBAN, D. & ZUCKERMAN, Z. 1999. Elastoplastic buckling of rectangular plates in biaxial compression/tension. *International Journal of Mechanical Sciences,* 41, 751-765.

EL-GHAZALY, H. A. & SHERBOURNE, A. N. 1986. Deformation theory for elasto-plastic buckling analysis of plates under non-proportional loading. *Computers and Structures* 22, 131-149.

ENGESSER, F. 1889. Die Knickfestigkeit gerader Stabe. *Z. Arch. Ing. Vereins Hannover,* 35.

ENGESSER, F. 1895. Ueber Knickfragen *Schweizerische Bauzeitung,* 26**,** 24-26.
EULER, L. 1744. Methodus Inveniendi Lineas Curvas Maximi Minimive Proprietate Gaudentes (Appendix, De Curvis Elasticis).
FAELLA, C., MAZZOLANI, F. M., PILUSO, V. & RIZZANO, G. 2000. Local buckling of aluminium members: Testing and classification. *Journal of Structural Engineering,* 126**,** 353-360.
GARDNER, L. & NETHERCOT, D. 2005. *Designers' Guide to EN 1993-1-1 Eurocode 3: Design of Steel Structures - General Rules and Rules for Buildings*, Thomas Telford Ltd.
GERARD, G. 1945. Secant modulus method for determining plate instability above the proportional limit. *Journal of Aeronautical Science,* 13.
GERE, J. M. & GOODNO, B. J. 2012. *Mechanics of Materials,* Canada, Global Engineering.
GJELSVIK, A. & LIN, G. S. 1987. Plastic Buckling of Plates with edge frictional shear effects. *Journal of Engineering Mechanics,* 113**,** 953-964.
HAAIJER, G. 1957. Plate buckling in the strain hardening range *Proceedings of ASCE, Engineering Mechanics Division,* 83.
HAAIJER, G. & THURLIMANN, B. 1958. On inelastic buckling of steel. *Proceedings of ASCE, Engineering Mechanics Division,* 84.
HANDELMAN, G. H. & PRAGER, W. 1948. Plastic buckling of a rectangular plate under edge thrusts. *National Advisory Commitee for Aeronautics, Report No. 946*.
HARDING, J. E., HOBBS, R. E. & NEAL, B. G. 1977. The elasto-plastic analysis of imperfect square plates under in-plane loading. *Proceedings of Institution of Civil Engineers, Part2,* 63**,** 137-158.
HENCKY, H. Z. 1924. Theorie Plastischer Deformationen und der hierdurch im Material hervorgerufenen Nachspannungen. *Journal of Applied Mathematics and Mechanics,* 4**,** 323-334.
HILL, R. 1950. *The Mathematical Theory of Plasticity,* Oxford, Oxford University Press.
HUTCHINSON, J. W. 1972. On the postbuckling behaviour of imperfection-sensitive structures in the plastic range. *Journal of Applied Mechanics,* 71**,** 155-161.
HUTCHINSON, J. W. 1973a. Imperfection-sensitivity in the plastic range. *Journal of Mechanical Physics and Solids,* 21**,** 191-204.
HUTCHINSON, J. W. 1973b. Post-bifurcation behaviour in the plastic range. *Journal of Mechanical Physics and Solids,* 21**,** 163-190.
HUTCHINSON, J. W. 1974. Plastic Buckling. *Advances in Applied Mechanics,* 14.
HUTCHINSON, J. W. & BUDIANSKY, B. 1974. Analytical and numerical study of the effects of initial imperfections on the inelastic buckling of a cruciform column. *Proceedings of the IUTAM Symposium on Buckling of Structures***,** 98-105.
HUTCHINSON, J. W. & NEALE, K. W. 1980. Finite strain J2 Deformation Theory *IUTAM Symposium*.
ILYUSHIN, A. A. 1947. The elasto-plastic stability of plates. *National Advisory Commitee for Aeronautics, Technical memorandum 1188*.
IZZUDDIN, B. & ELNASHAI, A. 1993. Adaptive space frame analysis. Part II: A distributed plasticity approach. *Proceedings of the ICE-Structures and Buildings,* 99**,** 317-326.

IZZUDDIN, B. & LI, Z. 2004. A co-rotational formulation for large displacement analysis of curved shells. *The 18th Australasian conference on the mechanics of structures & materials. Taylor & Francis Group, London*, 1247-1253.

IZZUDDIN, B. & SMITH, D. L. 1996. Large-displacement analysis of elastoplastic thin-walled frames. I: formulation and implementation. *Journal of Structural Engineering,* 122, 905-914.

IZZUDDIN, B. A. 1991. *Nonlinear dynamic analysis of framed structures.* PhD, Imperial College London

IZZUDDIN, B. A. 2006. Simplified buckling analysis of skeletal structures. *Proceedings of the ICE-Structures and Buildings,* 159, 217-228.

IZZUDDIN, B. A. 2007a. An optimisation approach towards lock-free finite elements.

IZZUDDIN, B. A. 2007c. Rotational Spring Analogy for Buckling Analysis. *Journal of Structural Engineering-asce,* 133.

IZZUDDIN, B. A. 2008. Simplified modelling of nonlinear structures-"spanning component to systems". *Proceedings of IASS-IACM*.

JASINSKI, F. 1895. Noch einWort zuden 'Knickfragen'. *Schweizerische Bauzeitung,* 25, 172-175.

JIRASEK, M. & BAZANT, P. B. 2001. *Inelastic Analysis of Structures*, John Wiley & Sons, ltd.

KIRCHHOFF, G. R. 1850. *J.Math. (Crelle),* 40.

KOITER, W. T. 1960. General theorems for elastic-plastic solids. *Progress in Solid Mechanics,* 1, 165-221.

LI, Z. X., IZZUDDIN, B. A. & VU-QUOC, L. 2008. A 9-node co-rotational quadrilateral shell element. *Computational Mechanics,* 42, 873-884.

LUNDQUIST, E. E. 1939. Local instability of symmetrical rectangular tubes under axial compression. *national Advisory Commitee for Aeronautics*.

MAPLESOFT, A. D. O. W. M. I. Maple 18. Waterloo, Ontario.

MUSHTARI, K. M. 1938. Certain generalisations of the theory of thin shells. *Izv Fiz Mat ob-va pri KazUn-te* 11.

NADAI, A. 1931. *Plasticity*, McGraw-Hill.

NEALE, K. W. 1975. Effect of imperfections on the plastic buckling of rectangular plates. *Journal of Applied Mechanics,* 42, 115-120.

NEEDLEMAN, A. & TEVERGAARD, V. 1976. An analysis of the imperfection sensitivity of square elastic-plastic plates under axial compression. *International Journal of Solids and Structures,* 12, 185-201.

NEEDLEMAN, A. & TVERGAARD, V. 1982. Aspects of plastic post-buckling behaviour. *Mechanics of Solids, The Rodney Hill 60th Anniversary Volume.* Pergamon Press Oxford.

ODQVIST, F. K. G. 1933. Plasticity Theory with Applications. *Royal Swedish Academy of Engineering Sciences*.

ONAT, E. T. & DRUCKER, D. C. 1953. Inelastic instability and incremental theories of plasticity. *Journal of Aeronautical Science,* 20, 181-186.

PEARSON, C. E. 1950. Bifurcation criterion and plastic buckling of plates and columns *Journal of Aeronautical Science,* 17, 417-424.

PRAGER, W. 1955. Probleme der Plastizitatstheorie. Basel, Stuttgart.

PRAGER, W. 1956. A new method of analysing stresses and strains in work hardening plastic solids *Journal of Applied Mechanics,* ASME 23, 493-496.

PRANDTL, L. 1925. Spannungsverteilung in plastischen Koerpern. *Proceedings of the 1st International Congress on Applied Mechanics*, 43-54.

PRIDE, R. A. & HEIMERL, G. J. 1949. Plastic buckling of simply supported compressed plates. *National Advisory Commitee for Aeronautics, Report No. 1817*.

RAMBERG, W. & OSGOOD, W. R. 1943. Description of stress-strain curves by three parameters. *National Advisory Commitee for Aeronautics, Report No. 902*.

REUSS, E. 1930. Beruecksichtigung der elastischen Formaenderungen in der Plastizitaetstheorie. *Journal of Applied Mathematics and Mechanics,* 10**,** 266-274.

ROS, M. & EICHINGER, A. 1932. Final report of the 1st Congress. *International Association of Bridge and Strcutural Engineering.*

SANDORFF, H. A. 1946. Strain distribution during column failure. Lockheed Aircraft Corporation

SEWELL, M. J. 1964. A general theory of elastic and inelastic plate failure II. *Journal of Mechanical Physics and Solids,* 12**,** 279-297.

SHANLEY, F. R. 1946. The Column Paradox. *Journal of the Aeronautical Sciences,* 13**,** 678-678.

SHANLEY, F. R. 1947. Inelastic Column Theory. *Journal of the Aeronautical Sciences,* 14**,** 261-268.

SHRIVASTAVA, S. C. 1979. Inelastic buckling of plates including shear effects. *International Journal of Solids and Structures,* 15**,** 567-575.

SHRIVASTAVA, S. C. & BLEICH, H. H. 1976. Inelastic buckling of plates allowing for shear effects. Office of Naval Research, Project No. 64-428.

STANDARDS, E. 2005. Eurocode 3- Design of steel structures- Part 1-1: General rules and rules for buildings.

STANDARDS, E. 2006. Eurocode 3- Design of steel structures- Part 1-5: Plated structural elements.

STOWELL, E. Z. 1948. A unified theory of plastic buckling of columns and plates. *National Advisory Commitee for Aeronautics, Report No. 898*.

TEMPLIN, R. L., STURM, R. G., HARTMANN, E. C. & HOLT, M. 1938. Column strength of various aluminium alloys. Pittsburgh: Aluminium Company of America

TIMOSHENKO, S. 1936. *Theory of elastic stability,* New York, McGraw-Hill.

TIMOSHENKO, S. & GERE, J. M. 1961. *Theory of elastic stability*, McGraw-Hill.

TIMOSHENKO, S. P. 1910. *Z. Math.Physik,* 58.

TRAHAIR, N. S., BRADFORD, M. A., NETHERCOT, D. A. & GARDNER, L. 2008. *The behaviour and design of steel structures to EC3*, Taylor & Francis.

TUGCU, P. 1991. Plate buckling in the plastic range. *International Journal of Mechanical Sciences,* 33**,** 1-11.

VAN DEN BROEK, J. A. 1945. Column formula for materials of variable modulus (Developed by the theory of limit design). *The Engineering Journal (Canada)*.

VAN DER HEIJDEN, A. M. A. 1979. A study of Hutchinson's plastic buckling model *Journal of Mechanical Physics and Solids,* 27**,** 441-464.

VLASOV, V. Z. 1964. General theory of shells and its application in engineering. Washington DC: NASA Technical Translation TTF-99.

VON KARMAN, T. 1910. Untersuchungen uber die Knickfestigkeit, Mitteilungen uber Forschungsarbeiten auf dem Gebiete des Ingenieurwensen *Springer,* 81.

VON MISES, R. 1913. Mechanik der festen Körper im plastisch deformablen Zustand. *Göttin. Nachr. Math. Phys.,* 1.

WANG, C. M., ZIANG, Y. & CHAKRABARTY, J. 2001. Elastic/plastic buckling of thick plates. *International Journal of Solids and Structures,* 38**,** 8617-8640.
ZIEGLER, H. 1959. A modification to Prager's hardening rule. *Quarterly Journal of Applied Mathematics,* 17**,** 55-65.